EXPANDING THE APPLICATION POTENTIAL OF GLYCOSIDE PHOSPHORYLASES THROUGH PROCESS ENGINEERING

ir. Karel De Winter


UNIVERSITEIT GENT

FACULTEIT BIO-INGENIEURSWETENSCHAPPEN

Members of the jury

Prof. dr. Tom Desmet (Ghent University) (promotor)

Prof. dr. ir. Wim Soetaert (Ghent University) (promotor)

Prof. dr. ir. Stefaan De Smet (Ghent University) (chairman)

Prof. dr. ir. Matthias D'hooghe (Ghent University) (secretary)

Prof. dr. ir. John Van Camp (Ghent University)

Prof. dr. Ludo Diels (University of Antwerp)

Dr. ir. Manu De Groeve (Ablynx NV)

Promotors

Prof. dr. Tom Desmet (Ghent University)

Prof. dr. ir. Wim Soetaert (Ghent University)

Centre for Industrial Biotechnology and Biocatalysis

Department of Biochemical and Microbial Technology

Ghent University, Belgium

Dean

Prof. dr. ir. Marc Van Meirvenne

Rector

Prof. dr. Anne De Paepe

Karel De Winter was supported by the Fund for Scientific Research-Flanders (FWO-Vlaanderen, doctoral scholarship) and the European Commission FP7-project Novosides (grant agreement nr. KBBE-4-265854).

ir. Karel De Winter

EXPANDING THE APPLICATION POTENTIAL OF GLYCOSIDE PHOSPHORYLASES THROUGH PROCESS ENGINEERING

Thesis submitted in fulfillment of the requirements for the degree of
Doctor (PhD) in Applied Biological Sciences

Dutch translation of the title

Verruiming van de toepassingsmogelijkheden van glycoside fosforylasen door procesoptimalisatie

To refer to this thesis

K. De Winter, **2016**, Expanding the application potential of glycoside phosphorylases through process engineering, PhD thesis, Faculty of Bioscience Engineering, Ghent University, Ghent.

Printed by University Press, Zelzate.

ISBN number: 978-90-5989-867-7

DANKWOORD

Een doctoraat schrijven wordt wel eens beschouwd als één van de meest eenzame bezigheden ter wereld. Hoewel dit wellicht waar is, kan de periode die hieraan voorafgaat allerminst eenzaam genoemd worden. Vandaar dat ik van deze gelegenheid gebruik wil maken om een aantal mensen die rechtstreeks of onrechtstreeks hebben bijgedragen tot het behalen van mijn doctoraat, te bedanken.

In eerste instantie wil ik mijn promotoren, professor Tom Desmet en professor Wim Soetaert bedanken om mij de mogelijkheid te geven onderzoek uit te voeren in een goed uitgerust labo. De mentale, wetenschappelijke en financiële ondersteuning, de vrijheid om weer eens iets nieuws op poten te zetten, het vertrouwen, en de eindeloze diepgaande discussies werden enorm geapprecieerd. Ook professor Vladimír Křen, die mij de mogelijkheid gaf gedurende 3 maanden onderzoek ter verrichten in Praag, wens ik hiervoor te bedanken.

Een speciaal woord van dank gaat ook naar de juryleden. Professor Ludo Diels, professor John Van Camp, professor Matthias D'hooghe, professor Stefaan De Smet en dokter Manu De Groeve; bedankt voor de oprechte interesse, het kritisch nalezen van mijn doctoraat, en de uitdagende vragen.

"Een goede werksfeer draagt bij tot het dagelijks geluk, en stimuleert het streven naar resultaat", desalniettemin een onderschatting van het belang van collega's als je het mij vraagt. Eerst en vooral wens ik mijn voorgangers te bedanken voor de vele praktische hulp, raad en uitleg. Bedankt An, Jef, Giang, Koen, Dirk en Tommeke! Maar ook het huidige glycodirect team mag er zeker zijn. Bedankt Barbara, Magali, Margo, Griet, Jorick, Stevie, Koen, Maarten en Renfei om zowel tijdens de uren, na de uren, en zelfs op de skipiste steeds voor een goede sfeer te zorgen. Mareike, Marieke, Paul; het was aangenaam samenwerken met jullie. Collega's van Inbio: bedankt voor de goede sfeer en assistentie!

Een oprecht woord van dank aan mijn thesisstudenten is zeker eveneens op zijn plaats. Kristien, Saskia, Bram, Tim, Kathleen, Jeroen, Lena, Lisa, Griet, Bert, Anoek en Sylvie;

bedankt voor de inzet, de talloze herhalingen, het gemotiveerd blijven ondanks tegenslagen, het nachtwerk en de weekends of verjaardagsfeestjes die bij momenten wat later bleken aan te vangen. Zonder jullie was dit resultaat niet mogelijk, bedankt!

Tenslotte rest mij nog een woord van dank te richten aan de mensen die mij van kleins af alle kansen en ondersteuning hebben gegeven. Mama, papa, lieve zus, meter, opa, meme, pepe; bedankt voor de onvoorwaardelijke steun, raad, en de mooie momenten samen. Margo, niet alleen Emile en Leon komen graag thuis, ook voor mij is thuiskomen steevast het mooiste moment van de dag! Je steun, aanvoelen (jij weet echt wat ik denk of ga zeggen), geduld, bereidheid om alles om het even wanneer te bespreken, en heerlijke maaltijden maken van ons gezin de mooiste plaats op aarde. Bedankt!

TABLE OF CONTENTS

ABBREVIATIONS

[BMIM][BF_4]	1-Butyl-3-methylimidazolium tetrafluoroborate
[BMIM][dca]	1-Butyl-3-methylimidazolium dicyanamide
[BMIM][I]	1-Butyl-3-methylimidazolium iodide
[EMIM][dca]	1-Ethyl-3-methylimidazolium dicyanamide
[EMIM][$EtSO_4$]	1-Ethyl-3-methylimidazolium ethylsulfate
[MMIM][$MeSO_4$]	1-Methyl-3-methylimidazolium methylsulfate
ABTS	2,2'-Azino-bis(3-ethylbenzothiazoline-6-sulphonic acid)
CAN	Acetonitrile
AMMOENG 101	Quaternary ammonium compounds, coco alkylbis (hydroxyethyl)methyl, ethoxylated, chlorides, methyl chloride
APG	Alkyl polyglucoside
ATP	Adenosinetriphosphate
BaSP	*Bifidobacterium adolescentis* sucrose phosphorylase
BCA	Bicinchoninic acid
BHT	2,6-Bis(1,1-dimethylethyl)-4-methylphenol
BMGY	Buffered glycerol-complex
BMMY	Buffered methanol-complex
BSM	Basal salts medium
BuOAc	Butyl acetate
CAZymes	Carbohydrate-active enzymes
CDP	Cellodextrin phosphorylase
CLEA	Cross-linked enzyme aggregate
CP	Cellobiose phosphorylase
CsCDP	*Clostridium stercorarium* cellodextrin phosphorylase
CtCP	*Clostridium thermocellum* cellobiose phosphorylase
CV	Coefficient of variation
DMF	Dimethylformamide
DMSO	Dimethyl sulfoxide
DNA	Deoxyribonucleic acid
dNTP	Deoxynucleotide triphosphate

DO	Dissolved oxygen
DPPH	2,2-Diphenyl 1-picrylhydrazyl
EC_{50}	Half maximal effective concentration
EC-HFA	Enzyme carrier hetero-functional amino
EDTA	Ethylenediaminetetraacetic acid
ELSD	Evaporative light scattering detector
EtOAc	Ethyl acetate
EtOH	Ethanol
FA	Formic acid
G6P-DH	Glucose-6-phosphate dehydrogenase
GA	Glutaraldehyde
gCOSY	Gradient correlation spectroscopy
GH	Glycoside hydrolase
gHMBC	Gradient heteronuclear multiple bond coherence
gHSQC	Gradient heteronuclear single quantum coherence
GI	Glucose isomerase
GP	Glycoside phosphorylase
GT	Glycosyl transferase
HIV	Human immunodeficiency virus
HPAEC	High performance anion exchange chromatography
HPLC	High-performance liquid chromatography
HSQC-TOCSY	Heteronuclear single quantum coherence-total correlation spectroscopy
Hz	Hertz
iCLEA	Imprinted cross-linked enzyme aggregate
ICUMSA	International commission for uniform methods of sugar analysis
IL	Ionic liquid
IPA	Isopropyl alcohol
IPTG	Isopropyl β-D-thiogalactopyranoside
K_m	Michaelis–Menten constant
LB	Lysogeny broth
MeOH	Methanol

MES	2-(*N*-morpholino)ethanesulfonic acid
MOPS	3-(*N*-morpholino)propanesulfonic acid
MTBE	Methyl-*tert*-butylether
NAD	Nicotinamide adenine dinucleotide
NF-kB	Nuclear factor kappa-light-chain-enhancer of activated B cells
Ni-NTA	Nickel-nitrilotriacetic acid
NMR	Nuclear magnetic resonance
OD	Optical density
OG	Octyl β-D-glucopyranoside
PAD	Pulsed amperometric detection
PEG	Polyethylene glycol
PGM	Phosphoglucomutase
Pi	Inorganic phosphate
PNP	*p*-Nitrophenol
R_f	Retardation factor
Rpm	Revolutions per minute
SHIME	Simulation of human intestinal microbial ecosystem
SP	Sucrose phosphorylase
t_{50}	Half-life time
TG	Transglycosidase
TLC	Thin layer chromatography
TOCSY	Total correlation spectroscopy
TtSPP	*Thermoanaerobacterium thermosaccharolyticum* sucrose phosphorylase
TtSPP_R134A	R134A mutant of the *Thermoanaerobacterium thermosaccharolyticum* sucrose phoshorylase
U	Unit of enzymatic activity
UDP-Glc	Uridine diphosphate glucose
Vvm	Volume of air per volume of liquid per minute
WT	Wild type
YNB	Yeast nitrogen base
YPD	Yeast extract peptone dextrose

αG1P	α-D-Glucose 1-phosphate
αGal1P	α-D-Galactose 1-phosphate
αGG	α-Glucosyl glycerol

Introduction

Carbohydrates provide energy in living organisms and are a structural component of the cell wall. Over the past decade, certain carbohydrates have also been associated with the growth of beneficial bacteria in the human gut. Prominent examples of such 'prebiotics' include inulin[1], trans- galactooligosaccharides[2], resistant starches[3] and mannan oligosaccharides[4, 5]. Carbohydrates also play a pivotal role in recognition processes when attached to proteins or lipids[6]. Moreover, glycosylation, the attachment of a carbohydrate moiety, can drastically change both the physicochemical and biological properties compared to the aglycon.

Indeed, glycosylation is known to improve the stability of labile compounds such as vitamin C[7], modulate the activity spectrum of antibiotics[8], and enhance the solubility of flavonoids and stilbenoids[9]. Vancomycin, for example, exhibits its antibacterial activity by binding essential bacterial cell wall mucopeptide precursors terminating in the sequence L-Lys–D-Ala–D-Ala, which blocks their further processing into peptidoglycans. Although this binding is ensured by five hydrogen bonds between amide protons of the aglycon and the cellwall precursors, the carbohydrate moieties were found to be crucial in the required dimerization and anchoring of the antibiotic to the cell membrane[8]. The increased hydrophilicity, on the other hand, significantly influences the pharmacokinetic and dynamic properties of drugs, while glycosylation also allows targeting to specific organs, thus enabling the use of smaller doses[10]. In addition, glycosylation often leads to a modified perception of flavors and fragrances. A prime example is glycyrrhizin, found in sweetwood (*Glycirhyza glabra*). The latter terpenoid glycoside loses most of its sweetness upon hydrolysis[11]. The α-glucoside of L-menthol, in turn, is only slowly hydrolyzed in the mouth, resulting in a prolonged sensation of freshness[12]. Consequently, the development of a cheap and efficient glycosylation technology is highly desirable.

Chemical glycosylation is typically performed based on the Fischer or Koenings-Knorr reaction[13]. The former is performed by reacting an aldose or ketose with an alcohol in the presence of an acid catalyst, while the latter uses glycosyl halides, activated with silver salts, as glycosyl donors. Unfortunately, the substrates of the Fisher glycosylation are limited to simple alcohols, and product isolation is hampered by the formation of different isomers and anomers[14]. In contrast, the regioselectivity of Koenings-Knorr

glycosylations can be controlled by applying appropriate protection strategies, while the anomeric configuration is strongly dependent on the neighboring group participation of the C2 substituent and the type of solvents and catalysts used[15].

Despite the continuous development of new procedures, including the use of glycosyl trichloroacetimidates[16] and the more stable *n*-pentenyl glycosides[17], chemical synthesis of glycosides still suffers from a number of drawbacks. Indeed, labor-intensive activation and protection procedures require the use of toxic catalysts and solvents, resulting in the generation of large amounts of (toxic) waste. Moreover, the commonly used multistep synthetic routes often result in low yields, while limiting the overall productivity[13, 15]. Biocatalytic approaches are, therefore, an attractive alternative that enables one-step reactions with high regio- and stereoselectivity[18]. Enzymatic glycosylation reactions typically generate 5-fold less waste and have a 15-fold higher space-time yield, a tremendous improvement in the eco-efficiency[19].

In general, four types of carbohydrate-active enzymes (CAZymes) can be used to transfer glycosyl moieties (Figure I.1). Glycoside hydrolases (GH) are *in vivo* hydrolytic enzymes, transferring the cleaved glycosyl moieties to water[20]. However, GHs can also be used for synthetic purposes when applied under either kinetic (transglycosylation) or thermodynamic (reverse hydrolysis) control[21]. Although many specificities have been reported, the yields are typically low. Indeed, the presence of water is essential to retain enzymatic activity, but inevitably also leads to hydrolysis of the substrates or products. As a result, the water activity of the reaction mixtures should be carefully balanced, compromising high yields, and generally resulting in poor productivities.

Glycosyl transferases (GT), on the other hand, can be considered nature's catalysts for glycosylation reactions. These enzymes have evolved over millions of years to optimally catalyze glycosyl transfer reactions, and thus combine high yields and productivities with excellent regio- and stereocontrol[22]. Unfortunately, their application is hampered by the high price of the required nucleotide-activated donor substrates (e.g., uridine diphosphate glucose (UDP-Glc)). Furthermore GTs are often membrane-associated enzymes originating from plants, complicating expression and purification procedures[23]. As a result, the overall productivity, also taking the production of active enzyme into

consideration, is rather limited. Although many GTs have nowadays been identified in microorganisms[24], and the *in situ* formation of UDP-Glc from sucrose and UDP has been described[25], the use of GTs is limited to the field of therapeutic compounds like complex oligosaccharides[26].

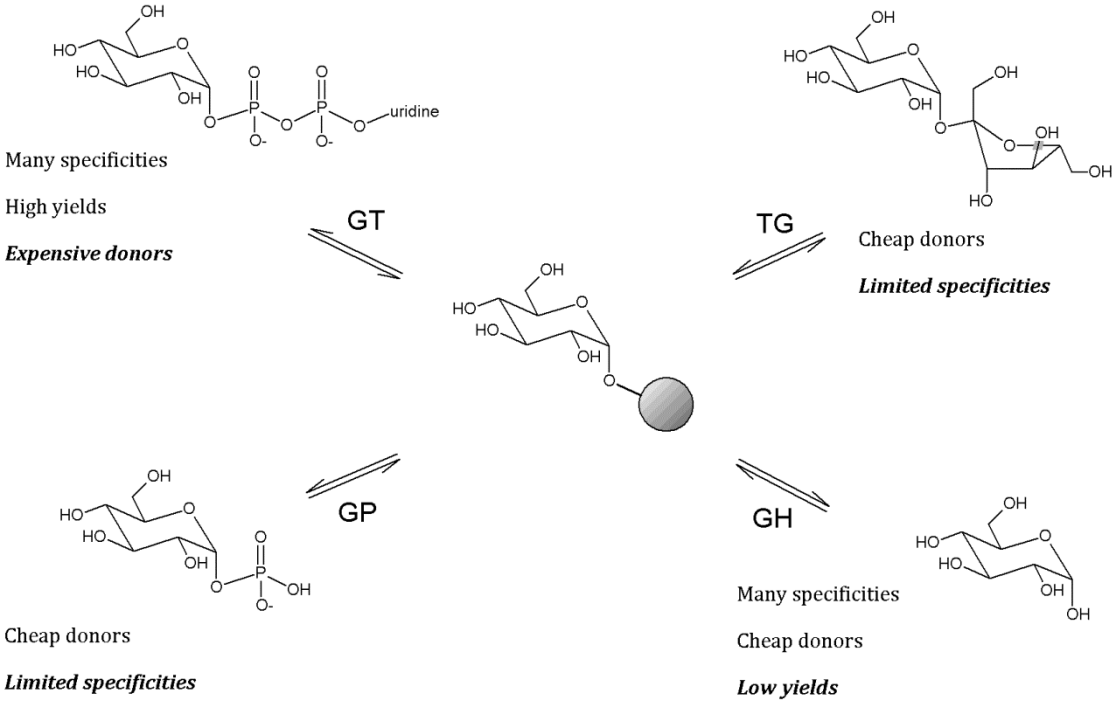

Figure I.1 Glycosylation reactions catalyzed by glycosyl transferases (GT), transglycosidases (TG), glycoside phosphorylases (GP) and glycoside hydrolases (GH). The four classes of CAZymes are listed with their respective benefits and drawbacks; adapted from[27].

Two types of glycosyl transferring enzymes have properties that lay between GHs and GTs. These enzymes are capable of achieving moderate yields, without the need for expensive nucleotide-activated donor substrates. Transglycosidases (TG), on the one hand, employ non-activated carbohydrates (e.g., sucrose) for the transfer of a glycosyl group[28]. Glycoside phosphorylases (GP), on the other hand, require glycosyl phosphates (e.g., α-D-glucose 1-phosphate (αG1P)) as donor[29]. TGs have been successfully applied for the synthesis of prebiotic oligosaccharides[30] and various glycoconjugates[31-33]. Nevertheless, their application is hampered by the limited availability of specificities, typically only allowing the transfer of α-glucosyl or β-fructosyl moieties to a narrow range of acceptors[27]. Indeed, their low affinity towards non-carbohydrate acceptors, combined with the loss of activity due to the use of solvents, generally limits the productivity of these enzymes for the glycosylation of small organic compounds.

In vivo, glycoside phosphorylases degrade di- and oligosaccharides using inorganic phosphate; thereby producing a glycosyl phosphate and a saccharide of reduced chain length. The phosphate moiety can be conveniently transferred from C1 to C6 by a phosphomutase, allowing its use in the glycolysis without further activation by a kinase[34]. Moreover, the high-energy content of the produced glycosyl phosphates allows the reactions to be reversed, enabling the application of GPs for synthetic purposes *in vitro*. This property has already been vastly exploited, resulting in the synthesis of several unnatural tri- and disaccharides using cellobiose phosphorylase (CP)[35, 36]. Besides CP, also cellodextrin phosphorylase (CDP) and sucrose phosphorylase (SP) have been used to glycosylate a variety of compounds. Indeed, the former has been applied for the glycosylation of oligosaccharides[37], alkyl glucosides[38] and phenolic glucosides[39], while the latter has been described for the synthesis of 2-*O*-α-D-glucopyranosyl L-ascorbic acid[7] and 2-*O*-(α-D-glucopyranosyl) *sn*-glycerol[40]. Despite many endeavors in the field of enzyme engineering[39, 41-43], the industrial applicability of these enzymes is still hampered by the limited number of specificities and the availability of αG1P.

Therefore, an efficient strategy for the production of αG1P was first developed (CHAPTER 1). The use of the recently reported *Bifidobacterium adolescentis* SP Sepabeads[44], combined with a yeast treatment and crystallization step allowed the isolation of large quantities of pure αG1P. Besides enzyme engineering, process engineering (i.e. optimizing the reaction temperature, pH, substrate concentrations and the use of solvents) and molecular imprinting are valuable tools to expand the applicability of enzymes. In view of the recently reported SP cross-linked enzyme aggregates (CLEA)[45], a new technology combining covalent immobilization and molecular imprinting was established in CHAPTER 2. The latter technique was developed to combine an enhanced selectivity towards alternative substrates with an improved thermostability. Next, the glycosylation potential of SP was scrutinized using various cosolvents (CHAPTER 3) and biphasic reaction systems (CHAPTER 4). A broad range of solvents and operational conditions were evaluated, identifying the IL AMMOENG 101 and ethyl acetate as potent solvents for glycosylation reactions. Moreover, the use of the optimized reaction conditions allowed the synthesis of a broad range of challenging α-glucosides.

The optimized reaction conditions obtained in CHAPTER 3 and 4 were then combined with the αG1P produced in CHAPTER 1, allowing the synthesis of various β-glucosides with cellobiose phosphorylase. In addition, the concept of imprinted cross-linked enzyme aggregates (iCLEAs) was revisited using CP (CHAPTER 5). Next, the use of cosolvents and biphasic catalysis with the α-L-rhamnosidase from *Aspergillus terreus* was evaluated (CHAPTER 6), thereby expanding the diversity of glycosides to α-L-rhamnosides. The previously obtained glucosides were then further glycosylated using cellodextrin phosphorylase and αG1P as donor. Careful optimization of the reaction conditions allowed the synthesis of numerous cellobiosides and cellotriosides, while the performance of the CDP originating from *Clostridium stercorarium* was further improved by enzyme engineering (CHAPTER 7). Next, the previously studied GPs were combined for the synthesis and isolation of a wide range of glycosylated antioxidants. The solubility, thermal stability and radical scavenging properties of the established antioxidant library was then scrutinized, thereby revealing the application potential of glycosylated antioxidants (CHAPTER 8). Finally, a recently developed SP mutant[43] was evaluated for the production of kojibiose. The use of an integrated approach during the design of the process, allowed the synthesis and isolation of crystalline kojibiose with high yields (CHAPTER 9).

CHAPTER 1

Operational stability of immobilized sucrose phosphorylase: continuous production of α-glucose 1-phosphate at elevated temperatures

This chapter has been published as:

K. De Winter, A. Cerdobbel, W. Soetaert and T. Desmet, **2011**, Operational stability of immobilized sucrose phosphorylase: Continuous production of α-glucose 1-phosphate at elevated temperatures, *Process Biochemistry*, 46, 2074-2078.

1 ABSTRACT

Sucrose phosphorylase (SP) is a useful biocatalyst for the selective transfer of α-glucosyl residues to a variety of acceptor molecules. At the industrial scale, however, conversions of sucrose would preferably be performed at 60 °C or higher. Previous research has shown that the stability of the SP from *Bifidobacterium adolescentis* can be significantly improved by immobilization on Sepabeads EC-HFA. Therefore, this biocatalyst has now been applied for the continuous production of α-D-glucose 1-phosphate from sucrose. To lower the costs, the enzyme has only been partially purified prior to immobilization. Interestingly, the presence of the substrate sucrose was found to dramatically enhance the stability of the biocatalyst, allowing its use in a packed-bed reactor for more than 2 weeks at 60 °C without loss of activity. The overall process generated a space-time yield of 179 g/L/h, and the product could be recovered in crystalline form with a yield of 86 %.

2 INTRODUCTION

Glycosyl phosphates, such as α-D-glucose 1-phosphate (αG1P), are key intermediates in the synthesis of nucleotide sugars, the activated donors of glycosyl transferases[46]. They are, however, also efficient glycosyl donors in their own right, for both chemical and enzymatic glycosylation reactions[47]. Moreover, αG1P can also be used for a number of other applications. Among these are the stimulation of active calcium transport in intestines as nutritional supplement, and its use in medicine as a substitute of inorganic phosphate in parenteral nutrition[48, 49].

Glycosyl phosphates can be produced by chemical synthesis, but these procedures suffer from low yields and lack of anomeric selectivity[50]. Biocatalytic synthesis typically relies on kinases, which require adenosinetriphoshpate (ATP) as phosphate donor. Although several strategies have been developed to recycle this cofactor, the high costs involved with the latter strategy hamper large-scale applications[51]. In that respect, glycoside phosphorylases are a very attractive alternative, as they only require cheap inorganic phosphate for the production of glucose 1-phosphate from a di- or oligosaccharide[52]. The β-form has, for example, been produced at 60 °C using the thermostable trehalose phosphorylase from *Thermoanaerobacter brockii*[53]. Interestingly, α-D-galactose 1-phosphate has recently also become available as product thanks to the creation of variants of cellobiose phosphorylase with activity towards lactose[41, 54].

Similarly, sucrose phosphorylase can be used for the production of αG1P by the phosphorolysis of sucrose into αG1P and fructose[52]. Moreover, a variety of glycosylated compounds can be produced with this enzyme, thanks to its broad acceptor specificity[55]. For example, an exceptionally efficient process for the production of 2-*O*-(α-D-glucopyranosyl) *sn*-glycerol has recently been developed with SP[40, 56]. The product is commercially available under the tradename Glycoin® and is used as a moisturizing agent in cosmetics.

At the industrial scale, however, all these conversions of sucrose would preferably be performed at 60 °C or higher, mainly to avoid microbial contamination and to lower the viscosity of the reaction solution[57-59]. We have recently shown that immobilization of the

SP from *Bifidobacterium adolescentis* significantly enhances its stability. Indeed, covalent binding to Sepabeads EC-HFA resulted in a biocatalyst with a half-life of more than 10 h at 60 °C[44], while a cross-linked enzyme aggregate (CLEA) of SP did not lose any activity even after 10 days incubation at 60 °C[45].

In this chapter, a continuous production process for αG1P was developed with immobilized SP operating at 60 °C. For that purpose, Sepabeads were preferred over CLEAs because the latter are not well suited for use in a packed-bed reactor[60]. The immobilization of heat purified enzyme has been evaluated, thereby avoiding the expensive and labor-intensive His-tag purification. The operational stability of the obtained biocatalyst was examined, and an efficient downstream-processing procedure for αG1P was established.

3 RESULTS & DISCUSSION

3.1 Immobilization of heat purified SP

Immobilization of the His-tag purified SP from *B. adolescentis* on Sepabeads EC-HFA results in a highly stable biocatalyst with an increased temperature optimum[44]. For industrial applications, however, the purification of an enzyme by chromatographic techniques prior to immobilization is rather expensive. We have recently shown that the contaminating phosphatase activity present in the *E. coli* host can also be efficiently removed by heat treatment of crude cell extracts[45]. We have, therefore, now evaluated the immobilization efficiency of heat purified SP.

Under optimal conditions, immobilization of 0.25 mg heat purified protein on 1 g Sepabeads EC-HFA was found to result in an immobilization yield of 60 %, which is lower than the 72 % obtained with the His-tag purified enzyme at the same protein/resin ratio[44]. However, in previous work we found that His-tag purification is hampered by a yield of only 45 %, compared to nearly 100 % for heat purification[44, 45]. Therefore, the overall yield of purification and immobilization is higher for the latter process (60 %), than for the former (33 %). Characterization of the new immobilized SP preparation revealed that its thermal behavior is similar to that of the His-tag purified

immobilizate, i.e. an optimal temperature for phosphorolytic activity of 65 °C (Figure S1.1) and a residual activity of 75 % after 16 h incubation at 60 °C.

SP is known to catalyze a minor hydrolytic reaction[27], which could have a negative impact on the product yield. The specificity of the immobilized enzyme has therefore also been determined (Figure 1.1).

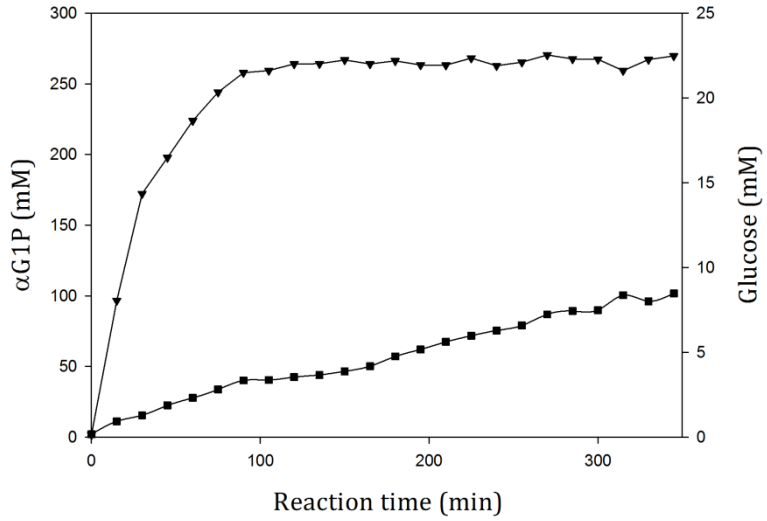

Figure 1.1 Phosphorolysis and hydrolysis of sucrose by immobilized SP. Experiments were performed with 2.5 U/mL enzyme and 400 mM substrate at pH 7.0 and 60 °C. Both the release of αG1P (▼) and glucose (■) were followed in time.

Using 400 mM sucrose as substrate at 60 °C and pH 7, the hydrolytic activity was found to be only 0.4 % of the phosphorolytic activity, resulting in the release of small amounts of glucose. Once the equilibrium of the phosphorolytic reaction is reached, slow hydrolysis of the formed αG1P is also observed. Consequently, the conversion must be stopped at the appropriate time, although the product loss would only become substantial after several hours. Similar results were obtained with the free enzyme (Figure S1.2), which indicates that the latter immobilization does not influence the specificity of SP.

Finally, the operational stability of both the His-tag purified and heat purified immobilized biocatalysts was evaluated by recycling the beads for consecutive batch reactions at 60 °C (Figure 1.2).

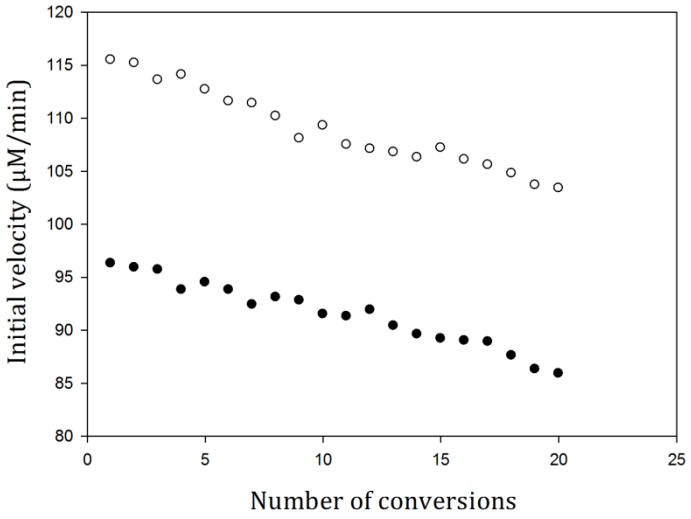

Figure 1.2 Repeated batch conversion of sucrose by immobilized SP at 60 °C. The initial velocity of the His-tag purified (○) and heat purified (●) immobilized biocatalysts was measured after each conversion. Both enzyme preparations were immobilized on Sepabeads EC-HFA by offering 4 U to the resin under optimal conditions. The initial velocity was determined in 25 mL substrate at 60 °C.

Both resins were found to retain 90 % of their initial activity after 20 reaction cycles. In spite of this promising characteristic, a continuous production process in a packed-bed reactor was believed to be more appropriate for industrial applications, as this would results in a much higher space-time yield.

3.2 Continuous production of αG1P

Different amounts of the new SP preparation, obtained by immobilizing 111 U/mL resin, were packed in a plug-flow reactor to identify the optimal conditions for the continuous production of αG1P (Figure 1.3). A substrate solution consisting of 400 mM sucrose in 400 mM phosphate buffer at pH 7.0 and 60 °C was then pumped through the columns at a flow rate of 0.75 mL/min. The maximal substrate conversion (69 %) of this equilibrium reaction could nearly be reached when 18 mL of resin was used (average residence time of 24 min). Increasing the resin volume, therefore, would lower the productivity of the reactor. Indeed, the space-time yield dropped from 179 to 92 g/L/h when 36 mL of resin was used, as the additional 18 mL resin could not further increase the αG1P concentration. In contrast, lowering the resin volume allows for a more economical use of the immobilized enzyme, albeit at the expense of the degree of conversion. With 9 mL of resin, for example, the space-time yield increased to 254 g/L/h

but only 49 % of the substrate was converted to αG1P. The choice of the optimal reactor configuration will thus depend on the price of the biocatalyst and the substrate.

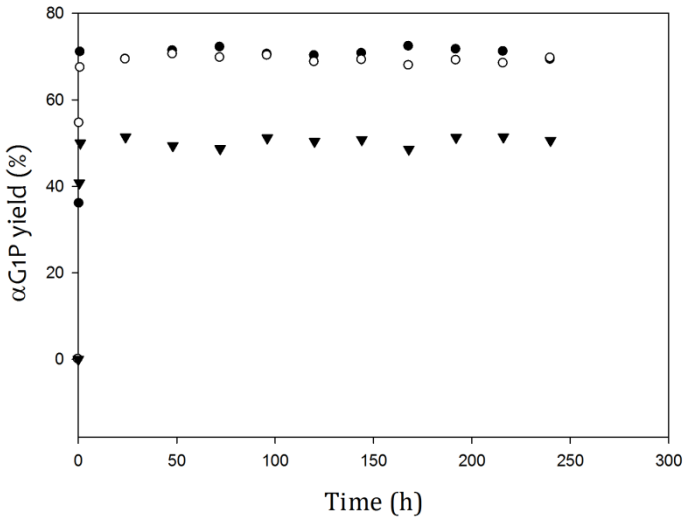

Figure 1.3 Continuous production of αG1P by immobilized SP at 60 °C. The αG1P yield for packed bed reactors with 36 (●), 18 (○) and 9 (▼) ml Sepabeads EC-HFA respectively was determined. Substrate containing 400 mM sucrose in 400 mM phosphate buffer at pH 7.0 was pumped through each packed bed at a constant flow rate of 0.75 mL/min.

Interestingly, we found that the conversion rate remained constant up to extended reaction times of 240 h. Nevertheless, the immobilized enzyme is known to lose 25 % of its activity after only 16 h incubation at 60 °C. The latter indicates that the presence of the substrate sucrose has a dramatic effect on the stability of the biocatalyst, emphasizing the excellent performance of immobilized SP under the operational conditions. It is well known that enzymes can be stabilized through interactions with their substrate[61] or with sugars in general[62]. We have previously shown that sucrose can also increase the yield of the immobilization process[44]. Clearly, the interactions between sucrose and SP are crucial to maintain the structural integrity of the enzyme as much as possible.

3.3 Purification and crystallization of αG1P

After the continuous production of αG1P, the product was purified from the reaction mixture that also contained sucrose, phosphate, fructose and traces of glucose, released by the minor hydrolytic activity of SP. Conveniently, these contaminating carbohydrates could be efficiently removed by treatment with yeast (Figure 1.4).

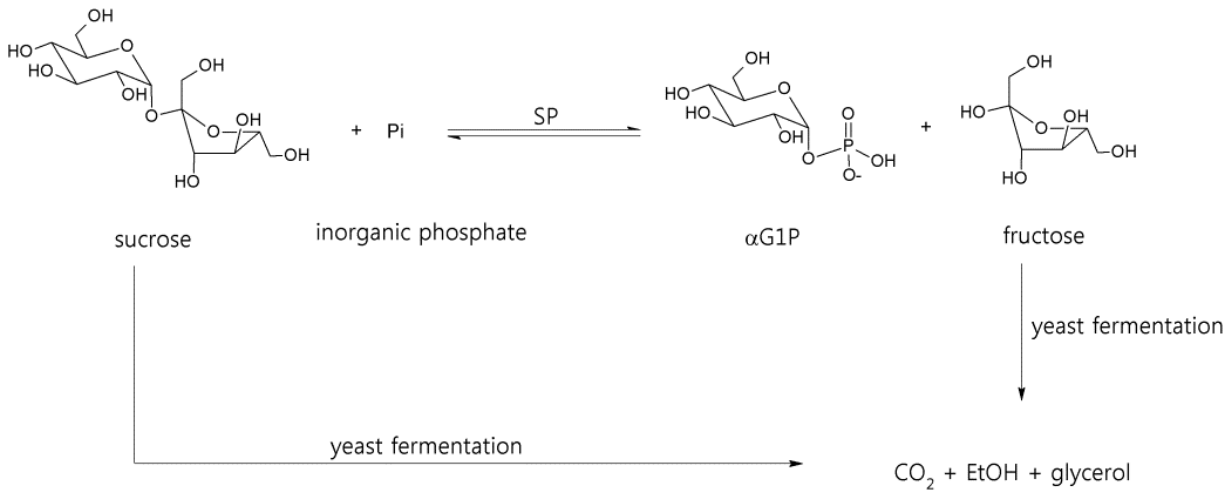

Figure 1.4 General scheme for the production and purification of αG1P. Sucrose is converted to fructose and αG1P by immobilized SP at 60 °C. Contaminating carbohydrates can then be removed by treatment with yeast at 30 °C.

Initially, sucrose was rapidly hydrolyzed to glucose and fructose by the yeast's invertase activity. Glucose and fructose were then completely metabolized within 2 and 6 hours respectively, resulting in the formation of ethanol, CO_2 and minor amounts of glycerol. In contrast to the undesired carbohydrates, αG1P was not consumed by the yeast as the latter charged compound cannot pass through the yeast's membrane (Figure 1.5). Afterwards, the yeast was removed by filtration, resulting in a near quantitative recovery of αG1P.

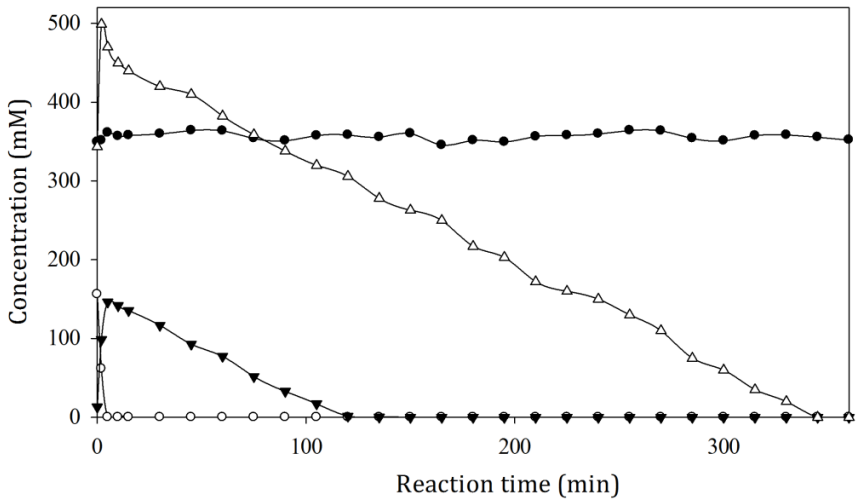

Figure 1.5 Removal of contaminating carbohydrates from αG1P by treatment with yeast. Time courses of the concentration of αG1P (●), fructose (Δ), glucose (▼) and sucrose (○). Baker's yeast was added to a concentration of 20 g/L and gently stirred during 8 h at 30 °C.

The product, however, still contained the remaining inorganic phosphate present in the reaction mixture. This contamination can be removed by chemical precipitation of phosphate followed by filtration[63]. Although 94 % recovery was achieved, crystals of αG1P could not be generated. The latter is most likely caused by interference of some compounds present in the precipitation liquid, e.g. acetic acid or Mg^{2+} ions[53].

To circumvent this problem, the production process was adapted to minimize the amount of phosphate, eliminating the need for its removal. To that extent, the phosphorolysis of sucrose (500 mM) was performed with varying concentrations of phosphate, allowing the reactions to proceed until apparent equilibrium. Lower phosphate concentrations at the start of the reaction evidently resulted in lower phosphate concentrations at equilibrium, but also decreased the degree of sucrose conversion (Table 1.1).

Table 1.1 Concentration of αG1P and phosphate at apparent equilibrium after the phosphorolysis of 500 mM sucrose at 60 °C and pH 7.0 (HPLC analysis). The concentration of phosphate at the start of the reaction was varied.

$[P_i]^a$ (mM)	$[\alpha G1P]^b$ (mM)	$[P_i]^b$ (mM)	conversion[c] (%)
100	97.6 ± 2.2	2.4 ± 0.3	19.5
200	175.1 ± 4.1	25.0 ± 0.9	35.0
300	245.5 ± 4.9	54.6 ± 1.2	49.1
400	321.1 ± 5.8	78.9 ± 2.6	64.2
500	354.5 ± 7.3	145.6 ±3.3	70.9

[a] at the start of the reaction; [b] at apparent equilibrium.; [c] of sucrose

The optimal sucrose/phosphate ratio thus depends on the required specifications for the process, i.e. either high yields or a high purity. At a ratio of 5, crystals of αG1P could be generated with a yield of 86 %, exhibiting a contamination with phosphate of less than 1 %. However, if phosphate contamination of the product is no constraint, a ratio of 1 will result in a higher αG1P yield towards sucrose.

4 CONCLUSION

In this chapter, a continuous production process for αG1P was developed with immobilized sucrose phosphorylase. The use of heat purified SP was found to be a practical alternative to the His-tag purified enzyme, yielding a biocatalyst preparation that is cheaper but still free from contaminating phosphatase activity. In that way, a packed-bed reactor was constructed, allowing a space-time yield of 179 g/L/h at 60 °C. Interestingly, the substrate sucrose was found to have a significant effect on the stability of the enzyme, which does not lose activity even after 2 weeks of continuous operation at 60 °C. The produced αG1P could be conveniently purified by yeast treatment and, recovered in crystalline form with a yield of 86 %.

This is the first time that a continuous production process with SP is described at elevated temperatures. Enzymatic synthesis of αG1P with the immobilized SP from *Leuconostoc mesenteroides* has been reported previously, but all these processes were carried out at 30 or 37 °C in contrast with the 60 °C reported here[52, 64-66]. This process can thus serve as proof of principle for the development of other glycosyl transfer reactions catalyzed by immobilized SP at the industrial scale. Indeed, the procedures reported here can be easily scaled-up, as is nicely illustrated by the established use of immobilized glucose isomerase in a similar packed-bed reactor[67].

5 MATERIALS & METHODS

5.1 Materials

Amino-epoxy (EC-HFA) Sepabeads were kindly provided by Resindion S.R.L (Mitsubishi Chemical Corporation). Instant baker's yeast was purchased from Algist Bruggeman. All other chemicals were analytical grade and purchased from Sigma-Aldrich.

5.2 Enzyme production and purification

E. coli XL10-Gold cells were used for transformation with the constitutive expression plasmid pCXshP34_BaSP[68]. The resulting strain was cultivated in 1 L shake flasks incubated at 37 °C using LB medium (10 g/L tryptone, 5 g/L yeast extract, 5 g/L NaCl, pH 7.0) supplemented with 100 mg/L ampicillin. After 8 h of growth and expression, the

cells were harvested by centrifugation (10 000 g, 4 °C, 20 min), and frozen until further use. Cell extracts were prepared by treatment of frozen pellets with the EasyLyse Bacterial Protein Extraction Solution (Epicentre). Subsequently, cell debris was removed by centrifugation (18 000 g, 4 °C, 30 min). The crude enzyme preparation was heat purified by incubation at 60 °C for 1 h, followed by centrifugation (18 000 g, 4 °C, 30 min). Alternatively, the *N*-terminal His_6-tagged protein was purified by nickel-nitrilotriacetic acid (Ni-NTA) metal affinity chromatography, as described by the supplier (Qiagen).

5.3 Enzyme immobilization

Unless stated otherwise, immobilization was performed by adding 0.1 g Sepabeads EC-HFA to 5 mL of a SP solution (0.8 U/mL) containing 500 mM sucrose in 40 mM phosphate buffer at pH 7.2. The mixture was incubated during 22 h at 25 °C and gently stirred at 150 rpm. After immobilization, the resin was washed intensively with 100 mM phosphate buffer at pH 7.0. The immobilization yield is defined as the ratio of the activity detected on the Sepabeads and the activity present in the original enzyme solution. Recycling of the beads was evaluated by performing consecutive batch reactions of 1 hour at 60 °C. To that purpose, 4 U of either His-tag purified or heat purified SP were offered to Sepabeads EC-HFA at the same protein:resin ratio. The obtained biocatalysts were allowed to react with 25 mL substrate consisting of 400 mM sucrose in 400 mM phosphate buffer at pH 7.0 in a Thermoshaker (Eppendorf) at 750 rpm and 60 °C. The biocatalysts were recovered by sedimentation and washed five times with 100 mM phosphate buffer at pH 7.0 in between reaction cycles.

5.4 Activity assays

The activity of the free enzyme was determined discontinuously by measuring the release of the reducing sugar fructose from the non-reducing substrate sucrose with the bicinchoninic acid (BCA) method[69]. One unit (U) of activity was defined as the amount of enzyme that releases 1 µmol of fructose per minute from a 100 mM phosphate buffer containing 100 mM sucrose at pH 7.0 and 37 °C. The activity of immobilized SP was determined by adding the total amount of washed immobilized enzyme (0.1 g) into 40 mL substrate solution. The mixture was incubated in a thermoshaker (Eppendorf) with

constant shaking (750 rpm) at 37 °C and samples were analyzed with the BCA method. The ratio of hydrolysis over phosphorolysis was determined by measuring the release of glucose and αG1P in parallel. The former was determined with the glucose oxidase/peroxidase assay[70], and the latter with a coupled enzymatic assay based on the action of phosphoglucomutase (PGM) and glucose-6-phosphate dehydrogenase (G6P-DH)[71, 72]. The assay solution consisted of 2 mM EDTA, 10 mM $MgSO_4$, 2 mM β-NAD, 10 µM glucose-1,6-bisphosphate, 1.2 U PGM, 1.2 U G6P-DH and 100 mM sucrose in 100 mM phosphate buffer at pH 7.0 and 37 °C. All reported errors correspond to the standard errors.

5.5 Thermal stability assay

The immobilized enzyme was placed in 100 mM phosphate buffer at pH 7.0 and incubated at 60 °C in a thermoshaker (Eppendorf) with constant shaking (750 rpm). After 16 h, the remaining activity was determined using the BCA method.

5.6 Continuous production of αG1P

About 4000, 2000 and 1000 U of heat purified SP were immobilized on 36, 18 and 9 mL Sepabeads EC-HFA, respectively. The obtained immobilized biocatalysts were packed in three identical columns (diameter of 1.4 cm, volume of 50 mL), equipped with a water jacket at 60 °C. The packing height of the columns was 23.4, 11.7 and 5.8 cm respectively. The columns were equilibrated with 400 mM phosphate buffer, pH 7.0. The substrate solution contained 400 mM sucrose in 400 mM phosphate buffer at pH 7.0, and was brought to reaction temperature (60 °C) through incubation in a water bath. The temperature of the effluent was monitored. The solution was pumped through each packed bed at a constant flow rate of 0.75 mL/min delivered by a MasterFlex pump (type 77521). At regular intervals, 1 mL samples were analyzed on a Varian ProStar HPLC using an aminex HPX-87H column (Bio-Rad) at 30 °C. The eluent consisted of 5 mM H_2SO_4 in milliQ at a flow rate of 0.6 mL/min. Adequate detection was achieved with a refractive index detector.

5.7 Purification and crystallization of αG1P

The product was purified by removal of sucrose, fructose and glucose by treatment with baker's yeast (20 g/L) for 8 h at 30 °C. At certain times, 1 mL samples were analyzed by HPLC, as described above. If required, phosphate was precipitated by the addition of magnesium acetate and ammonia[63]. Biomass and precipitated phosphate were removed by filtration through a Seitz EKS filter. The filtrate was brought to a pH of 7.0 and was subsequently concentrated in a rotary evaporator (Büchi, Rotavapor R-134) at 60 °C to a brix of 45 (measured with an Atago hand refractometer). The solution was then slowly cooled to 0 °C over a period of 4 h, and incubated overnight on ice to promote crystal growth. Finally, the crystals were filtered through Whatman paper, washed with ethanol and dried overnight at 70 °C in an oven.

6 SUPPLEMENTARY INFORMATION

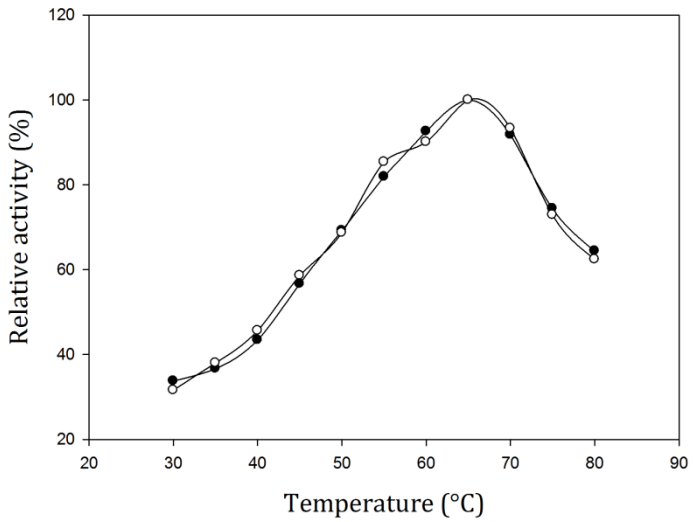

Figure S1.1 Thermoactivity of His-tag (●) and heat purified (○) SP. Experiments were performed with 100 mM sucrose in a 100 mM phosphate buffer at pH 7.0.

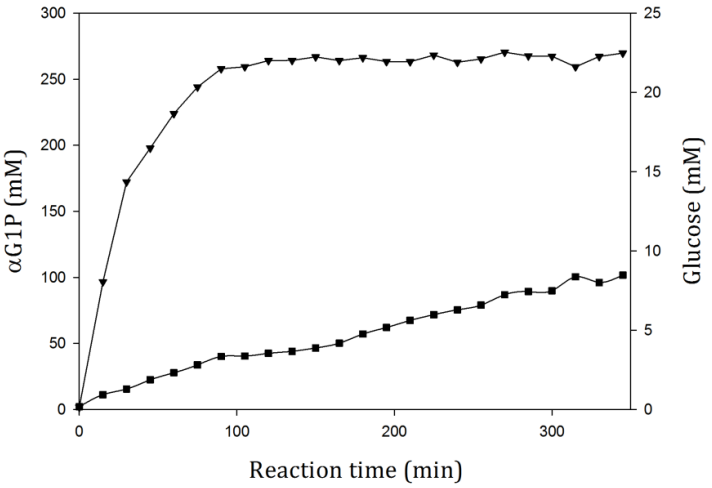

Figure S1.2 Phosphorolysis and hydrolysis catalyzed by free SP originating from *B. adolescentis*. Experiments were performed with 2.5 U/mL enzyme and 400 mM substrate at pH 7.0 and 60 °C. Both the release of αG1P (▼) and glucose (■) were followed in time.

CHAPTER 2

An imprinted cross-linked enzyme aggregate (iCLEA) of sucrose phosphorylase: combining improved stability with altered specificity

This chapter has been published as:

K. De Winter, W. Soetaert and T. Desmet, **2012**, An imprinted cross-linked enzyme aggregate (iCLEA) of sucrose phosphorylase: Combining improved stability with altered specificity, *International Journal of Molecular Sciences*, 13, 11333-11342.

1 ABSTRACT

The industrial use of sucrose phosphorylase (SP), an interesting biocatalyst for the selective transfer of α-glucosyl residues to various acceptor molecules, has been hampered by a lack of long-term stability and low activity towards alternative substrates. Recent research indicated that the stability of the SP from *Bifidobacterium adolescentis* can be significantly improved by immobilization on Sepabeads or the formation of a cross-linked enzyme aggregate (CLEA). In this chapter, it is shown that the transglucosylation activity of such a CLEA can also be improved by molecular imprinting with a suitable substrate. To obtain proof of concept, SP was imprinted with α-glucosyl glycerol and subsequently cross-linked with glutaraldehyde. As a consequence, the enzyme's specific activity towards glycerol as acceptor substrate was increased two-fold while simultaneously providing an exceptional stability at 60 °C. This procedure can be performed in an aqueous environment and gives rise to a new enzyme formulation called iCLEA.

2 INTRODUCTION

Sucrose phosphorylase catalyzes the reversible phosphorolysis of sucrose into α-D-glucose 1-phosphate (αG1P) and D-fructose (CHAPTER 1). Although it is formally classified as a glycosyl transferase (EC 2.4.1.7), the enzyme belongs to the glycoside hydrolase family 13[73] and follows the typical double displacement mechanism of retaining glycosidases[74]. The crystal structure of the enzyme from *Bifidobacterium adolescentis* has been determined and consists of a $(\beta/\alpha)_8$ barrel containing Asp192 (nucleophile) and Glu232 (acid/base) as catalytic residues[75]. Besides the synthesis of αG1P (CHAPTER 1), SP can be employed for the transfer of glucose to a wide variety of carbohydrates as well as non-carbohydrate molecules[55]. For example, an exceptionally efficient process for the production of α-glucosyl glycerol (αGG) has been developed with SP[40, 56]. The product is a moisturizing agent for cosmetics and is commercially available under the tradename Glycoin.

Unfortunately, the use of SP as industrial biocatalyst has been limited by a lack of long-term stability and low activity on alternative substrates[76, 77]. Very recently, however, significant improvements in the thermostability of the SP from *B. adolescentis* have been realized by immobilization on Sepabeads (CHAPTER 1)[44], formation of a cross-linked enzyme aggregate (CLEA)[45, 78] and introduction of specific mutations[79]. In contrast, an enzyme with a modified specificity has not yet been reported, although studies aiming to alter the acceptor specificity of SP by protein engineering have revealed insight into the glycosylation mechanism[80] and succeeded to suppress the hydrolytic activity without affecting the ability of phenolic compounds to act as acceptor[81].

Molecular imprinting is an attractive alternative to mutagenesis for the manipulation of enzymatic properties[82]. Indeed, the three-dimensional structure of a protein can be modified by noncovalent interactions with an imprinting molecule in mild denaturing conditions[83]. Unfortunately, imprinted enzymes are only able to maintain their new conformation when transferred to a non-aqueous environment or when immobilized by cross-linking[84, 85]. For the latter strategy, a radical polymerization procedure has been reported that requires transfer to organic solvents and derivatization of the enzyme[86-88].

In this chapter, the molecular imprinting of the SP from *B. adolescentis* using cross-linking by glutaraldehyde[78] instead of radical polymerization in pure organic solvents, is described. Indeed, the use of an aqueous environment yields a considerably simpler imprinting procedure resulting in an imprinted cross-linked enzyme aggregate (iCLEA) exhibiting altered acceptor specificity as well as excellent stability at 60 °C.

3 RESULTS & DISCUSSION

3.1 Production of iCLEAs

For the preparation of the imprinted cross-linked enzyme aggregate (iCLEA), the stabilized LNFI variant of the SP from *B. adolescentis* was used[79]. The enzyme was recombinantly expressed in *E. coli* and partially purified by means of heat treatment, which has shown to remove the contaminating phosphatase activity[45]. The next steps in the preparation of the iCLEA then consist of imprinting, followed by precipitation (Figure 2.1).

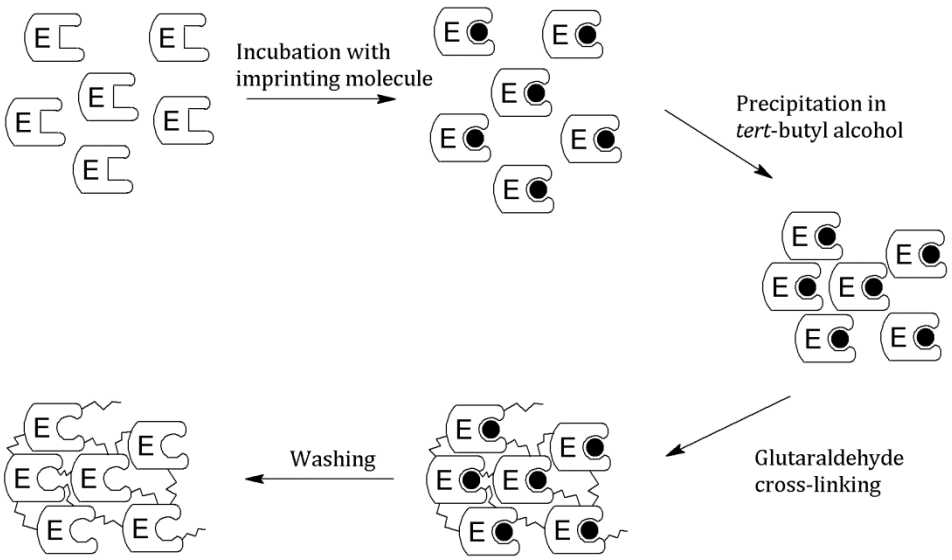

Figure 2.1 General scheme for the production of imprinted cross-linked enzyme aggregates (iCLEAs).

To that end, the precipitation of SP in the presence of a number of possible imprinting molecules was first evaluated (Table 2.1). Previous research has identified *tert*-butyl alcohol as the precipitant of choice[45]. However, the presence of phosphate or αG1P (100-500 mM) resulted in the appearance of a second phase upon addition of *tert*-butyl alcohol, excluding these molecules from use as imprinters. Also, addition of sucrose in a

concentration higher than 200 mM was found to inhibit the precipitation of SP, whereas glycerol and αGG did not affect precipitation. Clearly, these results indicate the importance of evaluating precipitation thoroughly, prior to the production of an iCLEA.

Table 2.1 Precipitation of SP in the presence of different imprinting molecules. Precipitation was achieved by adding 6 mL *tert*-butyl alcohol to 4 mL enzyme solution under agitation at 4 °C.

Imprinting molecule	[C][a] (M)	Precipitation (%)	$SP_{residual}$[b] (%)
None	/	97.8	1.2
Sucrose	0.2	96.4	1.6
Sucrose	0.5	52.1	38.5
Sucrose	1	40.6	56.8
Glycerol	0.5	98.2	1.1
Glycerol	1	96.6	1.3
Glycerol	2	97.6	1.4
Sucrose + glycerol	0.5 + 2	68.9	25.6
Sucrose + glycerol	0.2 + 2	96.6	1.5
αGG	0.2	97.3	1.4

[a] of the imprinting molecules; [b] after precipitation.

Finally, the aggregated enzyme molecules were chemically cross-linked with glutaraldehyde to obtain the corresponding immobilizates. A typical immobilization yield of 30 % has been reported for SP[45], and this value was also obtained in the presence of glycerol or αGG. However, the addition of sucrose during precipitation was found to increase the immobilization yield by roughly 10 %. This result is in accordance with work published by Wang and collaborators, who reported a sugar-assisted precipitation strategy to increase the activity of a Penicillin G Acylase CLEA[89].

The specificity of the obtained formulations was then examined and compared with that of a non-imprinted CLEA. More specifically, their activity towards phosphate (phosphorolysis) and glycerol (transglucosylation) as acceptor was determined (Figure 2.1).

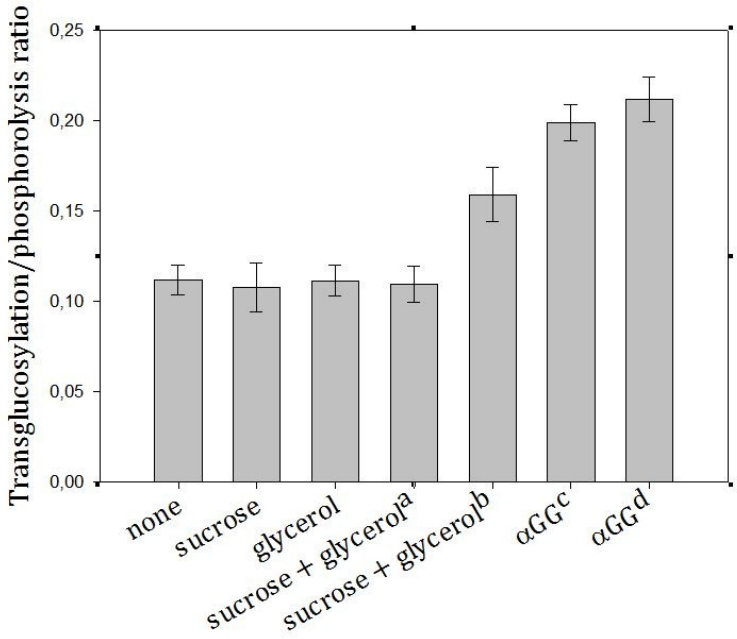

Figure 2.2 Transglucosylation/phosphorolysis ratio for different CLEA formulations. [a] Cross-linking was initiated upon addition of the imprinting molecules. [b] Cross-linking was initiated after 30 min incubation. [c] 200 mM αGG was used. [d] 1 M αGG was used.

Imprinting with sucrose, glycerol or a combination of both was found to have no influence on the specificity of the enzyme preparation. However, initiating aggregation and cross-linking after 30 min incubation with sucrose and glycerol did significantly increase the transglucosylation activity. This must mean that the presence of glycosylated product is required to modify the enzyme's acceptor specificity. Indeed, imprinting with 200 mM αGG (enzyme/αGG ratio ≅ 1:11 000) almost doubled the specific activity on glycerol, from 2.22 U/mg for the non-imprinted CLEA to 4.12 U/mg for the iCLEA. Increasing the αGG concentration to 1 M (enzyme/αGG ratio ≅ 1:55 000) during imprinting, however, did not significantly improve the acceptor specificity much further.

3.2 Characterization of the iCLEAs

When SP is used for transglucosylation reactions, both primary and secondary hydrolysis can decrease the atom economy[27, 55]. Although αGG itself is a very poor substrate, hydrolysis of sucrose can be quite significant and even lead to the formation of inhibiting products[40, 90]. Therefore, the hydrolytic activity of the CLEA and iCLEA were examined in the presence of sucrose and glycerol as substrates. Hydrolysis was found to

be identical for both biocatalysts, meaning that the ratio with transglucosylation is only half as high for the iCLEA than for the CLEA. To further asses its applicability in carbohydrate conversions, the thermostability of the iCLEA preparation was evaluated by incubation at 60 °C and measuring the residual activity at several points in time (Figure 2.3).

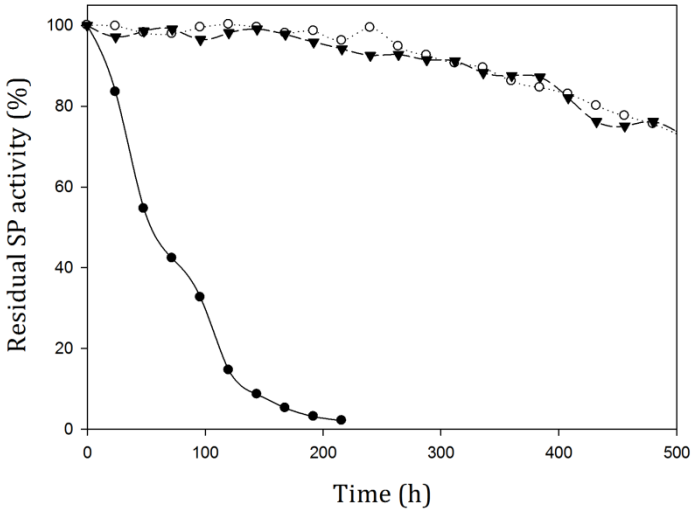

Figure 2.3 Stability of different SP formulations at 60°C. The residual activity of soluble SP (●), CLEAs (○) and iCLEAs (▼) was measured every 24 h.

The iCLEA was found to exhibit a comparable thermostability to the non-imprinted CLEA, and thus to be drastically more stable than the soluble enzyme. Indeed, an impressive 75 % of the initial activity was still present after three weeks incubation at 60 °C. Next, the efficiency of the newly formed iCLEA was demonstrated by comparing its performance with that of the reference CLEA in a batch production of αGG at 60 °C (Figure 2.4). This clearly showed that the maximal transfer yield of 84 %[40] could be reached twice as fast with the iCLEA compared to its non-imprinted counterpart. Furthermore, the newly formed iCLEA also proved its excellent operational stability by losing no activity during five consecutive batch conversions.

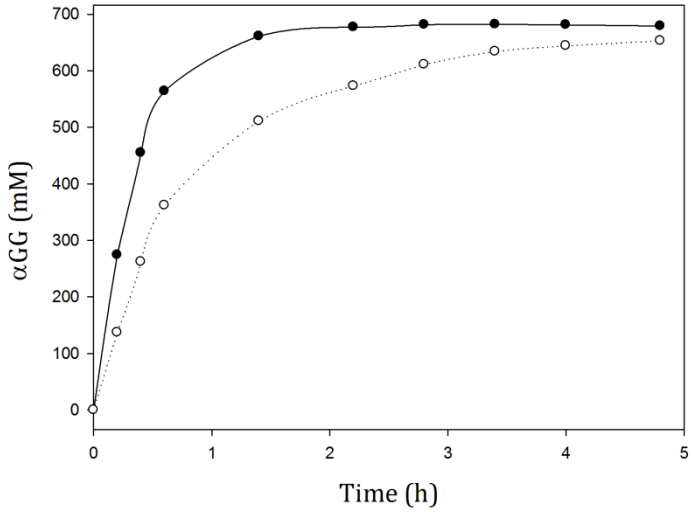

Figure 2.4 Synthesis of αGG with immobilized SP at 60 °C. The conversions were performed with 5 mg/mL CLEAs (○) or iCLEAs (●) in a 50 mM MOPS buffer pH 7.0 containing 800 mM sucrose and 2 M glycerol.

4 CONCLUSION

Although molecular imprinting of a cross-linked enzyme aggregate (iCLEA) has been described for improving the activity of the hydroxynitrile lyase from *Linum usitatissimum*[91], this is the first time it is used to alter the transglycosylation specificity of a biocatalyst. As proof of concept, sucrose phosphorylase was imprinted with α-glucosyl glycerol and subsequently cross-linked with glutaraldehyde. As a result, the enzyme's specificity towards glycerol as acceptor was increased two-fold. Furthermore, the obtained biocatalyst was extremely stable, and could be used for an industrially relevant production process at 60 °C. This convenient procedure thus allows to simultaneously improve stability and specificity, and could find widespread application in the field of enzyme engineering.

5 MATERIALS & METHODS

5.1 Materials

Glucosyl glycerol was produced as previously described[40]. *Tert*-butyl alcohol, glutaraldehyde, and sodium borohydride were purchased from Aldrich-Chemie, Fisher and Acros, respectively. All other reagents were analytical grade and purchased from Sigma-Aldrich.

5.2 Enzyme production and purification

E. coli BL21 (DE3) (Novagen) cells were used for transformation with the constitutive expression plasmid pCXshP34_BaSP_LNFI[68, 79]. The resulting strain was routinely grown in 50 mL LB medium (CHAPTER 1). After overnight growth, the culture was inoculated into 1 L of double LB medium (20 g tryptone/L, 10 g yeast extract/L, 5 g NaCl/L; pH7.0) supplemented with 30 g/L glucose and 100 mg/L ampicillin in a 2 L Biostat M reactor (B. Braun Biotech Inc). Fermentation was done at 37 °C and 550 rpm with aeration at 1.2 vvm. When necessary, antifoam was added manually to prevent foaming. After approximately 8 h of growth (OD_{600} ~ 25), the cells were harvested by centrifugation (10 000 g, 4 °C, 20 min). The obtained pellets were frozen at -20 °C until further use.

Cell extracts were prepared by treatment of frozen pellets with 50 mM MOPS pH 7.0 supplemented with 1 mg/mL lysozyme for 30 min at room temperature, followed by 2 x 2 min sonification (Branson 250 Sonifier, level 3, 50 % duty cycle). Subsequently, cell debris was removed by centrifugation (18 000 g, 4 °C, 30 min). Finally, the crude enzyme preparation was heat purified by incubation at 60 °C for 60 min as described in CHAPTER 1.

5.3 Preparation of the iCLEA

The heat purified SP enzyme was diluted to a final protein concentration of 2 mg/mL and allowed to react with the imprinting molecules for 30 min at 37 °C. Next, 6 mL of *tert*-butanol was added to 4 mL of the imprinted SP solution under agitation. After 30 min, 1.36 mg glutaraldehyde was gently added to cross-link the enzyme aggregate, and the mixture was kept under stirring for 60 min. Reduction of the formed imine bonds

was achieved by adding 10 mL of a solution containing 1 mg/mL sodium borohydride in 0.1 M sodium bicarbonate buffer at pH 10.0. After 15 min, another 10 mL was added and allowed to react for 15 min. Finally, the iCLEA was harvested by centrifugation (10 000 g, 4 °C, 30 min) and washed five times with 50 mM MOPS buffer at pH 7.0. All steps were performed in a thermoshaker (Eppendorf) at 750 rpm and 4 °C. The immobilization yield is defined as the ratio of the activity detected in the iCLEA preparation to that present in the original enzyme solution.

5.4 Activity assays

Phosphorolysis of sucrose was measured discontinuously with an enzymatic assay, in which the production of αG1P is coupled to the reduction of NAD^+ in the presence of phosphoglucomutase and glucose-6-phosphate dehydrogenase[72]. The reactions were analyzed by inactivation of samples (5 min at 95 °C) at regular intervals, followed by measurement of the absorbance at 340 nm in a microplate reader 680XR (Bio-Rad). One unit of phosphorolysis activity corresponds to the release of 1 µmol fructose per minute from 100 mM sucrose in 100 mM phosphate buffer at pH 7.0 and 37 °C.

The transglucosylation activity of SP towards glycerol was determined indirectly by measuring the increase in reducing sugars. More specifically, the release of fructose (and glucose) from sucrose as donor substrate was determined discontinuously with the BCA method (CHAPTER 1). In parallel, the release of glucose through hydrolysis was determined discontinuously with the glucose oxidase/peroxidase assay (CHAPTER 1). When glucose was detected, its concentration was subtracted twice from the concentration of reducing sugars measured with the BCA method, to calculate the net transglucosylation activity. One unit of transglucosylation activity corresponds to the production of 1 µmol αGG per minute from 800 mM sucrose and 2 M glycerol in 50 mM MOPS buffer at pH 7.0 and 60 °C.

Alternatively, the concentration of αGG was determined directly by HPLC analysis using an aminex HPX-87C column (Bio-Rad) with milliQ water as the mobile phase at a constant flow rate of 0.6 mL/min and 85 °C. The hydrolytic activity was quantified using 50 mM donor and 65 mM acceptor, which is identical to the conditions used to assess the transglucosylation potential of SP[77]. Protein concentrations were measured

according to the Lowry method[92], using bovine serum albumin as standard. All reported errors correspond to the standard errors.

5.5 Stability assays

The thermostability of the iCLEAs was determined by incubation in 50 mM MOPS buffer pH 7.0 in a water bath at 60 °C. Every 24 h, samples were taken and the residual activity was analyzed using the BCA method. In addition, the operational stability was evaluated by using the iCLEAs for consecutive batch conversions of 800 mM sucrose and 2 M glycerol at 60 °C. After each reaction, the iCLEAs were recuperated by centrifugation (10 000 g, 4 °C, 30 min) and washed three times with 50 mM MOPS buffer at pH 7.0.

CHAPTER 3

Ionic liquids as cosolvents for glycosylation by sucrose phosphorylase: balancing acceptor solubility and enzyme stability.

This chapter has been published as:

K. De Winter, K. Verlinden, V. Kren, L. Weignerova, W. Soetaert and T. Desmet, **2013**, Ionic liquids as cosolvents for glycosylation by sucrose phosphorylase: balancing acceptor solubility and enzyme stability, *Green Chemistry*, 15, 1949–1955.

1 ABSTRACT

Over the past decade, disaccharide phosphorylases have received increasing attention as promising biocatalysts for glycoside synthesis. Unfortunately, these enzymes typically have a very low affinity for non-carbohydrate acceptors, which urges the addition of cosolvents to increase the dissolved concentration of these acceptors. However, commonly applied solvents such as methanol and dimethyl sulfoxide (DMSO) are not compatible with many intended applications of carbohydrate-derived products. In this chapter, the solubility of a wide range of relevant acceptors was assessed in the presence of ionic liquids (ILs) as alternative and 'green' solvents. The IL AMMOENG 101 was found to be the most effective cosolvent for compounds as diverse as medium- and long-chain alcohols, flavonoids, alkaloids, phenolics and terpenes. Moreover, this IL was shown to be less deleterious to the stability and activity of sucrose phosphorylase than the commonly used dimethyl sulfoxide. To demonstrate the usefulness of this solvent system, a process for the resveratrol glycosylation was established in a buffer containing 20 % AMMOENG 101, 1 M sucrose and saturated amounts of acceptor. A single regioisomer 3-*O*-α-D-glucopyranosyl (*E*)-resveratrol was obtained as proven by NMR spectroscopy.

2 INTRODUCTION

Glycosylation of small molecules can substantially improve their physicochemical and biological properties, thereby extending their application potential in various industries[10, 19, 23, 93]. Prominent examples include the increased solubility of therapeutic flavonoids[94], the prolonged stability of ascorbic acid in cosmetic formulations[95], and the modified perception of flavors and fragrances[12]. Despite the continuous development of new procedures, chemical synthesis of glycosides still suffers from low yields because of the need for (de)protection and activation steps[13, 15]. Biocatalytic approaches are, therefore, an attractive alternative that enables one-step reactions with high regio- and stereoselectivity[18]. Enzymatic glycosylation reactions typically generate 5-fold less waste and have a 15-fold higher space-time yield, which is a tremendous improvement in the eco-efficiency[19].

Currently, few enzymes are available to perform glycosylation reactions cost-efficiently at the industrial scale[96]. On the one hand, glycosyl transferases (GT) require nucleotide-activated sugars that are relatively expensive[97] and glycoside hydrolases (GH) suffer from low yields when used in the synthetic direction[27]. Consequently, disaccharide phosphorylases have received increasing attention in recent years as promising biocatalysts for glycoside synthesis[29, 98, 99]. These enzymes catalyze the reversible phosphorolysis of glycosidic bonds, and thus only require a glycosyl phosphate as donor substrate for synthetic reactions.

Unfortunately, disaccharide phosphorylases typically have a very low affinity (K_m > 1 M) for non-carbohydrate acceptors[77, 100]. The catalytic efficiency of sucrose phosphorylase (SP) towards such compounds is usually not significantly higher than the contaminating hydrolytic activity[77]. Nevertheless, an efficient process for the production of 2-*O*-(α-D-glucopyranosyl) *sn*-glycerol has been developed with this enzyme by careful optimization of the substrate concentrations[40, 101]. Moreover, it was shown in CHAPTER 2 that the efficiency of the SP biocatalyst could be further increased by molecular imprinting. For hydrophobic acceptors like flavonoids and other polyphenols, however, concentrations compensating for the high K_m values are not readily achieved in aqueous solutions. Enzymatic glycosylation of these compounds is, therefore, commonly

performed in the presence of organic cosolvents, such as DMSO or methanol. However, these solvents are not compatible with numerous applications of carbohydrate-derived products[102], and their presence can lead to the partial inactivation of the biocatalyst[33, 77, 79].

Ionic liquids (ILs) have emerged recently as a completely new class of solvents for biocatalytic applications[103, 104]. These green solvents consist of salts with a low melting point (<100 °C) that possess no vapor pressure and are inflammable[105]. Due to their ability to dissolve both polar and hydrophobic substrates, ILs have been successfully applied for the synthesis of glycosidic compounds[106-109]. For example, the yield for the galactosylation of *N*-acetylglucosamine with β-galactosidase from *Bacillus circulans* could be doubled upon addition of 25 % [MMIM][$MeSO_4$][105]. However, no attention has yet been paid to the use of ILs as cosolvents for disaccharide phosphorylases.

In this chapter, the stability and activity of the SP from *Bifidobacterium adolescentis* was evaluated in the presence of various ILs, and the solubility of relevant acceptors in these systems was determined.

3 RESULTS & DISCUSSION

3.1 Solubility of acceptors in IL cosolvent systems

The enzymatic glycosylation of hydrophobic compounds is complicated by their low solubility in aqueous systems[9, 33]. Therefore, the effect of various ILs (Figure S3.2) on solubility was evaluated, and compared with that of conventional cosolvents at a concentration of 20 % (Table 3.1). Optimal values (pH 6.5 and 60 °C) for the sucrose phosphorylase from *B. adolescentis*[44] were used. Furthermore, the influence of sucrose (1 M) was also assessed, since this substrate serves as glycosyl donor for SP and will thus be present during the actual reactions. The initial screening was performed with resveratrol and quercetin as target compounds with powerful anti-oxidant and anti-inflammatory properties, but a very low solubility in water[110-112].

Table 3.1 Solubility at pH 6.5 and 60 °C, in the presence of 20 % cosolvent and 1 M sucrose.

	Solubility resveratrol (mM)		Solubility quercetin (mM)	
Solvent	- sucrose	+ sucrose	- sucrose	+ sucrose
Water	0.2 ± 0.1	2.4 ± 0.3	< 0.1	< 0.1
MeOH	2.2 ± 0.2	5.8 ± 0.6	0.2 ± 0.1	0.4 ± 0.1
DMSO	37.5 ± 2.9	46.3 ± 3.8	9.4 ± 0.9	12.1 ± 1.1
Tween 20	44.5 ± 3.3	56.1 ± 4.2	10.5 ± 1.1	11.8 ± 2.0
Triton X-100	11.5 ± 1.3	18.6 ± 0.9	1.6 ± 0.2	2.2 ± 0.4
[MMIM] [$MeSO_4$]	13.8 ± 1.3	15.4 ± 0.8	0.5 ± 0.1	0.5 ± 0.2
[BMIM][BF_4]	10.1 ± 1.2	12.6 ± 1.1	0.4 ± 0.1	0.5 ± 0.2
[BMIM][dca]	11.8 ± 1.6	16.4 ± 1.8	0.5 ± 0.1	0.6 ± 0.1
[BMIM][I]	39.5 ± 3.2	47.3 ± 3.9	0.8 ± 0.2	1.2 ± 0.3
[EMIM][$EtSO_4$]	14.6 ± 1.2	18.1 ± 1.4	0.6 ± 0.1	0.9 ± 0.1
[EMIM][dca]	130.4 ± 9.8	145.1 ± 11.6	1.5 ± 0.2	1.8 ± 0.4
AMMOENG 101	246.6 ± 15.2	286.5 ± 12.9	21.2 ± 1.1	24.9 ± 2.0

As expected, only traces of resveratrol or quercetin could be dissolved in the cosolvent-free system. The addition of 20 % ILs resulted in a remarkable increase in solubility, without affecting the ability to dissolve 1 M sucrose. All ILs easily outranked methanol as cosolvent. Furthermore, both [EMIM][dca] and AMMOENG 101 proved to better dissolve resveratrol compared to DMSO, which was recently used for the enzymatic synthesis of resveratrol glucosides[9]. The nature of the anion as well as the cation appears to be important for the imidazolium-based ILs, which is in agreement with previous observations[102, 113]. Interestingly, the presence of 1 M sucrose was found to further increase the solubility, although the effect was rather limited in most cases. The highest solubility was obtained when using AMMOENG 101 (Figure 3.1), an ethoxylated quaternary ammnonium salt manufactured by Solvent Innovation. This IL, also commercialized by Evonik Industries as TEGO K5, has already been used to capture carbon dioxide from fuel gas streams[114], and to solubilize water-insoluble ketones[115].

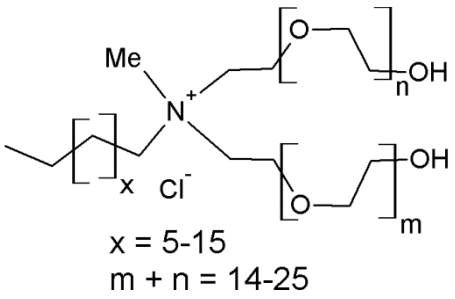

Figure 3.1 Chemical structure of the ethoxylated quaternary ammnonium salt AMMOENG 101.

The solubilizing properties of AMMOENG 101 were then examined in more detail, by varying the amount of cosolvent added (Figure 3.2). As could be expected, increasing the concentration of IL resulted in an increased solubility of the acceptors. However, a maximum was observed at 60 % AMMOENG 101, after which the solubility decreased. Resveratrol could be dissolved up to an impressive 2 M, whereas the highest solubility of quercetin was found to be 0.2 M.

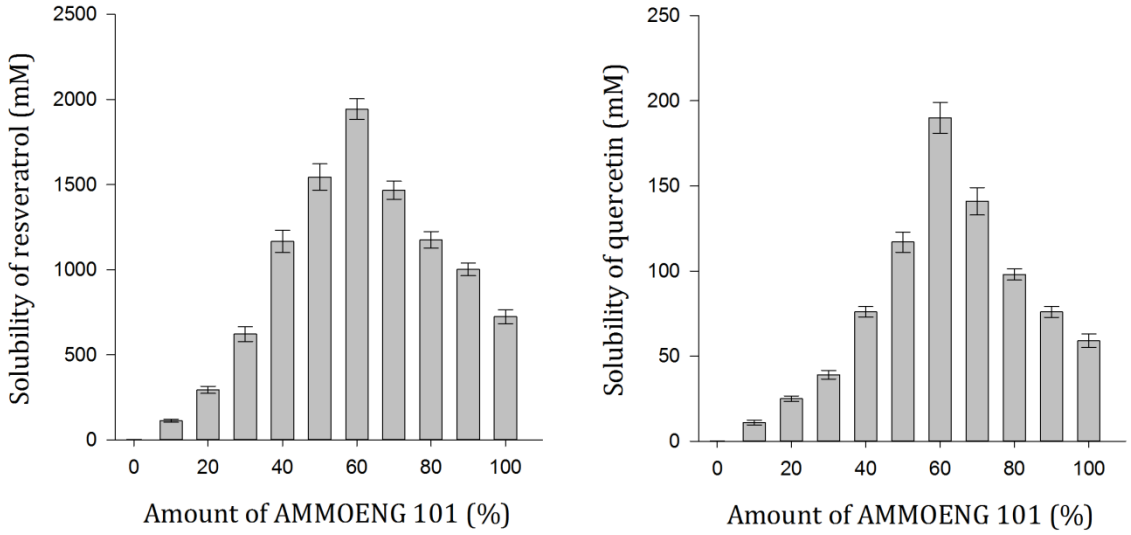

Figure 3.2 Solubility at pH 6.5 and 60 °C in the presence of various concentrations of AMMOENG 101.

Finally, the solubility of other glycosylation acceptors was determined in both DMSO and AMMOENG 101 cosolvent systems (Table 3.2). Based on their structure, these acceptors can be divided into five classes, i.e. flavonoids, medium- and long-chain alcohols, terpenes, alkaloids and phenolics. The addition of a cosolvent enhanced the solubility of all of them but the IL was remarkably more efficient than DMSO. For example, the

solubility of sparingly soluble substances such as curcumin and dodecanol could be increased to 46 mM and 510 mM, respectively, by the addition of 40 % AMMOENG 101. The same condition resulted in a tenfold increased solubility of 3-hydroxy-2-nitropyridine and cinnamyl alcohol. Solubility of hexanol and geraniol was increased by two orders of magnitude, resulting in a concentration of 3.1 M for the former. In conclusion, the IL was found to boost the solubility of various chemicals, from rather hydrophilic to very hydrophobic, regardless of their type.

Table 3.2 Solubility of various compounds at 60 °C in a 50 mM MES buffer at pH 6.5 containing 20 and 40 % DMSO and AMMOENG 101 respectively.

Compound	Solubility (mM)				
	Buffer	DMSO		AMMOENG 101	
		20 %	40 %	20 %	40 %
Resveratrol	0.2 ± 0.1	37.5 ± 2.9	97.5 ± 6.9	246 ± 15	1166 ± 95
Quercetin	< 0.1	9.4 ± 0.9	22.1 ± 1.3	21.2 ± 1.1	76.5 ± 5.2
Curcumin	< 0.1	8.2 ± 0.5	19.1 ± 1.1	13.5 ± 0.8	45.9 ± 1.8
Dodecanol	1.3 ± 0.2	3.6 ± 0.2	18.1 ± 1.7	268 ± 18	508 ± 39
Hexanol	6.3 ± 0.8	12.3 ± 0.9	31.1 ± 2.2	1664 ± 106	3108 ± 159
Geraniol	4.3 ± 0.3	9.3 ± 0.3	19.1 ± 1.4	403 ± 26	1861 ± 94
Linalool	5.2 ± 0.6	7.3 ± 0.4	16.1 ± 1.2	294 ± 18	1130 ± 82
3-Hydroxypyridine	255 ± 20	457 ± 26	923 ± 68	654 ± 51	1395 ± 109
3-Hydroxy-2-nitropyridine	261 ± 18	602 ± 54	1356 ± 96	968 ± 63	2652 ± 153
Saligenin	352 ± 16	409 ± 11	920 ± 48	721 ± 52	2560 ± 192
Salicylic acid	7.3 ± 0.7	61.8 ± 3.6	162 ± 12	271 ± 21	854 ± 66
Vanillyl alcohol	70.4 ± 5.9	452 ± 11	796 ± 66	817.3 ± 75.6	1018 ± 72
Cinnamyl alcohol	17.4 ± 1.3	40.6 ± 2.9	137 ± 9	937 ± 46	2751 ± 196
4-Nitrophenol	167 ± 12	187 ± 16	442 ± 31	642 ± 52	1219 ± 86

3.2 Stability and activity in IL cosolvent systems

Although the addition of ILs allows dissolving a wide variety of compounds, their presence could negatively affect the stability of the biocatalyst[33, 106]. Therefore, the half-life (t_{50}) of the SP from *B. adolescentis* was determined in the presence of different cosolvents (Table 3.3). In agreement with previous studies on other enzymes, [MMIM][$MeSO_4$], AMMOENG 101 and DMSO were found to be less deleterious for the stability of SP than for example [BMIM][I], [BMIM][BF_4] and methanol[106, 107, 115, 116]. Moreover, in accordance to the results in CHAPTER 1 and CHAPTER 2, the presence of sucrose appears to be a critical parameter for the enzyme's stability. Indeed, the addition of 1 M sucrose resulted in a 25-fold increased half-life when 20 % DMSO or AMMOENG 101 is present. Similar patterns were obtained with the well-known protectant trehalose,[117] which is not a substrate of SP. The results indicate that stabilization does not originate from the binding of substrate in the active site but rather from non-specific interactions at the protein surface[118, 119].

Table 3.3 Stability of SP at pH 6.5 and 60 °C, in the presence of 20 % cosolvent and 1 M sucrose.

	t_{50} (min)	
Solvent	- sucrose	+ sucrose
Water	3210 ± 126	4261 ± 192
[EMIM][$EtSO_4$]	16.0 ± 2.1	54.7 ± 3.2
[EMIM][dca]	5.1 ± 0.3	32.5 ± 2.6
[BMIM][dca]	4.8 ± 0.2	29.5 ± 1.9
[BMIM][I]	<1	2.1 ± 0.1
[BMIM][BF_4]	3.2 ± 0.1	33.8 ± 2.7
[MMIM]][$MeSO_4$]	32.6 ± 3.2	85.3 ± 6.6
AMMOENG 101	128 ± 6	3162 ± 198
DMSO	106 ± 9	2622 ±144
MeOH	3.2 ± 0.5	26.8 ± 2.4

Next, the stability of SP was determined at varying concentrations of both AMMOENG 101 and DMSO (Figure 3.3), the former being superior allowing a 24 h half-life at the concentration of 60 %, whereas such a t_{50} was already reached at a DMSO concentration of only 30 %. Activity of SP in both cosolvents was assessed as well. The enzyme displayed a relative activity of 98 and 87 % in 20 and 40 % IL, respectively, compared to 86 and 34 % in identical concentrations of DMSO. According to these results, the IL AMMOENG 101 is a much better cosolvent than the commonly used DMSO.

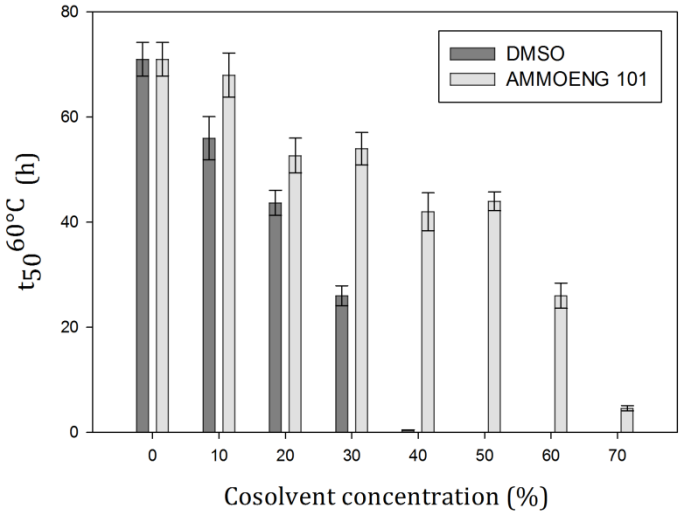

Figure 3.3 Half-life of SP at pH 6.5 and 60 °C, in the presence of 1 M sucrose and varying cosolvent concentrations.

Although the SP from *B. adolescentis* already is quite stable, a stabilized variant ('LNFI') containing 6 mutations has recently been created[79]. Furthermore, immobilized preparations of the enzyme have also been prepared, either by the covalent coupling to Sepabeads[44] or by the production of a cross-linked enzyme aggregate (CLEA)[45, 78]. All of these are known to be more thermostable than the native enzyme and they are shown here to be also more resistant to the presence of 20 % AMMOENG 101 (Figure 3.4). Indeed, the enzyme's t_{50} could be increased by about 15 and 40 h when using the LNFI variant or Sepabeads immobilizate, respectively. The CLEA was the most stable, and exhibited an impressive half-life of 100 h. These results support previous findings that thermal and solvent stability are closely related[106, 120, 121].

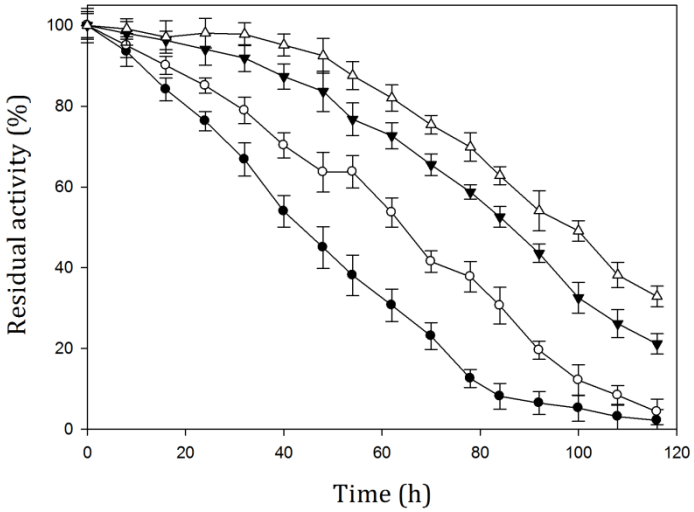

Figure 3.4 Stability of various SP formulations at 60 °C and pH 6.5, in the presence of 20 % AMMOENG 101 and 1 M sucrose. Wild-type enzyme (●), LNFI variant (○), Sepabeads immobilizate (▼) and CLEA immobilizate (Δ).

3.3 Production of glycosides in ILs

The applicability of AMMOENG 101 as cosolvent for the production of glycosides with SP was assessed using the glycosylation of resveratrol as case study (Figure 3.5). After 24 h reaction of sucrose with resveratrol saturated in 20 % AMMOENG 101, a single new peak could be observed at 8.5 min, next to the signal of resveratrol at 10.9 min (Figure 3.6).

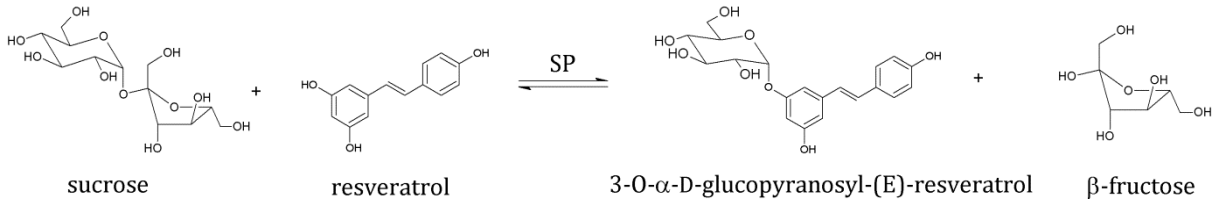

Figure 3.5 Enzymatic glucosylation of resveratrol catalyzed by thermostable SP in an ionic liquid cosolvent system.

The product was purified by silica gel chromatography, and identified as 3-*O*-α-D-glucopyranosyl (*E*)-resveratrol by NMR spectroscopy. Glycosylation of resveratrol has already been achieved with *Bacillus cereus* and *Streptococcus mutans* as whole-cell biocatalysts[122, 123]. More recently, the synthesis of a mixture of α-glucosyl derivatives using cyclodextrin glucanotransferase was described[9]. However, this is the first report

on the use of a purified enzyme for the glucosylation of resveratrol yielding a single product.

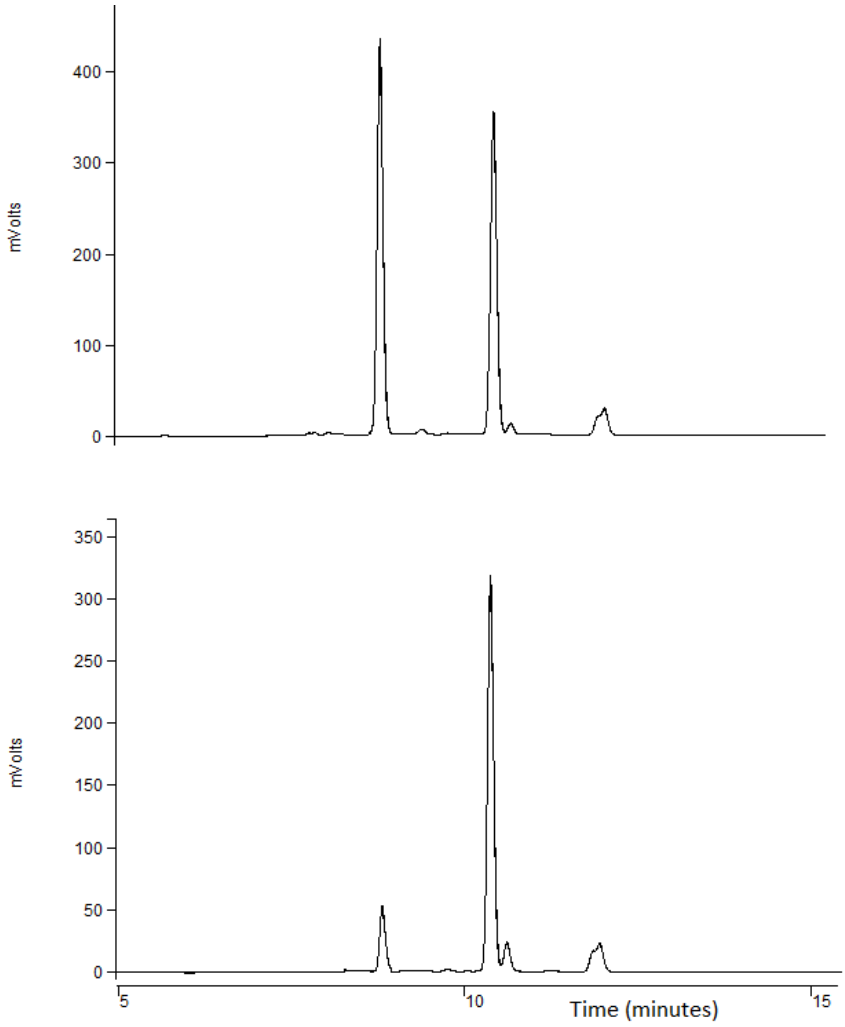

Figure 3.6 Production of α-glycosyl resveratrol (8.5 min) with SP at pH 6.5 and 60 °C, using 1 M sucrose and resveratrol (10.9 min) saturated in 20 % AMMOENG 101 (above) or DMSO (beneath) after 24 h incubation.

In contrast, about 10 times less product was formed when DMSO was used as cosolvent under optimal reaction conditions. The difference was even more pronounced with quercetin as acceptor substrate. Indeed, numerous attempts using 20 and 40 % of DMSO, DMF, methanol, ethanol and acetone as organic cosolvents failed to yield product. Only minor amounts of quercetin could be dissolved in 20 % of these solvents, whereas the addition of 40 % resulted in rapid inactivation of the enzyme. However, glycosylated products could clearly be detected when quercetin was saturated in 20 % AMMOENG

101 (Figure S3.1). In addition, the glycosylation of all compounds from Table 3.2 was evaluated using similar reaction conditions. Glucosides of hexanol, geraniol, 3-hydroxypyridine, saligenin, vanillyl alcohol and cinnamyl alcohol were observed by means of TLC analysis. These results identified the IL AMMOENG 101 as a powerful tool for glycosylation reactions with disaccharide phosphorylases, efficiently balancing acceptor solubility and enzyme stability.

4 CONCLUSION

Following the work on glycoside synthesis with SP in conventional solvents[55], this is the first report on the use of ionic liquids with disaccharide phosphorylases. The stability and activity of SP, as well as the solubility of a wide range of interesting acceptors was assessed. The results show that the solubility of flavonoids, medium- and long-chain alcohols, terpenes, alkaloids and phenolics can be improved significantly by addition of AMMOENG 101. Moreover, this IL was found to be less deleterious to the stability and activity of SP compared to organic solvents like DMSO or methanol. The presence of 1 M sucrose as a substrate significantly improves the enzyme stability in the presence of cosolvents. As proof of concept, the production of 3-*O*-α-D-glucopyranosyl (*E*)-resveratrol was demonstrated to be much more efficient in AMMOENG 101 compared to DMSO as cosolvent. Consequently, the use of ILs could find widespread application for glycoside synthesis with disaccharide phosphorylases.

5 MATERIALS & METHODS

5.1 Materials

AMMOENG 101 and amino-epoxy (EC-HFA) Sepabeads were kindly provided by Evonik Industries AG and Resindion S.R.L (Mitsubishi Chemical Corporation), respectively. The other ILs were purchased from IoLiTec Ionic Liquids Technologies GmbH, and had a purity of at least 99 %. All other chemicals were analytical grade and purchased from Sigma-Aldrich. Recombinant SP was produced and partially purified by heat treatment as described in CHAPTER 2. The immobilized SP variants were produced according to the protocols described in CHAPTER 1 and 2.

5.2 HPLC analysis

HPLC analysis was performed on a reversed phase column (Alltech Prevail C-18, 250 mm × 4.6 mm), with milliQ water (solvent A) and methanol (solvent B), both containing 0.05 % formic acid, as the mobile phase. The flow rate and temperature were set at 1.0 mL/min and 30 °C, respectively. The gradient elution was as follows: 100 % of solvent A (0 - 2 min), 0 to 90 % solvent B (2 - 20 min), 90 % solvent B (20 – 25 min), 90 to 0 % solvent B (25 – 30 min) and 100 % solvent A (30 – 38 min). Adequate detection was obtained with an Alltech 2000ES evaporative light scattering detector (ELSD) for dodecanol, hexanol, geraniol, linalool, 3-hydroxypyridine, 3-hydroxy-2-nitropyridine, saligenin and salicylic acid. The tube temperature, gas flow and gain were set at 25 °C, 1.5 L/min and 4, respectively. The other compounds were quantified using a Varian Prostar 320 UV/Vis detector at 306, 373, 335, 254, 317 and 246 nm for resveratrol, quercetin, curcumin, cinnamyl alcohol, 4-nitrophenol and vanillyl alcohol, respectively. The obtained peaks were calibrated using standard curves of the specific compounds, prepared in DMSO or methanol. All HPLC analyses were performed in triplicate.

5.3 Solubility measurements

The dissolution of all compounds in the different cosolvent systems was performed in a water bath at 60 °C with ± 0.1 °C accuracy. Varying amounts of cosolvent and sucrose were added to 50 mM MES buffer at pH 6.5, and transferred to a 10 mL falcon. Next, the desired compounds were added until clear precipitation was observed. The samples were vortexed multiple times and allowed to equilibrate for 48 h. Undissolved solids were removed by filtration through a 0.45 µm microporous membrane at the same temperature. Finally, the obtained solutions were diluted in DMSO or methanol, and subjected to HPLC analysis.

5.4 Stability assays

The thermostability of SP was determined by incubating 25 U/mL in 50 mM MES buffer at pH 6.5 in a water bath at 60 °C. If required, sucrose and cosolvents were added. At regular intervals, samples were taken and diluted 100 times in 50 mM MOPS buffer at pH 7.0. The samples were stored at 4 °C, and the activity at 37 °C was determined using the continuous αG1P assay (CHAPTER 1). The t_{50}-values were calculated from the

equations obtained by fitting the linear part of the stability curves. The stability of the immobilized biocatalysts was evaluated by incubating 1 and 15 mg of CLEAs and Sepabeads, respectively, in 300 µL 50 mM MES buffer at pH 6.5 containing 20 % IL AMMOENG 101 and 1 M sucrose. At regular intervals, samples were taken and diluted 100 times in 50 mM MOPS buffer at pH 7.0. The samples were stored at 4 °C, and the activity at 37 °C was determined using the discontinuous αG1P assay (CHAPTER 1). All reported errors correspond to the standard errors.

5.5 Production and purification of glycosides

The glycosylation of flavonoids was carried out at 10 mL scale in a 50 mM MES buffer at pH 6.5 containing 1 M sucrose and 20 % cosolvent. The substrate solutions were saturated with resveratrol or quercetin, and 50 U/mL of the SP variant 'LNFI' was added. After 24 h, the reactions were stopped by inactivation (10 min at 95 °C) and centrifuged (12 000 g, 4 °C, 15 min) to remove all particulates. Next, the supernatant was diluted, and subjected to HPLC analysis. Alternatively, the aqueous buffer was evaporated *in vacuo* and the residue was purified by column chromatography on silica gel (EtOAC/MeOH/H_2O = 30:5:4). TLC analysis (EtOAC/MeOH/H_2O = 30:5:4) was conducted on Merck Silica gel 60 F_{254} precoated plates. Detection was achieved by spraying with 10 % (v/v) H_2SO_4 and heating.

5.6 Structure elucidation of glucosides

The chemical structure of the purified resveratrol glycoside was inferred from the combination of 1D NMR (^{1}H NMR and ^{13}C NMR) and 2D NMR (gCOSY, gHSQC and gHMBC) spectroscopic analysis; *J* values are given in Hz. According to the COSY experiment, the proton spectrum displays a –CH=CH- group, AA'BB' and AMX spin systems of para-disubstituted and 1,3,5-trisubstituted aromatic rings, and one saccharide unit. The set of extracted vicinal constants (d, *J* = 3.5 Hz) identified α-glucose, while the magnitude of $J_{7\text{-H, }8\text{-H}}$ (16.3 Hz) proved the *E*-conformation of resveratrol. The position of the glycosylation was confirmed by the HMBC contact of the C-3 with 1"-H. Spectral analysis and interpretation was kindly performed by the group of Prof. Vladimír Křen at the Institute of Microbiology (Czech Republic).

3-*O*-α-D-Glucopyranosyl (*E*)-resveratrol

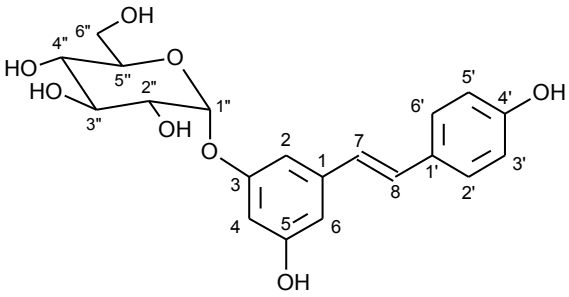

^{1}H NMR (400 MHz; CD_3OD): 7.39 (2 H, d, *J* = 8.6, 2'-H and 6'-H), 7.04 (1 H, d, *J* = 16.3, 8-H), 6.87 (1 H, d, *J* = 16.3, 7-H), 6.86 (1 H,s, 2-H),6.80 (2 H, d, *J* = 8.6, 3'-H and 5'-H), 6.62 (1 H, s, 6-H), 6.54 (1 H, s, 4-H), 5.50 (1 H, d, *J* = 3.5, 1"-H), 3.87 (1 H, dd, *J* = 9.7 and 8.9, 3"-H), 3.76 (2 H, m, 6"-Ha, 6"-Hb), 3.72 (1 H, ddd, *J* = 9.7, 4.2 and 2.5, 5"-H), 3.60 (1 H, dd, *J* = 9.7 and 3.6, 2"-H) and 3.48 (1 H, dd, *J* = 9.7 and 8.9, 4"-H).

^{13}C NMR (100 MHz; CD_3OD): 160.23 (C-3), 159.87 (C-5), 158.73 (C-4'), 141.75 (C-1), 130.63 (C-1'), 130.25 (C-8), 129.18 (C-2' and C-6'), 127.01 (C-7), 116.83 (C-3' and C-5'), 108.70 (C-6), 107.85 (C-2), 104.88 (C-4), 99.61 (C-1"), 75.28 (C-3"), 74.63 (C-5"), 73.64 (C-2"), 71.81 (C-4"), 62.63 (C-6").

6 SUPPLEMENTARY INFORMATION

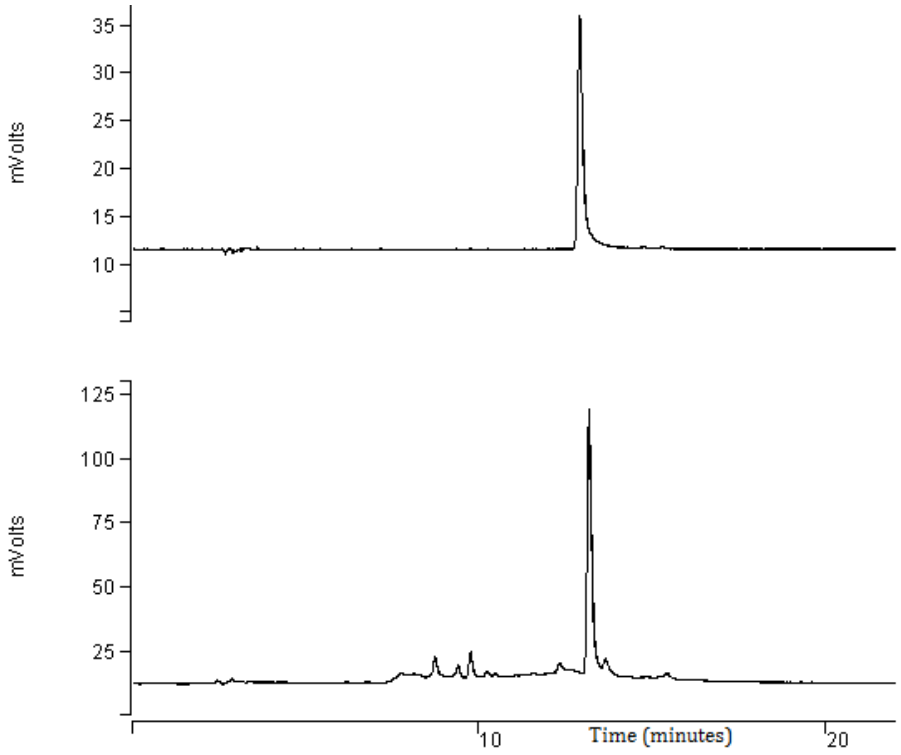

Figure S3.1 Production of quercetin glucosides (7 - 12 min) with SP at pH 6.5 and 60 °C, using 1 M sucrose and quercetin (14.1 min) saturated in 20 % DMSO (above) or AMMOENG 101 (beneath) after 24 h incubation.

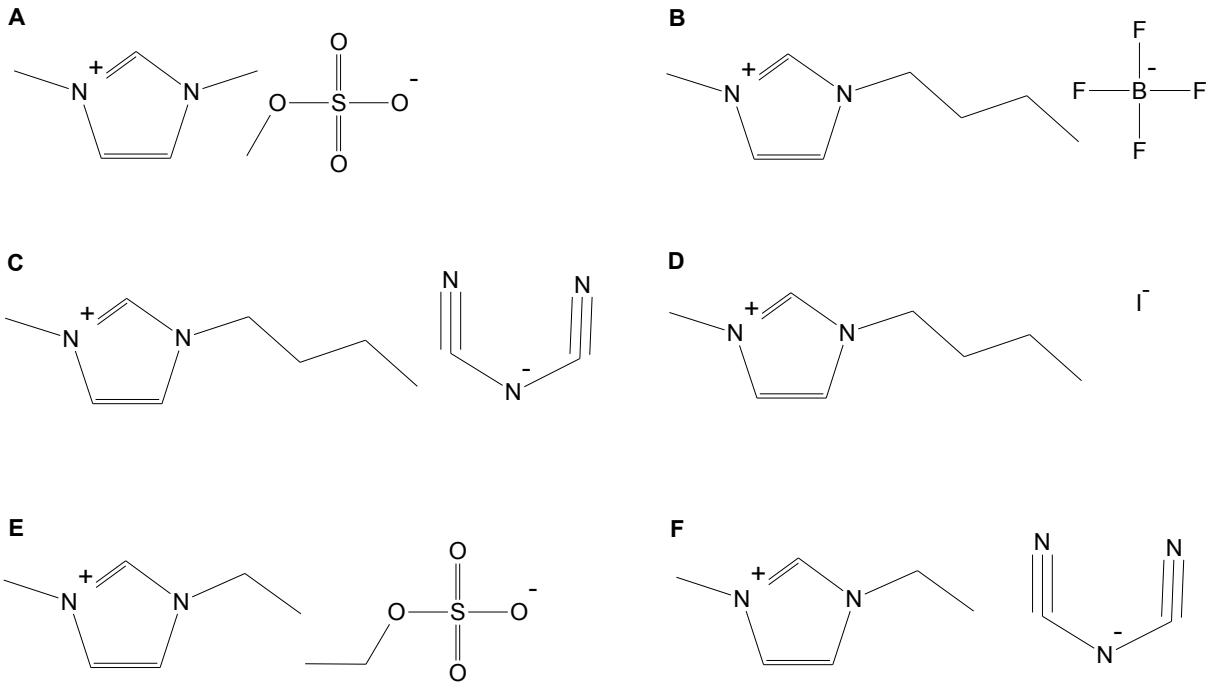

Figure S3.2 Structure of the various ionic liquids used during this research: [MMIM] [MeSO4] (A), [BMIM][BF4] (B), [BMIM][dca] (C), [BMIM][I] (D), [EMIM][EtSO4](E) and [EMIM][dca] (F).

CHAPTER 4

Biphasic catalysis with sucrose phosphorylase: chemoenzymatic synthesis of α-D-glucosides.

This chapter has been published as:

K. De Winter, T. Desmet, T. Devlamynck, L. Van Renterghem, T. Verhaeghe, H. Pelantova, V. Kren and W. Soetaert, **2014**, Biphasic catalysis with disaccharide phosphorylases: Chemoenzymatic synthesis of α-D-glucosides using sucrose phosphorylase, *Organic Process Research & Development*, 18, 781-787.

1 ABSTRACT

Thanks to its broad acceptor specificity, sucrose phosphorylase (SP) has been exploited for the transfer of glucose to a wide variety of acceptor molecules. Unfortunately, the low affinity (K_m > 1 M) of SP towards these acceptors typically urges the addition of cosolvents, which often either fail to dissolve sufficient substrate or progressively give rise to enzyme inhibition and denaturation. In this work, a buffer/ethyl acetate ratio of 5:3 was identified to be the optimal solvent system, allowing the use of SP in biphasic systems. Careful optimization of the reaction conditions enabled the synthesis of a range of α-D-glucosides, such as cinnamyl α-D-glucopyranoside, geranyl α-D-glucopyranoside, 2-*O*-α-D-glucopyranosyl pyrogallol and series of alkyl gallyl 4-*O*-α-D-glucopyranosides. The usefulness of biphasic catalysis was further illustrated by comparing the glucosylation of pyrogallol in a cosolvent and biphasic reaction system. The acceptor yield for the former reached only 17.4 %, whereas roughly 60 % of the initial pyrogallol was converted when using biphasic catalysis.

2 INTRODUCTION

Numerous biologically active molecules exist as glycosides in nature. Glycosylation can expand structural diversity[8], induce targeting of drugs to specific organs and tissues[124], and improve the solubility of hydrophobic compounds[94]. Furthermore, glycosylation is known to drastically extend the stability of labile molecules[95] and mediate the controlled release of flavors and fragrances[12]. Unfortunately, large-scale chemical synthesis of these molecules is limited by low yields, the use of toxic catalysts and the generation of waste[13, 15]. Biocatalytic approaches, allowing one-step reactions with high regio- and stereoselectivity, have therefore attracted much attention over the past decade[18].

Enzymatic glycosylation is typically performed with glycosyltransferases (GTs) or glycoside hydrolases (GH). However, the former requires relatively expensive nucleotide-activated sugars[97] while the latter suffers from low yields when used in the synthetic direction[27]. Less research has been done with disaccharide phosphorylases, although they show potential as biocatalysts for glycoside synthesis[29, 98, 99]. Indeed, these enzymes use a glycosyl phosphate donor, which is much cheaper than the activated sugar nucleotides required by GTs and can be synthesized by phosphorolysis of their natural substrates[29].

Sucrose phosphorylase (SP) catalyzes the reversible phosphorolysis of sucrose into α-D-glucose 1-phosphate (αG1P) and D-fructose. Its broad acceptor specificity has been exploited for the transfer of glucose to a wide variety of acceptor molecules, such as polyols[40], phenolics[125, 126], hydroxyfuranones[127] and stilbenoids[128]. Unfortunately, the low affinity (K_m > 1 M) of SP towards these acceptors typically urges the addition of cosolvents like DMSO or methanol. However, low concentrations of these cosolvents often fail to dissolve sufficient substrate, whereas high concentrations progressively give rise to enzyme inhibition and denaturation[33, 79].

Besides the use of ionic liquids (CHAPTER 3), the application of liquid-liquid biphasic systems containing water and a water-immiscible organic solvent, however, provides an interesting alternative. The aqueous phase contains the enzymes and water soluble substrates, while hydrophobic substrates are dissolved in the organic phase. Stirring or

shaking will transfer these substrates from the organic to the aqueous phase, where they can be converted by the enzymes. Improved enzyme stability and ease of product recovery, while avoiding substrate and product inhibition, are among the major advantages of biphasic systems[129, 130]. The usefulness of this type of catalysis has been widely illustrated for numerous applications, including the synthesis of oligosaccharides[131] and glycosides[132, 133] with glycosidases.

Although SP has recently been successfully applied for glycosylation reactions in ILs (CHAPTER 3) and supercritical carbon dioxide[100], no reports on its use in biphasic reaction systems are available to date. In this chapter, the glycosylation of various acceptors with the SP from *Bifidobacterium adolescentis* in biphasic systems is described.

3 RESULTS & DISCUSSION

3.1 Exploring biphasic catalysis with SP

The β-D-glucoside of cinnamyl alcohol has recently gained attention from the pharmaceutical industry due to its claimed anti-fatigue, anti-aging, antioxidant, and immune enhancing properties[134-136]. The enzymatic glucosylation of cinnamyl alcohol has already been reported in an IL based cosolvent system using the SP from *B. adolescentis* (BaSP) (CHAPTER 3). Unfortunately, the latter synthesis suffered from low yields and labor intensive product recovery. Consequently, the use of a cosolvent was avoided by reacting 250 µL of the alcohol with 250 µL MES buffer at pH 6.5 supplemented with 2 M sucrose and 50 U/mL BaSP. TLC analysis of the reaction mixture after 48 h incubation at 60 °C revealed a clear new spot having an R_f higher than sucrose and lower than cinnamyl alcohol (Figure S4.1). The product was purified by silica gel chromatography and identified to be cinnamyl α-D-glucopyranoside by NMR spectroscopy.

Encouraged by these results, conditions enabling the efficient enzymatic glucosylation with BaSP were further optimized. Indeed, a number of factors are known to influence the glycosylation efficiency, including the pH, the type and concentration of both donor and acceptor, as well as the reaction temperature[21]. A full factorial design experiment was performed to determine their relative importance on the glucosylation of cinnamyl

alcohol. The cheap and readily available donor sucrose was used, and the temperature was fixed at 37 °C (Table 4.1).

Table 4.1 Optimization of SP catalyzed synthesis of cinnamyl α-D-glucopyranoside in a biphasic system: 2^3 factorial design. The reaction mixtures were incubated during 48 h at 37 °C.

Run	pH	[Sucrose] (M)	Buffer/acceptor ratio	Product spot intensity
1	6	0.5	5:1	++
2	6	0.5	1:1	+
3	6	2	5:1	+++
4	6	2	1:1	++++
5	7.5	0.5	5:1	++
6	7.5	0.5	1:1	+
7	7.5	2	5:1	+++++
8	7.5	2	1:1	++++

The glucosylation yield was found to be strongly influenced by the buffer/acceptor (solvent) ratio, while high sucrose concentrations were generally required to obtain proper glucosylation. Indeed, a product concentration of 4.8 g/L was achieved when using 2 M sucrose at pH 7.5 with a 5:1 solvent ratio. The pH was found to only influence the product spot intensity when reacting 2 M sucrose with a 5:1 solvent ratio. However, the limited differences can be explained by the low product concentrations obtained for the other conditions, and the narrow pH range (6 to 7.5) applied. Next, the pH (5 to 9) and solvent ratio (10:1 to 1:5) were varied to identify optima at pH 7.5 and a ratio of 5:3. Although higher sucrose concentrations were not feasible due to viscosity limitations, the glycosylation efficiency could be further improved by increasing the reaction temperature to 50 °C. Finally, the optimal reaction conditions were found to be a solvent ratio of 5:3, 2 M sucrose, pH 7.5 and 50 °C, resulting in the production of 6.4 g/L cinnamyl α-D-glucopyranoside. Interestingly, using αG1P as donor resulted in significantly less product formation (4.1 g/L compared to 6.4 g/L), confirming sucrose to be the preferred donor substrate[55].

3.2 Selection of a suitable water-immiscible solvent

Although these results confirmed the SP mediated transfer of a glucose moiety using biphasic catalysis, a suitable water immiscible solvent is required to allow glycosylation of solid acceptors. The latter solvent should be able to dissolve high amounts of acceptor, without impairing the glucosylation reaction catalyzed by the enzyme. Various solvents were supplemented with 50 mg/mL cinnamyl alcohol and reacted under the optimal conditions (Figure 4.1).

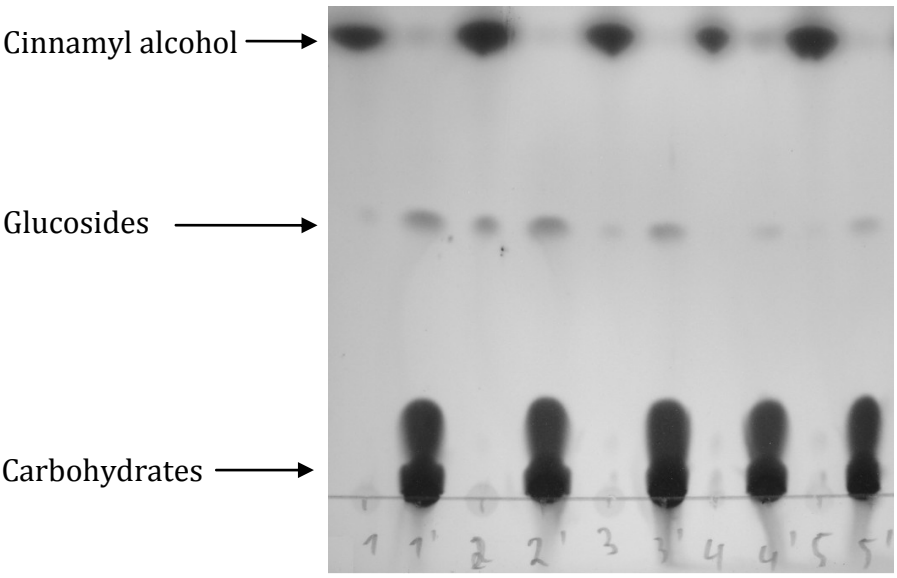

Figure 4.1 Biphasic glycosylation of cinnamyl alcohol with BaSP. The acceptor was dissolved to 50 mg/mL in butyl acetate (1), ethyl acetate (2), methyl-*tert*-butylether (3), octane (4) and diethyl ether (5). The organic and aqueous (') phase was spotted for each reaction.

TLC analysis revealed the highest conversion when using ethyl acetate (EtOAc). However, SP mediated glucosylation of cinnamyl alcohol was also observed when butyl acetate (BuOAc), methyl-*tert*-butylether (MTBE), octane, diethyl ether, cyclohexene and pentane were used.

Next, the solubility of different acceptors was evaluated in the most promising solvents (Table S4.1). Although the solubility of all compounds was found to be very low in octane, the majority of the evaluated acceptors could be dissolved in BuOAc, MTBE and EtOAc. The latter was found to be less deleterious for the glycosylation activity of SP, and was therefore used in all further experiments (Figure 4.1). Finally, the concentration of cinnamyl alcohol in the organic phase was varied to reveal optimal glucoside formation at 100 mg/mL.

3.3 Evaluation of the glycosylation potential of SP

The glycosylation potential of SP was then evaluated by incubating various acceptors under optimal glucosylation conditions. Semi-quantative data for a large number of acceptors was obtained through TLC analysis (Table 4.2), while HPLC experiments allowed detailed analysis of a limited amount of reactions (Table 4.3).

Table 4.2 Glycosylation potential of the SP from *B. adolescentis* in a biphasic reaction system. TLC analysis was performed after 48 h incubation at 50 °C.

Acceptor	Product spot intensity	Acceptor	Product spot intensity
Pentanol[a]	+++	Cinnamyl alcohol[a]	+++
Hexanol[a]	++	Menthol[b]	-
Heptanol[a]	+	Saligenin[b]	++++
Octanol[a]	+	*p*-Nitrophenol[b]	+
Nonanol[a]	-	Phenol[b]	-
Decanol[a]	-	Hydroquinone[b]	+
Dodecanol[a]	-	Catechol[b]	+++
Cyclohexanol[a]	++++	Resorcinol[b]	+++
2-Hexanol[a]	+++	Pyrogallol [b]	+++++
Linalool[a]	-	Methyl gallate[b]	++++
Eugenol[a]	++	Ethyl gallate[b]	++++
Nerolidol[a]	-	Propyl gallate[b]	+++
β-Citronellol[a]	+	Lauryl gallate[b]	-
Geraniol[a]	++	Salicylic acid methyl ester[a]	+
2-Phenylethanol[a]	+	Curcumin[b]	-
1*R*-Phenylethanol[a]	+++++	Resveratrol[b]	+
1*S*-Phenylethanol[a]	+++++	Quercetin[b]	+
Benzyl alcohol[a]	++	Vanillin[b]	++
Anisyl alcohol[a]	+	Vanillyl alcohol[b]	+++

[a] Glycosylation was performed using the acceptor as organic phase. [b] Glycosylation was performed using EtOAc supplemented with 100 mg/mL acceptor as organic phase.

These results illustrate the versatile applicability of biphasic catalysis for the production of glycosides with SP. The structure of numerous glucosides was confirmed by NMR spectroscopy. Aliphatic alcohols could be glycosylated up to octanol, but the obtained product concentrations decreased with increasing chain lengths.

Table 4.3 Glycosylation of various acceptors with the SP from *B. adolescentis*. HPLC analysis was performed after 48 h incubation at 50 °C.

Acceptor	[Glucoside] (mM)	[Glucoside] (g/L)	Glucoside[d] (g)	$Yield_{Acceptor}$ (%)	$Yield_{Donor}$ (%)
Geraniol[a]	20.4	6.5	0.65	0.9	1.6
1*R*-Phenylethanol[a]	133.2	37.9	3.79	4.3	10.7
1*S*-Phenylethanol[a]	126.7	36.0	3.60	4.1	10.1
Cinnamyl alcohol[a]	21.5	6.4	0.64	0.8	1.7
Cinnamyl alcohol[b]	16.2	4.8	0.48	5.8	1.3
Hydroquinone[b]	2.6	0.7	0.07	0.7	0.2
Resorcinol[b]	27.1	7.4	0.74	7.9	2.2
Pyrogallol [b]	175.8	50.6	5.06	59.1	14.1
Pyrogallol [c]	112.6	32.4	3.24	75.7	9.0
Methyl gallate[b]	87.4	30.2	3.02	42.9	7.0
Ethyl gallate[b]	50.9	18.3	1.83	26.9	4.0
Propyl gallate[b]	24.7	9.2	0.92	14.0	1.9

[a] Glycosylation was performed using the acceptor as organic phase. [b] Glycosylation was performed using EtOAc supplemented with 100 mg/mL acceptor as organic phase. [c] Glycosylation was performed using EtOAc supplemented with 50 mg/mL acceptor as organic phase. [d] Glucoside produced in a 100 mL reaction.

Surprisingly, secondary alcohols were found to be more easily glycosylated compared to primary alcohols. Indeed, 48 h incubation under optimal reaction conditions resulted in glucoside concentrations of 37.9 and 36.0 g/L for 1*R*- and 1*S*-phenylethanol, respectively, while only traces of product were detected when reacting 2-phenylethanol. The structure of *R*- and *S*-1-phenylethyl α-D-glucopyranoside was confirmed by NMR spectroscopy. Also, BaSP was found to glycosylate a range of structurally diverse compounds with olfactory properties. Examples include the monoterpenoids geraniol and β-citronellol, aromatic alcohols such as benzyl alcohol, anisyl alcohol, cinnamyl

alcohol and vanillyl alcohol, as well as the phenylpropanoid eugenol and the phenolic aldehyde vanillin. Although these glycosides were generally produced in significantly lower concentrations compared to secondary alcohols (Table 4.3), we were able to confirm the formation of geranyl α-D-glucopyranoside and cinnamyl α-D-glucopyranoside by NMR spectroscopy.

In contrast to earlier work with the SP from *L. mesenteroides*[125], we failed to obtain any glycosides of phenol. However, we were able to couple a glucose moiety to hydroquinone, catechol, resorcinol and pyrogallol, indicating the necessity of additional phenolic hydroxyl groups to ensure correct positioning in the active site. Indeed, the formation of 1-*O*-α-D-glucopyranosyl hydroquinone (0.7 g/L), 1-*O*-α-D-glucopyranosyl resorcinol (7.4 g/L) and 2-*O*-α-D-glucopyranosyl pyrogallol (50.6 g/L) was confirmed by NMR spectroscopy. In addition, glucosylation of a series of gallic acid esters was observed, as confirmed by NMR spectroscopy. These potent antioxidants, including ethyl gallate (E313) and propyl gallate (E310), are commonly applied in foods, cosmetics and hair products[137, 138]. The methyl ester glucoside could be produced up to 30 g/L, while longer alkyl chains were found to result in lower glucoside concentrations (Table 4.3).

In conclusion, a wide variety of glucosides could be synthesized using the SP from *B. adolescentis*. Industrially relevant glucoside concentrations of several g/L were obtained for a number of acceptors[96, 139]. Not surprisingly, the acceptor yields were much lower when using the pure acceptor as organic phase (Table 4.3). The latter, however, could be increased from 0.8 to 5.8 % for cinnamyl alcohol, by dissolving 100 mg/mL of the acceptor in EtOAc, rather than using the alcohol in its undiluted form. Moreover, the acceptor yield for pyrogallol could be improved from 59.1 to 75.7 % by decreasing the acceptor concentration from 100 to 50 mg/mL. However, these increased yields were achieved at the expense of lower product concentrations (Table 4.3).

The donor yields, on the contrary, were less than 20 % for all acceptors (Table 4.3). Indeed, higher concentrations of sucrose were added to stabilize the enzyme (CHAPTER 3), and push the conversion in the synthesis direction. Therefore, considerable amounts of sucrose remained present at the end of the reaction (Figure 4.2). Moreover, SP is known to exhibit an undesirable hydrolytic side reaction, yielding D-glucose and D-

fructose as products. The liberated glucose can then be glucosylated by SP, resulting in the formation of 'glucobiose' products[55, 90]. Unfortunately, this competition between D-glucose and the acceptor compound was found to further decrease the donor yield.

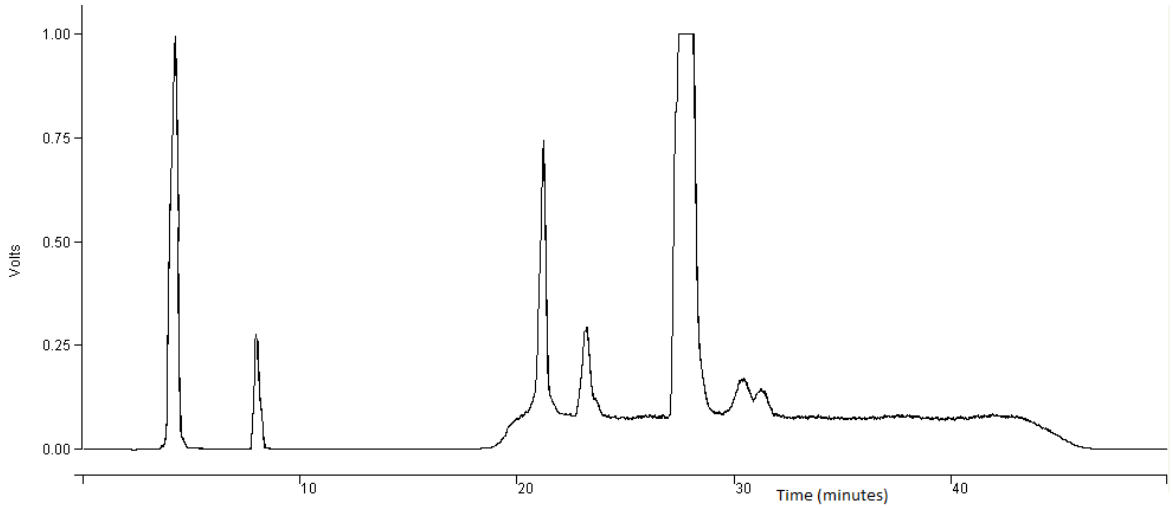

Figure 4.2 HPLC chromatogram showing the glucosylation of propyl gallate and formation of glucobiose products with SP. The sample was analyzed after 24 h incubation under optimal biphasic reaction conditions at 50 °C: gallic acid propyl ester (4.9 min), propyl gallyl 4-*O*-α-D-glucopyranoside (8.2 min), D-fructose (21.7 min), D-glucose (23.2 min), sucrose (28.3 min) and glucobiose products (30.2 – 31.9 min).

3.4 Cosolvent or biphasic catalysis?

Finally, the performance of biphasic catalysis was compared with a recently reported cosolvent system (CHAPTER 3), using the glycosylation of pyrogallol as a case study. Therefore, the water immiscible EtOAc was replaced by the IL AMMOENG 101, which has been successfully applied for the SP mediated synthesis of 3-*O*-α-D-glucopyranosyl (*E*)-resveratrol[128]. All other parameters were identical for both reactions (Figure 4.3).

Interestingly, the acceptor yield for the cosolvent system reached only 17.4 %, while roughly 60 % of the initial pyrogallol was converted when using a biphasic system. This significant difference can be explained by the transfer ratio of the enzyme under the operational conditions. Indeed, a ratio of 5.7 for the biphasic system, compared to 1.1 for the cosolvent system, indicates that less hydrolysis (and synthesis of glucobioses) occurs upon application of biphasic catalysis. In addition, the course of product formation reveals the absence of secondary hydrolysis (i.e. the degradation of 2-*O*-α-D-glucopyranosyl pyrogallol), as previously reported by the Nidetzky group for α-glucosyl glycerol[40] (Figure 4.3).

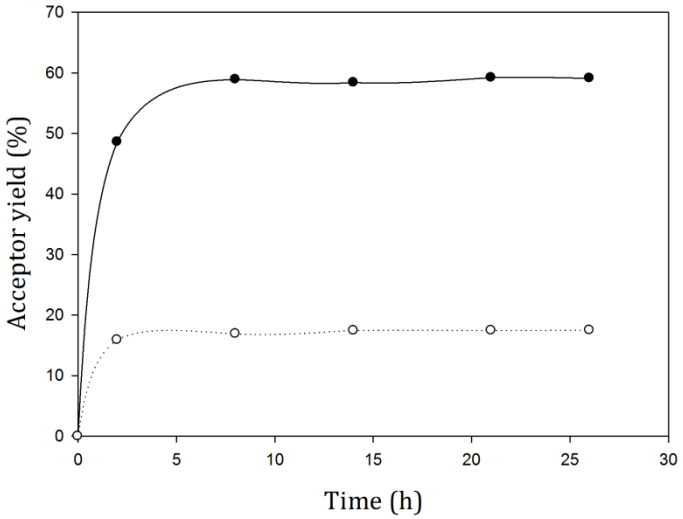

Figure 4.3 Synthesis of 2-*O*-α-D-glucopyranosyl pyrogallol in a cosolvent (○) and biphasic (●) reaction system. The reaction mixture consisted of 62.5 % aqueous MOPS buffer at pH 7.5 containing 2 M sucrose and 50 U/mL SP, and 37.5 % EtOAc supplemented with 100 mg/mL pyrogallol. For the cosolvent system, EtOAc was replaced by the IL AMMOENG 101.

4 CONCLUSION

Following the work on SP mediated glycoside synthesis in conventional solvents[55], ILs (CHAPTER 3) and supercritical carbon dioxide[100], this is the first report on the use of disaccharide phosphorylases in biphasic reaction systems. Careful optimization allowed the glucosylation of aliphatic alcohols, monoterpenoids, aromatic alcohols and phenolics. In addition a series of alkyl gallyl 4-*O*-α-D-glucopyranosides were successfully synthesized up to 30 g/L. These glucosylations were achieved by reacting 62.5 % aqueous MOPS buffer at pH 7.5 containing 2 M sucrose and 50 U/mL SP, and 37.5 % EtOAc supplemented with 100 mg/mL acceptor. Also, the production of 2-*O*-α-D-glucopyranosyl pyrogallol was compared in cosolvent and biphasic systems. The transfer ratio was found to be 5 times higher when using the latter system, resulting in less hydrolysis and formation of glucobiose side product. Consequently, the use of biphasic catalysis was identified to be a valuable alternative for glycoside synthesis with disaccharide phosphorylases.

5 MATERIALS & METHODS

5.1 Materials

The IL AMMOENG 101 was kindly provided by Evonik Industries AG, and ethyl acetate was bought from Fiers. All other chemicals were analytical grade and purchased from Sigma-Aldrich. The recombinant SP from *B. adolescentis* was produced and partially purified by heat treatment as described in CHAPTER 2. The activity of the enzyme was determined as shown in CHAPTER 2, and one unit of SP was defined as the activity that corresponds to the release of 1 µmol fructose per minute from 100 mM sucrose in 100 mM phosphate buffer at pH 7.0 and 37 °C. NMR spectra were measured on a Bruker AVANCE III 600 MHz spectrometer (600.23 MHz for ^{1}H, and 150.94 MHz for ^{13}C) in CD_3OD at 25 °C. HPLC measurements were performed on a Varian Prostar.

5.2 Glycosylation reactions with SP

Small scale biphasic glycosylation reactions were performed in a Thermoshaker (Eppendorf) at 1400 rpm. Varying amounts of different water immiscible acceptors were added to 500 µL aqueous buffer in a 1.5 mL eppendorf. Alternatively, water immiscible organic solvents containing 100 mg/mL acceptor were used. The acidity of the aqueous phase was varied by using a citrate-phosphate buffer (pH 5.0-5.4), MES buffer (pH 5.5-6.5), MOPS buffer (pH 6.6-7.5) or tricine buffer (pH 7.6-9). Unless stated otherwise, the reactions were incubated at 50 °C in the presence of 2 M sucrose and 50 U/mL SP. The acceptor ($Yield_{Acceptor}$) and donor yield ($Yield_{Donor}$) are defined as the ratio of the amount of product formed to the amount of acceptor and donor added to the reaction, respectively (mol/mol).

5.3 Solubility measurements

The dissolution of various acceptor molecules in different water immiscible solvents was performed in a water bath at 50 °C with ± 0.1 °C accuracy. Varying amounts of acceptor were added to a 2 mL eppendorf, and solvent was added to 1 mL. Next, the samples were vortexed multiple times and allowed to equilibrate for 48 h, after which the samples were checked for remaining particles. The latter technique allows to map

the solubilizing properties of various solvents, whilst avoiding the time consuming HPLC analyses required by the method described in CHAPTER 3.

5.4 TLC analysis

TLC analysis was performed on Merck Silica gel 60 F_{254} precoated plates. The eluens was a mixture of EtOAC/MeOH/H_2O = 30:5:4, and spots were visualized by UV detection at 254 nm, or charring with 10 % (v/v) H_2SO_4. All TLC plates of a single experiment were visually compared, thereby rating the intensity of product spots between +++++ and + for the highest intensity and a barely visible spot respectively. Both the aqueous and the solvent phase were spotted on TLC. The intensity of both product spots was combined to yield a single rating.

5.5 HPLC analysis

HPLC analysis was performed on an X-bridge amide column (250 mm × 4.6 mm, 3.5 µm, Waters, USA) with milliQ water (solvent A) and acetonitrile (solvent B), both containing 0.2 % triethylamine, as the mobile phase. The flow rate and temperature were set at 1.0 mL/min and 30 °C, respectively. The gradient elution was as follows: 95 % of solvent A (0 - 12 min), 5 to 25 % solvent B (12 - 15 min), 25 % solvent B (15 - 40 min), 25 to 5 % solvent B (40 - 41 min) and 95 % solvent A (41 - 50 min). Adequate detection was obtained with an Alltech 2000ES evaporative light scattering detector (ELSD). The tube temperature, gas flow and gain were set at 30 °C, 1.5 L/min and 1, respectively. Homogeneous samples containing both phases were obtained after intensive mixing. These samples were then diluted in DMSO, and subjected to HPLC analysis. The resulting concentrations thus refer to the amount of product present in the total reaction volume. The obtained peaks were calibrated using authentic standard curves prepared in milliQ water or methanol. All HPLC analyses were performed in triplicate.

5.6 Comparison of biphasic and cosolvent glycosylation reactions

The glycosylation of pyrogallol was carried out at 10 mL scale. The reaction mixture consisted of 62.5 % aqueous MOPS buffer at pH 7.5 containing 2 M sucrose and 50 U/mL SP, and 37.5 % EtOAc supplemented with 100 mg/mL pyrogallol. Alternatively, EtOAc was replaced by the IL AMMOENG 101. Reaction mixtures were incubated in a

thermoshaker (Eppendorf) at 750 rpm and 50 °C. The concentration of 2-*O*-α-D-glucopyranosyl pyrogallol and fructose was determined by means of HPLC analysis. The transfer ratio is defined as the ratio of the amount of glucose transferred to the acceptor over the sum of the free glucose and the glucose incorporated in glucobioses. The former was calculated based on the glucoside concentration, while the latter was obtained by subtracting the amount of glucoside from the obtained fructose concentration.

5.7 Production and purification of glucosides

The glycosylation of hydroquinone, resorcinol, pyrogallol, methyl gallate, ethyl gallate and propyl gallate was carried out at 100 mL scale in magnetically stirred flasks. Biphasic reaction mixtures were created by adding 62.5 mL aqueous buffer to 37.5 mL organic solvent. The aqueous buffer consisted of 50 mM MOPS at pH 7.5 containing 2 M sucrose and 50 U/mL SP. EtOAc supplemented with 100 mg/mL hydroquinone, resorcinol, pyrogallol, methyl gallate, ethyl gallate or propyl gallate was used as organic phase. Alternatively, glycosylation of 1-phenylethanol, geraniol and cinnamyl alcohol was performed by substituting the EtOAc by the pure acceptor. Reactions were terminated after 48 h incubation at 50 °C, after which the reaction mixtures were heated (10 min at 95 °C) and centrifuged (12 000 g, 4 °C, 15 min) to remove debris. The samples were then evaporated *in vacuo* and the residue was purified by column chromatography (silicagel, EtOAC/MeOH/H_2O = 30:5:4).

5.8 Structure elucidation of glucosides

The structures of the newly formed glucosides were determined by a combination of 1D NMR (^{1}H NMR and ^{13}C NMR) and 2D NMR (gCOSY, gHSQC and gHMBC) spectroscopy. Residual signals of solvent were used as internal standard (δ_H 3.330 ppm, δ_C 49.30 ppm), and digital resolution enabled us to report δ_H to three and δ_C to two decimal places. The proton spin systems were assigned by COSY, and then the assignment was transferred to carbons by HSQC. HMBC experiments enabled us to assign quaternary carbons and to join individual spin systems together. Chemical shifts are given in δ-scale [ppm], and coupling constants in Hz. Spectral analysis and interpretation was kindly performed by the group of Prof. Vladimír Křen at the Institute of Microbiology (Czech Republic).

1-*O*-α-D-Glucopyranosyl hydroquinone

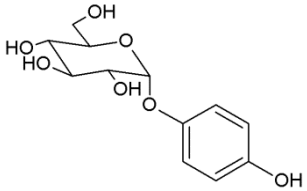

^{1}H NMR (600.23 MHz, CD_3OD, 25 °C): 3.427 (1H, dd, *J* = 9.7, 8.9 Hz, H-4), 3.543 (1H, dd, *J* = 9.8, 3.7 Hz, H-2), 3.722 (1H, dd, *J* = 11.3, 4.9 Hz, H-6u), 3.752 (1H, ddd, *J* = 9.7, 4.9, 2.0 Hz, H-5), 3.791 (1H, dd, *J* = 11.3, 2.0 Hz, H-6d), 3. 863 (1H, dd, *J* = 9.8, 8.9 Hz, H-3), 5.310 (1H, d, *J* = 3.7 Hz, H-1), 6.720 (2H, m, Σ*J* = 8.9 Hz, H-*meta*), 7.026 (2H, m, Σ*J* = 8.9 Hz, H-*ortho*)

^{13}C NMR (150.94 MHz, CD_3OD, 25 °C): 62.73 (C-6), 71.92 (C-4), 73.73 (C-2), 74.50 (C-5), 75.28 (C-3), 100.85 (C-1), 116.99 (C-*meta*), 120.17 (C-*ortho*), 152.22 (C-*ipso*), 154.14 (C-*para*)

1-*O*-α-D-Glucopyranosyl resorcinol

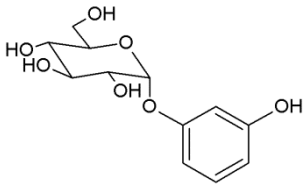

^{1}H NMR (600.23 MHz, CD_3OD, 25 °C): 3.462 (1H, dd, *J* = 9.9, 8.9 Hz, H-4), 3.569 (1H, dd, *J* = 9.8, 3.7 Hz, H-2), 3.671 (1H, ddd, *J* = 9.9, 4.4, 2.7 Hz, H-5), 3.728 (1H, dd, *J* = 12.0, 4.4 Hz, H-6u), 3.762 (1H, dd, *J* = 12.0, 2.7 Hz, H-6d), 5.457 (1H, d, *J* = 3.7 Hz, H-1), 6.548 (1H, ddd, *J* = 8.1, 2.3, 0.8 Hz, H-6'), 6.636 (1H, dd, *J* = 2.3, 2.3 Hz, H-2'), 6.662 (1H, ddd, *J* = 8.2, 2.3, 0.8 Hz, H-4'), 7.087 (1H, dd, *J* = 8.2, 8.1 Hz, H-5')

^{13}C NMR (150.94 MHz, CD_3OD, 25°C): 62.58 (C-6), 71.75 (C-4), 73.63 (C-2), 74.58 (C-5), 75.26 (C-3), 99.52 (C-1), 105.85 (C-2'), 109.57 (C-4'), 110.83 (C-6'), 131.14 (C-5'), 159.90 (C-3'), 160.09 (C-1')

2-*O*-α-D-Glucopyranosyl pyrogallol

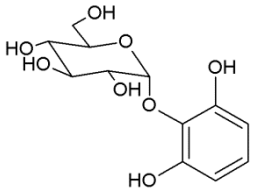

^{1}H NMR (600.23 MHz, CD_3OD, 25 °C): 3.441 (1H, dd, *J* = 10.1, 8.9 Hz, H-4), 3.604 (1H, dd, *J* = 9.6, 3.9 Hz, H-2), 3.771 (1H, dd, *J* = 11.8, 5.5 Hz, H-6u), 3.881 (1H, dd, *J* = 9.6, 8.9 Hz, H-3), 3.902 (1H, dd, *J* = 11.8, 2.4 Hz, H-6d), 4.234 (1H, ddd, *J* = 10.1, 5.5, 2.4 Hz, H-5), 5.024 (1H, d, *J* = 3.9 Hz, H-1) 6.385 (2H, d, *J* = 8.2 Hz, H-*meta*), 6.813 (1Ht, *J* = 8.2 Hz, H-*para*)

^{13}C NMR (150.94 MHz, CD_3OD, 25 °C): 62.60 (C-6), 71.41 (C-4), 73.66 (C-2), 75.30 (C-3), 75.56 (C-5), 106.01 (C-1), 108.95 (C-*meta*), 126.47 (C-*para*), 136.12 (C-*ipso*), 152.27 (C-*ortho*)

Methyl gallyl 4-*O*-α-D-glucopyranoside

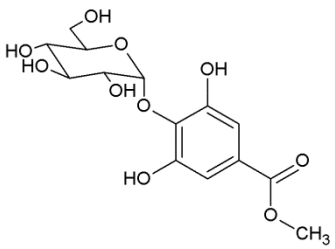

^{1}H NMR (600.23 MHz, CD_3OD, 25 °C): 3.482 (1H, dd, *J* = 10.1, 9.2 Hz, H-4), 3.619 (1H, dd, *J* = 9.6, 3.8 Hz, H-2), 3.796 (1H, dd, *J* = 11.9, 4.9 Hz, H-6u), 3.860 (3H, s, H-1'), 3.868 (1H, dd, *J* = 11.9, 2.5 Hz, H-6d), 3.902 (1H, dd, *J* = 9.6, 9.2 Hz, H-3), 4.243 (1H, ddd, *J* = 10.1, 4.9, 2.5 Hz, H-5), 5.149 (1H, d, *J* = 3.8 Hz, H-1), 7.063 (2H, s, H-*meta*)

^{13}C NMR (150.94 MHz, CD_3OD, 25°C): 52.88 (C-1'), 62.41 (C-6), 71.18 (C-4), 73.66 (C-2), 75.22 (C-3), 75.46 (C-5), 105.45 (C-1), 110.34 (C-*meta*), 128.10 (C-*para*), 139.75 (C-*ipso*), 152.31 (C-*ortho*), 168.60 (CO)

Ethyl gallyl 4-*O*-α-D-glucopyranoside

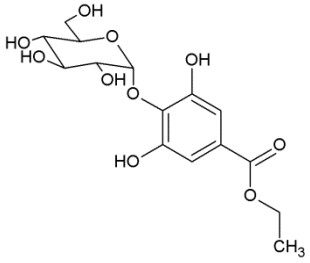

^{1}H NMR (600.23 MHz, CD_3OD, 25 °C): 1.372 (3H, t, *J* = 7.1 Hz, H-2'), 3.479 (1H, dd, *J* = 10.1, 9.2 Hz, H-4), 3.619 (1H, dd, *J* = 9.6, 3.8 Hz, H-2), 3.793 (1H, dd, *J* = 11.8, 5.0 Hz, H-6u), 3.872 (1H, dd, *J* = 11.8, 2.5 Hz, H-6d), 3.901 (1H, dd, *J* = 9.6, 9.2 Hz, H-3), 4.242 (1H, ddd, *J* = 10.1, 5.0, 2.5 Hz, H-5), 4.317 (1H, q, *J* = 7.1 Hz, H-1'), 5.146 (1H, d, *J* = 3.8 Hz, H-1), 7.068 (2H, s, H-*meta*)

^{13}C NMR (150.94 MHz, CD_3OD, 25°C): 14.85 (C-2'), 62.36 (C-1'), 62.45 (C-6), 71.22 (C-4), 73.67 (C-2), 75.24 (C-3), 75.50 (C-5), 105.51 (C-1), 110.31 (C-*meta*), 128.47 (C-*para*), 139.72 (C-*ipso*), 152.29 (C-*ortho*), 168.13 (CO)

Propyl gallyl 4-*O*-α-D-glucopyranoside

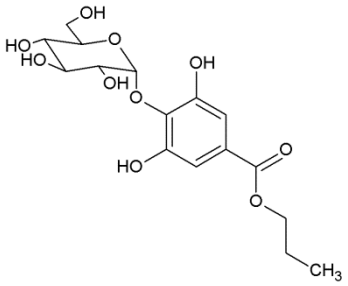

^{1}H NMR (600.23 MHz, CD_3OD, 25 °C): 1.038 (3H, t, *J* = 7.4 Hz, H-3'), 1.778 (2H, tq, *J* = 7.4, 6.6 Hz, H-2'), 3.485 (1H, dd, *J* = 10.0, 9.2 Hz, H-4), 3.622 (1H, dd, *J* = 9.6, 3.8 Hz, H-2), 3.798 (1H, dd, *J* = 11.9, 4.9 Hz, H-6u), 3.872 (1H, dd, *J* = 11.9, 2.5 Hz, H-6d), 3.906 (1H, dd, *J* = 9.6, 9.2 Hz, H-3),4.223 (2H, t, *J* = 6.6 Hz, H-1'), 4.246 (1H, ddd, *J* = 10.0, 4.9, 2.5 Hz, H-5), 5.153 (1H, d, *J* = 3.8 Hz, H-1), 7.070 (2H, s, H-*meta*)

^{13}C NMR (150.94 MHz, CD_3OD, 25°C): 11.07 (C-3'), 23.40 (C-2'), 62.41 (C-6), 67.92 (C-1'), 71.17 (C-4), 73.64 (C-2), 75.21 (C-3), 75.45 (C-5), 105.44 (C-1), 110.28 (C-*meta*), 128.39 (C-*para*), 139.69 (C-*ipso*), 152.28 (C-*ortho*), 168.16 (CO)

1*R*-Phenylethyl α-D-glucopyranoside

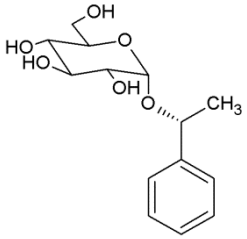

^{1}H NMR (600.23 MHz, CD_3OD, 25 °C): 1.493 (3H, d, *J* = 6.6 Hz, H-2'), 3.304 (1H, dd, *J* = 9.8, 8.9 Hz, H-4), 3.333 (1H, dd, *J* = 9.8, 3.8 Hz, H-2), 3.709 (1H, m, H-6u), 3.735 (1H, m, H-5), 3.775 (1H, dd, *J* = 9.7, 8.9 Hz, H-3), 3.886 (1H, m, H-6d), 4.626 (1H, d, *J* = 3.8 Hz, H-1), 4.909 (1H, q, *J* = 6.6 Hz, H-1'),7.272 (1H, m, H-*para*), 7.345 (2H, m, H-*meta*), 7.455 (2H, m, H-*ortho*)

^{13}C NMR (150.94 MHz, CD_3OD, 25°C): 24.92 (C-2'), 63.13 (C-6), 72.34 (C-4), 73.78 (C-2), 74.19 (C-5), 74.59 (C-1'), 75.40 (C-3), 97.14 (C-1), 128.19 (C-*ortho*), 128.90 (C-*para*), 129.71 (C-*meta*), 144.30 (C-*ipso*)

1*S*-Phenylethyl α-D-glucopyranoside

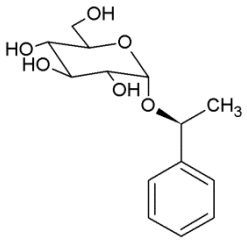

^{1}H NMR (600.23 MHz, CD_3OD, 25 °C): 1.499 (3H, d, *J* = 6.5 Hz, H-2'), 3.323 (1H, dd, *J* = 10.0, 8.5 Hz, H-4), 3.362 (1H, ddd, *J* = 10.0, 4.3, 2.3 Hz, H-5), 3.429 (1H, dd, *J* = 9.7, 3.8 Hz, H-2), 3.435 (1H, dd, *J* = 11.8, 2.3 Hz, H-6u), 3.543 (1H, dd, *J* = 11.9, 4.3 Hz, H-6d), 3.664 (1H, dd, *J* = 9.7, 8.5 Hz, H-3), 4.808 (1H, q, *J* = 6.5 Hz, H-1'), 5.058 (1H, d, *J* = 3.8 Hz, H-1), 7.254 (1H, m, H-*para*), 7.326 (2H, m, H-*meta*), 7.427 (2H, m, H-*ortho*)

^{13}C NMR (150.94 MHz, CD_3OD, 25°C): 22.44 (C-2'), 62.33 (C-6), 71.81 (C-4), 73.88 (C-2), 75.38 (C-3), 77.17 (C-1'), 78.42 (C-5), 99.34 (C-1), 127.73 (C-*ortho*), 128.65 (C-*para*), 129.54 (C-*meta*), 145.60 (C-*ipso*)

Cinnamyl α-D-glucopyranoside

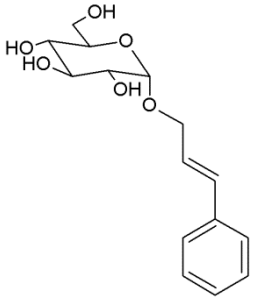

^{1}H NMR (600.23 MHz, CD_3OD, 25 °C): 3.325 (1H, dd, *J* = 10.0, 8.9 Hz, H-4), 3.446 (1H, dd, *J* = 9.7, 3.7 Hz, H-2), 3.661 (1H, ddd, *J* = 10.0, 5.7, 2.3 Hz, H-5), 3.707 (1H, dd, *J* = 11.7, 5.7 Hz, H-6u), 3.714 (1H, dd, *J* = 9.7, 8.9 Hz, H-3), 3.851 (1H, dd, *J* = 11.7, 2.3 Hz, H-6d), 4.240 (1H, ddd, *J* = 12.8, 6.6, 1.4 Hz, H-1'u), 4.407 (1H, ddd, *J* = 12.8, 5.8, 1.6 Hz, H-1'd), 4.922 (1H, d, *J* = 3.7 Hz, H-1), 6.410 (1H, ddd, *J* = 16.0, 6.6, 5.8 Hz, H-2'), 6.714 (1H, ddd, *J* = 16.0, 1.6, 1.4 Hz, H-3'), 7.242 (1H, m, H-*para*), 7.321 (2H, m, H-*meta*), 7.439 (2H, m, H-*ortho*)

^{13}C NMR (150.94 MHz, CD_3OD, 25 °C): 63.03 (C-6), 69.44 (C-1'), 72.18 (C-4), 73.87 (C-2), 74.15 (C-5), 75.44 (C-3), 99.61 (C-1), 126.89 (C-2'), 127.82 (C-*ortho*), 129.01 (C-*para*), 129.89 (C-*meta*), 134.21 (C-3'), 138.52 (C-*ipso*)

Geranyl α-D-glucopyranoside

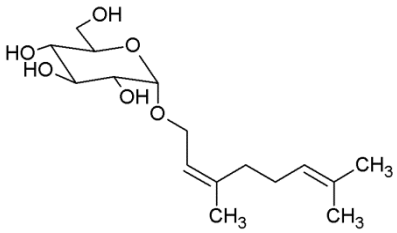

^{1}H NMR (600.23 MHz, CD_3OD, 25 °C): 1.630 (3H, s, H-9'), 1.695 (3H, q, *J* = 1.0 Hz, H-8'), 1.715 (3H, s, 3'-Me), 2.067 (2H, m, H-4'), 2.141 (2H, m, H-5'), 3.316(1H, dd, *J* = 9.9, 8.8 Hz, H-4), 3.403 (1H, dd, *J* = 9.7, 3.8 Hz, H-2), 3.608 (1H, ddd, *J* = 9.9, 5.5, 2.4 Hz, H-5), 3.658 (1H, dd, *J* = 9.7, 8.8 Hz, H-3), 3.704 (1H, ddd, *J* = 11.8, 5.5 Hz, H-6u), 3.824 (1H, dd, *J* = 11.8, 2.4 Hz, H-6d), 4.121 (1H, dd, *J* = 12.1, 7.5 Hz, H-1'u), 4.242 (1H, dd, *J* = 12.1, 6.4 Hz, H-1'd), 4.838 (1H, d, *J* = 3.8 Hz, H-1), 5.128 (1H, m, H-6'), 5.409 (1H, m, H-2')

^{13}C NMR (150.94 MHz, CD_3OD, 25 °C): 16.79 (3'-Me), 18.04 (C-9'), 26.17 (C-8'), 27.74 (C-5'), 41.01 (C-4'), 62.96 (C-6), 65.11 (C-1'), 72.12 (C-4), 73.85 (C-2), 73.97 (C-5), 75.49 (C-3), 99.17 (C-1), 121.95 (C-2'), 125.36 (C-6'), 132.82 (C-7'), 141.86 (C-3')

6 SUPPLEMENTARY INFORMATION

Table S4.1 Solubility of various acceptors in ethyl acetate, octane, butyl acetate and methyl-*tert*-butylether at 50 °C.

Acceptor	Solubility (mg/mL)			
	EtOAc	BuOAc	MTBE	octane
Gallic acid ethyl ester	200 – 210	50 – 60	90 – 100	< 10
Hydroquinone	170 – 180	50 – 60	60 – 70	< 10
Pyrogallol	490 – 500	210 – 220	240 – 250	< 10
Saligenin	450 – 460	230 – 240	250 – 260	< 10
Curcumin	10 – 20	10 – 20	< 10	< 10
Resveratrol	10 – 20	< 10	< 10	< 10
p-Nitrophenol	740 – 750	480 – 490	540 – 550	< 10
Vanillyl alcohol	20 – 30	< 10	< 10	< 10

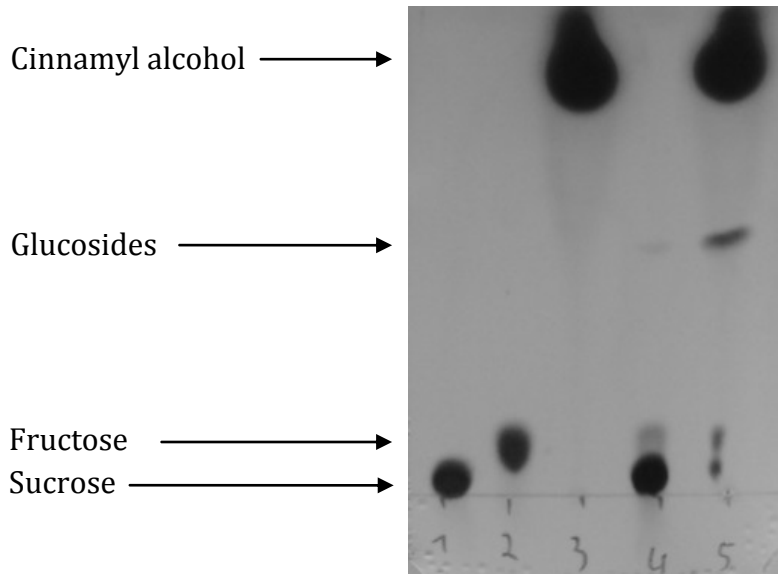

Figure S4.1 Glycosylation of cinnamyl alcohol with sucrose phosphorylase from *B. adolescentis*. Standards of sucrose (1), fructose (2) and cinnamyl alcohol (3) were spotted along the aqueous phase (4) and the cinnamyl alcohol phase (5) after 48 h incubation at 60 °C.

CHAPTER 5

Chemoenzymatic synthesis of β-D-glucosides using cellobiose phosphorylase from *Clostridium thermocellum.*

This chapter has been published as:

K. De Winter, L. Van Renterghem, K. Wuyts, H. Pelantova, V. Kren, W. Soetaert and T. Desmet, **2015**, Chemoenzymatic synthesis of β-D-glucosides using cellobiose phosphorylase from *Clostridium thermocellum*, *Advanced Synthesis & Catalysis*, 357, 1961-1969.

1 ABSTRACT

As illustrated in the previous chapters, disaccharide phosphorylases have been successfully applied for the synthesis of numerous α-glucosides. In contrast, much less research has been done with respect to the production of β-glucosides. Although cellobiose phosphorylase (CP) was already successfully used for the synthesis of various disaccharides and branched trisaccharides, its glycosylation potential towards small organic compounds hasn't been explored to date. Unfortunately, disaccharide phosphorylases typically have a very low affinity for non-carbohydrate acceptors, which urges the addition of solvents. The IL AMMOENG 101 and EtOAc were identified as the most promising solvents, allowing the synthesis of various β-glucosides. Next to hexyl, heptyl, octyl, nonyl, decyl and undecyl β-D-glucopyranoside, also the formation of vanillyl 4-O-β-D-glucopyranoside, 2-phenylethyl β-D-glucopyranoside, β-citronellyl β-D-glucopyranoside and 1-O-β-D-glucopyranosyl hydroquinone was confirmed by NMR spectroscopy. Moreover, the stability of CP could be drastically improved by creating cross-linked enzyme aggregates, while the efficiency of the biocatalyst for the synthesis of octyl β-D-glucopyranoside was doubled by imprinting with octanol. The usefulness of the latter system was illustrated by performing three consecutive batch conversions with octanol iCLEAs, yielding roughly 2 g of octyl β-D-glucopyranoside.

2 INTRODUCTION

Despite the continuous development of new procedures, the synthesis of glycosides still remains a challenge to date[15]. Numerous chemical routes have been described for the production of these molecules, but their application is limited by poor yields, the use of toxic catalysts and the generation of waste[13]. Consequently, biocatalytic approaches have received increasing attention in recent years as promising alternative for glycoside synthesis[18]. Indeed, enzymatic glycosylation reactions enable one-step conversions with high regio- and stereoselectivity; thereby generating 5-fold less waste[19].

Over the past decade, disaccharide phosphorylases have been identified as potent enzymes for the synthesis of glycosides. While glycosyltransferases require expensive nucleotide-activated sugars[97] and glycoside hydrolases suffer from unfavorable equilibrium constants[18], these enzymes use cheap glycosyl phosphate donors and can be efficiently used in the synthesis direction[29]. Examples include the α-glucosylation of alcohols with maltose phosphorylase[140] and the synthesis of 2-*O*-α-D-glucopyranosyl glycerol[40] (CHAPTER 2), 1-*O*-α-D-glucopyranosyl hydroquinone[125] (CHAPTER 4), 2-*O*-α-D-glucopyranosyl L-ascorbic acid,[7] and geranyl α-D-glucopyranoside[141] (CHAPTER 4) using sucrose phosphorylase (SP). In CHAPTER 3, it is shown that the efficiency of these glucosylation reactions can be vastly improved by the addition of ionic liquids (ILs), while CHAPTER 4 illustrated the usefulness of biphasic catalysis. Moreover, various immobilization techniques have been successfully applied resulting in biocatalysts with enhanced activity and stability, while allowing their recycling in repetitive batch conversions (CHAPTER 1 and 2). In contrast to the extended work on α-glucosides, only a single report describing the synthesis of β-glucosides with disaccharide phosphorylases is known to date[142]. Nevertheless, numerous biologically active molecules exist as β-glucosides in nature. For example arbutin, the β-glucoside of hydroquinone, can be found in wheat, pear skins and *Bergenia crassifolia*[143]. This skin whitening compound is used in cosmetics to reduce irritation caused by hydroquinone[144] and treat urogenital tract infections[145]. Alkyl β-glucosides, on the other hand, are potent non-ionic surfactants with good emulsifying and antimicrobial properties[146]. These compounds are widely used in pharmaceuticals, detergents, and food ingredients[147].

Cellobiose phosphorylase (CP) catalyzes the reversible phosphorolysis of cellobiose and inorganic phosphate to α-D-glucose 1-phosphate (αG1P) and D-glucose[148]. Unlike SP, CP is an inverting phosphorylase following a single displacement reaction, thereby forming glycosides with opposite anomeric configuration compared to the donor substrate[149]. Thanks to its relatively broad acceptor specificity with respect to carbohydrates, CP has been successfully used for the synthesis of various disaccharides[150] and branched trisaccharides[36]. More recently, mutant CPs with enhanced activity towards alkyl[42] and aryl β-glucosides[151] have been reported. Nevertheless, all of these acceptors contain a glucose moiety as point of attachment whereas the direct glycosylation of non-carbohydrate acceptors such as long-chain alcohols, flavonoids, alkaloids, phenolics and terpenes has not been achieved yet.

In this chapter, the glycosylation of various small organic compounds with the CP from *Clostridium thermocellum* is described in IL cosolvent and biphasic systems. Moreover, the enzyme was immobilized and imprinted to increase both the stability and activity of the biocatalyst.

3 RESULTS & DISCUSSION

3.1 Development of a suitable glycosylation system

Although much work has been done with the CP from *C. thermocellum* (CtCP), limited information on the kinetic thermostability of the enzyme is known to date. Nevertheless, carbohydrate conversions are preferably performed at elevated temperatures[58]. Therefore, the stability of the CtCP was evaluated at various temperatures (Figure 5.1).

In contrast to the rapid inactivation at 60 °C, CP was found to be remarkably stable at 37 °C. However, applying enzymes much below their optimal temperature typically comes at the expense of a lower turnover. A balance between stability and activity was found for CP at 50 °C, retaining over 58 % of its initial activity after 24 h, while operating at roughly 80 % of its maximal velocity[152].

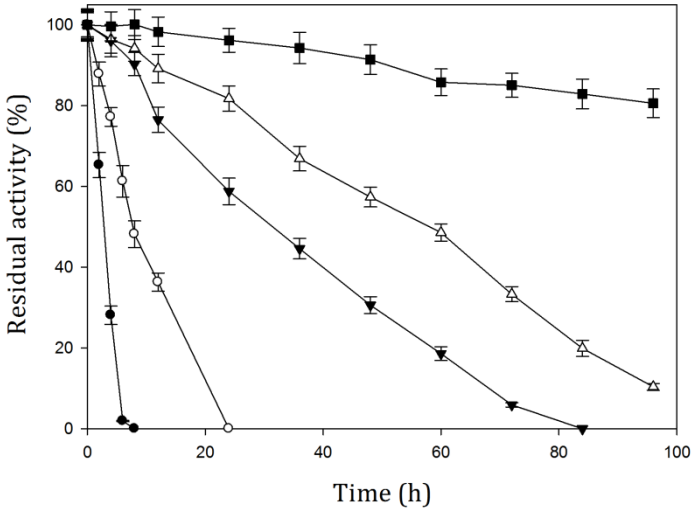

Figure 5.1 Kinetic thermostability of the CP from *C. thermocellum*. The enzyme was dissolved in MES buffer (50 mM, pH 6.5) an incubated at 37 (■), 45 (Δ), 50 (▼), 55 (○) and 60 °C (●).

In addition, the typically very low affinity of disaccharide phosphorylases for non-carbohydrate acceptors urges the addition of solvents[77]. Therefore, the half-life (t_{50}) of CtCP was also determined in the presence of some commonly used organic cosolvents, as well as in some ILs (Table 5.1).

Table 5.1 Stability of the CP from *C. thermocellum* at pH 6.5 and 50 °C, in the presence of various organic solvents and ILs.

	t_{50}[a] [min]	
Solvent	20 %	37.5 %
MeOH	229 ± 12	11.2 ± 0.9
EtOH	42.1 ± 3.3	3.5 ± 0.3
DMSO	736 ± 49	256 ± 19
[BMIM][dca]	24.2 ± 2.2	3.5 ± 0.2
[BMIM][I]	<1	<1
[BMIM][BF_4]	3.2 ± 0.1	<1
[MMIM] [$MeSO_4$]	82.6 ± 6.2	10.3 ± 0.6
AMMOENG 101	1092 ± 96	654 ± 48
EtOAc	966 ± 78	902 ± 64

[a] The time required to reduce the initial enzymatic activity by 50 % at 50 °C.

Both methanol and ethanol were found to destabilize CP, reducing the t_{50} at 50 °C from over 32 h to less than 4 and 1 h, respectively. Moreover, these short chain alcohols can be glycosylated by CP[142], impairing their application as cosolvent. In parallel to SP, also the ILs [BMIM][dca], [BMIM][I] and [BMIM][BF_4] were found to destabilize CP, while DMSO and the quaternary ammonium salt AMMOENG 101 were less deleterious for the stability of CP. Interestingly, the enzyme was also found to be compatible with EtOAc, allowing the use of biphasic catalysis. In contrast to the application of cosolvents, increasing the EtOAc concentration from 20 to 37.5 % did not significantly influence the stability of CP (Table 5.1). Next, the activity of the enzyme was assessed in the most promising solvent systems. CP displayed a relative activity of 94 and 92 % in 20 % IL and 37.5 % EtOAc respectively, thus allowing its use in the latter solvent systems.

3.2 Exploring the glycosylation potential of CP

Having established adequate cosolvent and biphasic catalysis conditions, the glycosylation potential of CP towards various small organic compounds was evaluated. Table 5.2 illustrates the broad acceptor promiscuity of the CP from *C. thermocellum.* The synthesis of alkyl β-glucosides was found to show similar characteristics to glycosidases[153]. Indeed, increasing the chain length resulted in decreased glucoside concentrations, and primary alcohols were found to be more easily glycosylated compared to secondary alcohols. For example, after 48 h incubation under optimal reaction conditions, 70.6 and 68.4 mM hexyl and octyl β-D-glucopyranoside were obtained. In contrast barely any glucosides could be detected when using 2-hexanol or 2-octanol as acceptor.

Interestingly, the glycosylation potential of CP is not limited to linear aliphatic alcohols. Next to cyclohexanol, some substituted alcohols with olfactory properties were successfully glucosylated. Despite being produced in lower concentrations, we were able to confirm the formation of vanillyl 4-*O*-β-D-glucopyranoside, β-citronellyl β-D-glucopyranoside and 2-phenylethyl β-D-glucopyranoside. Glycosylation of both *R* and *S*-1-phenylethanol failed, confirming the difficult glycosylation of secondary alcohols.

Table 5.2 Glycosylation potential of the CP from *C. thermocellum*. TLC or HPLC analysis was performed after 48 h incubation at 50 °C.

Acceptor	Product (mM)	Acceptor	Product (mM)
Pentanol	+ [a, d]	1*R*-phenylethanol	- [a]
Hexanol	70.6 [a]	1*S*-phenylethanol	- [a]
Heptanol	72.2 [a]	2-Phenylethanol	58.7 [a]
Octanol	68.4 [a]	Cinnamyl alcohol	+ [a]
Nonanol	54.6 [a]	Menthol	- [b], - [c]
Decanol	48.3 [a]	Vannillyl alcohol	24.5[b], 26.3[c]
Dodecanol	29.6 [a]	Phenol	- [b], - [c]
Cyclohexanol	+ [a]	*p*-Nitrophenol	- [b], - [c]
2-Hexanol	+ [a]	Hydroquinone	1.9 [b], 1.8[c]
2-Octanol	+ [a]	Catechol	- [b], - [c]
Linalool	- [a, e]	Resorcinol	- [b], - [c]
Eugenol	- [a]	Pyrogallol	+ [b], + [c]
β-Citronellol	19.8 [a]	Curcumin	- [b], - [c]
Geraniol	+ [a]	Quercetin	- [b], - [c]
Nerolidol	- [a]	Resveratrol	- [b], - [c]
Anisyl alcohol	+ [a]	Vanillin	+ [b], + [c]

[a] Glycosylation was performed using 37.5 % acceptor as organic phase. [b] Glycosylation was performed using 37.5 % EtOAc as organic phase. [c] Glycosylation was performed in a cosolvent system containing 20 % IL. [d] +, Product was detected by TLC analysis. [e] -, No product was detected by TLC analysis.

CtCP was also able to couple a glucose moiety to the phenolic hydroxyl groups of hydroquinone, pyrogallol and vanillin. Although these reactions were rather inefficient compared to SP, 1-*O*-β-D-glucopyranosyl hydroquinone could be isolated, and its structure was confirmed by NMR spectroscopy. Remarkably, no significant differences were observed between the IL based cosolvent and biphasic system.

3.3 Cross-linked enzyme aggregates of CP

Over the past decade, immobilization has proven to be a valuable technique to enhance the operational stability of enzymes[154]. Unlike other immobilization techniques, the formation of cross-linked enzyme aggregates (CLEAs) does not require expensive carriers, and avoids dilution of the enzyme's activity[155]. First, the precipitation of CP was

evaluated in the presence of *tert*-butanol (Figure 5.2). While 80 % of the enzyme remained soluble after the addition of 20 % *tert*-butanol, all CP was precipitated after 30 min incubation at a solvent concentration of 50 %. Lower concentrations or shorter incubation failed to yield complete precipitation (Figure 5.2).

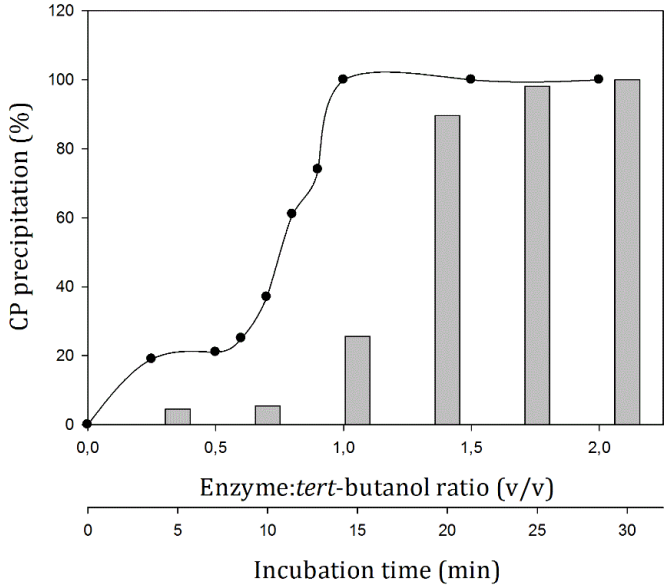

Figure 5.2 Precipitation of the CP from *C. thermocellum*. Various ratios of CtCP and *tert*-butanol were incubated during 30 min at 4 °C (●). The incubation time was varied at a volumetric ratio of 1 (bars).

Next, the glutaraldehyde (GA) based cross-linking step was optimized by varying the amount of cross-linker and the incubation time (Figure 5.3).

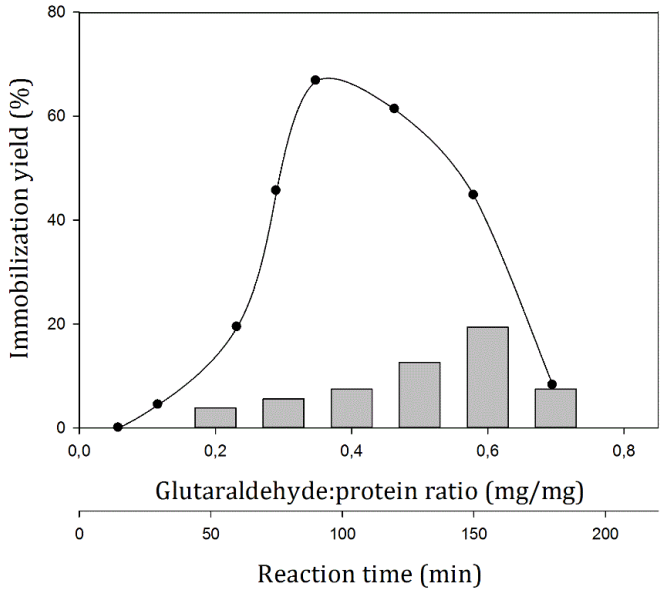

Figure 5.3 Optimization of CP CLEA formation. The gluateraldehyde:protein ratio was varied using a reaction time of 1h (bars), while the reaction time was varied at a ratio of 0.6 (●).

A maximal yield of 67 % was reached when incubating the enzyme at a GA:protein ratio of 0.6 for 90 min. Lower ratios or shorter incubation resulted in less CLEA, while further increasing the amount of GA or the incubation time strongly reduced the activity of the immobilized biocatalyst (Figure 5.3).

In parallel with previous studies on SP, the optimal temperature of the obtained CP CLEAs shifted from 70 °C for the soluble enzyme, to an impressive 90 °C (Figure 5.4)[45]. The observed difference can be explained by the increased mobility of the reactants at this elevated temperature (enhanced substrate diffusion), while maintaining the enzyme in a stable conformation through immobilization. The increased optimal temperature can thus been considered an indirect effect caused by the increased stability of the immobilized biocatalyst. Moreover, the pH range was found to have broadened (Figure S5.1), indicating enhanced operational stability.

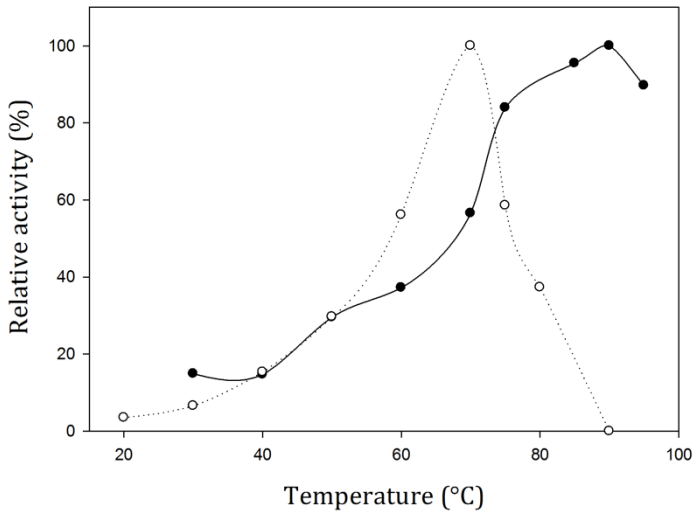

Figure 5.4 The effect of temperature on the activity of soluble (○) and immobilized (●) CP from *C. thermocellum*. The activity was measured in a MES buffer (50 mM, pH 6.5) containing 50 mM αG1P and 50 mM glucose.

The latter was further investigated by determining the stability of the CP CLEAs at 50 °C (Figure 5.5). Immobilization boosted the half-life at 50 °C from 34 h to almost 11 days. A similar pattern was observed upon addition of the IL AMMOENG 101 or EtOAc, revealing close correlation between thermal and solvent stability.

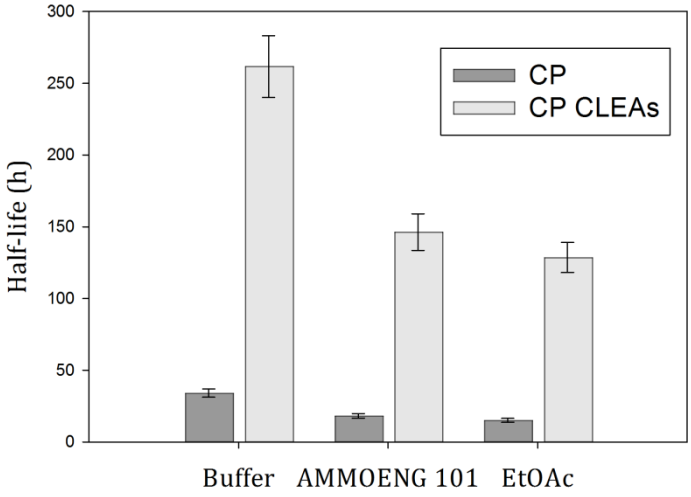

Figure 5.5 Half-life of CP and CP CLEAs at 50 °C. The biocatalysts were incubated in MES buffer (50 mM, pH 6.5) containing 20 % AMMOENG 101 or 37.5 % EtOAc.

3.4 Imprinted cross-linked enzyme aggregates of CP

In CHAPTER 2, it has been shown that the activity of CLEAs can be improved by molecular imprinting. The applicability of the latter technique was evaluated using the glycosylation of octanol as case study. To that end, CP was incubated with 250 mM octanol or octyl β-D-glucopyranoside (OG) prior to the formation of CLEAs. The effectiveness of the obtained immobilizates for the synthesis of OG was then evaluated (Figure 5.6).

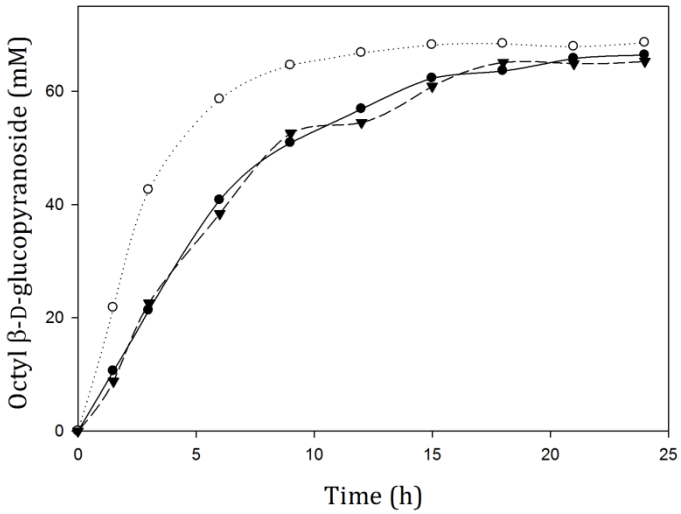

Figure 5.6 Synthesis of octyl β-D-glucopyranoside at 50 °C. Biphasic catalysis was performed with CP CLEAs (●), octyl β-D-glucopyranoside iCLEAs (▼) or octanol iCLEAs (○).

Imprinting with OG did not significantly increase the transglycosylation activity of the enzyme, but the addition of octanol roughly doubled the initial rate of OG synthesis (Figure 5.6). Interestingly, the activity of both iCLEAs towards glucose was decreased by 80 and 45 %, respectively, further illustrating their altered specificity. In contrast to SP (CHAPTER 2) imprinting with the acceptor molecule rather than the glucoside was found to enhance the desired glycosylation activity.

Finally, the applicability and reusability of the octanol iCLEAs was assessed at 50 mL scale. After 24 h incubation at 50 °C, the iCLEAs were recuperated by centrifugation and the reaction mixture was subjected to hydrophobic membrane filtration. Next, the octanol phase was evaporated *in vacuo*, yielding 674 mg octyl β-D-glucopyranoside. This procedure was repeated three times without loss of productivity, revealing excellent mechanical stability and recyclability of the biocatalyst.

4 CONCLUSION

In this chapter, the stability of CP was assessed at elevated temperatures in the presence of various solvents. CtCP was found to be compatible with the IL AMMOENG 101 and EtOAc, allowing the glycosylation of aliphatic alcohols, monoterpenoids, aromatic alcohols and phenolics. The stability of the biocatalyst could be improved by cross-linking the enzyme, resulting in an impressive half-life at 50 °C of 11 days. Moreover, the efficiency of the CLEAs for the synthesis of octyl β-D-glucopyranoside could be roughly doubled by molecular imprinting with octanol. As proof of concept, three consecutive batch productions of octyl β-D-glucopyranoside were performed, revealing the excellent operational stability and recyclability of the CP octanol iCLEAs. Consequently, CP was identified to be a valuable alternative for the synthesis of β-glucosides.

5 MATERIALS & METHODS

5.1 Materials

The IL AMMOENG 101 was kindly provided by Evonik Industries AG, and EtOAc was bought from Fiers. The other ILs were purchased from IoLiTec Ionic Liquids Technologies GmbH, and had a purity of at least 99 %. All other chemicals were analytical grade and purchased from Sigma-Aldrich.

5.2 Production and purification of cellobiose phosphorylase

Overexpression of CP was carried out using *E. coli* JW0987 cells transformed with the expression vector pTrc99a harboring the codon optimized CP gene from *Clostridium thermocellum* YM4. The strain was routinely grown at 37 °C on 500 mL LB medium (10 g/L tryptone, 5 g/L yeast extract, 5 g/L NaCl) supplemented with ampicillin (100 mg/L). After overnight growth, the culture was inoculated into 15 L of double LB medium (20 g/L tryptone, 10 g/L yeast extract, 5 g/L NaCl) supplemented with glucose (30 g/L) and ampicillin (100 mg/L) in a 30 L Biostat C reactor (B. Braun Biotech Inc., Pennsylvania). The temperature, pH and stirrer speed were set at 37 °C, 7 and 800 rpm respectively. Adequate aeration was achieved by passing 1.1 vvm air through the reactor, and foaming was prevented by manually adding anti-foam (10 % (v/v) antifoam silicone Snapsil RE 20, VWR BDH Prolabo) when required. Induction was performed by adding IPTG to a final concentration of 0.1 mM as soon as the OD_{600} reached 0.6. After 8 h of growth (OD_{600} ~ 34), the cells were harvested by centrifugation (10 000 g, 4 °C, 20 min), and frozen at -20 °C.

Next, the obtained pellets were lysed as described in CHAPTER 2 and the *N*-terminal His_6-tagged protein was purified by nickel-nitrilotriacetic acid metal affinity chromatography. The protocol as described by the supplier (Qiagen) was used, except for the imidazole concentration of the elution buffer, which was reduced to 175 mM. The obtained enzyme solution was washed with MES buffer (50 mM, pH 6.5) and concentrated using Centricons (Amicon Ultra 30K, Millipore).

5.3 Preparation of CLEAs and iCLEAs

Cross-linked enzyme aggregates of CP were prepared by adding 100 µL *tert*-butanol to 100 µL His_6-tagged purified protein (2.4 mg/mL) under agitation in a thermoshaker (Eppendorf) at 1000 rpm. After 30 min incubation at 4 °C, varying amounts of glutaraldehyde (25 % (v/v)) were added and the mixture was kept under stirring for 15, 30, 60, 75, 90, 120, 150 or 180 min. Reduction of the formed imine bonds was achieved by adding 500 µL sodium bicarbonate buffer (100 mM, pH 10.0) supplemented with sodium borohydride (1 mg/mL). After 15 min incubation at 4 °C, another 500 µL was added and allowed to react during 15 min. Next, the resulting CLEAs were harvested by

centrifugation (17 000 g, 4 °C, 15 min), and subsequently washed 5 times with 1 mL MES buffer (50 mM, pH 6.5). iCLEAs were prepared by incubating CP with 250 mM octanol (3.25 mg) or octyl β-D-glucopyranoside (7.31 mg) during 30 min at 37 °C prior to the addition of *tert*-butanol.

Large-scale production of CLEAs and iCLEAs was performed by adding 4 mL *tert*-butanol to 4 mL His_6-tagged purified protein (2.4 mg/mL) in 50 mL falcons. The glutaraldehyde:protein ratio was set at 0.6 (5.76 mg), and the reaction mixture was incubated during 90 min at 4 °C. Next, two times 10 mL sodium bicarbonate buffer (100 mM, pH 10.0) supplemented with sodium borohydride (1 mg/mL) was added. The CLEAs were then harvested by centrifugation (10 000 g, 4 °C, 20 min), washed 5 times with 20 mL MES buffer (50 mM, pH 6.5) and freeze-dried (Alpha 1-4, Christ).

5.4 Activity assays

The activity of CP and CP CLEAs was determined in the synthesis direction by measuring the release of phosphate from αG1P with the method of Gawronski and Benson[156]. One unit of CP activity corresponds to the release of 1 µmol phosphate per minute from 50 mM αG1P and 50 mM glucose in a 50 mM MES buffer at pH 6.5 and 37 °C. The activity of the CLEAs was determined by adding 1 mL substrate buffer (50 mM αG1P and 50 mM glucose in 50 mM MES buffer pH 6.5) to the obtained biocatalyst. The reactions were performed in a thermoshaker (Eppendorf) at 1000 rpm. Alternatively, a citrate-phosphate buffer (pH 4.0-5.4), MES buffer (pH 5.5-6.5), MOPS buffer (pH 6.6-7.5) and tricine buffer (pH 7.6-9.0) were used. Unless stated otherwise, the temperature was set at 37 °C. The immobilization yield is defined as the ratio of the activity detected in the CLEA preparation to that present in the original enzyme solution. Protein concentrations were measured according to the Lowry method, using bovine serum albumin as standard[92]. All assays were performed in triplicate and had a CV of less than 10 %. All reported errors correspond to the standard errors.

5.5 Stability assays

The kinetic thermostability was determined by diluting 20 U/mL CP in a 50 mM MES at pH 6.5. If required, solvents were added and the mixtures were incubated in a water bath at various temperatures. At regular intervals, samples were taken and diluted 200 times in 50 mM MES buffer at pH 6.5. The diluted samples were stored at 4 °C, and their activity was determined at 37 °C using the Gawronski method. The stability of the CLEAs was evaluated by incubating 6 mg CP CLEA in 1.5 mL MES buffer (50 mM, pH 6.5) in a thermoshaker (Eppendorf) at 1000 rpm. Alternatively, the MES buffer contained 20 % AMMOENG 101 or 37.5 % EtOAc. At regular intervals, homogeneous samples (100 µL) were taken after intensive mixing, centrifuged (17 000 g, 4 °C, 15 min) and washed three times with 1 mL MES buffer (50 mM, pH 6.5). The samples were stored at 4 °C, and the activity was determined at 37 °C using the Gawronski assay. The t_{50}-values, which is the time required to reduce the initial enzymatic activity by 50 % at a certain temperature, were calculated from the equations obtained by fitting the linear part of the stability curves.

5.6 Analytical methods

The formation of glucosides was assessed by TLC or HPLC. Separation and detection were achieved on Merck Silica gel 60 F_{254} precoated plates as described in CHAPTER 4. The concentration of glucosides was determined by HPLC analysis. Adequate separation and detection was achieved using an X-bridge amide column (250 mm × 4.6 mm, 3.5 µm, Waters, USA) coupled with an Alltech 2000ES ELSD, as described in CHAPTER 4. When using biphasic catalysis, homogeneous samples, obtained after intensive mixing, were diluted in DMSO. The resulting concentrations thus refer to the amount of product present in the total reaction volume. All calibration curves were prepared with authentic samples.

5.7 Glycosylation reactions with CP

Biphasic catalysis was performed by adding water immiscible acceptors (300 µL) to 500 µL 50 mM MES buffer at pH 6.5 containing 200 mM αG1P. Alternatively, 300 µL EtOAc supplemented with various acceptors (30 mg) was used as organic phase. Cosolvent catalysis was achieved by adding 200 µL AMMOENG 101 and various

acceptors (37.5 mg) to 800 µL 50 mM MES buffer at pH 6.5 containing 200 mM αG1P. All reactions were performed in a thermoshaker (eppendorf) at 1000 rpm and 50 °C in the presence of 5 U/mL CP. After 24 h, samples were inactivated (10 min at 95 °C) and subjected to TLC or HPLC analysis.

5.8 Production and purification of glucosides

The glycosylation of hexanol, heptanol, octanol, nonanol, decanol, dodecanol, β-citronellol and 2-phenylethanol was carried out by adding the acceptors (18.75 mL) to 31.25 mL 50 mM MES buffer at pH 6.5 containing 200 mM αG1P. Glycosylation of vannillyl alcohol and hydroquinone was achieved by using EtOAc (18.75 mL) containing the acceptors (1.875 g) as organic phase. All reactions were performed in magnetically stirred flasks at 50 °C in the presence of 5 U/mL CP. After 48 h, the reaction mixtures were heated (10 min, 95 °C) and centrifuged (10 000 g, 4 °C, 20 min) to remove debris. The samples were then evaporated *in vacuo* and the residue was purified by column chromatography (silicagel, EtOAC/MeOH/H_2O = 30:5:4).

Synthesis of octyl β-D-glucopyranoside was carried out at 50 mL scale in a biphasic system consisting of octanol (18.75 mL) and 31.25 mL 50 mM MES buffer at pH 6.5 containing 200 mM αG1P. The reactions were performed in magnetically stirred flasks at 50 °C in the presence of 40 mg CP CLEA, octanol iCLEA or octyl β-D-glucopyranoside iCLEA respectively. At regular intervals, samples were inactivated (10 min at 95 °C) and subjected to HPLC analysis. Alternatively, the reaction was stopped after 24 h incubation at 50 °C. The octanol iCLEAs were recuperated by centrifugation (10 000 g, 4 °C, 20 min), and the reaction mixture was passed through a pretreated hydrophobic membrane (Accurel PP1E, Membrane, Germany). Prior to its application, the membrane was consecutively treated with 50 mL of the following solutions: hexadecane, hexadecane/water (50:50), octanol and finally an octanol/water (50:50). The resulting octanol phase was then evaporated *in vacuo* and the residue was weighed. The iCLEAs were recycled for the next batch conversion.

5.9 Structure elucidation of glucosides

NMR spectra were measured on a Bruker AVANCE III 700 MHz spectrometer (700.13 MHz for ^{1}H and 176.05 MHz for ^{13}C) in CD_3OD at 25 °C. Residual signals of solvent were used as an internal standard (δ_H 3.330 ppm, δ_C 49.3 ppm). ^{1}H NMR, ^{13}C NMR, COSY, HSQC, and HMBC spectra were measured using standard manufacturers' software (Topspin 3.2, Bruker BioSpin GmbH, Rheinstetten). Chemical shifts are given in δ-scale [ppm], and coupling constants in Hz. Digital resolution enabled us to report chemical shifts of protons to three and coupling constants to one and carbon chemical shifts to two decimal places. Some hydrogen chemical shifts were read out from HSQC and are reported to two decimal places. The proton spin systems were assigned by COSY, and then the assignment was transferred to carbons by HSQC. HMBC experiment enabled us to assign quaternary carbons and join individual spin systems together. Spectral analysis and interpretation was kindly performed by the group of Prof. Vladimír Křen at the Institute of Microbiology (Czech Republic).

Hexyl β-D-glucopyranoside

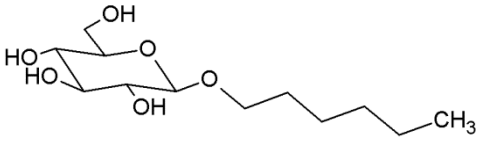

^{1}H NMR (CD_3OD): δ 0.926 (3H, t, *J* = 7.1 Hz, H-6'), 1.33 (2H, m, H-4'), 1.35 (2H, m, H-5'), 1.404 (2H, m, H-3'), 1.638 (2H, m, H-2'), 3.200 (1H, dd, *J* = 9.2, 7.8 Hz, H-2), 3.281 (1H, ddd, *J* = 9.6, 5.6, 2.3 Hz, H-5), 3.320 (1H, dd, *J* = 9.6, 8.7 Hz, H-4), 3.381 (1H, dd, *J* = 9.2, 8.7 Hz, H-3), 3.554 (1H, dt, *J* = 9.6, 6.8 Hz, H-1'u), 3.696 (1H, dd, *J* = 11.9, 5.6 Hz, H-6u), 3.880 (1H, dd, *J* = 11.9, 2.3 Hz, H-6d), 3.916 (1H, dt, *J* = 9.6, 6.9 Hz, H-1'd), 4.273 (1H, d, *J* = 7.8 Hz, H-1)

^{13}C NMR (CD_3OD): δ 14.68 (C-6'), 23.91 (C-5'), 27.01 (C-3'), 30.98 (C-2'), 33.10 (C-4'), 62.97 (C-6), 71.14 (C-1'), 71.83 (C-4), 75.28 (C-2), 78.05 (C-5), 78.29 (C-3), 104.54 (C-1)

Heptyl β-D-glucopyranoside

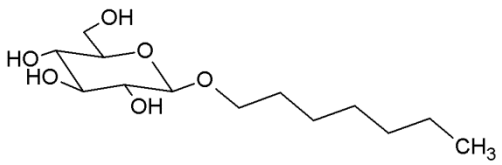

^{1}H NMR (CD_3OD): δ 0.921 (3H, t, *J* = 7.1 Hz, H-7'), 1.33 (2H, m, H-5'), 1.34 (2H, m, H-6'), 1.36 (2H, m, H-4'), 1.398 (2H, m, H-3'), 1.640 (2H, m, H-2'), 3.197 (1H, dd, *J* = 9.2, 7.8 Hz, H-2), 3.279 (1H, ddd, *J* = 9.6, 5.6, 2.3 Hz, H-5), 3.317 (1H, dd, *J* = 9.6, 8.7 Hz, H-4), 3.379 (1H, dd, *J* = 9.2, 8.7 Hz, H-3), 3.553 (1H, dt, *J* = 9.6, 6.8 Hz, H-1'u), 3.695 (1H, dd, *J* = 11.9, 5.6 Hz, H-6u), 3.880 (1H, dd, *J* = 11.9, 2.3 Hz, H-6d), 3.915 (1H, dt, *J* = 9.6, 6.9 Hz, H-1'd), 4.271 (1H, d, *J* = 7.8 Hz, H-1)

^{13}C NMR (CD_3OD): δ 14.72 (C-7'), 23.92 (C-6'), 27.31 (C-3'), 30.54 (C-4'), 31.04 (C-2'), 33.25 (C-5'), 62.99 (C-6), 71.14 (C-1'), 71.86 (C-4), 75.31 (C-2), 78.08 (C-5), 78.31 (C-3), 104.56 (C-1)

Octyl β-D-glucopyranoside

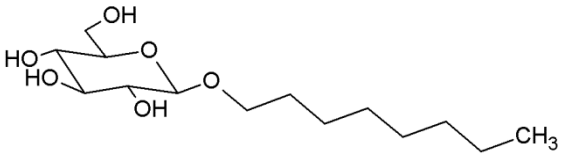

^{1}H NMR (CD_3OD): δ 0.921 (3H, t, *J* = 7.1 Hz, H-8'), 1.31 (2H, m, H-6'), 1.33 (4H, m, H-4', H-7'), 1.34 (2H, m, H-5'), 1.402 (2H, m, H-3'), 1.640 (2H, m, H-2'), 3.191 (1H, dd, *J* = 9.2, 7.8 Hz, H-2), 3.274 (1H, ddd, *J* = 9.6, 5.5, 2.2 Hz, H-5), 3.309 (1H, dd, *J* = 9.6, 8.6 Hz, H-4), 3.370 (1H, dd, *J* = 9.2, 8.6 Hz, H-3), 3.553 (1H, dt, *J* = 9.6, 6.8 Hz, H-1'u), 3.690 (1H, dd, *J* = 11.9, 5.5 Hz, H-6u), 3.881 (1H, dd, *J* = 11.9, 2.2 Hz, H-6d), 3.917 (1H, dt, *J* = 9.6, 6.9 Hz, H-1'd), 4.267 (1H, d, *J* = 7.8 Hz, H-1)

^{13}C NMR (CD_3OD): δ 14.72 (C-8'), 24.00 (C-7'), 27.39 (C-3'), 30.70[a] (C-4'), 30.87[a] (C-5'), 31.08 (C-2'), 33.29 (C-6'), 63.04 (C-6), 71.18 (C-1'), 71.92 (C-4), 75.38 (C-2), 78.16 (C-5), 78.38 (C-3), 104.62 (C-1); [a] might be interchanged

Nonyl β-D-glucopyranoside

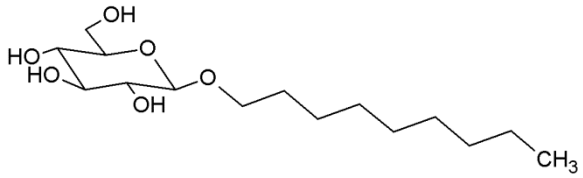

^{1}H NMR (CD_3OD): δ 0.921 (3H, t, *J* = 7.1 Hz, H-9'), 1.31 (2H, m, H-7'), 1.32 (2H, m, H-8'), 1.33 (6H, m, H-4', H-5', H-6'), 1.403 (2H, m, H-3'), 1.640 (2H, m, H-2'), 3.187 (1H, dd, *J* = 9.2, 7.8 Hz, H-2), 3.271 (1H, ddd, *J* = 9.6, 5.5, 2.2 Hz, H-5), 3.303 (1H, dd, *J* = 9.6, 8.5 Hz, H-4), 3.363 (1H, dd, *J* = 9.2, 8.5 Hz, H-3), 3.553 (1H, dt, *J* = 9.6, 6.8 Hz, H-1'u), 3.686 (1H, dd, *J* = 11.9, 5.5 Hz, H-6u), 3.881 (1H, dd, *J* = 11.9, 2.2 Hz, H-6d), 3.918 (1H, dt, *J* = 9.6, 6.9 Hz, H-1'd), 4.265 (1H, d, *J* = 7.8 Hz, H-1)

^{13}C NMR (CD_3OD): δ 14.73 (C-9'), 24.03 (C-8'), 27.42 (C-3'), 30.73[a] (C-6'), 30.94[a] (C-5'), 31.02[a] (C-4'), 31.11 (C-2'), 33.36 (C-7'), 63.08 (C-6), 71.20 (C-1'), 71.97 (C-4), 75.43 (C-2), 78.21 (C-5), 78.44 (C-3), 104.67 (C-1); [a] might be interchanged

Decyl β-D-glucopyranoside

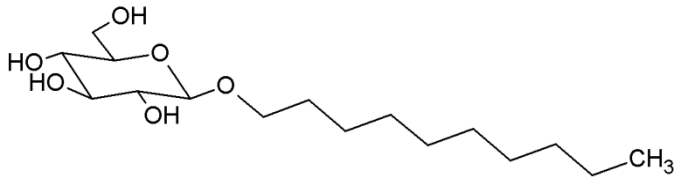

^{1}H NMR (CD_3OD): δ 0.920 (3H, t, *J* = 7.1 Hz, H-10'), 1.30 (2H, m, H-8'), 1.32 (2H, m, H-7'), 1.33 (8H, m, H-4', H-5', H-6', H-9'), 1.403 (2H, m, H-3'), 1.640 (2H, m, H-2'), 3.189 (1H, dd, *J* = 9.2, 7.8 Hz, H-2), 3.273 (1H, ddd, *J* = 9.6, 5.5, 2.2 Hz, H-5), 3.305 (1H, dd, *J* = 9.6, 8.5 Hz, H-4), 3.365 (1H, dd, *J* = 9.2, 8.5 Hz, H-3), 3.553 (1H, dt, *J* = 9.6, 6.8 Hz, H-1'u), 3.688 (1H, dd, *J* = 11.9, 5.5 Hz, H-6u), 3.882 (1H, dd, *J* = 11.9, 2.2 Hz, H-6d), 3.918 (1H, dt, *J* = 9.6, 6.9 Hz, H-1'd), 4.266 (1H, d, *J* = 7.8 Hz, H-1)

^{13}C NMR (CD_3OD): δ 14.74 (C-10'), 24.03 (C-9'), 27.41 (C-3'), 30.77[a] (C-7'), 30.93[a] (C-6'), 31.01[a] (C-5'), 31.05[a] (C-4'), 31.10 (C-2'), 33.36 (C-8'), 63.07 (C-6), 71.20 (C-1'), 71.95 (C-4), 75.41 (C-2), 78.20 (C-5), 78.42 (C-3), 104.66 (C-1); [a] might be interchanged

Dodecyl β-D-glucopyranoside

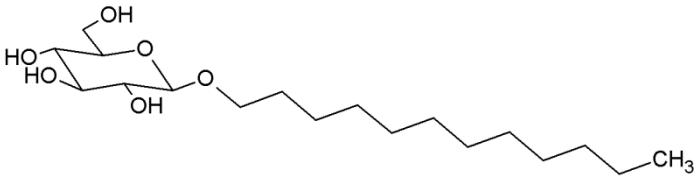

^{1}H NMR (CD_3OD): δ 0.920 (3H, t, *J* = 7.1 Hz, H-11'), 1.31 (4H, m, H-8', H-9'), 1.32 (6H, m, H-4', H-5', H-6'), 1.33 (4H, m, H-7', H-10'), 1.402 (2H, m, H-3'), 1.640 (2H, m, H-2'), 3.189 (1H, dd, *J* = 9.2, 7.8 Hz, H-2), 3.272 (1H, ddd, *J* = 9.6, 5.5, 2.2 Hz, H-5), 3.305 (1H, dd, *J* = 9.6, 8.5 Hz, H-4), 3.365 (1H, dd, *J* = 9.2, 8.5 Hz, H-3), 3.553 (1H, dt, *J* = 9.6, 6.8 Hz, H-1'u), 3.688 (1H, dd, *J* = 11.9, 5.5 Hz, H-6u), 3.881 (1H, dd, *J* = 11.9, 2.2 Hz, H-6d), 3.918 (1H, dt, *J* = 9.6, 6.9 Hz, H-1'd), 4.266 (1H, d, *J* = 7.8 Hz, H-1)

^{13}C NMR (CD_3OD): δ 14.74 (C-11'), 24.03 (C-10'), 27.41 (C-3'), 30.77[a] (C-8'), 30.93[a] (C-7'), 31.05[a] (C-5', C-6'), 31.10[a] (C-4', C-2'), 33.37 (C-9'), 63.07 (C-6), 71.20 (C-1'), 71.95 (C-4), 75.41 (C-2), 78.20 (C-5), 78.42 (C-3), 104.66 (C-1); [a] might be interchanged

2-Phenylethyl β-D-glucopyranoside

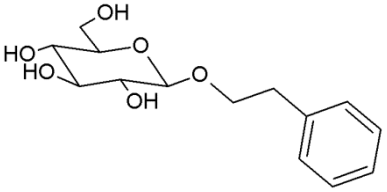

^{1}H NMR (CD_3OD): δ 2.941 (1H, m, Σ*J* = 25.0 Hz, H-2'u), 2.973 (1H, m, Σ*J* = 25.0 Hz, H-2'd), 3.205 (1H, dd, *J* = 9.2, 7.8 Hz, H-2), 3.286 (1H, m, H-5), 3.305 (1H, m, H-4), 3.369 (1H, dd, *J* = 9.2, 8.6 Hz, H-3), 3.684 (1H, dd, *J* = 11.9, 5.5 Hz, H-6u), 3.779 (1H, ddd, *J* = 9.7, 8.2, 6.7 Hz, H-1'u), 3.882 (1H, dd, *J* = 11.9, 2.1 Hz, H-6d), 4.111 (1H, ddd, *J* = 9.7, 8.2, 6.8 Hz, H-1'd), 4.322 (1H, d, *J* = 7.8 Hz, H-1), 7.197 (1H, m, H-*para*), 7.267 (4H, m, H-*ortho*, H-*meta*)

^{13}C NMR (CD_3OD): δ 37.53 (C-2'), 63.05 (C-6), 71.94 (C-4), 72.01 (C-1'), 75.40 (C-2), 78.26 (C-5), 78.40 (C-3), 104.68 (C-1), 127.50 (C-*para*), 129.64 (C-*meta*), 130.32 (C-*ortho*), 140.36 (C-*ipso*)

β-Citronellyl β-D-glucopyranoside

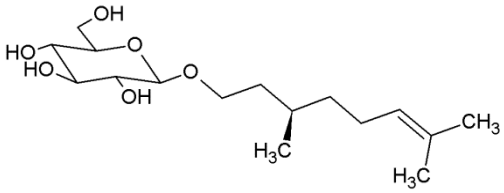

^{1}H NMR (CD_3OD): δ 0.935 (3H, d, J = 6.6 Hz, 3'-Me), 1.18 (1H, m, H-4'u), 1.37 (1H, m, H-4'd), 1.44 (1H, m, H-2'u), 1.610 (1H, m, H-3'), 1.627 (3H, d, *J* = 1.3 Hz, 7'-Me), 1.68 (1H, m, H-2'd), 1.692 (3H, d, *J* = 1.3 Hz, H-8'), 1.999 (1H, m, H-5'u), 2.040 (1H, m, H-5'd), 3.184 (1H, dd, *J* = 9.2, 7.8 Hz, H-2), 3.275 (1H, ddd, *J* = 9.6, 5.4, 2.2 Hz, H-5), 3.305 (1H, dd, *J* = 9.6, 8.5 Hz, H-4), 3.365 (1H, dd, *J* = 9.2, 8.5Hz, H-3), 3.606 (1H, ddd, J = 9.6, 8.0, 5.8 Hz, H-1'), 3.691 (1H, dd, *J* = 11.9, 5.4 Hz, H-6u), 3.885 (1H, dd, *J* = 11.9, 2.2 Hz, H-6d), 3.956 (1H, ddd, J = 9.6, 7.8, 6.8 Hz, H-1'd), 4.267 (1H, d, *J* = 7.8 Hz, H-1), 5.127 (1H, m, H-6')

^{13}C NMR (CD_3OD): δ 18.02 (7'-Me), 20.21 (3'-Me), 26.19 (C-8'), 26.77 (C-5'), 30.88 (C-3'), 38.04 (C-2'), 38.73 (C-4'), 63.07 (C-6), 69.43 (C-1'), 71.97 (C-4), 75.41 (C-2), 78.21 (C-5), 78.45 (C-3), 104.64 (C-1), 126.19 (C-6'), 132.25 (C-7')

Vanillyl 4-*O*-β-D-glucopyranoside

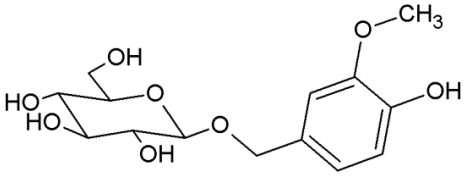

^{1}H NMR (CD_3OD): δ 3.253 (1H, dd, *J* = 9.1, 7.8 Hz, H-2), 3.272 (1H, ddd, *J* = 9.5, 5.8, 2.3 Hz, H-5), 3.311 (1H, dd, *J* = 9.5, 8.7 Hz, H-4), 3.354 (1H, dd, *J* = 9.1, 8.7 Hz, H-3), 3.710 (1H, dd, *J* = 11.9, 5.8 Hz, H-6u), 3.878 (3H, s, 3'-OMe), 3.918 (1H, dd, *J* = 11.9, 2.3 Hz, H-6d), 4.336 (1H, d, *J* = 7.8 Hz, H-1), 4.609 (1H, d, *J* = 11.4 Hz, CH_2 u), 4.838 (1H, d, *J* = 11.4 Hz, CH_2 d), 6.769 (1H, d, *J* = 8.0 Hz, H-5'), 6.845 (1H, dd, *J* = 8.0, 2.0 Hz, H-6'), 7.071 (1H, d, *J* = 2.0 Hz, H-2')

^{13}C NMR (CD_3OD): δ 56.67 (3'-OMe), 63.14 (C-6), 72.04[a] (CH_2), 72.05[a] (C-4), 75.42 (C-2), 78.32 (C-5), 78.40 (C-3), 103.04 (C-1), 113.62 (C-2'), 116.09 (C-5'), 122.76 (C-6'), 130.60 (C-1'), 147.65 (C-4'), 149.23 (C-3')); [a] might be interchanged

1-*O*-β-D-Glucopyranosyl hydroquinone

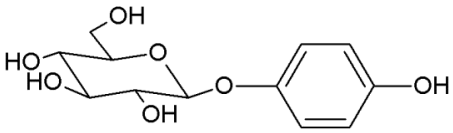

^{1}H NMR (CD_3OD): δ 3.395 (2H, m, H-4, H-5), 3.428 (1H, dd, *J* = 9.2, 7.5 Hz, H-2), 3.460 (1H, m, H-3), 3.718 (1H, m, H-6u), 3.902 (1H, m, H-6d), 4.755 (1H, d, *J* = 7.5 Hz, H-1), 6.718 (2H, m, Σ*J* = 9.1 Hz, H-*meta*), 6.985 (2H, m, Σ*J* = 9.1 Hz, H-*ortho*)

^{13}C NMR (CD_3OD): δ 62.84 (C-6), 71.72 (C-4), 75.27 (C-2), 78.27 (C-3), 78.32 (C-5), 103.92 (C-1), 116.90 (C-*meta*), 119.67 (C-*ortho*), 152.72 (C-*ipso*), 154.08 (C-*para*)

6 SUPPLEMENTARY INFORMATION

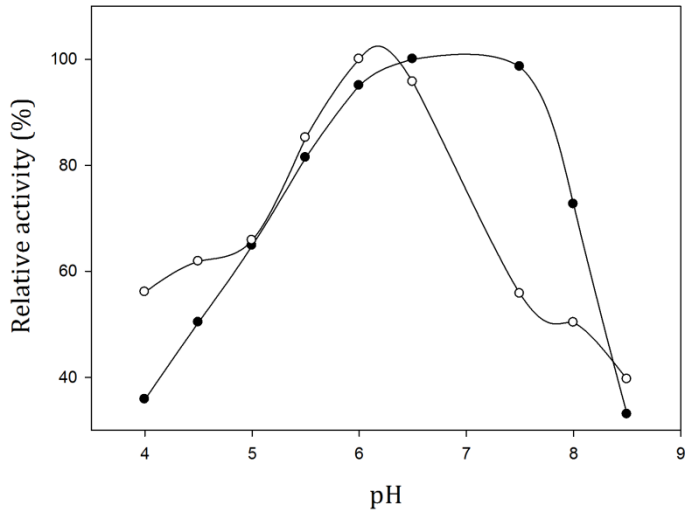

Figure S5.1 The effect of pH on the activity of soluble (○) and immobilized (●) CP from C. thermocellum. The activity was measured in a 50 mM buffer containing 50 mM αG1P and 50 mM glucose at 37 °C.

CHAPTER 6

Chemoenzymatic synthesis of α-L-rhamnosides using recombinant α-L-rhamnosidase from *Aspergillus terreus*

This chapter has been published as:

K. De Winter, D. Simcikova, B. Schalck, L. Weignerova, H. Pelantova, W. Soetaert, T. Desmet and V. Kren, **2013**, Chemoenzymatic synthesis of α-L-rhamnosides using recombinant α-L-rhamnosidase from *Aspergillus terreus*, *Bioresource Technology*, 147, 640-644.

1 ABSTRACT

This chapter describes an efficient, large scale fermentation of the recombinant α-L-rhamnosidase originating from *Aspergillus terreus*. High-cell-density *Pichia pastoris* fermentation resulted in yields up to 627 U/L/h. The recombinant enzyme was used for the reverse rhamnosylation of various small organic compounds. A full factorial experimental design setup was applied to identify the importance of temperature, substrate concentrations, solvent type and concentration as well as the acidity of the reaction mixture. Careful optimization of these parameters allowed the synthesis of a range of α-L-rhamnosides among which cyclohexyl α-L-rhamnopyranoside, anisyl α-L-rhamnopyranoside and 2-phenylethyl α-L-rhamnopyranoside. In addition, α-L-rhamnosylation of phenolic hydroxyls in phenols such as hydroquinone, resorcinol, catechol and phenol was observed, which is a rather unique reaction catalyzed by glycosidases.

2 INTRODUCTION

L-Rhamnose is widely distributed in plants and bacteria as a component of the cell walls[157] and of various natural products. Rhamnose is typically produced by the biocatalytic cleavage of rutin[158]. Some rhamnosides are important bioactive compounds, e.g., cytotoxic saponins[159], antifungal plant glycoalkaloids[160], and bacterial virulence factors[161]. Clear correlations between the presence of specific sugar residues and the biological activity of these molecules have been demonstrated in a plethora of examples[10]. In plants, L-rhamnose is also bound to some volatile compounds, e.g., aroma terpenol glycosides of wine[162]. Finally, *Citrus* spp. accumulate large amounts of L-rhamnose-containing flavonoid glycosides (e.g., naringin and hesperidin), having different flavors and important antioxidant and anti-inflammatory activity[163].

Quite recently α-L-rhamnose and/or α-L-rhamnosides were found to interact with the specific receptors on keratinocytes, which play an important role in cell and tissue aging[164]. This finding triggered a vigorous research in the cosmetic application of rhamnosides. Indeed, the use of rhamnose and rhamnosides has been patented[165] and the respective preparations have already reached the market. Later, it was found that rhamnose itself does not penetrate the skin but when conjugated, e.g. in the form of pentyl rhamnoside, its concentration in stratum corneum and epidermis is doubled[166]. Another rhamnoside, e.g. undecyl rhamnoside has anti-inflamatory activity in the skin, which is mediated by release inhibition of prostaglandin 2 and by the inhibition of NF-kB transcription factor. This demonstrates clearly the importance of the preparation of rhamnosides especially by enzymatic methods, which do not involve any harmful and irritant chemicals, making the products applicable in the cosmetics and food industry.

α-L-Rhamnosidase (EC 3.2.1.40) is known to be an inverting enzyme, not being able to catalyze transglycosylation reactions. Recently, the alkali- and thermo-stable α-L-rhamnosidase from *Aspergillus terreus* was described[167]. This extracellular α-L-rhamnosidase was purified, characterized, sequenced and expressed in *Pichia pastoris*. This chapter describes large scale fermentation of the α-L-rhamnosidase and reverse rhamnosylation of series aliphatic and aromatic alcohols using this recombinant

enzyme. To our best knowledge the glycosylation of phenolic OH groups catalyzed by glycosidases has not been described yet.

3 RESULTS & DISCUSSION

3.1 Production of recombinant α-L-rhamnosidase

The production of α-L-rhamnosidase by *Aspergillus terreus* has already been optimized yielding an expression level of 5.5 U/mL after 8 days of cultivation[158]. The encoding gene has also been expressed in *Pichia pastoris* KM71H, resulting in yields up to 8 U/mL after a 6 day batch fermentation[167]. Here, a high-cell-density *P. pastoris* fermentation was established to circumvent the high material costs related to the use of BMGY and BMMY media, as well as the poor space time productivity reported to date. A 2 L fermenter was inoculated with 100 mL preculture, routinely grown on BMGY medium. A sharp increase in the dissolved oxygen (DO) indicated the end of the glycerol batch phase after approximately 12 h (Figure 6.1). At this moment, the OD_{600} reached 30.2. Next, a 6.6 g/L/h glycerol feed was started resulting in exponential growth to an OD_{600} of roughly 150 after 26 h. Higher feed rates were found to result in anoxic conditions, while lower rates decreased the space time yield of the fermentation.

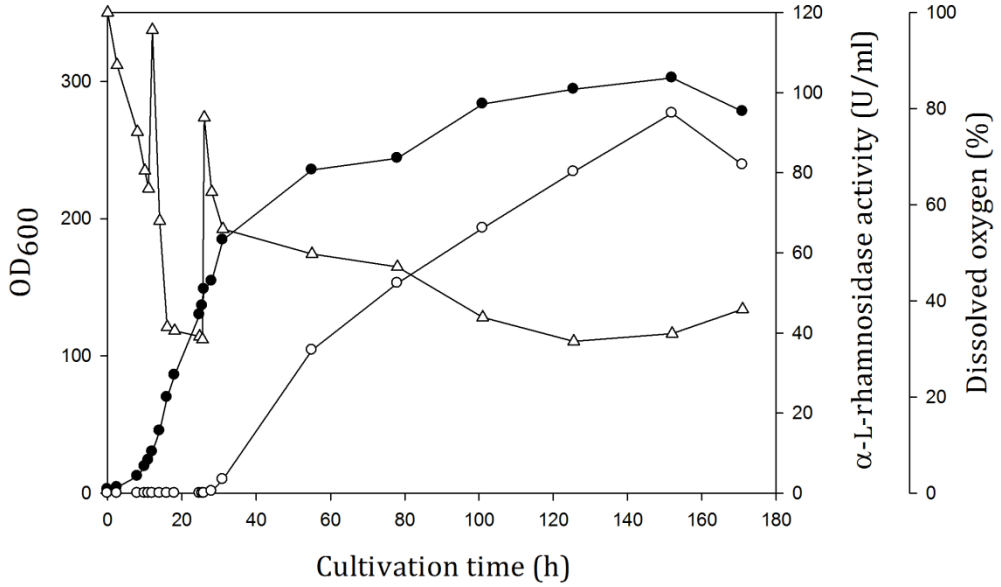

Figure 6.1 Production of α-L-rhamnosidase in a 2 L high-cell-density *P. pastoris* fermentation. The optical density (●), α-L-rhamnosidase activity (○) and dissolved oxygen (Δ) were monitored during 7 days.

The glycerol feed was stopped after 26 h, and the addition of methanol was commenced. The methanol feed was linearly increased from 0.8 g/L/h to 2.1 g/L/h over the next 10 h of fermentation. This feed rate was maintained during 5 days, resulting in an OD_{600} of 302 and the secretion of 95.3 U/mL α-L-rhamnosidase. Prolonged fermentation resulted in a decrease of α-L-rhamnosidase activity (Figure 6.1). Thus the space time yield was increased to an impressive 627 U/L/h, compared to previously reported values of 28.6 and 55.6 U/L/h[158, 167]. This efficient fermentation should allow the production of α-L-rhamnosidase at a lower cost, enabling the development of new applications at the industrial scale.

3.2 Reverse hydrolysis with α-L-rhamnosidase

The hydrolysis of rutin to quercetin-3-β-D-glucopyranoside (isoquercitrin) by α-L-rhamnosidase has recently been achieved at the kilogram scale[158]. Isoquercitrin and rhamnose were added to 150 mg/mL and 1.5 M respectively in a 50 mM MOPS buffer at pH 7.0 and 37 °C in the presence of 20 U/mL α-L-rhamnosidase. However, no rutin could be detected after three days. Nevertheless, when DMSO was added to 50 %, a new strong spot was observed on TLC after 24 h. The product was identified to be the expected rutin by TLC co-chromatography with an authentic sample (Figure 6.2).

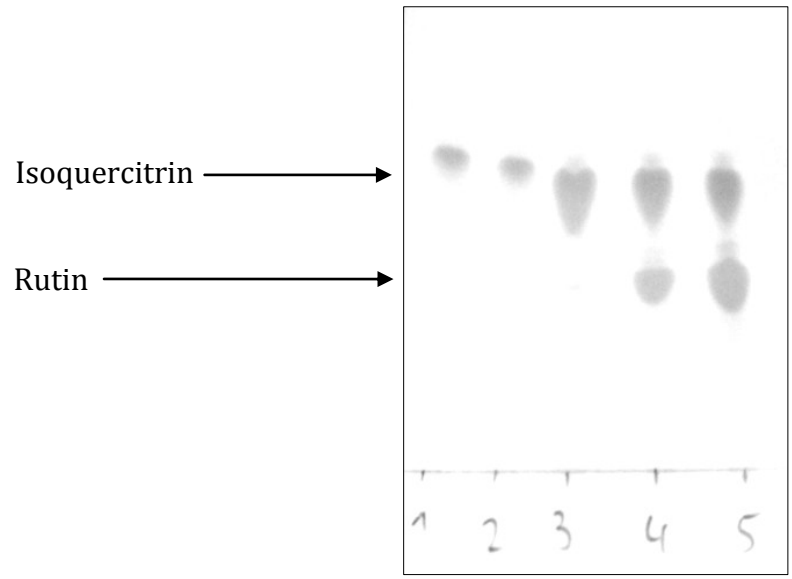

Figure 6.2 Synthesis of rutin from isoquercitrin and rhamnose (1.5 M) in the presence of 20 U/mL α-L-rhamnosidase at 37 °C. Isoquercitrin was saturated in a 50 mM MOPS buffer at pH 7.0 (blanc (1), reaction (2)). Alternatively 50 % DMSO was added (blanc (3), reaction (4)). Co-chromatography of sample 4 with 50 mg/mL rutin was also performed (5).

Encouraged by the successful synthesis of rutin from isoquercitrin and rhamnose, the rhamnosylation of three simple phenolic compounds was evaluated. To that end, 750 mg/mL phenol, catechol or pyrogallol was added to a 50 mM MOPS buffer at pH 7.0. Alternatively, they were dissolved to 50 mg/mL. The glycosylation of these compounds was tested in the presence of 50 % DMSO. A single new spot having R_f higher than rhamnose and lower than the acceptor appeared after 24 h in case of catechol (50 mg/mL), while the other two phenols failed to yield any glycosides (Figure S6.1). The product was purified by silica gel chromatography and identified to be 1-*O*-α-L-rhamnopyranosyl catechol by NMR spectroscopy. Therefore, conditions enabling the efficient enzymatic rhamnosylation (reverse glycosylation or more correctly "condensation") with *A. terreus* α-L-rhamnosidase were further optimized.

3.3 Influence of solvents on the glycosylation activity of α-L-rhamnosidase

Reverse hydrolysis is based on the reaction equilibrium shift towards synthesis of the glycosidic linkage. According to thermodynamics, this can be achieved either by increasing substrate concentrations, decreasing the water activity, or by the combination of both. Enzymatic glycosylation *via* reverse hydrolysis is, therefore, commonly performed in the presence of organic cosolvents, such as DMSO or acetone. However, these solvents often tend to inactivate biocatalysts[168], urging a balance between cosolvent addition and enzyme stability.

Hence, the activity of *A. terreus* α-L-rhamnosidase towards catechol was evaluated at various DMSO concentrations (Table S6.1). The addition of cosolvent was found to be crucial for effective rhamnosylation. Product formation was observed between 20 and 60 % DMSO with the maximum yield at 40 %. Higher concentrations of DMSO resulted in a lower yield due to the enzyme inactivation compared to the gain caused by the improved equilibrium conditions. Therefore, the rhamnosylation activity of *A. terreus* α-L-rhamnosidase was assessed in the presence of various cosolvents. Short chain alcohols, such as methanol and ethanol have been identified as good acceptors, impeding thus their use as cosolvent[169]. Due to the ability to dissolve both polar and hydrophobic substrates, ionic liquids (ILs) have recently been successfully employed for the synthesis of glycosidic compounds (CHAPTER 3). Therefore, a range of organic solvents as well as some ILs were evaluated for the rhamnosylation of catechol (Table 6.1).

Table 6.1 Influence of various cosolvents on the catechol glycosylation activity of α-L-rhamnosidase. Catechol and L-rhamnose were dissolved to 50 mg/mL and 1.5 M respectively in a 50 mM MES buffer at pH 7.0 containing 40 % cosolvent. Samples were analyzed after 24 h incubation at 37 °C.

Solvent	Product spot intensity	Solvent	Product spot intensity
Acetone	+++++	[MMIM][$MeSO_4$]	-
tert-Butyl alcohol	+++	[BMIM][BF_4]	-
Acetonitrile	+++	[BMIM][dca]	-
DMSO	+++++	[BMIM][I]	-
DMF	++	[EMIM][$EtSO_4$]	-
PEG M_n 300	+++++	[EMIM][dca]	-
PEG M_n 4000	+++++	AMMOENG 101	+

The enzyme was found to maintain the highest glycosylation activity in commonly used solvents such as DMSO, polyethylene glycol and acetone. However, rhamnosylation of catechol was also achieved when using 40 % dimethylformamide, acetonitrile, *tert*-butyl alcohol, or the IL AMMOENG 101, which was recently used for the glycosylation of resveratrol (CHAPTER 3). The addition of other ILs failed to yield any glycosides. Acetone is readily available, easy to remove by evaporation and exhibits excellent solubilizing properties and it was, therefore, used in all further experiments. Additional tests (Table 6.2) confirmed 40 % acetone to be the optimal cosolvent concentration.

Table 6.2 Influence of acetone on the glycosylation activity of α-L-rhamnosidase. Catechol and rhamnose were dissolved to 50 mg/mL and 1.5 M respectively in a 50 mM MOPS buffer at pH 7.0. Samples were analyzed after 24 h at 37 °C.

[acetone] (%)	Product spot intensity	[acetone] (%)	Product spot intensity
10	-	60	+
20	++	70	+
30	+++	80	-
40	+++++	90	-
50	+++	100	-

3.4 Optimization of reverse hydrolysis conditions

Besides the cosolvent, a number of other factors can influence the glycosylation efficiency, including the pH, concentration of both substrates, as well as the temperature[170]. A full factorial design experiment was performed to determine their relative importance on the glycosylation yield of catechol (Table 6.3). Thermodynamic considerations predict more product formation when higher concentrations of substrate are used. Indeed, despite the inhibition of α-L-rhamnosidase by rhamnose[167], similar conditions using 1.5 M rhamnose compared to 0.5 M were found to yield more product. However, no glycosides could be detected when 500 mg/mL catechol was added, revealing strong destabilizing or inhibitory effects of the acceptor at high concentrations.

Table 6.3 Optimization of α-L-rhamnosidase catalyzed synthesis of catechol-rhamnoside: 2^3 factorial design. The temperature was fixed at 37 °C.

Run	pH	[Rhamnose] (M)	[Catechol] (mg/mL)	Product spot intensity
1	5.5	0.5	50	+++
2	5.5	0.5	500	-
3	5.5	1.5	50	+++++
4	5.5	1.5	500	-
5	7.5	0.5	50	++
6	7.5	0.5	500	-
7	7.5	1.5	50	++++
8	7.5	1.5	500	-

Next, the pH (4 to 10) and catechol concentration (10 to 500 mg/mL) were varied to indentify 40 % acetone, 1.5 M rhamnose, 200 mg/mL catechol, pH 6.0 and 37 °C to be optimal conditions for the reverse hydrolysis glycosylation of catechol with α-L-rhamnosidase (Table S6.2). Higher rhamnose concentrations were not feasible in a 40 % acetone buffer, whereas higher temperatures were found to result in a lower product formation, most likely caused by the combined destabilizing effect of elevated temperatures and high catechol concentrations.

3.5 Reverse hydrolysis in biphasic systems

The glycosylation of alcohols through the reverse hydrolysis action of glycosidases has been reported frequently. Indeed, various alkyl glucosides have been synthesized using both α and β-glucosidases[170], β-galactosidases[171] and β-*N*-acetylhexosaminidases[172]. In contrast, the synthesis of alkyl α-L-rhamnosides has only been reported for methanol, ethanol and 2-propanol[169]. Here, the effect of the pH and the concentration of both substrates on the α-L-rhamnosidase catalyzed synthesis of hexyl α-L-rhamnopyranoside in a biphasic system was investigated. A full factorial design experiment was performed to determine the relative importance of these factors on the glycosylation yield (Table 6.4).

Table 6.4 Optimization of α-L-rhamnosidase catalyzed synthesis of hexyl rhamnoside in a biphasic system: 2^3 factorial design. The temperature was fixed at 37 °C.

Run	pH	[Rhamnose] (M)	Buffer/hexanol ratio	Product spot intensity
1	5.5	0.5	5	+++++
2	5.5	0.5	0.5	+
3	5.5	2	5	++++
4	5.5	2	0.5	+
5	7.5	0.5	5	+++
6	7.5	0.5	0.5	+
7	7.5	2	5	+++
8	7.5	2	0.5	+

Both the pH and hexanol amount were found to strongly influence the glycosylation yield. Interestingly, the rhamnose concentration did not significantly influence the rhamnosylation of hexanol. Further experiments were conducted to obtain optimal conditions at pH 5.5, 50 °C, 0.5 M rhamnose, and a buffer/hexanol ratio of 2.5 (Table S6.3).

3.6 Synthesis of α-L-rhamnosides

The glycosylation potential of the α-L-rhamnosidase from *A. terreus* was then evaluated by incubating various acceptors under optimal rhamnosylation conditions (Figure 6.3).

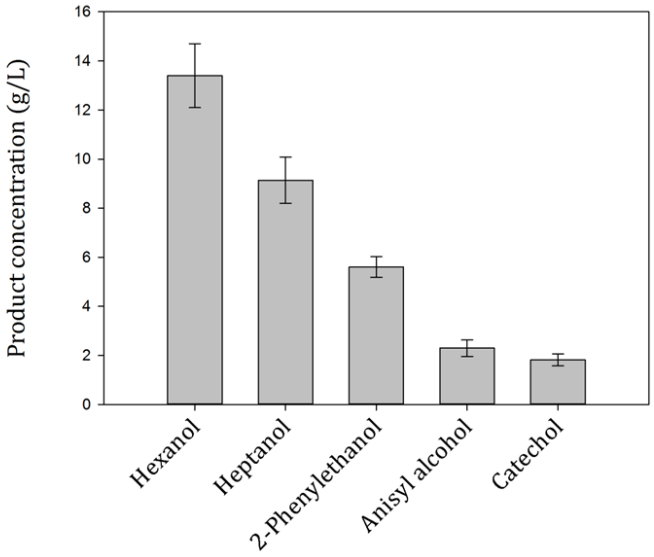

Figure 6.3 Glycosylation of various small organic compounds with α-L-rhamnosidase under optimal reaction conditions for cosolvent (catechol) and biphasic (hexanol, heptanol, anisyl alcohol and 2-phenylethanol) systems.

The synthesis of alkyl α-L-rhamnosides by reverse hydrolysis was found to show similar characteristics to other glycosidases[153]. The longer the alkyl chain, the lower the reaction yield (Table 6.5). Indeed 48 h incubation under optimal reaction conditions, resulted in rhamnoside concentrations of 13.4 and 9.1 g/L for hexanol and heptanol respectively (Figure 6.3). Also, primary alcohols were found to be more easily glycosylated compared to secondary alcohols.

NMR confirmation of hexyl α-L-rhamnopyranoside, heptyl α-L-rhamnopyranoside and cyclohexyl α-L-rhamnopyranoside was obtained. However, no alkyl rhamnosides could be isolated when reacting 2-hexanol or 2-octanol (Table 6.5). Interestingly, the rhamnosylation potential of the enzyme is not limited to aliphatic alcohols. Various flavors and fragrances, such as for example the monoterpenoids geraniol and β-citronellol were rhamnosylated as well[162]. Moreover, aromatic compounds with olfactory properties such as anisyl alcohol, cinnamyl alcohol and 2-phenylethanol were successfully glycosylated. Although anisyl α-L-rhamnopyranoside (2.3 g/L) and 2-phenylethyl α-L-rhamnopyranoside (5.6 g/L) were produced in substantially lower concentrations compared to aliphatic alkyl α-L-rhamnosides (Figure 6.3), confirmation of these glycosides was achieved by NMR spectroscopy.

Table 6.5 Glycosylation potential of the α-L-rhamnosidase from *A. terreus*. TLC analysis was performed after 48 h.

Acceptor	Product spot intensity	Acceptor	Product spot intensity
Hexanol[a]	+++++[c]	*S*-1-Phenylethanol[a]	-
Heptanol[a]	++++[d]	Benzyl alcohol[a]	+
Octanol[a]	+++[e]	Anisyl alcohol[a]	+++
Nonanol[a]	++[f]	Cinnamyl alcohol[a]	++++
Decanol[a]	+[g]	Saligenin[b]	+++
Dodecanol[a]	-	4-Phenoxyphenol[b]	+
Cyclohexanol[a]	+++++	Phenol[b]	+
2-Octanol[a]	-	Pinacol[b]	-
2-Hexanol[a]	-	Gallic acid[b]	-
Linalool[a]	-	Vanillin[b]	+
Eugenol[a]	-	Ethyl gallate[b]	-
Penta-erythritol[a]	-	Vanillyl alcohol[b]	+++
Nerolidol[a]	-	Pyrogallol[b]	-
β-Citronellol[a]	+	*p*-Nitrophenol[b]	-
Geraniol[a]	+++	Resveratrol[b]	+
Salicylic acid methyl ester[a]	+	Hydroquinone[b]	+++
2-Phenylethanol[a]	++++	Catechol[b]	+++
R-1-Phenylethanol[a]	-	Resorcinol[b]	+++

[a] Glycosylation was performed in a biphasic system. The acceptor was used as second phase. [b] Glycosylation was performed in a cosolvent system. [c] Corresponds to a product concentration ≥ 10 g/L. [d] Corresponds to a product concentration between 5 and 10 g/L. [e] Corresponds to a product concentration between 2 and 5 g/L. [f] Corresponds to a product concentration between 1 and 2 g/L. [g] Corresponds to a product concentration ≤ 1 g/L.

Glycosylation of both *R* and *S*-1-phenylethanol failed illustrating thus the difficult glycosylation of secondary alcohols. Surprisingly, hydroquinone, resorcinol and catechol could be easily rhamnosylated. Indeed, the formation of 1-*O*-α-L-rhamnopyranosyl hydroquinone, 1-*O*-α-L-rhamnopyranosyl resorcinol and 1-*O*-α-L-rhamnopyranosyl catechol was confirmed by NMR spectroscopy. In contrast to the formation of 1.8 g/L 1-*O*-α-L-rhamnopyranosyl catechol after 2 days, glycosylation of phenol was found to be much less efficient, while no pyrogallol rhamnosides could be obtained. These results

emphasize the importance of optimizing reaction conditions. Indeed, the initial reaction conditions only allowed the glycosylation of catechol, while no glycosides of phenol could be detected. Following the work on short alkyl α-L-rhamnoside production[169], this is probably the first report on the use of glycosidases for the synthesis of phenolic glycosides.

4 CONCLUSION

In this chapter, the glycosylation potential of α-L-rhamnosidase originating from *Aspergillus terreus* was evaluated. The recombinant expression in *P. pastoris* was substantially improved to 627 U/L/h, allowing thus the cost-effective production of α-L-rhamnosidase at the industrial scale. The obtained enzyme was used to explore rhamnosylation of various alcohols. Careful optimization of the reaction conditions allowed the synthesis of numerous alkyl α-L-rhamnosides. In addition, rhamnosylation of small phenolics such as hydroquinone, resorcinol, catechol and phenol was observed. Consequently, the use of α-L-rhamnosidase could find widespread application for glycoside synthesis in the cosmetics and food industry.

5 MATERIALS & METHODS

5.1 Materials

NMR spectra were measured on a Bruker AVANCE III 400 MHz spectrometer (400.00 MHz for ^{1}H, and 100.59 MHz for ^{13}C) and 600 MHz spectrometer (600.23 MHz for ^{1}H, and 150.93 MHz for ^{13}C) in CD_3OD at 25 and 30 °C. HPLC measurements were performed on a Varian Prostar, and absorbance at 405 nm was measured in a Bio-Rad microplate reader 680XR.

5.2 α-L-Rhamnosidase production

Pichia pastoris KM71H (Invitrogen, USA) containing the gene encoding for α-L-rhamnosidase from *Aspergillus terreus* was grown on YPD (yeast extract peptone dextrose: 1 % (w/v) yeast extract, 2 % (w/v) peptone, 2 % (w/v) glucose) medium and stored on YPD plates (YPD medium with 2 % (w/v) agar). Alternatively, the culture was cryopreserved at -80 °C in 15 % (v/v) glycerol. A single colony was inoculated in 100 mL BMGY (buffered glycerol-complex: 1 % (w/v) yeast extract, 2 % (w/v) peptone, 100 mM

potassium phosphate pH 6.0, 1.34 % (w/v) YNB (yeast nitrogen base, BD Difco, USA), 4 × 10^{-5} % (w/v) biotin and 1 % (v/v) glycerol) medium on a rotary shaker at 30 °C and 200 rpm. After 24 h growth, the culture was inoculated into 1 L of BSM (basal salts medium: 26.7 mL/L H_3PO_4 (85 % (w/v)), 0.93 g/L $CaSO_4$. 2 H_2O, 18.2 g/L K_2SO_4, 14.9 g/L $MgSO_4$. 7 H_2O and 4.13 g/L KOH) medium with 4.35 mL PTM_1 salts (6.0 g/L $CuSO_4$. 5 H_2O, 0.08 g/L NaI, 30 g/L $MnSO_4$. H_2O, 0.2 g/L Na_2MoO_4 . 2 H_2O, 0.02 g/L H_3BO_3, 0.5 g/L $CoCl_2$, 20.0 g/L $ZnCl_2$, 65.0 g/L $FeSO_4$. 7 H_2O, 0.2 g/L biotin and 5 mL/L H_2SO_4 conc.) and 10 g/L glycerol in a 2 L Biostat M reactor. Fermentation was performed at 30 °C and 1000 rpm with aeration at 1.5 vvm (set point DO 100 %). A pulsed feed of anti-foam (10 % (v/v) antifoam silicone Snapsil RE 20, VWR Prolabo) was controlled to administer 1 drop every 30 min to prevent foaming. The pH was set and maintained at 5 by addition of aqueous ammonium hydroxide (28 % (w/v) NH_3) or 5 M sulfuric acid. The initial batch phase was continued until the glycerol had been consumed, and was followed by a glycerol fed-batch phase. To that end, the fermenter was supplemented with a continuous feed of 6.6 g/L/h of 50 % (v/v) glycerol containing 12 mL/L PTM_1 salts during 14 h. To induce AOX transcription, methanol supplemented with 12 mL/L PTM_1 salts was added at a rate of 0.8 g/L/h. The feeding rate of methanol was gradually increased to 2.1 g/L/h over 10 h and maintained for the remainder of the fermentation.

5.3 Enzyme purification and concentration

The culture supernatant was harvested 5 days after induction by centrifugation (10 min, 10 000 g, 4 °C), and subjected to dialysis against 10 mM MES buffer at pH 6. Finally the obtained enzyme solution was washed with 50 mM MES buffer and concentrated using centricons (Amicon Ultra 30K, Millipore).

5.4 Activity assays

α-L-Rhamnosidase activity was assayed by mixing 200 µL MES buffer containing 50 mM *p*-nitrophenyl α-L-rhamnopyranoside (Sigma Aldrich, USA) with 400 µL of a diluted enzyme solution. The reactions were followed discontinuously by adding 50 µL samples to 150 µL of a 0.5 M Na_2CO_3 solution at regular intervals. The liberated *p*-nitrophenol (PNP) was determined spectrophotometrically at 405 nm in a microplate reader. One unit of α-L-rhamnosidase activity was defined as the amount of enzyme releasing 1 µmol

of PNP per minute in a 50 mM MES buffer at pH 6.0 and 37 °C. All assays were performed in triplicate and had a CV of less than 10 %.

5.5 Reverse hydrolysis with α-L-rhamnosidase

Glycosylation reactions were performed in a 50 mM MES buffer at pH 6. Alternatively, a citrate-phosphate buffer (pH 3.0 - 5.4), MES buffer (pH 5.5 - 6.5), MOPS buffer (pH 6.6 - 7.5) and tricine buffer (pH 7.6 – 9.0) were used. Varying amounts of solvents and substrate were added, and unless stated otherwise, the reactions were incubated at 37 °C in the presence of 1.5 M rhamnose and 20 U/mL α-L-rhamnosidase.

5.6 Analytical techniques

HPLC analysis was performed on an X-bridge amide column (250 mm × 4.6 mm, 3.5 µm, Waters, USA) with milliQ water (solvent A) and acetonitrile (solvent B), both containing 0.2 % triethylamine, as the mobile phase. The flow rate and temperature were set at 1.0 mL/min and 30 °C, respectively. The gradient elution was as follows: 95 % of solvent A (0 - 12 min), 5 to 25 % solvent B (12 - 15 min), 25 % solvent B (15 - 40 min), 25 to 5 % solvent B (40 - 41 min) and 95 % solvent A (41 - 50 min). Detection was accomplished with an Alltech 2000ES evaporative light scattering detector (ELSD). The tube temperature, gas flow and gain were set at 25 °C, 1.5 L/min and 4, respectively. In the case of biphasic reaction systems, homogeneous samples, obtained after intensive mixing, were dissolved in dimethyl sulfoxide (DMSO) and subjected to HPLC analysis. The resulting concentrations refer to the amount of product present in the total reaction volume. TLC analysis was performed as described in CHAPTER 4. All reported errors correspond to the standard errors.

5.7 Production and purification of glycosides

The glycosylation of hydroquinone, catechol and resorcinol was carried out at 20 mL scale in a 50 mM MES buffer at pH 6.5 containing 40 % acetone. Rhamnose, acceptor and α-L-rhamnosidase were added to a concentration of 1.5 M, 200 mg/mL (1.82 M) and 20 U/mL, respectively. Alternatively, rhamnosylation of hexanol, heptanol, cyclohexanol, anisyl alcohol and 2-phenylethanol was performed in a biphasic system consisting of 6 mL acceptor and 15 mL 50 mM MES buffer at 5.5, supplemented with 500 mM

rhamnose and 20 U/mL α-L-rhamnosidase. Reactions were terminated after 48 h incubation at 37 or 50 °C for cosolvent and biphasic reaction systems, respectively. The reaction mixtures were heated (10 min at 95 °C) and centrifuged (12 000 g, 4 °C, 15 min) to remove debris. The samples were then evaporated *in vacuo* and the residue was purified by column chromatography (silicagel, EtOAC/MeOH/H_2O = 30:5:4).

5.8 Structure elucidation of rhamnosides

The structures of new glycosides were determined by a combination of 1D NMR (^{1}H NMR and ^{13}C NMR) and 2D NMR (gCOSY, gHSQC and gHMBC) spectroscopy. Residual signals of solvent were used as an internal standard (δ_H 3.330 ppm, δ_C 49.30 ppm). Digital resolution enabled the reporting of δ_H to three and δ_C to two decimal places. Some hydrogen chemical shifts were read out from HSQC and are reported to two decimal places. The proton spin systems were assigned by COSY, and then the assignment was transferred to carbons by HSQC. HMBC experiments enabled to assign quaternary carbons and to join individual spin systems together. Chemical shifts are given in δ-scale [ppm], and coupling constants in Hz. Spectral analysis and interpretation was kindly performed by the group of Prof. Vladimír Křen at the Institute of Microbiology (Czech Republic).

1-*O*-α-L-Rhamnopyranosyl hydroquinone

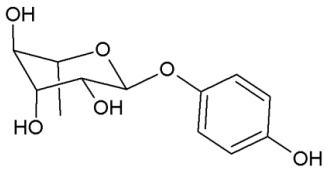

^{1}H NMR (600.23 MHz, CD_3OD, 25 °C): 1.256 (3H, d, *J* = 6.2 Hz, H-6), 3.466 (1H, dd, *J* = 9.5, 9.5 Hz, H-4), 3.725 (1H, dq, *J* = 9.5, 6.2 Hz, H-5), 3.842 (1H, dd, *J* = 9.5, 3.4 Hz, H-3), 4.000 (1H, dd, *J* = 3.4, 1.8 Hz, H-2), 5.268 (1H, d, *J* = 1.8 Hz, H-1), 6.726 (2H, m, Σ*J* = 8.9 Hz, H-*meta*), 6.911 (2H, m, Σ*J* = 8.9 Hz, H-*ortho*)

^{13}C NMR (150.94 MHz, CD_3OD, 25°C): 18.28 (C-6), 70.71 (C-5), 72.50 (C-2), 72.57 (C-3), 74.23 (C-4), 101.24 (C-1), 117.08 (C-*meta*), 119.35 (C-*ortho*), 151.39 (C-*ipso*), 153.92 (C-*para*)

1-*O*-α-L-Rhamnopyranosyl resorcinol

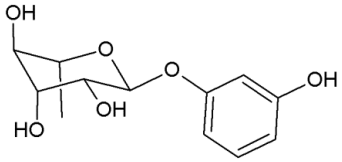

^{1}H NMR (600.23 MHz, CD_3OD, 25°C): 1.256 (3H, d, *J* = 6.2 Hz, H-6), 3.467 (1H, dd, *J* = 9.5, 9.5 Hz, H-4), 3.671 (1H, dq, *J* = 9.5, 6.2 Hz, H-5), 3.845 (1H, dd, *J* = 9.5, 3.5 Hz, H-3), 3.991 (1H, dd, *J* = 3.5, 1.8 Hz, H-2), 5.383 (1H, d, *J* = 1.8 Hz, H-1), 6.466 (1H, m, H-6'), 6.546 (1H, m, H-2'), 6.551 (1H, m, H-4'), 7.087 (1H, m, H-5')

^{13}C NMR (150.94 MHz, CD_3OD, 25°C): 18.32 (C-6), 70.86 (C-5), 72.41 (C-2), 72.55 (C-3), 74.18 (C-4), 100.13 (C-1), 105.16 (C-2'), 108.98 (C-4'), 110.62 (C-6'), 131.21 (C-5'), 159.37 (C-1'), 159.96 (C-3'); C-4'and 6'might be interchanged

1-*O*-α-L-Rhamnopyranosyl catechol

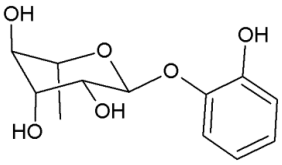

^{1}H NMR (600.23 MHz, CD_3OD, 25°C): 1.266 (3H, d, *J* = 6.2 Hz, H-6), 3.485 (1H, dd, *J* = 9.5, 9.5 Hz, H-4), 3.817 (1H, dq, *J* = 9.5, 6.2 Hz, H-5), 3.962 (1H, dd, *J* = 9.5, 3.5 Hz, H-3), 4.136 (1H, dd, *J* = 3.5, 1.8 Hz, H-2), 5.383 (1H, d, *J* = 1.8 Hz, H-1), 6.779 (1H, ddd, *J* = 8.1, 7.1, 1.9 Hz, H-4'), 6.857 (1H, dd, *J* = 7.9, 1.9 Hz, H-6'), 6.890 (1H, ddd, *J* = 7.9, 7.1, 1.5 Hz, H-5'), 7.115 (1H, dd, *J* = 8.1, 1.5 Hz, H-3')

^{13}C NMR (150.94 MHz, CD_3OD, 25°C): 18.26 (C-6), 70.98 (C-5), 72.29 (C-2), 72.47 (C-3), 74.23 (C-4), 101.50 (C-1), 117.64 (C-6'), 119.17 (C-3'), 121.14 (C-4'), 124.57 (C-5'), 146.06 (C-1'), 149.06 (C-2'); spin system 3'-4'-5'-6'might be interchanged for the opposite order 6'-5'-4'-3'

Hexyl α-L-rhamnopyranoside

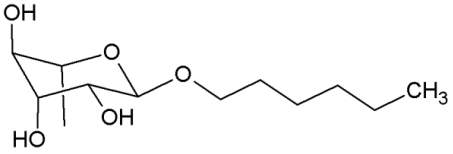

^{1}H NMR (400.00 MHz, CD_3OD, 30°C): 0.931 (3H, m, H-6'), 1.276 (3H, d, *J* = 6.2 Hz, H-6), 1.33 (2H, m, H-4'), 1.35 (2H, m, H-5'), 1.38 (2H, m, H-3'), 1.599 (2H, m, H-2'), 3.386 (1H, dd, *J* = 9.7, 9.3 Hz, H-4), 3.422 (1H, dt, *J* = 9.6, 6.4 Hz, H-1'u), 3.598 (1H, dq, *J* = 9.3, 6.2 Hz, H-5), 3.657 (1H, dd, *J* = 9.7, 3.4 Hz, H-3), 3.680 (1H, dt, *J* = 9.6, 6.7 Hz, H-1'd), 3.804 (1H, dd, *J* = 3.4, 1.7 Hz, H-2), 4.673 (1H, d, *J* = 1.7 Hz, H-1)

^{13}C NMR (100.58 MHz, CD_3OD, 30°C): 14.64 (C-6'), 18.26 (C-6), 23.92 (C-5'), 27.29 (C-3'), 30.88 (C-2'), 33.04 (C-4'), 68.89 (C-1'), 70.03 (C-5), 72.67 (C-2), 72.79 (C-3), 74.31 (C-4), 101.93 (C-1)

Heptyl α-L-rhamnopyranoside

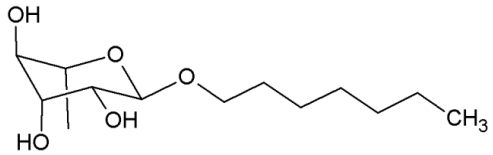

^{1}H NMR (600.23 MHz, CD_3OD, 30°C): 0.925 (3H, m, H-7'), 1.276 (3H, d, *J* = 6.2 Hz, H-6), 1.32 (2H, m, H-5'), 1.34 (2H, m, H-6'), 1.35 (2H, m, H-4'), 1.39 (2H, m, H-3'), 1.600 (2H, m, H-2'), 3.385 (1H, dd, *J* = 9.6, 9.4 Hz, H-4), 3.423 (1H, dt, *J* = 9.6, 6.3 Hz, H-1'u), 3.597 (1H, dq, *J* = 9.4, 6.2 Hz, H-5), 3.655 (1H, dd, *J* = 9.6, 3.4 Hz, H-3), 3.680 (1H, dt, *J* = 9.6, 6.7 Hz, H-1'd), 3.802 (1H, dd, *J* = 3.4, 1.7 Hz, H-2), 4.672 (1H, d, *J* = 1.7 Hz, H-1)

^{13}C NMR (150.94 MHz, CD_3OD, 30°C): 18.23 (C-6), 25.12 (C-5'), 25.36 (C-3'), 27.08 (C-4'), 32.77 (C-6'), 34.76 (C-2'), 70.15 (C-5), 72.76 (C-3), 73.15 (C-2), 74.44 (C-4), 76.37 (C-1'), 99.92 (C-1)

Cyclohexyl α-L-rhamnopyranoside

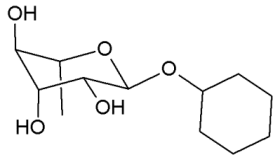

^{1}H NMR (400.00 MHz, CD_3OD, 30°C): 1.262 (3H, d, *J* = 6.3 Hz, H-6), 1.29 (1H, m, H-4'u), 1.31 (1H, m, H-5'u), 1.32 (1H, m, H-6'u), 1.34 (1H, m, H-3'u), 1.40 (1H, m, H-2'u), 1.55 (1H, m, H-4'd), 1.74 (1H, m, H-5'd), 1.76 (1H, m, H-3'd), 1.87 (1H, m, H-2'd), 1.88 (1H, m, H-6'd), 3.384 (1H, dd, *J* = 9.5, 9.5 Hz, H-4), 3.603 (1H, m, H-1'), 3.676 (1H, dq, *J* = 9.5, 6.3 Hz, H-5), 3.676 (1H, dd, *J* = 9.5, 3.4 Hz, H-3), 3.767 (1H, dd, *J* = 3.4, 1.7 Hz, H-2), 4.838 (1H, d, *J* = 1.7 Hz, H-1)

^{13}C NMR (100.58 MHz, CD_3OD, 30°C): 18.23 (C-6), 25.12[a] (C-5'), 25.36[a] (C-3'), 27.08 (C-4'), 32.77[b] (C-6'), 34.76[b] (C-2'), 70.15 (C-5), 72.76 (C-3), 73.15 (C-2), 74.44 (C-4), 76.37 (C-1'), 99.92 (C-1); [a,b] might be interchanged

Anisyl α-L-rhamnopyranoside

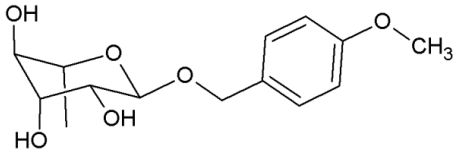

^{1}H NMR (600.23 MHz, CD_3OD, 25°C): 1.291 (3H, d, *J* = 6.2 Hz, H-6), 3.404 (1H, dd, *J* = 9.5, 9.5 Hz, H-4), 3.639 (1H, dq, *J* = 9.5, 6.2 Hz, H-5), 3.681 (1H, dd, *J* = 9.5, 3.5 Hz, H-3), 3.798 (3H, s, OMe), 3.812 (1H, dd, *J* = 3.5, 1.7 Hz, H-2), 4.449 (1H, d, *J* = 11.5 Hz, H-1'u), 4.623 (1H, d, *J* = 11.5 Hz, H-1'd), 4.756 (1H, d, *J* = 1.7 Hz, H-1), 6.909 (2H, m, Σ*J* = 8.7 Hz, H-*meta*), 7.279 (2H, m, Σ*J* = 8.7 Hz, H-*ortho*)

^{13}C NMR (150.94 MHz, CD_3OD, 25°C): 18.29 (C-6), 55.99 (OMe), 70.22 (C-5), 72.61 (C-2), 72.73 (C-3), 74.32 (C-4), 100.83 (C-1), 115.07 (C-*meta*), 131.02 (C-*ortho*), 131.30 (C-*ipso*), 161.18 (C-*para*)

2-Phenylethyl α-L-rhamnopyranoside

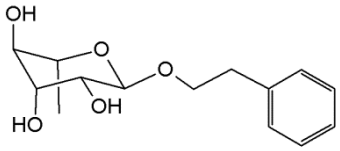

^{1}H NMR (600.23 MHz, CD_3OD, 25°C): 1.212 (3H, d, *J* = 6.2 Hz, H-6), 2.883 (2H, dd, *J* = 6.9, 6.6 Hz, H-2'), 3.356 (1H, dd, *J* = 9.5, 9.4 Hz, H-4), 3.419 (1H, dq, *J* = 9.5, 6.2 Hz, H-5), 3.619 (1H, dd, *J* = 9.4, 3.5 Hz, H-3), 3.654 (1H, dt, *J* = 9.7, 6.6 Hz, H-1'u), 3.782 (1H, dd, *J* = 3.5, 1.7 Hz, H-2), 3.877 (1H, dt, *J* = 9.7, 6.9 Hz, H-1'd), 4.669 (1H, d, *J* = 1.7 Hz, H-1), 7.194 (1H, m, H-*para*), 7.237 (2H, m, H-*ortho*), 7.282 (2H, m, H-*meta*)

^{13}C NMR (150.94 MHz, CD_3OD, 25°C): 18.24 (C-6), 37.41 (C-2'), 69.74 (C-1'), 70.08 (C-5), 72.56 (C-2), 72.70 (C-3), 74.18 (C-4), 101.89 (C-1), 127.52 (C-*para*), 129.63 (C-*meta*), 130.22 (C-*ortho*), 140.70 (C-*ipso*)

6 SUPPLEMENTARY INFORMATION

Table S6.1 Influence of DMSO on the glycosylation activity of α-L-rhamnosidase. Catechol and rhamnose were dissolved to 50 mg/mL and 1.5 M respectively in a 50 mM MOPS buffer at pH 7.0. Samples were analyzed after 24 h at 37 °C.

[DMSO] (%)	Product spot intensity
0	-
10	-
20	+
30	++
40	+++++
50	+++
60	++
70	-
80	-
90	-
100	-

Table S6.2 Optimization of α-L-rhamnosidase catalyzed synthesis of catechol-rhamnoside. The rhamnose and acetone concentrations were fixed at 1.5M and 40 % respectively.

pH	Temperature (°C)	[Catechol] (mg/mL)	Product spot intensity
4	37	50	++
5	37	50	+++
6	37	50	++++
7	37	50	+++
8	37	50	+++
9	37	50	+
10	37	50	-
6	37	10	++
6	37	100	++++
6	37	200	+++++
6	37	300	++
6	37	400	+
6	37	500	-
6	45	200	++++
6	50	200	+++

Table S6.3 Optimization of α-L-rhamnosidase catalyzed synthesis of hexyl-rhamnoside. The rhamnose concentration was fixed at 0.5M.

pH	Temperature (°C)	Buffer/hexanol ratio	Product spot intensity
4	37	5	+
5	37	5	++
5.5	37	5	+++
6	37	5	++
7	37	5	++
5.5	37	1	++
5.5	37	2.5	++++
5.5	37	7.5	++
5.5	37	10	++
5.5	45	2.5	++++
5.5	50	2.5	+++++
5.5	55	2.5	+++
5.5	60	2.5	++

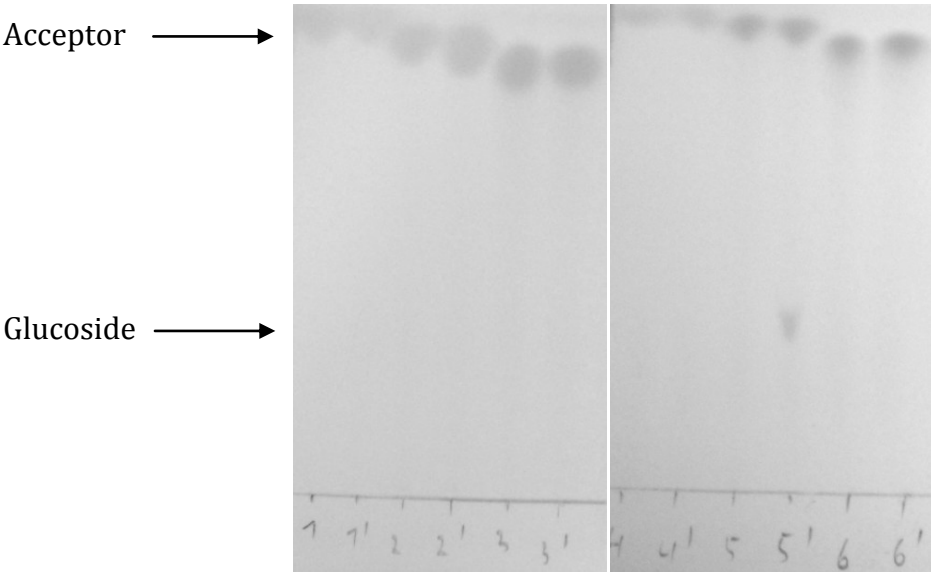

Figure S6.1 Reaction of 750 mg/mL phenol (1'), catechol (2') and pyrogallol (3') with rhamnose (1.5 M) in the presence of 20 U/mL α-L-rhamnosidase at 37 °C. Alternatively, 50 mg/mL phenol (4'), catechol (5') and pyrogallol (6') were used. All reactions were performed in a 50 mM MOPS buffer at pH 7.0 containing 50 % DMSO. For each condition, blancs (numbers without ') were analyzed next to the reactions.

CHAPTER 7

Extending glycosylation: Chain prolongation with cellodextrin phosphorylase through a combination of enzyme and process engineering

1 ABSTRACT

Although the efficient synthesis of numerous glycosides has been described in the previous chapters, prolongation of these compounds could further improve their properties. Unfortunately, sucrose and cellobiose phosphorylase are inefficient catalysts with respect to chain elongation, whereas chemical synthesis suffers from low yields and the generation of toxic waste. In this chapter, the cellodextrin phosphorylase from *Clostridium stercorarium* (CsCDP) was studied, and its activity towards various glucosides was determined. Interestingly, the enzyme was found to glycosylate a wide range of aliphatic and phenolic glucosides, among which next to the common β-glucosides also numerous α-glucosides. A number of complex glycosides, including salicyl 1-*O*-β-D-cellotriopyranoside and 6-*O*-β-D-cellobiopyranosyl esculetin were synthesized, isolated and analyzed by NMR spectroscopy. In addition, mutagenesis experiments were performed in the +2 subsite of the enzyme, revealing its importance for the activity of CsCDP. Remarkably, the specific activity of variant W168A towards octyl β-glucoside was found to be higher than the activity of the WT towards its natural substrate cellobiose.

2 INTRODUCTION

Glycosides are amongst the most widely distributed molecules in nature. In plants, for example, they play a role in accumulation, storage and transport of hydrophobic substances[173]. Indeed, compared to the free aglycone, glycosides show enhanced water solubility and decreased reactivity, allowing storage in the plant vacuole[174]. Examples include the cyanogenic glycoside amygdalin[175], the bitter tasting naringin[176] and the sweetner glycyrrhizin[11]. The former protects plants from herbivores by releasing the toxic hydrogen cyanide upon consumption[174], while the olfactory properties of the latter compounds are changed by their hydrolysis[177, 178].

Although chemical synthesis of glycosides still suffers from low yields, promising alternatives for the production of α- and β-glucosides have been described in CHAPTER 2, 3, 4 and 5. Prolongation of these glucosides, however, could further alter their properties. This has, for example, been nicely illustrated for carbohydrates connected to long alkyl chains, yielding compounds with good surfactant and emulsifying properties[179]. Indeed, by changing the aliphatic chain length[180] and the amount of glycosylation[181], alkyl polyglucosides (APGs) with varying properties can be obtained[182]. These interesting non-ionic surfactants find widespread application in detergents[183], lubricants[184] and cosmetics, and can be synthesized by Fischer condensation of carbohydrates and fatty acids[185]. Unfortunately, modification of the carbohydrate moiety by chemical methods is hampered by the need for numerous (de)protection and activation steps[15]. Therefore, enzymatic glycosylation of alkyl glucosides is a promising alternative[186].

Cellodextrin phosphorylase (CDP) (EC.2.4.1.49) catalyzes the reversible phosphorolysis of cello-oligosaccharides into cellodextrins with reduced chain length and α-glucose 1-phosphate (αG1P)[187]. The enzyme follows a similar single displacement reaction mechanism as cellobiose phosphorylase (CP), resulting in inversion of the anomeric configuration[38, 149]. Together with CP, it is involved in the natural degradation of cellulosic biomass[188, 189]. Because of the reversible nature of phosphorolytic reactions, however, CDP can also be used for glycosylation reactions *in vitro*. The enzyme is classified in the family GH-94 together with CP and chitobiose phosphorylase[190]. To date,

the crystal structure of CDP has not yet been determined. However, based on the crystal structure of chitobiose phosphorylase from *Vibrio proteolyticus*[191], a homology model for the CDP originating from *Clostridium stercorarium* (CsCDP) was created. In parallel with other GH-94 enzymes, it was shown that each monomer of the homodimeric structure of CDP consists of four different domains: a N-terminal β-sandwich domain, a short α-helical linker, the catalytic $(\alpha/\alpha)_6$ -barrel domain and a C-terminal β-sheet domain[39].

In contrast to the narrow donor specificity, the acceptor specificity of CDP is much more extended. Examples include oligosaccharides such as sophorose[152] and laminaritriose[37], alkyl glucosides such as methyl β-glucoside[38] and methyl β-cellobioside[192], surfactants among which sophorolipids and glucolipids[193], as well as the phenolic glucosides phenyl β-cellobioside[192] and PNP β-glucoside[39]. Remarkably, all of these compounds have at least one β-linked glucose unit in their structure. Moreover, when the CDP from *Clostridium stercorarium* was first discovered by Reichenbecher, the phosphorolysis of cellotriose was found to show the highest catalytic efficiency[38], indicating the presence of at least two acceptor subsites (+1 and +2). Interestingly, the residues in this +2 subsite were recently shown to be less conserved compared to the -1 and +1 subsite[39]. Indeed, while residue D474 (general catalytic acid)[194], residue D348 (hydrogen bonding of C2-OH and C3-OH in subsite -1)[149] and residue W472 (transition state stabilizer)[195] are highly conserved, no such homology could be observed for the important residues in the +2 subsite[39]. Despite these efforts, no detailed study on the promiscuity and application potential of this enzyme is available to date.

In this chapter, the glycosylation of various glucosides with the CDP from *Clostridium stercorarium* was evaluated. The specific activity towards different classes of acceptors was determined, and the influence of the residues in subsite +2 was scrutinized. Moreover, numerous glycosides were produced, isolated and characterized, while improved mutants for the synthesis of APGs were successfully obtained.

3 RESULTS & DISCUSSION

3.1 Production and purification of CDP

Although the recombinant production of the CDP originating from *Clostridium stercorarium* (CsCDP) has recently been described[39], moderate yields (12 U/mL culture volume) were obtained when applying the specified fermentation conditions. Increasing the induction time from 4 h to 16 h doubled the yield to 24 U/mL culture volume, while transferring the culture to a bioreactor allowed the production of roughly 500 000 U CsCDP in 15 L (33 U/mL). As illustrated in CHAPTER 5 for CP, purification of phosphorylases is crucial when using them in the synthesis direction. Therefore, also the His-tag purification of the obtained CsCDP crude cell extract was optimized.

First, the concentration of imidazole in the washing buffer was varied, identifying 25 mM as the optimal concentration. Lower concentrations hampered the purity of the protein, while higher imidazole concentrations decreased the purification yield. Next, the imidazole concentration in the elution buffer was varied between 250 and 500 mM. As a result, the purification yield could be increased from 20.4 % when using the initial conditions, to 65.3 % when applying the optimal wash conditions and eluting with 400 mM imidazole. Interestingly, also the level of purification increased from 4.3 to 6.7, indicating overall improved performance of the latter purification protocol.

3.2 Exploring the glycosylation potential of CDP

Although CDP is known to glucosylate various glucosides, its activity towards aglycons such as alcohols, terpenoids, phenols and flavanoids hasn't been reported to date. Indeed, the larger active site of this enzyme might allow the glucosylation of bulky acceptors such as resveratrol and quercetin. Therefore, the activity of the CDP from *Clostridium stercorarium* was evaluated towards a broad range of acceptors (Table S7.1). In contrast to SP (CHAPTER 4) and CP (CHAPTER 5), CDP was not able to glucosylate any of these compounds, indicating the necessity of a glucose moiety in the +1 subsite.

In order to screen a large number of glucosides, a suitable separation system was first developed. The eluens used to separate glucosides from their non-glycosylated

counterparts suffered from a low resolution when applied to analyze a typical reaction mixture of CsCDP (Figure 7.1, lane 1). Therefore, the performance of various eluens compositions for the separation of 1-*O*-β-D-glucopyranosyl hydroquinone, 1-*O*-β-D-cellobiopyranosyl hydroquinone and 1-*O*-β-D-cellotriopyranosyl hydroquinone (as obtained by reacting αG1P and 1-*O*-β-D-glucopyranosyl hydroquinone in the presence of CsCDP) was evaluated (Figure 7.1).

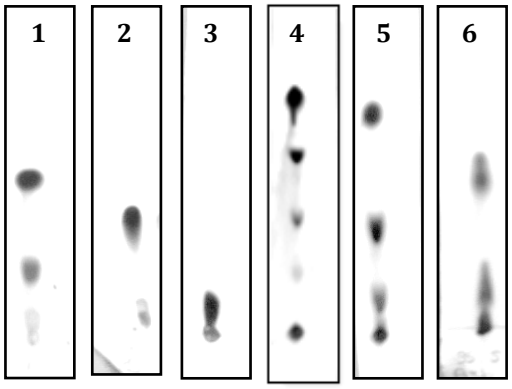

1. EtOAc/MeOH/H_2O = 30:5:4
2. EtOAc/MeOH = 8:1
3. EtOAc/H_2O = 8:1
4. Acetonitrile/H_2O = 85:15
5. EtOAC/butane/FA/H_2O = 3:3:1:1
6. Acetonitrile/H_2O = 95:5

Figure 7.1 Optimization of the separation of glucosides, cellobiosides and cellotriosides. Synthesis of glycosides was performed in a 50 mM MES buffer at pH 6.5 containing 100 mM αG1P, 100 mM 1-*O*-β-D-glucopyranosyl hydroquinone and 1 mg/mL CDP. Samples were analyzed after 24 h incubation at 37 °C.

Adequate separation was achieved when using an Acetonitrile/H_2O = 85:15 or an EtOAC/butane/FA/H_2O = 3:3:1:1 mixture. Unfortunately, the latter mixture contains formic acid, which may trigger hydrolysis of the formed glycosides upon isolation of the products. Therefore, the performance of the Acetonitrile/H_2O = 85:15 mixture was also evaluated for the separation of alkyl glycosides (Figure S7.1). Similar separation was achieved for both phenolic and aliphatic glycosides, revealing the generic character of the latter method.

Next, the activity of CsCDP towards a range of aliphatic and phenolic glucosides was scrutinized. Interestingly, the enzyme was active towards all tested compounds including the phenolic β-D-glucosides arbutin, esculin, salicin, polydatin, *p*-nitrophenyl β-glucoside, and aliphatic β-D-glucosides such as methyl β-glucopyranoside, butyl β-glucopyranoside, hexyl β-glucopyranoside, octyl β-glucopyranoside, nonyl β-glucopyranoside, decyl β-glucopyranoside and dodecyl β-glucopyranoside. Although less efficient (Figure S7.2), CDP was also able to transfer a glucose moiety to a number of α-glucosides including α-arbutin, methyl gallyl 4-α-D-glucopyranoside, ethyl gallyl 4-α-D-

glucopyranoisde, propyl gallyl 4-α-D-glucopyranoside, *p*-nitrophenyl 1-*O*-α-D-glucopyranoside and 3-*O*-α-D-glucopyranosyl resveratrol. Indeed, 24 h incubation at 37 °C resulted in 9 and 5 mM cellobioside and cellotrioside when using 1-*O*-α-D-glucopyranosyl hydroquinone as acceptor, whereas the product concentrations amounted to 24 and nearly 10 mM respectively upon addition of 1-*O*-β-D-glucopyranosyl hydroquinone (Table 7.1). Similar results were obtained for the PNP derivatives, indicating clear preference for β-linked glucose moieties.

Table 7.1 Synthesis of α and β-glycosides in a 50 mM MES buffer at pH 6.5 containing 1 mg/mL CDP, 100 mM αG1P and 100 mM acceptor. HPLC analysis was performed after 24 h of incubation at 37 °C.

	Concentration [mM]	
Acceptor	Cellobioside	Cellotrioside
1-*O*-α-D-Glucopyranosyl hydroquinone	9.4	5.4
1-*O*-β-D-Glucopyranosyl hydroquinone	24.1	9.9
p-Nitrophenyl 1-*O*-α-D-glucopyranoside	18.3	5.0
p-Nitrophenyl 1-*O*-β-D-glucopyranoside	22.2	13.7

Moreover, glycosylation was also observed when using the aliphatic α-D-glucosides of methanol, butanol or octanol as acceptor. Also here, a clear preference for β-glucosides was observed (Figure S7.2). Multiple newly formed glycosides were purified, and their structure was confirmed by NMR spectroscopy.

3.3 Mapping the acceptor specificity of CDP

Encouraged by these results, the acceptor specificity of CsCDP was analyzed in more detail. To that end, the specific activity of the enzyme towards various glucosides was determined (Figure 7.2). In accordance with the results obtained by Tran, a strong preference for the disaccharide cellobiose (3.4 U/mg) over the monosaccharide glucose (0.9 U/mg) was observed (Figure 7.2A)[39]. Maltose, α-(1,4)-linked glucobiose, was found to be a poor acceptor, exhibiting a specific activity of only 12 % (0.4 U/mg) when compared to cellobiose. Nevertheless, the formation of maltosyl β-(1,4)-glucopyranoside was confirmed by degradation with a β-glucosidase (Figure S7.3 and S7.4).

Next to carbohydrates, also a large group of glucosides with phenolic side chains were evaluated (Figure 7.2B). Interestingly, the highest activity of all tested acceptors was

found on PNP 1-*O*-β-D-glucopyranoside (10.1 U/mg) and arbutin (6.2 U/mg), followed by the β-cellobioside of PNP (5.9 U/mg). These numbers are substantially higher when compared to the activity towards cellobiose, confirming the importance of the acceptor subsite +2. Indeed, these results suggest the enzyme's preference for aryl over glucosyl side chains in +2 (Figure 7.3).

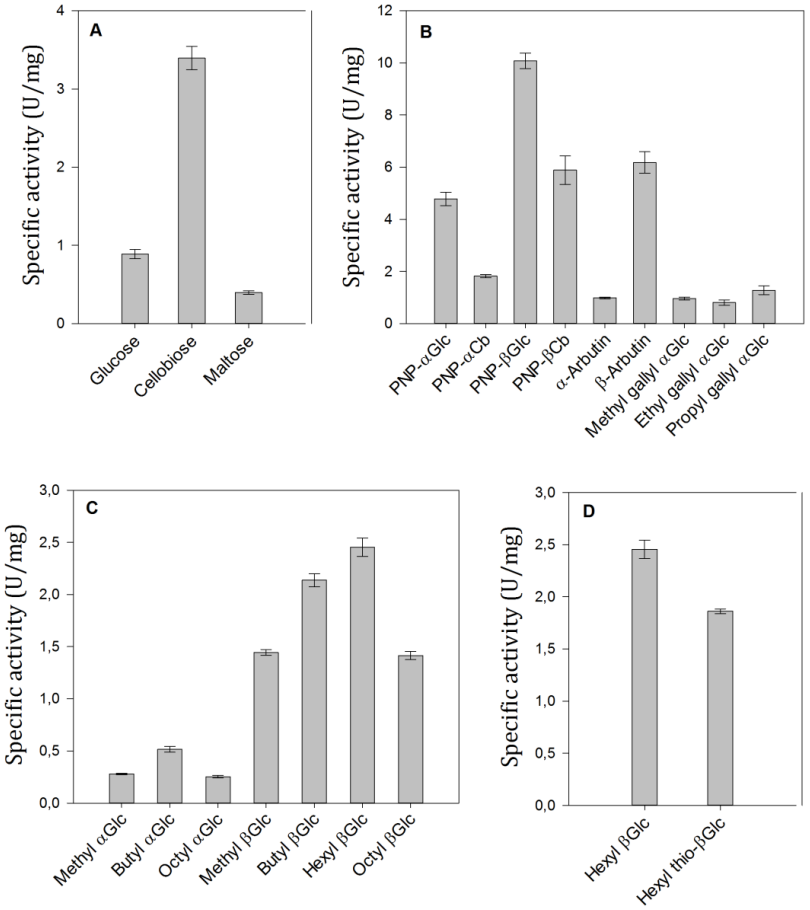

Figure 7.2 Specific activity of CDP towards carbohydrates (A), aromatic glucosides (B), aliphatic glucosides (C) and *O*- vs. *S*-β-glucosides (D). The specific activity was determined at 37 °C in a 50 mM MES buffer at pH 6.5 containing 50 mM αG1P and 50 mM acceptor. Abbreviations: PNP-αGlc, *p*-nitrophenyl 1-*O*- α-D-glucopyranoside; PNP-αCb, *p*-nitrophenyl 1-*O*-α-D-cellobiopyranoside; PNP-βGlc, *p*-nitrophenyl 1-*O*-β-D-glucopyranoside; PNP-βCb, *p*-nitrophenyl 1-*O*-β-D-cellobiopyranoside; Methyl gallyl αGlc, methyl gallyl 4-*O*-α-D-glucopyranoside; Ethyl gallyl αGlc, ethyl gallyl 4-*O*-α-D-glucopyranoside; Propyl gallyl αGlc, propyl gallyl 4-*O*-α-D-glucopyranoside; Methyl αGlc, methyl α-D-glucopyranoside; Butyl αGlc, butyl α-D-glucopyranoside; Octyl αGlc, octyl α-D-glucopyranoside; Methyl βGlc, methyl β-D-glucopyranoside; Butyl βGlc, butyl β-D-glucopyranoside; Octyl βGlc, octyl β-D-glucopyranoside; Hexyl βGlc, hexyl β-D-glucopyranoside; Hexyl thio-βGlc, hexyl thio-β-D-glucopyranoside.

Again, higher activities were found on β-bond glucosides compared to their α-linked counterparts. Indeed, while the specific activity towards *p*-nitrophenyl 1-*O*-β-D-glucopyranoside was found to be 10.1 U/mg, the activity was reduced to only 4.8 U/mg when using *p*-nitrophenyl 1-*O*-α-D-glucopyranoside as acceptor. Likewise, CsCDP was more active towards β-arbutin (6.2 U/mg) than α-arbutin (1.0 U/mg). Interestingly, CsCDP was also able to glycosylate a range of interesting antioxidants including methyl gallyl 4-*O*-α-D-glucopyranoside (1.0 U/mg), ethyl gallyl 4-*O*-α-D-glucopyranoside (0.8 U/mg) and propyl gallyl 4-*O*-α-D-glucopyranoside (1.3 U/mg).

In contrast to phenolic glucosides, moderate activities were observed when using acceptors with aliphatic side chains (Figure 7.2C). The activity towards hexyl β-D-glucopyranoside was found to be 2.5 U/mg, which is roughly 4 times lower compared to PNP 1-*O*-β-D-glucopyranoside. Both shorter and longer chains further decreased the enzymes efficiency, resulting in a specific activity of 1.4 U/mg for methyl and octyl β-D-glucopyranoside. In agreement with the observations for aromatic acceptors, CsCDP showed a clear preference for aliphatic β-glucosides compared to α-glucosides (Figure 7.2C). Although less efficient, the CDP from *Clostridium stercorarium* was also able to transfer a glucosyl moiety to thioglucosides (Figure 7.2D). In conclusion, CDP was found to strongly favor β-glucosides over α-glucosides. The highest activity was found towards glucosides with phenolic side chains, followed by glucosyl units and aliphatic side chains. These differences illustrate the importance of the +2 subsite regarding the activity of the CDP from *Clostridium stercorarium* (Figure 7.3).

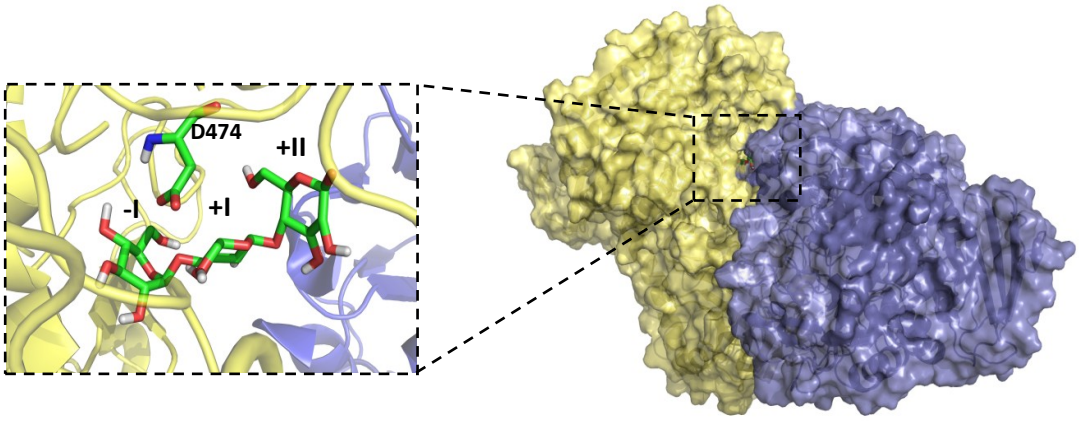

Figure 7.3 Homodimeric structure of the CDP from *Clostridium stercorarium*, docked with cellotriose. The catalytic residue D474, donor (-1) and acceptor (+1 and +2) subsites are indicated.

3.4 Altering the acceptor specificity of CDP by site directed mutagenesis

Although CsCDP was found to be a versatile glycosylation catalyst, its activity towards aliphatic glucosides is rather limited. Nevertheless, the synthesis of alkyl polyglucosides (APGs) remains of great value to date[183, 184, 193]. Based upon the obtained results, and previous studies on the CDP from *Clostridium stercorarium*[39], three positions in the +2 subsite were selected as potential 'hot-spots' for the selectivity of the enzyme (Figure 7.4).

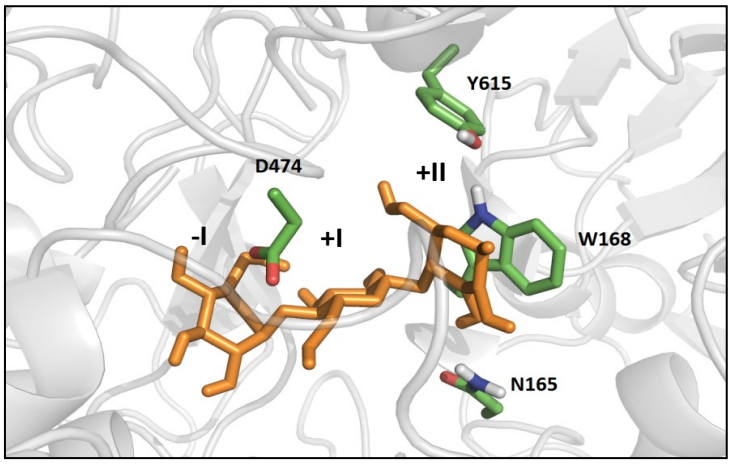

Figure 7.4 Predicted binding of cellotriose in the active site of the CDP from *Clostridium stercorarium*.

The asparangine residue N165 and the tryptophane residue W168 were chosen since these two residues have no counterpart in the structure of other glycoside phosphorylases[39]. Furthermore, the indole ring of residue W168 is most likely involved in stacking interactions when positioned parallel to the carbohydrate moiety or aryl unit of acceptor molecules[196, 197]. In addition, the tyrosine residue Y615 was chosen because of its interesting difference with CP. Indeed, the side chain of Y615 is flipped outwards in the case of CDP, thus avoiding a clash with bulky acceptors. Next, the three selected positions were mutated to alanine, and the activity of the obtained mutants towards a range of glucosides was determined (Table 7.2).

Table 7.2 Specific activity of the CDP from *Clostridium stercorarium* wild type (WT) and mutants. The specific activity (U/mg) was determined at 37 °C in a 50 mM MES buffer at pH 6.5 containing 50 mM αG1P and 50 mM acceptor.

Substrate	WT	Y615A	N165A	W168A
Cellobiose	3.40 ± 0.20	1.01 ± 0.07	3.02 ± 0.34	1.93 ± 0.21
PNP αGlc	4.78 ± 0.32	0.06 ± 0.01	0.34 ± 0.04	0.13 ± 0.02
PNP βGlc	10.08 ± 0.51	0.09 ± 0.01	2.29 ± 0.31	0.73 ± 0.08
Hexyl βGlc	2.45 ± 0.13	0.16 ± 0.02	3.20 ± 0.36	3.97 ± 0.50
Hexyl thio-βGlc	1.86 ± 0.08	0.19 ± 0.01	2.82 ± 0.35	3.74 ± 0.95
Octyl βGlc	1.41 ± 0.07	0.16 ± 0.02	2.37 ± 0.26	5.38 ± 0.64

Abbreviations: PNP-αGlc, *p*-nitrophenyl 1-*O*-α-D-glucopyranoside; PNP-βGlc, *p*-nitrophenyl 1-*O*-β-D-glucopyranoside; Hexyl βGlc, hexyl β-D-glucopyranoside; Hexyl thio-βGlc, hexyl thio-β-D-glucopyranoside; Octyl βGlc, octyl β-D-glucopyranoside.

Mutant Y615A displayed a significantly reduced activity towards all tested substrates (Table 7.2). Indeed, substitution of tyrosine Y615 by alanine decreased the specific activity by 70 % for the natural substrate cellobiose, while less than 10 % of the wild type activity was observed towards the unconventional substrates (Figure 7.5).

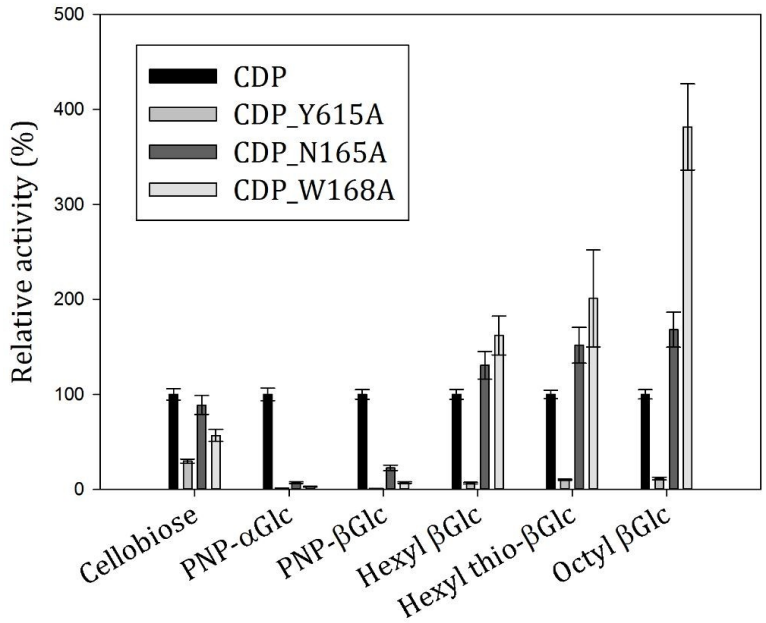

Figure 7.5 Relative activity of the WT and mutant (N165A, W168A, Y615A) CDP from *Clostridium stercorarium*. The activity was determined at 37 °C in a 50 mM MES buffer at pH 6.5 containing 50 mM αG1P and 50 mM acceptor. Abbreviations: PNP-αGlc, *p*-nitrophenyl 1-*O*-α-D-glucopyranoside; PNP-βGlc, *p*-nitrophenyl 1-*O*-β-D-glucopyranoside; Hexyl βGlc, hexyl β-D-glucopyranoside; Hexyl thio-βGlc, hexyl thio-β-D-glucopyranoside; Octyl βGlc, octyl β-D-glucopyranoside.

Residue Y615 was identified to be a determinant for the specificity of CDP and would therefore be an interesting target for further mutagenesis experiments. Substitution of asparangine 165 by alanine resulted in a significant loss of activity towards phenolic glucosides (i.e. residual activity of 7 and 23 % for *p*-nitrophenyl β or α-glucoside respectively). However, introducing alanine at position 165 did not affect the activity towards cellobiose, revealing interactions of N165 with aryl moieties in the +2 subsite (Table 7.2). Surprisingly, the latter substitution was also found to increase the activity towards aliphatic glucosides. Indeed, improved activities towards hexyl β-D-glucopyranoside (130 %), hexyl thio-β-D-glucopyranoside (151 %) and octyl β-D-glucopyranoside (167 %) were observed (Figure 7.5). Interestingly, these increased specific activities cannot be caused by a decreased K_m, as the Michaelis-Menten constants of the WT CDP (μM range) are much lower than the applied substrate concentrations (mM range)[39].

In parallel, replacing tryptophane 168 by alanine resulted in a significantly decreased activity towards the phenolic glucosides *p*-nitrophenyl β and α-glucoside. Moreover, also the activity towards cellobiose declined to 57 % (Figure 7.5). The latter results clearly suggest the importance of residue W168 in interactions with both aryl and glucosyl moieties. In contrast, the activity towards the aliphatic glucosides hexyl β-D-glucopyranoside, hexyl thio-β-D-glucopyranoside and octyl β-D-glucopyranoside increased substantially to 162, 201 and an impressive 381 % respectively. Docking experiments revealed the alkyl side chains turned towards the entrance of the active site (Figure 7.6). Indeed, substitution of the bulky tryptophane at position 168 by alanine reduces steric hindrance, thereby allowing increased reaction rates.

Next, both beneficial mutations (N165A and W168A) were combined in a double mutant. Although synergistic effects have previously been described[198, 199], the activity of the latter variant towards aliphatic glucosides was found to be decreased by 50 %. In conclusion, residues Y615, N165 and W168 were confirmed to be determinants for the specificity of CDP. Therefore, these positions can be considered 'hot-spots' for further mutagenesis experiments. However, significant improvements were already obtained, as the specific activity of variant W168A towards octyl β-glucopyranoside was found to be higher than the activity of the WT towards its natural substrate cellobiose.

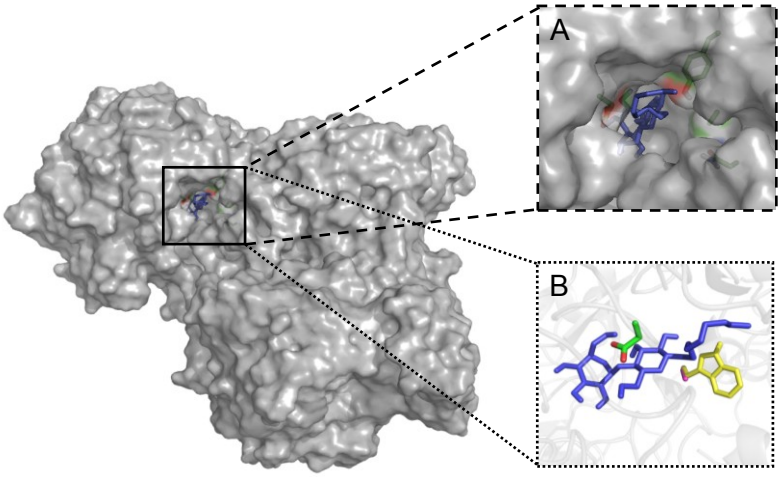

Figure 7.6 In silico docking of octyl β-cellobioside in modeled CDP_W168A variant. A: Entrance to the active site. B: Predicted binding of octyl β-cellobioside (blue). Residue 168 is shown both as tryptophane (yellow) and alanine (pink).

3.5 Efficient synthesis of octyl β-D-cellobiopyranoside

Finally, the applicability of the improved W168A mutant for the synthesis of octyl β-D-cellobiopyranoside was evaluated. To that end, two identical reactions with the wild type and W168A mutant were initiated, and the formation of the desired APG was followed by HPLC analysis (Figure 7.7).

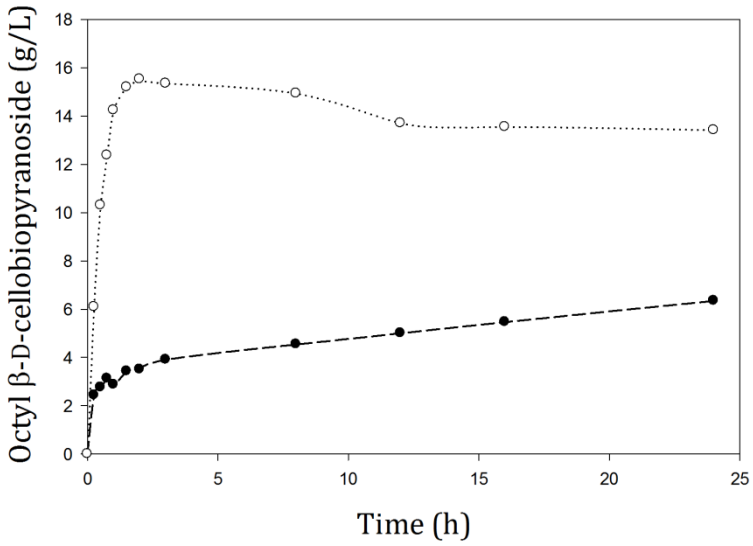

Figure 7.7 Synthesis of octyl β-D-cellobiopyranoside using the wild type (●) or mutant (○) CDP from *Clostridium stercorarium*. The reactions were performed at 37 °C in a 50 mM MES buffer at pH 6.5 containing 100 mM αG1P, 100 mM octyl β-D-glucopyranoside and 0.2 mg/mL CsCDP.

The octyl β-D-cellobiopyranoside concentration amounted up to 15 g/L after 2 h when using the W168A mutant, whereas only 1.7 g/L was formed under identical conditions with the wild type enzyme. Remarkably, the donor yield for the wild type reaction reached only 23.8 %, while 40.9 % of the initial αG1P was converted after 24 h when using the mutant enzyme. In conclusion, the W168A mutant clearly outperforms the wild type enzyme for the synthesis of octyl β-D-cellobiopyranoside, and can be considered a promising biocatalyst for the production of APGs.

4 CONCLUSION

Following the work on sucrose phosphorylase mediated α-glucosylation (CHAPTER 2, 3 and 4) and the synthesis of β-glucosides with cellobiose phosphorylase (CHAPTER 5), the prolongation of these glucosides with the cellodextrin phosphorylase from *Clostridium stercorarium* is described in this chapter. The specific activity of the enzyme towards various glucosides was assessed, revealing β-(1,4)-glucosylation of aliphatic and phenolic α/β-glucosides. Also, a range of complex cellobiosides and cellotriosides, among which salicyl 1-*O*-β-D-cellotriopyranoside and 6-*O*-β-D-cellobiopyranosyl esculetin, were synthesized, purified and confirmed by NMR spectroscopy. In addition, the function of the +2 subsite was scrutinized. Three proposed positions in the +2 subsite were mutated to alanine, and proved to be determinants for the activity of CDP. Remarkably, the specific activity of variant W168A towards octyl β-D-glucopyranoside was found to be higher than the activity of the WT towards its natural substrate cellobiose, revealing the potential of the newly created biocatalyst for the synthesis of APGs.

5 MATERIALS & METHODS

5.1 Materials

The IL AMMOENG 101 was kindly provided by Evonik Industries AG, and EtOAc was bought from Fiers. All other chemicals were analytical grade and purchased from Sigma-Aldrich.

5.2 Structural analysis of cellodextrin phosphorylase

The structural properties of the cellodextrin phosphorylase from *Clostridium stercorarium* were studied using a modeled structure, obtained by homology modeling in YASARA[200, 201] and visualization in PyMOL. A homology model was constructed based on the gene sequence of *C. stercorarium* CDP (DSM 8532) and the crystal structure of the chitobiose phosphorylase from *Vibrio proteolyticus* (PDB 1V7W)[39, 191, 202]. Three residues in subsite +2 (N165, W168, Y615) were selected for mutagenesis. Also, *in silico* docking experiments were carried out in YASARA using VINA[203, 204] and point charges assigned according to the AMBER03 force field[205].

5.3 Site-direct mutagenesis

Site-directed alanine mutants (Table 7.3) were created according to the Sanchis protocol. The latter method is based on the creation of a megaprimer from a mutagenic and a normal primer, which is afterwards used in a whole plasmid PCR[206].

Table 7.3 Overview of the created site directed mutants of the CDP from *C. stercorarium*.

Mutant	Fw primer	Rv primer	Megaprimer size
N165A	SAN_N165A	RV_ctrl	1875 bp
W168A	SAN_W168A	RV_ctrl	1915 bp
Y615A	FW_ctrl	SAN_RV_Y615A	1991 bp
N165A_W168A	SAN_N165A_W168A	RV_ctrl	1922 bp

The reaction mixture contained 2.5 U PfuUltra DNA Polymerase AD, 1x PfuUltra HF reaction buffer, 0.2 mM dNTP mix, 50 - 100 ng template DNA, 5 pmol forward primer and 5 pmol reverse primer (Table 7.4) in a total volume of 50 µL MilliQ. The PCR program starts with a hot start (3 min at 94 °C), and continues with 5 cycles of megaprimer formation (30 s denaturation at 94 °C, 60 seconds annealing at 55 °C and 1 min/kb elongation at 72 °C). In the second step, the created megaprimers were used in 20 cycles of whole-plasmid amplification (30 s denaturation at 94 °C and 2 min/kb for annealing and elongation at 68 °C). The program was finalized by a step of 2 min/kb at 72 °C, followed by subsequent cooling at 16 °C.

Table 7.4 Primers used for the site directed mutagenesis of the CDP *C. stercorarium* (5' - 3').

Primer name	Sequence
SAN_N165A	AATGGATCAGCAGGCGGTGGACTGGGTTCAGC
SAN_W168A	CAGCAGAATGTGGACGCAGTTCAGCAGATAAACC
SAN_N165A_W168A	AATGGATCAGCAGGCGGTGGACGCGGTTCAGCAGATAAACCAGGG
SAN_RV_Y615A	GCCCCCGGCGGTGCTGTGGTCATGCCCCCTATTTTC
FW_ctrl	GCCGACATCATAACGGTTCTG
RV_ctrl	TCTCTCATCCGCCAAAACAGC

After the PCR reaction, 20 U of *Dpn*I were added to the PCR mixtures and the latter were subsequently incubated during 1 h at 37 °C, resulting in digestion of methylated DNA. Next, an aliquot of 2.5 µL PCR-product was transformed into 50 µL of *E. coli* CGSC8974 electrocompetent cells using a Bio-Rad GenePulser (25 µF capacitance, 200 Ω resistance and a 10.0 kV/cm field strength). The cells were then incubated during 1 h at 37 °C and plated out on LB medium containing 100 µg/mL of ampicillin. After overnight incubation at 37 °C, the plates were stored at 4 °C. From these plates, three colonies were picked, added to 5 mL of liquid LB medium containing 100 µg/mL of ampicillin and incubated overnight at 37 °C while shaking at 200 rpm. Subsequently, 1 mL of medium was used for the creation of cryovials and 2 mL was used for plasmid extraction using the Qiagen Spin Miniprep kit. All constructs were subjected to nucleotide sequencing (LCG Genomics) to confirm the correct introduction of the desired mutations. Cryovials of the obtained strains were stored at -80 °C in presence of 70 % glycerol.

5.4 Production and purification of cellodextrin phosphorylase

Overexpression of CsCDP was carried out using *E. coli* JW0987 cells transformed with the expression plasmid pTrc99a harboring the codon optimized cellodextrin phosphorylase gene from *Clostridium stercorarium*. The strain was routinely grown at 37 °C on 500 mL LB medium (CHAPTER 5) supplemented with ampicillin (100 mg/L). After overnight growth, the culture was inoculated into 15 L of double LB medium (CHAPTER 5) supplemented with glucose (30 g/L) and ampicillin (100 mg/L) in a 30 L Biostat C reactor (B. Braun Biotech Inc.). The temperature, pH and stirrer speed were set at 37 °C, 7 and 800 rpm respectively. Adequate aeration was achieved by passing 1.1 vvm air through the reactor, and foaming was prevented by manually adding anti-

foam (10 % (v/v) antifoam silicone Snapsil RE 20, VWR BDH Prolabo) when required. Induction was performed by adding IPTG to a final concentration of 0.01 mM as soon as the OD_{600} reached 0.6. After 8 h of growth (OD_{600} ~ 34), the cells were harvested by centrifugation (10 000 g, 4 °C, 20 min), and frozen at -20 °C. The obtained pellets were lysed as described in CHAPTER 2 and the *N*-terminal His_6-tagged protein was purified by nickel-nitrilotriacetic acid metal affinity chromatography. The protocol as described by the supplier (Qiagen) was used, except for the imidazole concentration of the elution buffer, which was increased to 400 mM. The obtained enzyme solution was washed with MES buffer (50 mM, pH 6.5) and concentrated using Centricons (Amicon Ultra 30K, Millipore).

5.5 Activity assays

The activity of CDP was determined in the synthesis direction by measuring the release of phosphate from αG1P with the method of Gawronski and Benson[156]. One unit of CDP activity corresponds to the release of 1 µmol phosphate per minute from 50 mM αG1P and 50 mM acceptor in a 50 mM MES buffer at pH 6.5 and 37 °C. Protein concentrations were measured with the BCA Protein Assay kit (Pierce), using bovine serum albumin as standard. All assays were performed in triplicate and had a CV of less than 10 %. All reported errors correspond to the standard errors.

5.6 Analytical methods

The formation of glucosides was assessed by TLC, HPLC or HPAEC-PAD analysis. Separation and detection were achieved on Merck Silica gel 60 F_{254} precoated plates. Unless stated otherwise, the eluens was a mixture of ACN/H_2O = 85:15, and spots were visualized by UV detection at 254 nm, or charring with 10 % (v/v) H_2SO_4. Alternatively, the concentration of glycosides was determined by HPLC analysis. Adequate separation and detection was achieved using an X-bridge amide column (250 mm × 4.6 mm, 3.5 µm, Waters, USA) coupled with an Alltech 2000ES evaporative light scattering detector, as described in CHAPTER 4. The separation of carbohydrates was achieved by high performance anion exchange chromatography (HPAEC), while detection was performed with a pulsed amperometric detector (PAD). To that end, a CarboPack PA20 column installed on a Dionex ICS-5000 IC system was used. Elution was performed with a

gradient of eluent A (MilliQ), B (100 mM NaOH) and C (100 mM NaOH and 1 M NaOAc), as described in Table S7.2. All calibration curves were prepared with authentic samples.

5.7 Production and purification of glycosides

Glycosylation of a range of acceptor molecules (α-arbutin, arbutin, esculin, maltose, octyl β-D-glucopyranoside, *p*-nitrophenyl 1-*O*-α-D-glucopyranoside, *p*-nitrophenyl 1-*O*-β-D-glucopyranoside, polydatin, and salicin) was performed at 50 mL scale in falcons. To that end, 100 mM αG1P, 100 mM acceptor and 1 mg/mL CDP were added to a 50 mM MES buffer at pH 6.5. The reaction mixtures were incubated at 37 °C and 200 rpm. After 48 h, the reaction mixtures were heated (10 min, 95 °C) and centrifuged (10 000 g, 4 °C, 20 min) to remove debris. The samples were then evaporated *in vacuo* and the residue was purified by column chromatography (silicagel, ACN/H_2O = 85:15).

5.8 Structure elucidation of glycosides

NMR spectra were measured on a Bruker AVANCE III 700 MHz spectrometer (700.13 MHz for ^{1}H and 176.05 MHz for ^{13}C) in CD_3OD at 25 °C. Residual signals of solvent were used as an internal standard (δ_H 3.330 ppm, δ_C 49.3 ppm). ^{1}H NMR, ^{13}C NMR, COSY, HSQC, and HMBC spectra were measured using standard manufacturers' software (Topspin 3.2, Bruker BioSpin GmbH, Rheinstetten, DE). Chemical shifts are given in δ-scale [ppm], and coupling constants in Hz. Digital resolution enabled us to report chemical shifts of protons to three and coupling constants to one and carbon chemical shifts to two decimal places. Some hydrogen chemical shifts were read out from HSQC and are reported to two decimal places. The proton spin systems were assigned by COSY, and then the assignment was transferred to carbons by HSQC. HMBC experiments enabled to assign quaternary carbons and join individual spin systems together. Spectral analysis and interpretation was kindly performed by the group of Prof. Vladimír Křen at the Institute of Microbiology (Czech Republic).

6-*O*-β-D-Cellobiopyranosyl esculetin

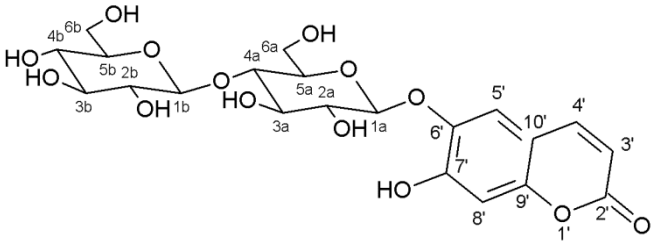

^{1}H NMR (CD_3OD): δ 3.268 (1H, dd, *J* = 9.1, 7.9 Hz, H-2b), 3.335 (1H, dd, *J* = 9.5, 8.9 Hz, H-4b), 3.386 (1H, ddd, *J* = 9.5, 5.8, 2.3 Hz, H-5b), 3.402 (1H, dd, *J* = 9.1, 8.9 Hz, H-3b), 3.611 (1H, dd, *J* = 9.0, 7.7 Hz, H-2a), 3.637 (1H, ddd, *J* = 9.5, 4.3, 2.4 Hz, H-5a), 3.670 (1H, dd, *J* = 9.0, 8.4 Hz, H-3a), 3.796 (1H, dd, *J* = 11.8, 5.8 Hz, H-6b). 3.706 (1H, dd, *J* = 9.5, 8.4 Hz, H-4a), 3.919 (1H, dd, *J* = 11.8, 2.3 Hz, H-6b), 3.929 (1H, dd, *J* = 12.2, 4.3 Hz, H-6a), 3.991 (1H, dd, *J* = 12.2, 2.4 Hz, H-6a), 4.466 (1H, d, *J* = 7.9 Hz, H-1b), 4.907 (1H, d, *J* = 7.7 Hz, H-1a), 6.225 (1H, d, *J* = 9.4, H-3'), 6.820 (1H, s, H-8'), 7.423 (1H, s, H-5'), 7.859 (1H, d, *J* = 9.4 Hz, H-4')

^{13}C NMR (CD_3OD): δ 61.96 (C-6a), 62.74 (C-6b), 71.69 (C-4b), 74.87 (C-2a), 75.23 (C-2b), 76.24 (C-3a), 77.26 (C-5a), 78.19 (C-3b), 78.46 (C-5b), 80.53 (C-4a), 104.34 (C-1a), 104.92 (C-1b), 105.11 (C-8'), 112.33[a] (C-3'), 116.68 (C-5'), 112.28[a] (C-10'), 145.40 (C-6'), 146.46 (C-4'), 153.36 (C-9'), 155.8 (C-7'), 164.35 (C-2'), [a]might be interchanged

Salicyl 1-*O*-β-D-cellobiopyranoside

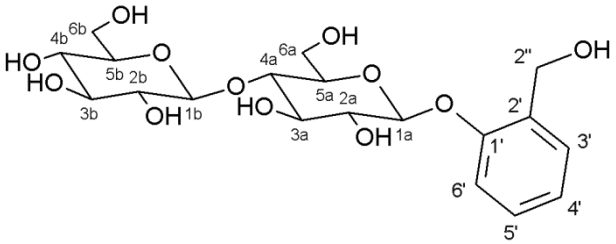

^{1}H NMR (CD_3OD): δ 3.059 (1H, dd, *J* = 9.4, 8.0 Hz, H-2b), 3.153 (1H, dd, *J* = 9.8, 9.1 Hz, H-4b), 3.23 (1H, m H-5b), 3.243 (1H, dd, *J* = 9.4, 9.1 Hz, H-3b), 3.413 (1H, m, H-2a), 3.47 (1H, m, H-6b), 3.48 (1H, m, H-3a), 3.49 (1H, m, H-4a), 3.49 (1H, m, H-5a), 3.577 (1H, dd, *J* = 12.3, 2.3 Hz, H-6a), 3.657 (1H, dd, *J* = 12.3, 2.4 Hz, H-6b), 3.712 (1H, d, *J* = 12.3 Hz, H-6a), 4.271 (1H, d, *J* = 8.0 Hz, H-1b), 4.423 (1H, d, *J* = 12.6 Hz, H-2''), 4.461 (1H, d, *J* = 12.6 Gz, H-2''), 4.888 (1H, d, *J* = 7.8 Hz, H-1a), 6.886 (1H, dd, *J* = 7.5, 7.5 Hz, H-4'), 6.946 (1H, d, *J* = 8.2 Hz, H-6'), 7.113 (1H, dd, *J* = 8.2, 7.5 Hz, H-5'), 7.144 (1H, d, *J* = 7.5 Hz, H-3')

^{13}C NMR (CD_3OD): δ 59.46 (C-2''), 60.05 (C-6a), 60.81 (C-6b), 69.70 (C-4b), 72.98 (C-2a), 73.40 (C-2b), 74.40 (C-3a), 75.17 (C-5a), 75.73 (C-3b), 76.24 (C-5b), 78.52 (C-4a), 100.53 (C-1a), 102.81 (C-1b), 115.53 (C-6'), 123.63 (C-4'), 129.65 (C-2'), 129.93[a] (C-3'), 129.94[a] (C-5'), 154.76 (C-1'), [a]might be interchanged

Salicyl 1-*O*-β-D-cellotriopyranoside

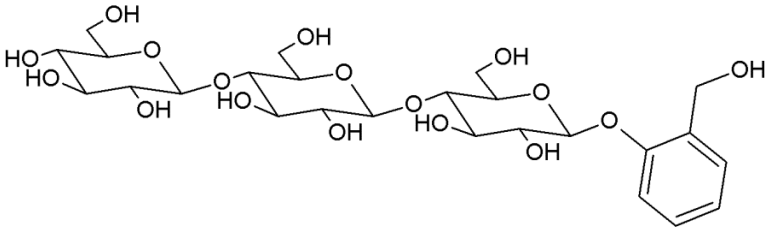

^{1}H NMR (CD_3OD): δ 3.044 (1H, dd, *J* = 9.4, 7.9 Hz, H-2c), 3.106 (1H, dd, *J* = 9.0, 7.9 Hz, H-2b), 3.144 (1H, dd, *J* = 9.1, 9.8 Hz, H-4c), 3.21 (1H, m, H-5c), 3.644 (1H, dd, H-6c), 3.236 (1H, dd, *J* = 9.4, 9.1 Hz, H-3c), 3.36 (1H, m, H-5b), 3.39 (1H, m, H-3b), 3.40 (1H, m, H-4b), 3.416 (1H, m, H-2a), 3.463 (1H, dd, *J* = 12.6, 5.8 Hz, H-6c), 3.49 (1H, m, H-3a), 3.50 (1H, m, H-4a), 3.50 (1H, m, H-5a), 3.570 (1H, dd, H-6b), 3.583 (1H, dd, H-6a), 3.714 (1H, d, H-6a), 3.725 (1H, d, H-6b), 4.241 (1H, d, *J* = 7.9 Hz, H-1c), 4.297 (1H, d, *J* = 7.9 Hz, H-1b), 4.425 (1H, d, *J* = 12.6 Hz, H-2''), 4.463 (1H, d, *J* = 12.6 Hz, H-2''), 4.890 (1H, d, *J* = 7.8 Hz, H-1a,), 6.894 (1H, dd, *J* = 7.5, 7.5 Hz, H-4'), 6.948 (1H, d, *J* = 8.2 Hz, H-6'), 7.115 (1H, dd, *J* = 8.2, 7.5 Hz, H-5'), 7.146 (1H, d, *J* = 7.5 Hz, H-3')

^{13}C NMR (CD_3OD): δ 59.46 (C-2''), 60.01 (C-6a), 60.14 (C-6b), 60.81 (C-6c), 69.69 (C-4c), 72.99 (C-2a), 73.19 (C-2b), 73.39 (C-2c), 74.29 (C-3b), 74.36 (C-3a), 75.08 (C-5b), 75.18 (C-5a), 75.72 (C-3c), 76.22 (C-5c), 78.63 (C-4b), 78.40 (C-4a), 100.55 (C-1a), 102.59 (C-1b), 102.81 (C-1c), 115.54 (C-6'), 123.63 (C-4'), 129.66 (C-2'), 129.93[a] (C-3'), 129.94[a] (C-5'), 154.76 (C-1'), [a]might be interchanged

para-Nitrophenyl 1-_O_-β-D-cellobiopyranoside

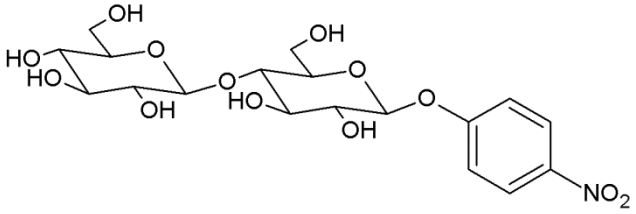

^{1}H NMR (CD_3OD): δ 3.277 (1H, dd, *J* = 9.2, 7.9 Hz, H-2b), 3.339 (1H, dd, *J* = 9.5, 8.8 Hz, H-4b), 3.386 (1H, ddd, *J* = 9.5, 5.8, 2.2 Hz, H-5b), 3.406 (1H, dd, *J* = 9.2, 8.8 Hz, H-3b), 3.594 (1H, dd, *J* = 8.8, 7.7 Hz, H-2a), 3.68 (1H, m, H-3a), 3.70 (1H, m, H-5a), 3.70 (1H, m, H-6b), 3.72 (1H, m, H-4a), 3.924 (1H, dd, *J* = 12.3, 3.6 Hz, H-6a), 3.919 (1H, dd, *J* = 11.9, 2.2 Hz, H-6b), 3.957 (1H, dd, *J* = 12.3, 2.1 Hz, H-6a), 4.473 (1H, d, *J* = 7.9 Hz, H-1b), 5.139 (1H, d, *J* = 7.7 Hz, H-1a), 7.257 (2H, m, *ΣJ* = 9.3 Hz, H-*ortho*), 8.240 (2H, m, *ΣJ* = 9.3 Hz, H-*meta*)
^{13}C NMR (CD_3OD): δ 61.81 (C-2a,), 62.75 (C-6a), 71.68 (C-4b), 74.74 (C-2a), 75.21 (C-2b), 76.50 (C-3a), 77.16 (C-5a), 78.18 (C-3b), 78.44 (C-5b), 80.29 (C-4a), 101.64 (C-1a), 104.87 (C-1b), 118.10 (C-*ortho*), 126.92 (C-*meta*), 144.23 (C-*para*), 164.08 (C-*ipso*)

para-Nitrophenyl 1-_O_-β-D-cellotriopyranoside

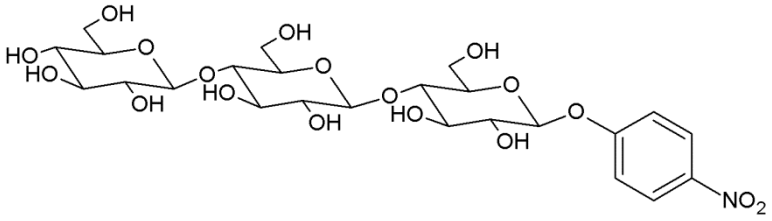

^{1}H NMR (CD_3OD): δ 3.25 (1H, m, H-2c), 3.34 (1H, m, H-4c), 3.35 (1H, m, H-2b), 3.36 (1H, m, H-5c), 3.39 (1H, m, H-3c), 3.52 (1H, m, H-5b), 3.57 (1H, m, H-3b), 3.59 (1H, m, H-2a), 3.63 (1H, m, H-4b), 3.69 (1H, m, H-3a), 3.69 (1H, m, H-6c), 3.70 (1H, m, H-5a), 3.72 (1H, m, H-4a), 3.91 (1H, m, H-6b), 3.91[a] (1H, m, H-6c), 3.95 (1H, m, H-6a), 3.95[a] (1H, m, H-6a), 3.95 (1H, m H-6b), 4.429 (1H, d, *J* = 7.4 Hz, H-1c), 4.513 (1H, d, *J* = 7.7 Hz, H-1b), 5.143 (1H, d, *J* = 7.3 Hz, H-1a), 7.26 (2H, m, H-*ortho*), 8.25 (2H, m, H-*meta*)
^{13}C NMR (CD_3OD): δ 61.71[a] (C-6b), 61.81[a] (C-6a), 62.75 (C-6c), 71.68 (C-4c), 74.76 (C-2a), 74.93 (C-2b), 75.21 (C-2c), 76.45 (C-3a), 76.51 (C-3b), 76.99 (C-5b), 77.15 (C-5a), 78.16 (C-3c), 78.44 (C-5c), 80.10 (C-4a), 80.48 (C-4b), 101.67 (C-1a), 104.63 (C-1b), 104.93 (C-1c), 118.01 (C-*ortho*), 126.92 (C-*meta*), 144.26 (C-*para*), 164.09 (C-*ipso*), [a]might be interchanged

para-Nitrophenyl 1-_O_-α-D-cellobiopyranoside

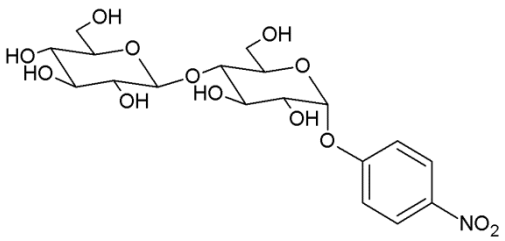

^{1}H NMR (CD_3OD): δ 3.255 (1H, dd, *J* = 9.0, 7.9 Hz, H-2b,), 3.336 (1H, dd, *J* = 9.5, 8.8 Hz, H-4b), 3.381 (1H, ddd, *J* = 9.5, 5.7, 2.2 Hz, H-5b), 3.394 (1H, dd, *J* = 9.0, 8.8 Hz, H-3b), 3.70[a] (1H, m, H-6a), 3.71 (1H, m, H-4a), 3.71 (1H, m, H-5a), 3.72 (1H, m, H-2a), 3.751 (1H, dd, *J* = 12.2, 1.9 Hz, H-6a), 3.890 (1H, dd, *J* = 12.2, 3.2 Hz, H-6a), 3.918 (1H, dd, *J* = 11.8, 2.2 Hz, H-6a), 4.004 (1H, m, *ΣJ* = 18.1 Hz, H-3a), 4.448 (1H, d, *J* = 7.9

Hz, H-1b), 5.691 (1H, d, *J* = 3.7 Hz, H-1a), 7.338 (2H, m, *ΣJ* = 9.3 Hz, H-*ortho*), 8.248 (2H, m, *ΣJ* = 9.3 Hz, H-*meta*)
^{13}C NMR (CD_3OD): δ 61.67 (C-6a), 62.75 (C-6b), 71.67 (C-4b), 73.05 (C-2a), 73.51 (C-3a), 73.80 (C-5a), 75.22 (C-2b), 78.15 (C-3b), 78.44 (C-5b), 80.55 (C-4a), 99.11 (C-1a), 104.93 (C-1b), 118.19 (C-*ortho*), 126.95 (C-*meta*), 144.23 (C-*para*), 163.67 (C-*ipso*)

para-Nitrophenyl 1-_O_-α-D-cellotriopyranoside

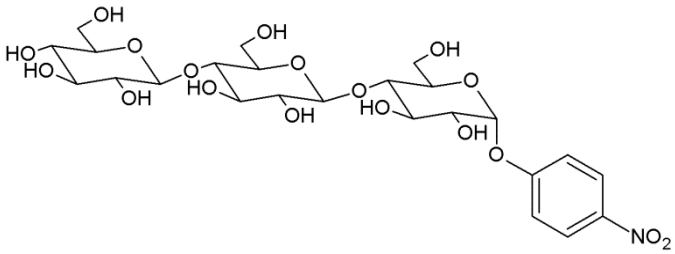

^{1}H NMR (CD_3OD): δ 3.252 (1H, dd, *J* = 9.2, 7.9 Hz, H-2c), 3.328 (1H, dd, *J* = 9.2, 7.9 Hz, H-2b), 3.325 (1H, dd, J = 9.6, 8.8 Hz, H-4c), 3.374 (1H, m, H-5c), 3.396 (1H, dd, *J* = 9.2, 8.8 Hz, H-3c), 3.521 (1H, ddd, *J* = 9.6, 4.2, 2.5 Hz, H-5b), 3.560 (1H, dd, *J* = 9.2, 8.8 Hz, H-3b), 3.627 (1H, dd, *J* = 9.6, 8.8 Hz, H-4b), 3.685 (1H, dd, *J* = 11.9, 5.8 Hz, H-6c), 3.71 (1H, m, H-5a), 3.72 (1H, m, H-2a), 3.72 (1H, m, H-4a,), 3.75 (1H, m, H-6a), 3.90 (1H, m, H-6a), 3.90 (1H, m, H-6b), 3.91 (1H, m, H-6c), 3.952 (1H, dd, *J* = 12.1, 2.5 Hz, H-6b), 4.011 (1H, dd, *J* = 9.8, 8.1 Hz, H-3a), 4.431 (1H, d, *J* = 7.9 Hz, H-1c), 4.493 (1H, d, *J* = 7.9 Hz, H-1b), 5.699 (1H, d, *J* = 3.7 Hz, H-1a), 7.340 (2H, m, *ΣJ* = 9.3 Hz, H-*ortho*), 8.251 (2H, m, *ΣJ* = 9.3 Hz, H-*meta*)
^{13}C NMR (CD_3OD): δ 61.56 (C-6a), 61.77 (C-6b), 62.71 (C-6c), 71.66 (C-4c), 73.05 (C-2a), 73.43 (C-3a), 73.79 (C-5a), 74.91 (C-2b), 75.18 (C-2c), 76.41 (C-3b), 76.96 (C-5b), 78.12 (C-3c), 78.42 (C-5c), 80.33 (C-4a), 80.45 (C-4b), 99.09 (C-1a), 104.65 (C-1b), 104.90 (C-1c), 118.20 (C-*ortho*), 126.96 (C-*meta*), 144.23 (C-*para*), 163.65 (C-*ipso*)

Octyl β-D-cellotriopyranoside

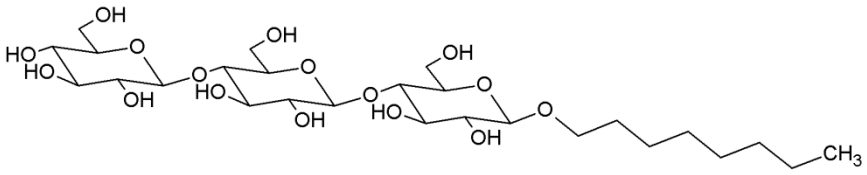

^{1}H NMR (CD_3OD): δ 0.922 (3H, t, *J* = 7.1 Hz, H-8'), 1.31 (2H, m, H-6'), 1.33 (2H, m, H-5'), 1.33 (2H, m, H-7'), 1.34 (2H, m, H-4'), 1.404 (2H, m, H-3'), 1.641 (2H, m, H-2'), 3.243 (1H, dd, *J* = 9.2, 7.9 Hz, H-2a), 3.253 (1H, dd, *J* = 9.2, 7.8 Hz, H-2c), 3.311 (1H, dd, *J* = 9.2, 7.9 Hz, H-2b), 3.321 (1H, dd, *J* = 9.7, 8.7 Hz, H-4a), 3.361 (1H, ddd, *J* = 9.7, 5.8, 2.3 Hz, H-5a), 3.385 (1H, dd, *J* = 9.2, 8.7 Hz, H-3a), 3.407 (1H, ddd, *J* = 9.6, 3.7, 2.8 Hz, H-5c), 3.498 (1H, ddd, *J* = 9.6, 4.2, 2.4 Hz, H-5b), 3.530 (1H, dd, *J* = 9.2, 8.8 Hz, H-3c), 3.550 (1H, dd, *J* = 9.2, 8.9 Hz, H-3b), 3.594 (1H, dd, *J* = 9.6, 8.8 Hz), 3.56 (1H, m, H-1'), 3.612 (1H, dd, *J* = 9.6, 8.9 Hz, H-4b), 3.681 (1H, dd, *J* = 11.9, 5.8 Hz, H-6a), 3.882 (1H, dd, *J* = 12.1, 4.2 Hz, H-6b), 3.896 (2H, m, H-6c), 3.898 (1H, m, H-6a), 3.90 (1H, m, H-1'), 3.926 (1H, dd, *J* = 12.1, 2.4 Hz, H-6b), 4.299 (1H, d, *J* = 7.8 Hz, H-1c), 4.420 (1H, d, *J* = 7.9 Hz, H-1a), 4.473 (1H, d, *J* = 7.9 Hz, H-1b)
^{13}C NMR (CD_3OD): δ 14.72 (C-8'), 24.02 (C-7'), 27.42 (C-3'), 30.72[a] (C-5'), 30.88[a] (C-4'), 31.09 (C-2'), 33.31 (C-6'), 62.08 (C-6b), 62.73 (C-6a), 71.27 (C-1'), 71.66 (C-4a), 74.94 (C-2b), 75.15 (C-2c), 75.20 (C-2a), 76.49 (C-3b), 76.72 (C-3c), 76.72 (C-5c), 76.95 (C-5b), 78.14 (C-3a), 78.43 (C-5a), 80.46 (C-4b), 80.87 (C-4c), 61.78 (C-6c), 104.53 (C-1c), 104.66 (C-1b), 104.91 (C-1a), [a]might be interchanged

Octyl β-D-cellotetrapyranoside

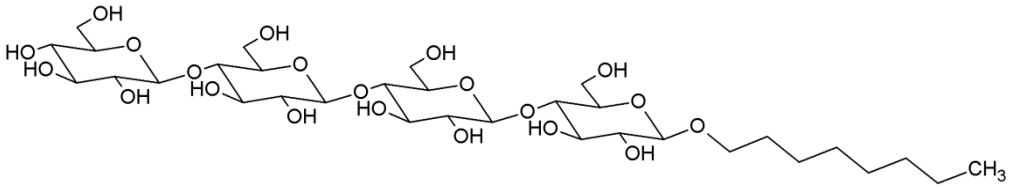

^{1}H NMR (CD_3OD): δ 0.589 (3H, m, H-8'), 1.00 (2H, m, H-6'), 1.00 (2H, m, H-7'), 1.03 (2H, m, H-4'), 1.03 (2H, m, H-5'), 1.082 (2H, m, H-3'), 1.351 (2H, m, H-2'), 3.024 (1H, dd, *J* = 9.0, 8.0 Hz, H-2d), 3.042 (1H, dd, *J* = 9.3, 7.9 Hz, H-2a), 3.086 (1H, dd, *J* = 9.3, 7.9 Hz, H-2b), 3.086 (1H, dd, *J* = 9.3, 7.9 Hz, H-2c), 3.144 (1H, dd, *J* = 9.3, 9.2 Hz, H-4a), 3.214 (1H, m, H-5a), 3.234 (1H, dd, *J* = 9.3, 9.2 Hz, H-3a), 3.307 (1H, m, H-5d), 3.349 (1H, m, H-5b), 3.349 (1H, m, H-5c), 3.356 (1H, m, H-3d), 3.356 (1H, m, H-4d), 3.397 (1H, m, H-3b), 3.397 (1H, m, H-4b), 3.397 (1H, m, H-3c), 3.397 (1H, m, H-4c), 3.40 (1H, m, H-1'), 3.463 (1H, m, H-6a), 3.555 (1H, m, H-6b), 3.555 (1H, m, H-6c), 3.64 (1H, m, H-1'), 3.643 (1H, m, H-6a), 3.704 (1H, m, H-6d), 3.707 (1H, m, H-6b), 3.707 (1H, m, H-6c), 3.896 (1H, m, H-6d), 4.201 (1H, d, *J* = 8.0 Hz, H-1d), 4.236 (1H, d, *J* = 7.9 Hz, H-1a), 4.261 (1H, d, *J* = 7.9 Hz, H-1b), 4.261 (1H, d, *J* = 7.9 Hz, H-1c)

^{13}C NMR (CD_3OD): δ 13.64 (C-8'), 22.25 (C-7'), 25.27 (C-3'), 28.61[a] (C-5'), 28.68[a] (C-4'), 28.96 (C-2'), 31.33 (C-6'), 60.08 (C-6c), 60.13 (C-6b), 60.26 (C-6d), 60.80 (C-6a), 69.69 (C-4a), 71.04 (C-1'), 73.16 (C-2d), 73.18 (C-2c), 73.19 (C-2b), 73.38 (C-2a), 74.25 (C-3c), 74.27 (C-3b), 74.59 (C-3d), 74.99 (C-5d), 75.06 (C-5c), 75.06 (C-5b), 75.72 (C-3a), 76.22 (C-5a), 78.48 (C-4c), 78.61 (C-4b), 78.79 (C-4d), 102.26 (C-1d), 102.58 (C-1c), 102.59 (C-1b), 102.80 (C-1a), [a]might be interchanged

6 SUPPLEMENTARY INFORMATION

Table S7.1 Glycosylation potential of the CDP from *C. stercorarium* towards aglycons. TLC analysis was performed after 24 h incubation at 37 °C.

Acceptor	Product spot	Acceptor	Product spot
Pentanol[a]	-	Cinnamyl alcohol[a]	-
Hexanol[a]	-	Menthol[b]	-
Heptanol[a]	-	Saligenin[b]	-
Octanol[a]	-	*p*-Nitrophenol[b]	-
Nonanol[a]	-	Phenol[b]	-
Decanol[a]	-	Hydroquinone[b]	-
Dodecanol[a]	-	Catechol[b]	-
Cyclohexanol[a]	-	Resorcinol[b]	-
2-Hexanol[a]	-	Pyrogallol [b]	-
Linalool[a]	-	Gallic acid methyl ester[b]	-
Eugenol[a]	-	Gallic acid ethyl ester[b]	-
Nerolidol[a]	-	Gallic acid propyl ester[b]	-
β-Citronellol[a]	-	Gallic acid lauryl ester[b]	-
Geraniol[a]	-	Salicylic acid methyl ester[a]	-
2-Phenylethanol[a]	-	Curcumin[b]	-
1*R*-Phenylethanol[a]	-	Resveratrol[b]	-
1*S*-Phenylethanol[a]	-	Quercetin[b]	-
Benzyl alcohol[a]	-	Vanillin[b]	-
Anisyl alcohol[a]	-	Vanillyl alcohol[b]	-

[a] Glycosylation was performed in a 50 mM MES buffer at pH 6.5 in the presence of 100 mM αG1P, 20 % acceptor and 1 mg/mL CsCDP. [b] Glycosylation was performed in a 50 mM MES buffer at pH 6.5 containing 20 % IL AMMOENG 101, in the presence of 100 mM αG1P, 100 mM acceptor and 1 mg/mL CsCDP.

Table S7.2 HPAEC-PAD elution was performed with a gradient of eluent A (MilliQ), B (100 mM NaOH) and C (100 mM NaOH and 1 M NaOAc) at a flow rate of 0.5 mL/min.

Time (min)	A (%)	B (%)	C (%)
0	80	20	0
4	80	20	0
8	0	100	0
10	0	100	0
45	15	85	15
46	80	20	0
55	80	20	0

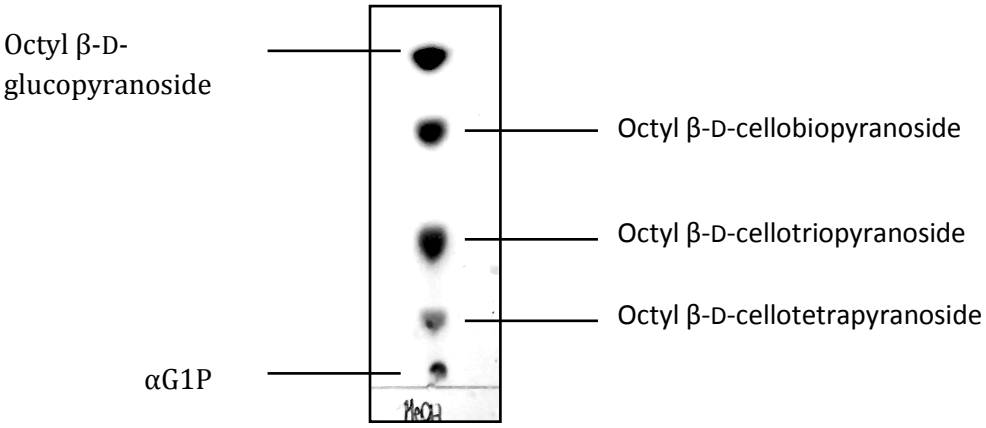

Figure S7.1 Separation of aliphatic glycosides with an Acetonitrile/H_2O = 85:15 mixture. Analysis was performed after reacting a 50 mM MES buffer at pH 6.5 containing 100 mM αG1P, 100 mM octyl β-D-glucopyranoside and 1 mg/mL CsCDP during 24 h at 37 °C.

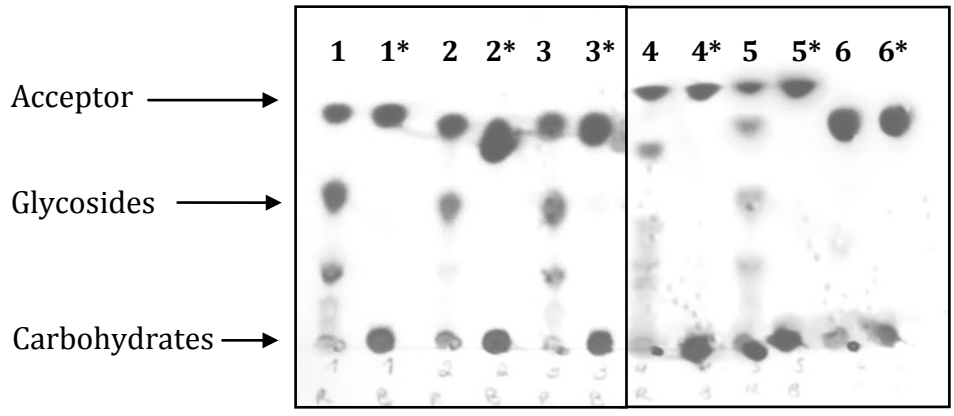

Figure S7.2 Glycosylation of various acceptors. TLC analysis was performed after 24 h of incubation at 37 °C. The reaction mixtures consisted of a 50 mM MES buffer at pH 6.5 supplemented with 100 mM αG1P, 1 mg/mL CDP and 100 mM of the following acceptors: arbutin (1), α-arbutin (2), salicin (3), methylgallyl 4-*O*-α-D-glucoside (4), octyl β-D-glucopyranoside (5) and octyl α-D-glucopyranoside (6). Lanes with * represent blank reactions, i.e. no addition of CsCDP.

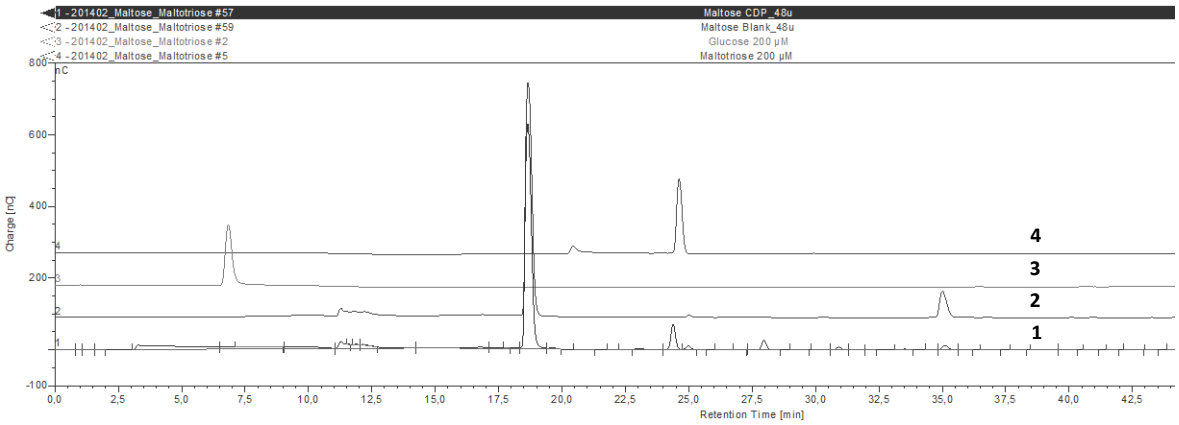

Figure S7.3 HPAEC-PAD analysis of [1] the glycosylation of maltose after 48 h of incubation at 37 °C. 100 mM αG1P and 100 mM maltose were reacted in a 50 mM MES buffer (pH 6.5), supplemented with 1 mg/mL CDP: maltose (18.9 min), unidentified peak (24.1 min), maltotriose trace (24.9 min), unidentified peak (28.0 min), G1P (35.2 min). [2] Blank reaction: maltose (18.9 min), maltotriose trace (24.9 min), αG1P (35.2 min). [3] Standard glucose (7.0 min). [4] Standard maltotriose (24.9 min).

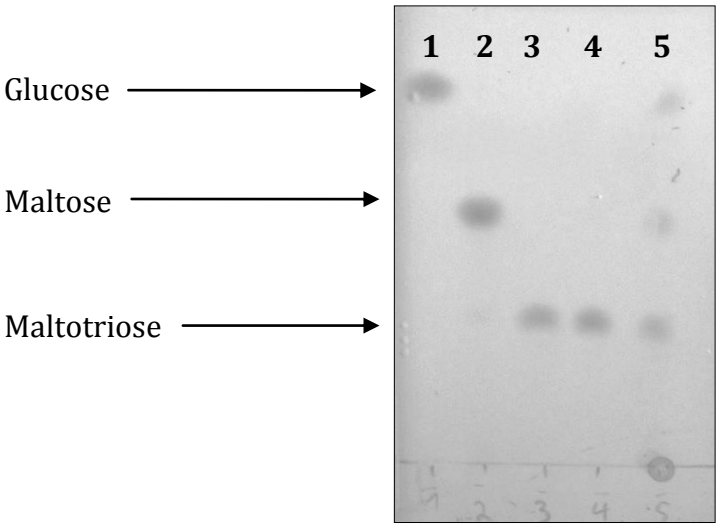

Figure S7.4 Structure confirmation of maltosyl β-(1,4)-D-glucopyranoside. Lane 1: glucose, Lane 2: maltose, Lane 3: maltotriose, Lane 4: purified product, no addition of β-glucosidase, Lane 5: purified product, incubated for 1 h with 5 U/mL β-glucosidase. TLC analysis was performed using three ascents of eluent Acetonitrile/H_2O = 85:15.

CHAPTER 8

Chemoenzymatic glycosylation of phenolic antioxidants: phosphorylase mediated synthesis and characterization.

This chapter has been published as:

K. De Winter, G. Dewitte, M.E. Dirks-Hofmeister, S. De Laet, H. Pelantova, V. Kren, and T. Desmet, **2015**, Enzymatic glycosylation of phenolic antioxidants: phosphorylase mediated synthesis and characterization, *Journal of Agricultural and Food Chemistry*, 63, 10131-10139.

1 ABSTRACT

Although numerous biologically active molecules exist as glycosides in nature, information on the activity, stability and solubility of glycosylated antioxidants is rather limited to date. In this chapter, a wide variety of antioxidants were glycosylated using different phosphorylase enzymes. The resulting antioxidant library, containing α/β-glucosides, different regio-isomers, cellobiosides and cellotriosides was then characterized. Glycosylation was found to substantially increase the solubility and stability of all evaluated compounds. Despite decreased radical scavenging abilities, most glycosides were identified to be potent antioxidants, outperforming the commonly used 2,6-bis(1,1-dimethylethyl)-4-methylphenol (BHT). Moreover, the point of attachment, the anomeric configuration, and the glycosidic chain length were found to influence the properties of these phenolic glycosides.

2 INTRODUCTION

Oxidation of fats and proteins quickly leads to deterioration of food through the undesirable formation of aldehydes, ketones and organic acids. To preserve the organoleptic properties of foodstuff, antioxidants are frequently applied[207-210]. Moreover, these compounds are common constituents of functional foods due to their putative health benefits[211-213]. Although diverse natural and synthetic antioxidants including the monophenolics ethyl and propyl gallate, flavonoids such as catechin and quercetin, and stilbenoids like resveratrol are available, the quest for antioxidants with altered properties continues to date[214, 215]. Indeed, antioxidants should be inexpensive, effective at low concentrations, stable enough to survive processing and storage in the finished product, while avoiding undesirable color, flavor or odor effects[211, 216].

In that respect, many chemical modifications of both natural and synthetic antioxidants have been explored. Examples include the methylation of flavonoids[217], the synthesis of lipophilic tyrosyl esters[218], and the glycosylation of hydroxytyrosol[219] and flavanoids[220]. The latter modification is of particular interest to increase the hydrophilicity of antioxidants[9]. Moreover, glycosylation is also known to improve the solubility of flavonoids in aqueous systems[221], enhance the stability of labile compounds[95, 222], and modulate the uptake of for example quercetin in the small intestine[223].

Unfortunately, chemical synthesis of these glycosides often requires numerous (de)protection and activation steps, resulting in low yields and (toxic) waste[13, 15]. In contrast, biocatalytic approaches enable one-step conversions with high regio- and stereoselectivity, typically generating 5-fold less waste[19]. Enzymatic synthesis of glycosides is typically performed with either glycosyltransferases or glycoside hydrolases. However, the former require relatively expensive nucleotide-activated donor substrates[97], while the latter suffer from low yields (~20%) when used in the synthetic direction[27].

Consequently, glycoside phosphorylases have gained increasing attention over the past decade, as they use a simple glycosyl phosphate as donor with relatively good yields (>50%)[29]. Continuous endeavors in this field enabled the α-glucosylation of for example

hydroquinone[125], glycerol (CHAPTER 2), resveratrol (CHAPTER 3) and propyl gallate (CHAPTER 4) by sucrose phosphorylase (SP), and chain elongation of glucosides using cellodextrin phosphorylase (CDP) (CHAPTER 7). Moreover, also β-glucosylation has been described with cellobiose phosphorylase (CP) (CHAPTER 5), while the R134A mutant of *Thermoanaerobacterium thermosaccharolyticum* SP (TtSPP) was found to be an even more efficient biocatalyst for the α-glycosylation of polyphenols[224].

In this chapter, the synthesis and characterization of a range of α-glucosides using either TtSPP_R134A or the SP from *Bifidobacterium adolescentis* (BaSP) is described. Also, the CDP originating from *Clostridium stercocarium* (CsCDP) was applied to produce a range of cellobiosylated and cellotriosylated antioxidants. The solubility, thermal stability, and antioxidant properties of the newly created compounds were determined and compared.

3 RESULTS & DISCUSSION

3.1 Synthesis and isolation of glycosylated antioxidants

Over the past decade, phosphorylase enzymes have been successfully applied for the synthesis of both α- and β-glucosides (CHAPTER 2, 3, 4, 5 and 7). Recently, the synthetic potential of these enzymes was broadened towards polyphenols[224]. Here, the SP from *B. adolescentis* (BaSP), the R134A mutant of the *T. thermosaccharolyticum* SP (TtSPP_R134A) and the CP from *C. thermocellum* (CtCP) were used to synthesize a variety of glucosylated antioxidants (Table 8.1).

Combining these enzymes allowed the creation of an antioxidant library with an extended structural diversity. Indeed, numerous aglycons ranging from simple phenols such as hydroquinone and pyrogallol, a series of gallate esters, and even polyphenols such as resveratrol, quercetin and catechin were successfully glucosylated. Moreover, different regio-isomers such as for example alkyl gallyl 3- and 4-*O*-α-D-glucopyranosides, 1- and 2-*O*-α-D-glucopyranosyl pyrogallol and 3′ - and 4′-*O*-α-D-glucopyranosyl quercetin were isolated (Table 8.1).

Table 8.1 Chemoenzymatic synthesis of glucosylated antioxidants.

Acceptor	Enzyme	Product	Abbreviation[d]	Isolated yield (%)
Hydroquinone	BaSP[a]	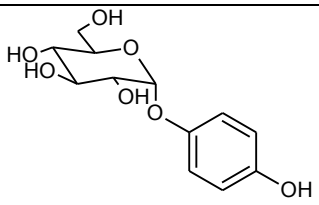	HQαGlc	0.7
	CtCP[b]	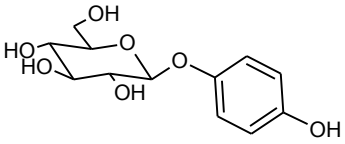	HQβGlc	1.6
Pyrogallol	TtSPP_R134A[c]	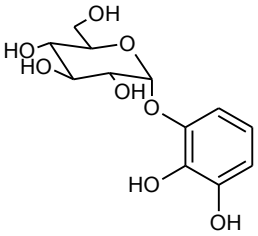	Pyr1αGlc	2.5
	BaSP[a]	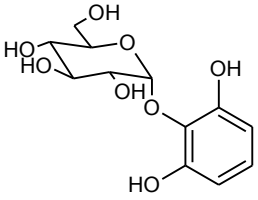	Pyr2αGlc	72.3
Methyl gallate	TtSPP_R134A[c]	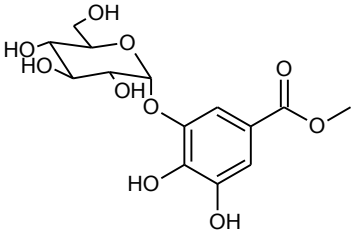	MG3αGlc	35.3
	BaSP[a]	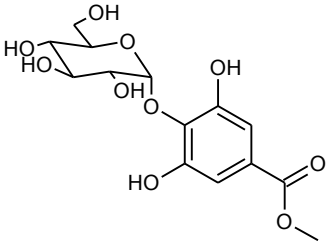	MG4αGlc	38.6
Ethyl gallate	TtSPP_R134A[c]	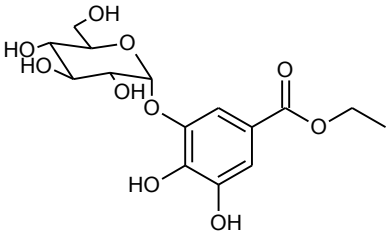	EG3αGlc	23.6

	BaSP[a]	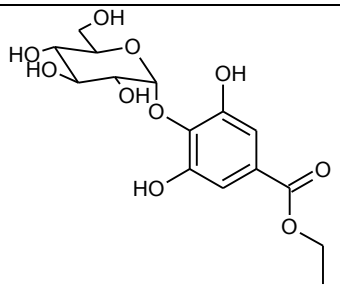	EG4αGlc	23.8
Propyl gallate	TtSPP_R134A[c]	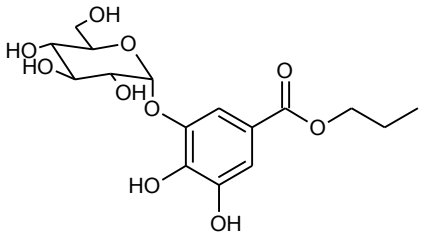	PG3αGlc	26.7
	BaSP[a]	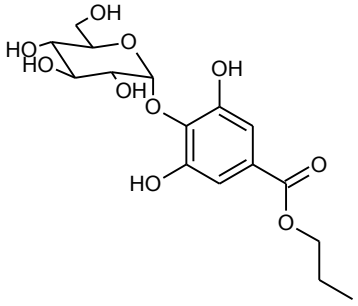	PG4αGlc	12.3
Lauryl gallate	TtSPP_R134A[c]	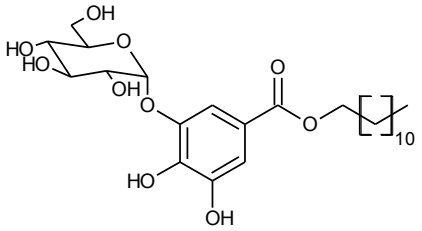	LG3αGlc	12.2
	TtSPP_R134A[c]	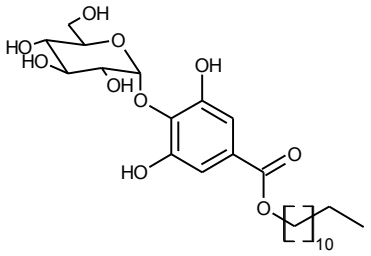	LG4αGlc	4.1
Resveratrol	TtSPP_R134A[c]	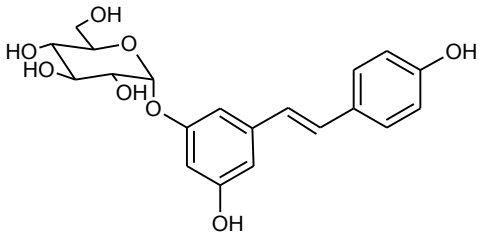	Res3αGlc	82.6

Quercetin	TtSPP_R134A[c]	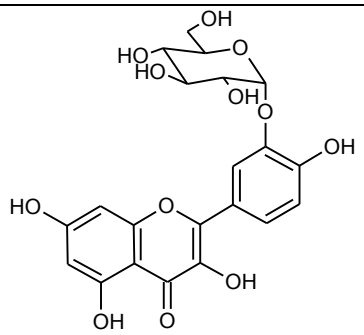	Qer3′αGlc	3.6
	TtSPP_R134A[c]	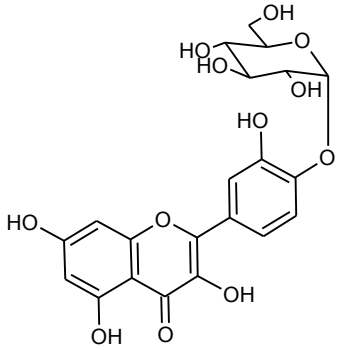	Qer4′αGlc	7.0
Catechin	TtSPP_R134A[c]	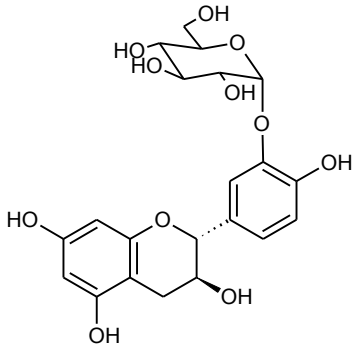	Cat3′αGlc	31.4
Epicatechin	TtSPP_R134A[c]	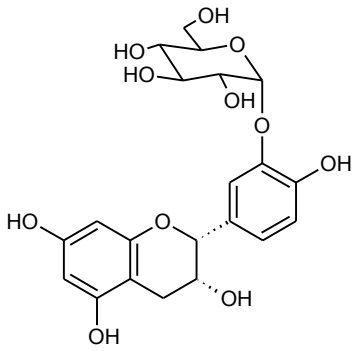	Epi3′αGlc	58.1

[a] Reaction conditions: 62.5 % 50 mM MOPS buffer at pH 7.5 containing 2 M (68 g/L) sucrose and 50 U/mL BaSP, 37.5 % EtOAc supplemented with 100 g/L acceptor, 48 h incubation at 50 °C. [b] Reaction conditions: 62.5 % 50 mM MES buffer at pH 6.5 containing 200 mM αG1P (52 g/L) and 5 U/mL CtCP, 37.5 % EtOAc supplemented with 100 g/L acceptor, 48 h incubation at 50 °C. [c] Reaction conditions: 50 mM MOPS buffer at pH 6.5 containing 200 mM sucrose (69 g/L), 10 g/L acceptor and 0.16 U/mL TtSPP_R134A, 24 h incubation at 55 °C. [d] Abbreviations: HQαGlc, 1-*O*-α-D-glucopyranosyl hydroquinone; HQβGlc, 1-*O*-β-D-glucopyranosyl hydroquinone; Pyr1αGlc, 1-*O*-α-D-glucopyranosyl pyrogallol; Pyr2αGlc, 2-*O*-α-D-glucopyranosyl pyrogallol; MG3αGlc, methyl gallyl 3-*O*-α-D-glucopyranoside; MG4αGlc, methyl gallyl 4-*O*-α-D-glucopyranoside; EG3αGlc, ethyl gallyl 3-*O*-α-D-glucopyranoside; EG4αGlc, ethyl gallyl 4-*O*-α-D-

glucopyranoside; PG3αGlc, propyl gallyl 3-*O*-α-D-glucopyranoside; PG4αGlc, propyl gallyl 4-*O*-α-D-glucopyranoside; LG3αGlc, lauryl gallyl 3-*O*-α-D-glucopyranoside; LG4αGlc, lauryl gallyl 4-*O*-α-D-glucopyranoside; Res3αGlc, 3-*O*-α-D-glucopyranosyl resveratrol; Qer3′αGlc, 3′-*O*-α-D-glucopyranosyl quercetin; Qer4′αGlc, 4′-*O*-α-D-glucopyranosyl quercetin; Cat3′αGlc, 3′-*O*-α-D-glucopyranosyl catechin and Epi3′αGlc, 3′-*O*-α-D-glucopyranosyl epicatechin

The antioxidant panel was further expanded by converting the obtained glucosides to their respective cellobiosides and cellotriosides using the CDP from *C. stercocarium* (Table 8.2). Although the CDP mediated glycosylation of saccharides,[152] alkyl β-glucosides,[38] nitrophenol β-glucoside[39] and phenyl β-cellobioside[192] has already been described, all of these acceptors contain a β-linked glucose moiety. As previously shown in CHAPTER 7, we were also able to elongate a range of α-glucosides, including those of hydroquinone, alkyl gallates and resveratrol (Table 8.2). The structures of all reported glycosides were confirmed by NMR spectroscopy.

Table 8.2 Cellodextrin phosphorylase mediated synthesis of various antioxidant cellobiosides and cellotriosides. The reactions were performed by reacting 100 mM αG1P (26 g/L) with 50 mM acceptor in a 50 mM MES buffer at pH 6.5 containing 5 U/mL CsCDP and 15 % EtOH. The products were isolated after 48 h incubation at 37 °C.

Acceptor	Product	Abbreviation[a]	Isolated yield (%)
HQαGlc	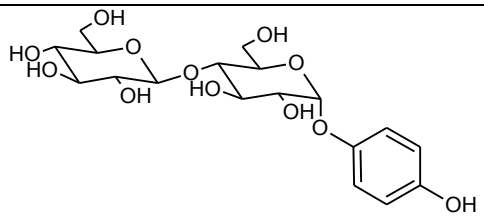	HQαCb	16.3
	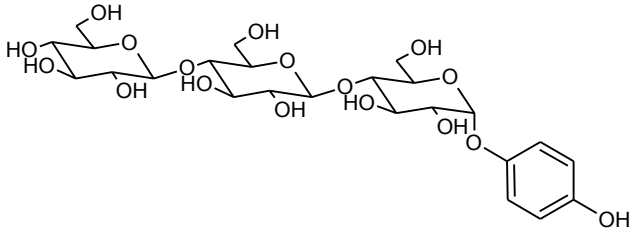	HQαCt	8.9
HQβGlc	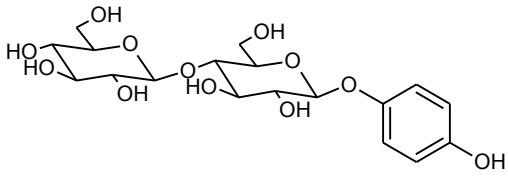	HQβCb	33.8

	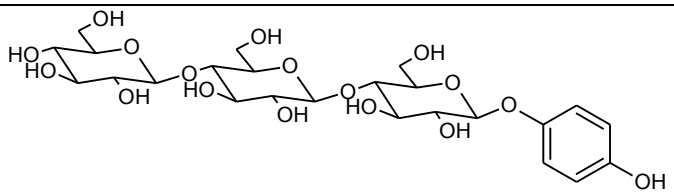	HQβCt	21.6
MG4αGlc	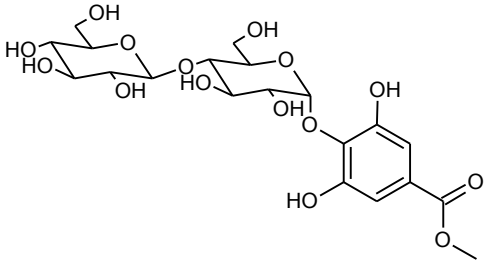	MG4αCb	7.1
	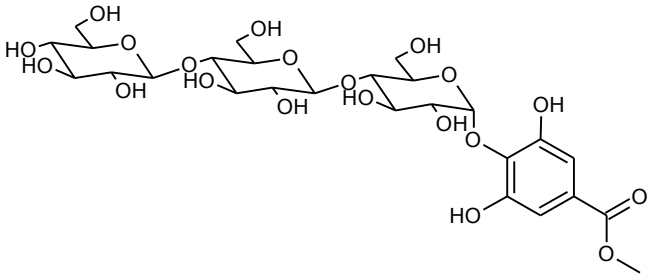	MG4αCt	1.9
EG4αGlc	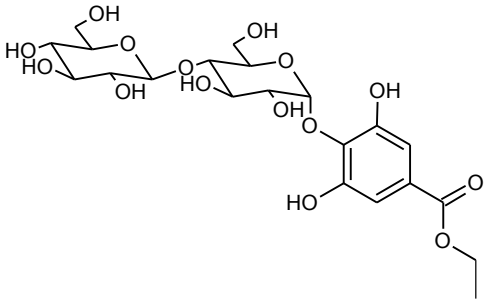	EG4αCb	8.3
PG4αGlc	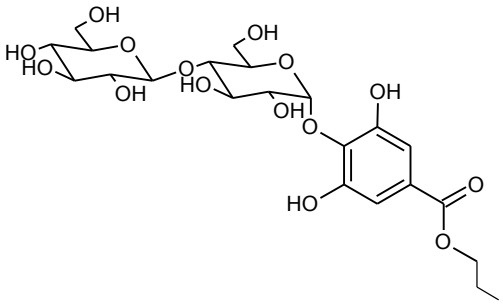	PG4αCb	10.5
	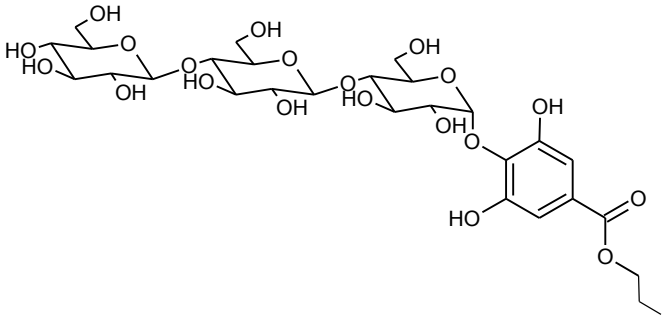	PG4αCt	2.6

Res3αGlc	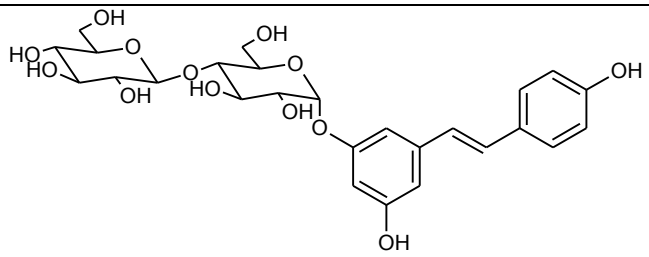	Res3αCb	3.5
	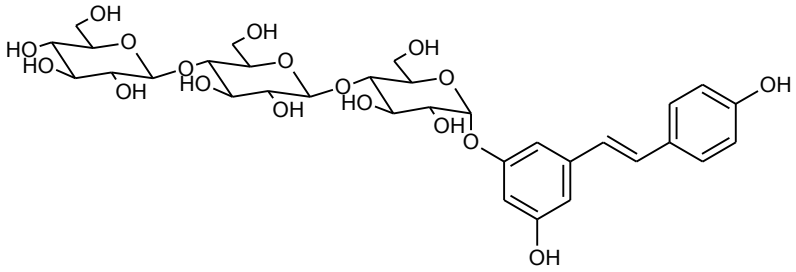	Res3αCt	3.2
Res3βGlc	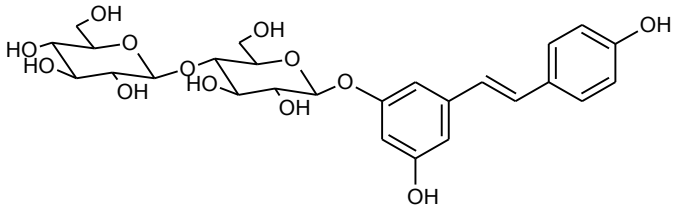	Res3βCb	9.7
	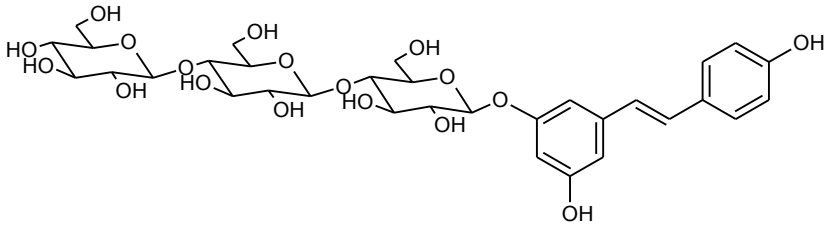	Res3βCt	5.1
Epi3′αGlc	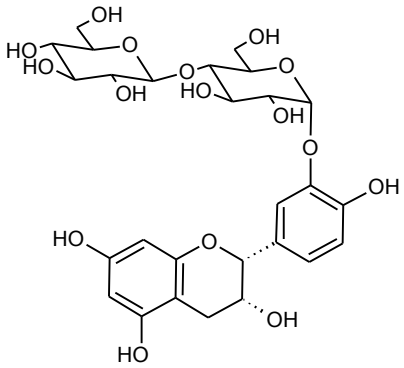	Epi3′αCb	2.9

[a]Abbreviations: HQαCb, 1-*O*-α-D-cellobiopyranosyl hydroquinone; HQαCt, 1-*O*-α-D-cellotriopyranosyl hydroquinone; HQβCb, 1-*O*-β-D-cellobiopyranosyl hydroquinone; HQβCt, 1-*O*-β-D-cellotriopyranosyl hydroquinone; MG4αCb, methyl gallyl 4-*O*-α-D-cellobiopyranoside; MG4αCt, methyl gallyl 4-*O*-α-D-cellotriopyranoside; EG4αCb, ethyl gallyl 4-*O*-α-D-cellobiopyranoside; PG4αCb, propyl gallyl 4-*O*-α-D-cellobiopyranoside; PG4αCt, propyl gallyl 4-*O*-α-D-cellotriopyranoside; Res3αCb, 3-*O*-α-D-cellobiopyranosyl resveratrol; Res3αCt, 3-*O*-α-D-cellotriopyranosyl resveratrol; Res3βCb, 3-*O*-β-D-cellobiopyranosyl resveratrol; Res3βCt, 3-*O*-β-D-cellotriopyranosyl resveratrol; Epi3′αCb, 3′-*O*-α-D-cellobiopyranosyl epicatechin

3.2 Solubility of glycosylated antioxidants

Next, the effect of glycosylation on the solubility of a variety of hydrophobic antioxidants was evaluated (Table 8.3). As could be expected, coupling a glucose moiety to these compounds increased their tendency to dissolve in aqueous solutions[222]. Indeed, while the solubility of epicatechin and catechin was limited to roughly 25 and 55 mM at pH 7.0, the corresponding 3′-α-glucosides could be dissolved to 326 mM and an impressive 1.1 M, respectively. Also the solubility of lauryl gallate, quercetin and resveratrol could be substantially increased by glucosylation (Table 8.3).

Table 8.3 Solubility of glycosylated antioxidants at 37 °C in a 10 mM phosphate buffer at pH 7.0.

Compound[a]	Solubility (mM)	Compound[a]	Solubility (mM)
Catechin	54.7 ± 3.8	Qer3′αGlc	0.69 ± 0.04
Cat3′αGlc	1104 ± 72	Qer4′αGlc	3.98 ± 0.26
Epicatechin	24.8 ± 1.9	Resveratrol	0.35 ± 0.02
Epi3′αGlc	326 ± 21	Res3αGlc	7.56 ± 0.52
Epi3′αCb	51.4 ± 3.1	Res3αCb	5.06 ± 0.46
Lauryl gallate	0.28 ± 0.02	Res3αCt	4.26 ± 0.33
LG3αGlc	4.56 ± 0.34	Res3βGlc	1.73 ± 0.12
LG4αGlc	9.68 ± 0.59	Res3βCb	0.82 ± 0.06
Quercetin	0.19 ± 0.01	Res3βCt	0.53 ± 0.04

[a]Abbreviations: see Table 8.1 and 8.2

In agreement with previous studies on quercetin[225] and epigallocatechin gallate[226], the glucosylation position was found to influence the solubility. The 3- and 3′-α-glucosides of lauryl gallate and quercetin could be dissolved up to 4.56 and 0.69 mM respectively, while the 4- and 4′-α-glucosides exhibited solubilities exceeding 9 and 4 mM. Moreover, the 3-α-glucoside of resveratrol was found to be roughly three times more soluble in a phosphate buffer at pH 7.0 compared to its β-glucosylated counterpart. In contrast to coupling additional glucose moieties directly to the polyphenol structure[227, 228], or extending the degree of glycosylation by adding α-(1,4)-linked glucose moieties (i.e. the synthesis of maltosides)[9], additional β-(1,4)-glucosylation was found to decrease solubility. Nevertheless, all cellobiosides and cellotriosides could be dissolved to higher concentrations than their respective aglycons (Table 8.3).

3.3 Antioxidant properties of glycosylated phenolics

Although glycosylation has been shown to generally increase solubility, the latter modification typically decreases the antioxidant capacity[222]. Therefore, the ability of the synthesized glucosides, cellobiosides and cellotriosides to scavenge DPPH and ABTS radicals was evaluated (Table 8.4).

Table 8.4 Antioxidant properties of glycosylated phenolics.

	EC_{50} (μM)			EC_{50} (μM)	
Compound[a]	DPPH	ABTS	Compound[a]	DPPH	ABTS
BHT	1040 ± 89	310 ± 18	PG4αGlc	136 ± 9	96.2 ± 2.3
Hydroquinone	95.0 ± 7.9	104 ± 2.9	PG4αCb	4439± 357	71.8 ± 2.6
HQαGlc	1530 ± 126	163 ± 5	PG4αCt	/	70.4 ± 2.7
HQαCb	2390 ± 169	126 ± 5	Lauryl gallate	39.2 ± 2.8	50.4 ± 1.9
HQαCt	2581 ± 205	75.4 ± 2.2	LG3αGlc	104 ± 6	151 ± 5
HQβGlc	1190 ± 81	116 ± 4	LG4αGlc	189 ± 12	115 ± 4
HQβCb	1550 ± 140	111 ± 3	Resveratrol	374 ± 27	69.2 ± 3.2
HQβCt	2042 ± 162	69.3 ± 1.9	Res3αGlc	592 ± 13	153 ± 4
Pyrogallol	63.2 ± 2.1	44.2 ± 1.7	Res3αCb	886 ± 65	297 ± 13
Pyr1αGlc	110 ± 9	117 ± 6	Res3αCt	988 ± 34	351 ± 20
Pyr2αGlc	888 ± 36	87.1 ± 3	Res3βGlc	398 ± 13	132 ± 8
Methyl gallate	33.8 ± 2.3	49.6 ± 1.1	Res3βCb	615 ± 19	443 ± 10
MG3αGlc	102 ± 9	154 ± 8	Res3βCt	663 ± 22	347 ± 9
MG4αGlc	312 ± 12	97 ± 1.4	Quercetin	75.1 ± 7.4	67.6 ± 3.8
MG4αCb	5040 ± 496	104 ± 3	Qer3′αGlc	108 ± 9	146 ± 9
MG4αCt	5623 ± 421	142 ± 6	Qer4′αGlc	83.1 ± 4.4	91.3 ± 3.2
Ethyl gallate	36.3 ± 1	51.2 ± 2.4	Catechin	111 ± 5	51.0 ± 1.9
EG3αGlc	100 ± 3	159 ± 5	Cat3′αGlc	487 ± 20	90.3 ± 2.0
EG4αGlc	241 ± 5	111 ± 3	Epicatechin	77.4 ± 6.1	51.2 ± 1.3
EG4αCb	4123± 262	111 ± 4	Epi3′αGlc	470 ± 5	89.4 ± 1.6
Propyl gallate	27.7 ± 1.5	52.0 ± 1.2	Epi3′αCb	490 ± 6	97.8 ± 4.8
PG3αGlc	100 ± 5	167 ± 3			

[a]Abbreviations: see Table 8.1 and 8.2

As expected, glycosylation was found to typically decrease the scavenging activity. In agreement with previous reports[229], the glucosylation position strongly influences the antioxidant capacity. Glycosylation of quercetin at the 4´ position, for example, reduces the scavenging activity to a lower extent compared to the 3´ position. Interestingly, alkyl gallyl 3-glucosides were found to be better DPPH scavengers than the corresponding 4-glucosides. The opposite was observed for ABTS radicals, indicating the different reactivity of ABTS and DPPH radicals. Also, glucosylation at the 2 position roughly doubled the EC_{50}^{ABTS} for pyrogallol, while the required concentration of 2-*O*-α-D-glucopyranosyl pyrogallol to scavenge 50 % of the DPPH radicals increased 14-fold. In contrast to the results obtained with the ABTS assay, the EC_{50}^{DPPH} of the 1-*O*-α-D-glucopyranosyl pyrogallol was found to be much lower, indicating the importance of the *ortho*-diphenolic structure of pyrogallol and alkyl gallate ester glucosides for DPPH scavenging.

In agreement with previous reports[230], the *para*-diphenolic structure of hydroquinone was found to be required for its DPPH scavenging activity. Indeed, while glucosylation barely affected the ability of hydroquinone to scavenge ABTS radicals, the EC_{50}^{DPPH} for α- and β-arbutin increased by a factor of 16 and 12, respectively. Interestingly, all evaluated β-linked glycosides showed better scavenging compared to their α-linked counterparts. Examples include 1-*O*-α/β-D-glucopyranosyl hydroquinone, 3-*O*-α/β-D-glucopyranosyl resveratrol, as well as their corresponding cellobiosides and cellotriosides (Table 8.4).

In general, extending glycosylation by adding β-(1,4)-linked glucose moieties further decreased the scavenging capacity. In contrast to the slightly reduced activity towards ABTS radicals, the ability of alkyl gallyl cellobiosides and cellotriosides to eliminate DPPH radicals was severely compromised. The latter reduced activity is most likely caused by steric hindrance, hampering the applicability of the DPPH assay for large compounds[231]. Remarkably, extending glycosylation was found to increase the ABTS scavenging activity of both hydroquinone α- and β-glucoside (Table 8.4). Much to our surprise, the EC_{50}^{ABTS} values of 1-*O*-α/β-D-cellotriosyl hydroquinone were even lower than the 104 µM obtained for hydroquinone.

3.4 Stability of glycosylated antioxidants

Despite some work on ascorbic acid[95] and quercetin glucosides[232, 233], reports describing the effect of glycosylation on the stability of antioxidants are rather scarce to date[234]. Therefore, the residual DPPH scavenging activity of a wide variety of glycosylated antioxidants after 24 h incubation at 60 °C was determined (Table 8.5).

Table 8.5 Thermal stability of glycosylated antioxidants. The residual DPPH scavenging capacity was determined after 24 h incubation at 60 °C and pH 7.

Compound[a]	Residual activity (%)	Compound[a]	Residual activity (%)
Hydroquinone	82.1 ± 3.6	EG4αGlc	82.3 ± 2.2
HQαGlc	99.1 ± 2.2	EG4αCb	99.2 ± 1.6
HQαCb	99.6 ± 3.4	Propyl gallate	69.4 ± 3.5
HQαCt	100.0 ± 2.6	PG3αGlc	85.7 ± 2.7
HQβGlc	99.4 ± 2.4	PG4αGlc	81.0 ± 3.2
HQβCb	99.7 ± 2.8	PG4αCb	99.6 ± 0.8
HQβCt	99.8 ± 2.1	Resveratrol	74.6 ± 2.7
Pyrogallol	24.5 ± 1.8	Res3αGlc	99.9 ± 1.6
Pyr1αGlc	27.9 ± 1.2	Res3αCb	99.6 ± 2.1
Pyr2αGlc	95.3 ± 3.2	Res3αCt	98.2 ± 3.5
Methyl gallate	83.6 ± 4.1	Res3βGlc	98.3 ± 2.6
MG3αGlc	96.7 ± 2.3	Res3βCb	99.5 ± 1.3
MG4αGlc	77.8 ± 2.1	Res3βCt	99.2 ± 1.7
MG4αCb	99.8 ± 1.1	Catechin	67.5 ± 3.8
MG4αCt	99.7 ± 2.1	Cat3′αGlc	95.6 ± 2.4
Ethyl gallate	71.9 ± 3.4	Epicatechin	64.4 ± 3.1
EG3αGlc	91.6 ± 2.3	Epi3′αGlc	94.4 ± 2.6

[a]Abbreviations: see Table 8.1 and 8.2

Glycosylation was found to substantially increase the stability of all evaluated antioxidants. The largest improvement was observed for pyrogallol, which lost over 75 % of its scavenging capacity after 24 h at 60 °C. In contrast, 2-*O*-α-D-glucopyranosyl pyrogallol retained roughly 95 % of its antioxidant capacity. Remarkably, the 1-*O*-α-D-glucopyranosyl pyrogallol retained only 28 % of its original scavenging activity,

indicating the importance of the glucosylation position. Indeed, although less pronounced, alkyl gallyl 3-glucosides were found to be more stable compared to the corresponding 4-glucosides. The anomeric configuration on the other hand, did not significantly affect the stability of hydroquinone and resveratrol glucosides, while all cellobiosides and cellotriosides remained fully active after 24 h at 60 °C (Table 8.5).

Next, the stability of propyl gallate and its glycosides was studied in more detail (Figure 8.1). Propyl gallate (E310), a common food additive, lost more than half of its scavenging capacity after 4 days incubation at 60 °C. The 3- and 4-glucosides performed much better, retaining roughly 80 and 75 % of their initial activity. However, propyl gallyl 4-*O*-α-D-cellobiopyranosyl retained all of its scavenging activity, even after 4 days incubation at 60 °C. Similar results were observed for hydroquinone and resveratrol cellobiosides, indicating the enhanced stability of the latter compounds.

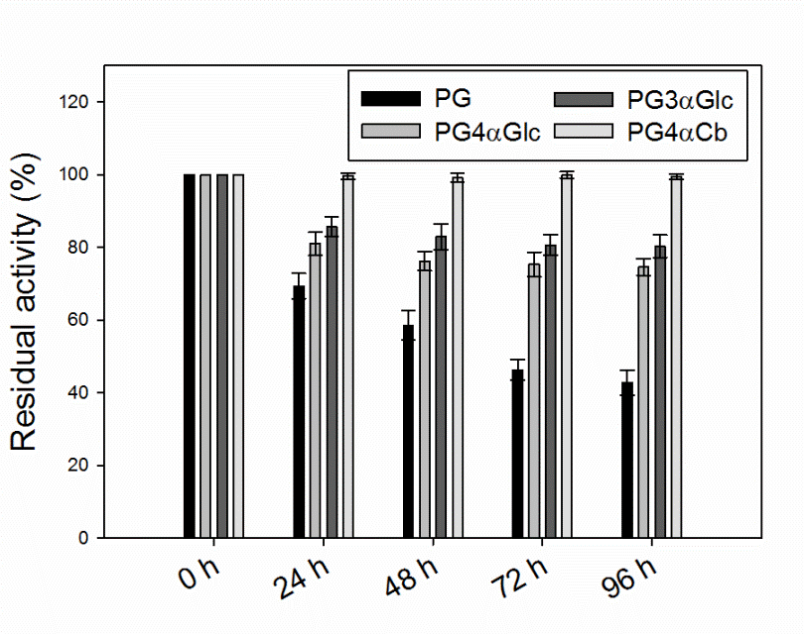

Figure 8.1 Stability of propyl gallate and its glycosides. The residual DPPH scavenging capacity was measured after incubation in a 10 mM phosphate buffer at pH 7.0 and 60 °C. Abbreviations: PG, propyl gallate; PG3αGlc, propyl gallyl 3-*O*-α-D-glucopyranoside; PG4αGlc, propyl gallyl 4-*O*-α-D-glucopyranoside and PG4αCb, propyl gallyl 4-*O*-α-D-cellobiopyranoside.

4 CONCLUSION

In conclusion, a wide variety of glycosylated antioxidants, including α-cellobiosides and cellotriosides, were produced. The glucosylation position was found to substantially influence the solubility of these compounds, while α-glucosides could be dissolved to higher concentrations compared to their β-linked counterparts. Moreover, glycosylation improved the stability of all evaluated antioxidants. Also, the point of attachment, the anomeric configuration, and the glycosidic chain length were found to influence the scavenging abilities of these glycosides. Despite decreased activities, most glycosylated compounds were identified as potent antioxidants, exhibiting lower EC_{50} values than BHT. Combined with their increased solubility and enhanced stability, these compounds might find widespread application in the food, feed and cosmetic industry.

5 MATERIALS & METHODS

5.1 Materials, enzymes and instruments

Ethyl acetate was bought from Fiers, all other chemicals were analytical grade and purchased from Sigma-Aldrich. The recombinant SPs were produced and heat purified as previously described (CHAPTER 3). The activity of these enzymes was determined as published earlier,[128] and one unit of SP was defined as the activity that corresponds to the release of 1 µmol fructose per minute from 100 mM sucrose in 100 mM phosphate buffer at pH 7.0 and 37 °C (CHAPTER 3). Overexpression in *E. coli* JW0987 cells, and His_6-Tag purification of CtCP and CsCDP was performed as described in CHAPTER 5 and 7, respectively. The activity of both enzymes was determined in the synthetic direction by measuring the release of phosphate from αG1P using the method of Gawronski and Benson[156]. One unit of CP or CDP activity corresponds to the release of 1 µmol phosphate per minute from 50 mM αG1P and 50 mM glucose or cellobiose respectively, in a 50 mM MES buffer at pH 6.5 and 37 °C. Absorbance measurements in cuvettes and microtiter plates were performed in a JASCO V-360 Bio Spectrophotometer (JASCO, The Netherlands) and Anthos Zenyth 200rt microplate reader (Biochrom, UK), respectively.

5.2 Production and purification of glucosides

The BaSP mediated glucosylation of hydroquinone, pyrogallol, methyl gallate, ethyl gallate and propyl gallate was carried out at 250 mL scale in magnetically stirred flasks. Biphasic catalysis was performed by adding 156 mL 50 mM MOPS at pH 7.5 containing 2 M (684 g/L) sucrose and 50 U/mL SP to 94 mL EtOAc supplemented with 100 g/L acceptor. The reaction mixtures were incubated during 48 h at 50 °C, and subjected to a heat treatment (10 min at 95 °C) and centrifugation step (12 000 g, 4 °C, 15 min) to remove debris. The samples were then evaporated *in vacuo* and the glucosides were isolated by column chromatography (silicagel, EtOAc/MeOH/water = 30:5:4).

Alternatively, α-glucosylation of pyrogallol, methyl gallate, ethyl gallate, propyl gallate, lauryl gallate, resveratrol, quercetin, catechin and epicatechin was performed in magnetically stirred flasks at 250 mL scale. The reaction mixtures consisted of a 50 mM MOPS buffer at pH 6.5 supplemented with 200 mM (69 g/L) sucrose, 10 g/L acceptor and 0.16 U/mL TtSPP_R134A. After 24 h incubation at 55 °C, NaCl was added to 300 g/L, and the mixtures were extracted with 250 mL isopropyl alcohol (IPA). Next the IPA phase was evaporated *in vacuo*, redissolved in MeOH, filtered over a Whatman paper and subjected to column chromatography (silicagel, EtOAc/MeOH/water = 30:5:4). The synthesis and isolation of 1-*O*-β-D-glucopyranosyl hydroquinone was performed as described in CHAPTER 5. The reported yields are based on the acceptor substrates.

5.3 Production and purification of cellobiosides and cellotriosides

The glycosylation of 1-*O*-α-D-glucopyranosyl hydroquinone (HQαGlc), 1-*O*-β-D-glucopyranosyl hydroquinone (HQβGlc), methyl gallyl 4-*O*-α-D-glucopyranoside (MG4αGlc), ethyl gallyl 4-*O*-α-D-glucopyranoside (EG4αGlc), propyl gallyl 4-*O*-α-D-glucopyranoside (PG4αGlc), 3-*O*-α-D-glucopyranosyl resveratrol (Res3αGlc), 3-*O*-β-D-glucopyranosyl resveratrol (Res3βGlc) and 3′-*O*-α-D-glucopyranosyl epicatechin (Epi3′αGlc) was carried out at 50 mL scale in falcons. The reaction mixtures consisted of 100 mM (26 g/L) αG1P and 50 mM of the above mentioned acceptors dissolved in a 50 mM MES buffer at pH 6.5 containing 5 U/mL CsCDP and 15 % EtOH. The reactions were terminated after 48 h incubation at 37 °C, after which the reaction mixtures were heated (10 min at 95 °C) and centrifuged (12 000 g, 4 °C, 15 min). The samples were then

evaporated *in vacuo* and the residue was purified by column chromatography (silicagel, EtOAc/MeOH/water = 20:5:3). The reported yields are based on the acceptor substrates.

5.4 Solubility measurements

The solubility of glycosylated antioxidants was determined in 1.7 mL eppendorfs containing 250 µL 10 mM phosphate buffer at pH 7.0. The antioxidants were added until clear precipitation was observed, after which the mixtures were incubated in a water bath at 37 °C with ± 0.1 °C accuracy. Next, the samples were vortexed multiple times and allowed to equilibrate for 24 h. Undissolved solids were removed by centrifugation (12 000 g, 37 °C, 5 min) at the same temperature. Next, the obtained solutions were diluted in MeOH, and their absorbance was measured at 306, 373, 283, 280 and 280 nm for resveratrol, quercetin, lauryl gallate, catechin and epicatechin glycosides respectively. All experiments were performed in triplicate, and the calibration curves were prepared with authentic samples dissolved in MeOH.

5.5 Determination of DPPH radical scavenging activity

The 2,2-diphenyl-1-picrylhydrazyl (DPPH) radical scavenging activity was determined by adding 100 µL MeOH, containing varying antioxidant concentrations, to 200 µL MeOH supplemented with 200 µM DPPH in microtiter plates. After intensive mixing, the samples were stored during 15 min at room temperature in darkness, after which the absorbance of the mixtures was measured at 517 nm. The required concentration to reduce the absorbance by 50 % (EC_{50}) was calculated from the equations obtained by fitting the linear part of the absorption curves. Butylated hydroxytoluene (BHT) was used as reference, and all analyses were performed in triplicate.

5.6 Determination of ABTS radical scavenging activity

The 2,2'-azino-bis(3-ethylbenzothiazoline-6-sulphonic acid) (ABTS) radical scavenging assay was used to evaluate the antioxidant properties of glycosylated phenolics. The ABTS cation radical was produced by reacting 1 part of milliQ water containing 14 mM ABTS with 1 part 4.9 mM potassium persulfate dissolved in milliQ. The obtained solution was stored in the dark at room temperature during 16 h, prior to its dilution with MeOH to an absorbance of 0.700 ± 0.020 at 734 nm. Next, 30 µL MeOH containing varying

antioxidant concentrations was added to 200 µL ABTS solution in microtiter plates. After intensive mixing, the samples were stored during 15 min at room temperature in darkness, after which the absorbance of the mixtures was measured at 734 nm. The EC_{50} was calculated as described above, and BHT was used as reference. All analyses were performed in triplicate, and had a CV of less than 10 %.

5.7 Stability assays

Thermal stability was determined by dissolving 1 mM of the glycosylated antioxidants in a 10 mM phosphate buffer at pH 7.0. Unless stated otherwise, the solutions were incubated in a hot water bath at 60 °C with ± 0.1 °C accuracy during 24 h. Next, the samples were cooled on ice, diluted in MeOH, and their EC_{50}^{DPPH} was determined. The residual activity was calculated as the ratio of the EC_{50} before and after heat treatment. All analyses were performed in triplicate, and had a CV of less than 10 %. All reported errors correspond to the standard errors.

5.8 Structure elucidation of glycosides

NMR spectra were measured on a Bruker AVANCE III 600 MHz spectrometer (600.13 MHz for ^{1}H and 150.93 MHz for ^{13}C) at 25 °C in CD_3OD (99.98 %D, ARMAR Chemicals, Döttingen, CH) and at 30 °C in D_2O (100.00 %D, ARMAR Chemicals, Döttingen, CH - samples 1-*O*-α-D-cellobiopyranosyl hydroquinone, 1-*O*-α-D-cellotriopyranosyl hydroquinone and 1-*O*-β-D-cellotriopyranosyl hydroquinone). Residual signals of solvents were used as an internal standard (CD_3OD: σ_H 3.330 ppm, σ_c 49.30 ppm, D_2O: σ_H 4.508 ppm). Carbon chemical shifts in D_2O were referenced to the signal of acetone (σ_c 30.50 ppm). NMR experiments: COSY, HSQC, HMBC, HSQC-TOCSY, and 1d-TOCSY were performed using standard manufacturers' software. ^{1}H NMR and ^{13}C NMR spectra were zero filled to fourfold data points and multiplied by window function before Fourier transformation. Two-parameter double-exponential Lorentz-Gauss function was applied for ^{1}H to improve resolution and line broadening (1 Hz) was applied to get better ^{13}C signal-to-noise ratio. Digital resolution enabled us to report chemical shifts of protons to three and carbon chemical shifts to two decimal places.

The assignment of proton spin systems was achieved by COSY, and then transferred to carbons by HSQC. The differentiation of individual sugar units in cellobiose and cellotriose moieties was also supported by 1d-TOCSY and HSQC-TOCSY experiments. The anomeric configuration was determined from the magnitude of $J_{H\text{-}1,H\text{-}2}$. The glycosidic linkage position was deduced using heteronuclear correlations in HMBC and from the downfield glycosylation shifts of the involved carbons C-4. The position of the glycosylation was confirmed by HMBC contact between anomeric proton H-1 and attached carbon of aglycon. The spectra of 1-*O*-α-D-glucopyranosyl hydroquinone, 1-*O*-β-D-glucopyranosyl hydroquinone, 2-*O*-α-D-glucopyranosyl pyrogallol, methyl gallyl 4-*O*-α-D-glucopyranoside, ethyl gallyl 4-*O*-α-D-glucopyranoside, propyl gallyl 4-*O*-α-D-glucopyranoside, 3-*O*-α-D-glucopyranosyl resveratrol were identical to those reported in CHAPTER 3, 4 and 5. Spectral analysis and interpretation was kindly performed by the group of Prof. Vladimír Křen at the Institute of Microbiology (Czech Republic).

1-*O*-α-D-Glucopyranosyl pyrogallol

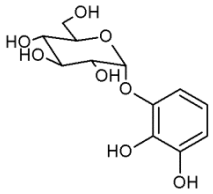

^{1}H NMR (600.23 MHz, MeOD): 3.452 (1H, dd, *J* = 9.8, 9.1 Hz, H-4), 3.596 (1H, dd, *J* = 9.7, 3.7 Hz, H-2), 3.746 (1H, dd, *J* = 11.5, 4.8 Hz, H-6u), 3.782 (1H, dddd, *J* = 9.8, 4.8, 2.1, 0.4 Hz, H-5), 3.819 (1H, dd, *J* = 11.5, 2.1 Hz, H-6d), 3.896 (1H, dd, *J* = 9.7, 9.1 Hz, H-3), 5.303 (1H, d, *J* = 3.7 Hz, H-1), 6.551 (1H, dd, *J* = 8.1, 1.5 Hz, H-4'), 6.621 (1H, dd, *J* = 8.2, 8.1 Hz, H-5'), 6.797 (1H, dd, *J* = 8.2, 1.5 Hz, H-6')

^{13}C NMR (150.95 MHz, MeOD): 62.65 (C-6), 71.67 (C-4), 73.78 (C-2), 74.76 (C-5), 75.17 (C-3), 101.86 (C-1), 110.81 (C-6'), 112.11 (C-5'), 120.29 (C-4'), 137.17 (C-2'), 147.53 (C-3'), 147.64 (C-1')

Methyl gallyl 3-*O*-α-D-glucopyranoside

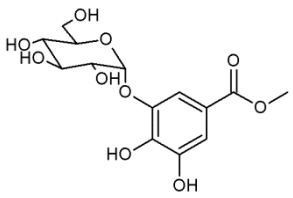

^{1}H NMR (600.23 MHz, MeOD): 3.496 (1H, dd, *J* = 9.8, 9.1 Hz, H-4), 3.634 (1H, dd, *J* = 9.7, 3.7 Hz, H-2), 3.741 (1H, ddd, *J* = 9.8, 4.5, 2.3 Hz, H-5), 3.773 (1H, dd, *J* = 11.9, 4.5 Hz, H-6u), 3.812 (1H, dd, *J* = 11.9, 2.3 Hz, H-6d), 3.852 (3H, s, H-1"), 3.903 (1H, dd, *J* = 9.7, 9.1 Hz, H-3), 5.391 (1H, d, *J* = 3.7 Hz, H-1), 7.254 (1H, d, *J* = 2.0 Hz, H-6'), 7.506 (1H, d, *J* = 2.0 Hz, H-2')

^{13}C NMR (150.95 MHz, MeOD): 52.71 (C-1"), 62.43 (C-6), 71.43 (C-4), 73.66 (H-2), 74.94 (C-5), 75.07 (C-3), 101.76 (C-1), 112.22 (C-2'), 113.53 (C-6'), 121.97 (C-1'), 142.28 (C-4'), 146.84 (C-3'), 147.28 (C-5'), 168.96 (CO)

Ethyl gallyl 3-*O*-α-D-glucopyranoside

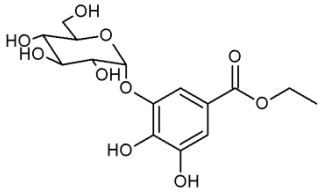

^{1}H NMR (600.23 MHz, MeOD): 1.371 (3H, t, *J* = 7.1 Hz, H-2”), 3.501 (1H, dd, *J* = 9.8, 9.1 Hz, H-4), 3.634 (1H, dd, *J* = 9.7, 3.7 Hz, H-2), 3.752 (1H, dddd, *J* = 9.8, 4.5, 2.3, 0.4 Hz, H-5), 3.779 (1H, dd, *J* = 11.7, 4.3 Hz, H-6u), 3.813 (1H, dd, *J* = 11.7, 2.3 Hz, H-6d), 3.905 (1H, dd, *J* = 9.7, 9.1 Hz, H-3), 4.315 (2H, q, *J* = 7.1 Hz, H-1”), 5.384 (1H, d, *J* = 3.7 Hz, H-1), 7.260 (1H, d, *J* = 2.0 Hz, H-6’), 7.506 (1H, d, *J* = 2.0 Hz, H-2’)

^{13}C NMR (150.95 MHz, MeOD): 14.94 (C-2”), 62.18 (C-1”), 62.43 (C-6), 71.43 (C-4), 73.67 (H-2), 74.93 (C-5), 75.07 (C-3), 101.85 (C-1), 112.28 (C-2’), 113.52 (C-6’), 122.28 (C-1’), 142.29 (C-4’), 146.85 (C-3’), 147.25 (C-5’), 168.50 (CO)

Propyl gallyl 3-*O*-α-D-glucopyranoside

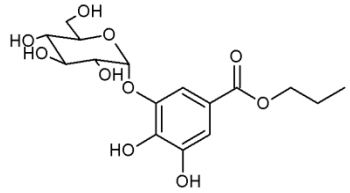

^{1}H NMR (600.23 MHz, MeOD): 1.042 (3H, t, *J* = 7.4 Hz, H-3”), 1.783 (2H, m, H-2”), 3.511 (1H, dd, *J* = 9.8, 9.0 Hz, H-4), 3.637 (1H, dd, *J* = 9.7, 3.7 Hz, H-2), 3.752 (1H, ddd, *J* = 9.8, 4.1, 2.6 Hz, H-5), 3.783 (1H, dd, *J* = 11.9, 4.1 Hz, H-6u), 3.812 (1H, dd, *J* = 11.9, 2.6 Hz, H-6d), 3.908 (1H, dd, *J* = 9.7, 9.0 Hz, H-3), 4.224 (2H, t, *J* = 6.6 Hz, H-1”), 5.385 (1H, d, *J* = 3.7 Hz, H-1), 7.266 (1H, d, *J* = 2.0 Hz, H-6’), 7.509 (1H, d, *J* = 2.0 Hz, H-2’)

^{13}C NMR (150.95 MHz, MeOD): 11.10 (C-3”), 23.48 (C-2”), 62.41 (C-6), 67.76 (C-1”), 71.39 (C-4), 73.66 (H-2), 74.90 (C-5), 75.06 (C-3), 101.87 (C-1), 112.28 (C-2’), 113.50 (C-6’), 122.25 (C-1’), 142.28 (C-4’), 146.86 (C-3’), 147.25 (C-5’), 168.55 (CO)

Lauryl gallyl 3-*O*-α-D-glucopyranoside

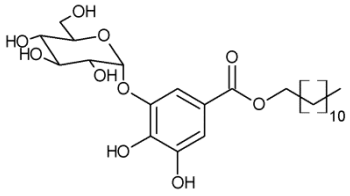

^{1}H NMR (600.23 MHz, MeOD): 0.913 (3H, t, *J* = 7.1 Hz, H-12”), 1.30-1.36 (14H, m, H-5”- H-11”), 1.395 (2H, m, H-4”), 1.461 (2H, m, H-3”), 1.760 (2H, m, H-2”), 3.513 (1H, dd, *J* = 9.9, 8.9 Hz, H-4), 3.636 (1H, dd, *J* = 9.7, 3.7 Hz, H-2), 3.751 (1H, ddd, *J* = 9.9, 4.1, 2.7 Hz, H-5), 3.785 (1H, dd, *J* = 12.0, 4.1 Hz, H-6u), 3.812 (1H, dd, *J* = 12.0, 2.7 Hz, H-6d), 3.908 (1H, dd, *J* = 9.7, 8.9 Hz, H-3), 4.263 (2H, m, H-1”), 5.384 (1H, d, *J* = 3.7 Hz, H-1), 7.261 (1H, d, *J* = 2.0 Hz, H-6’), 7.503 (1H, d, *J* = 2.0 Hz, H-2’)

^{13}C NMR (150.95 MHz, MeOD): 14.73 (C-12”), 24.03 (C-11”), 27.44 (C-3”), 30.14 (C-2”), 30.68 (C-4”), 30.77 (C-9”), 30.95, 31.00, 31.05, 31.05 (C-5”, C-6”, C-7”, C-8”), 33.36 (C-10”), 62.42 (C-6), 66.29 (C-1”), 71.39 (C-4), 73.66 (H-2), 74.91 (C-5), 75.06 (C-3), 101.88 (C-1), 112.28 (C-2’), 113.52 (C-6’), 122.26 (C-1’), 142.28 (C-4’), 146.87 (C-3’), 147.25 (C-5’), 168.55 (CO)

Lauryl gallyl 4-*O*-α-D-glucopyranoside

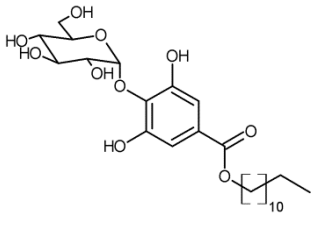

^{1}H NMR (600.23 MHz, MeOD): 0.914 (3H, t, *J* = 7.1 Hz, H-12”), 1.30-1.37 (14H, m, H-5”- H-11”), 1.396 (2H, m, H-4”), 1.467 (2H, m, H-3”), 1.763 (2H, m, H-2”), 3.479 (1H, dd, *J* = 10.1, 9.1 Hz, H-4), 3.616 (1H, dd, *J* = 9.7, 3.7 Hz, H-2), 3.794 (1H, dd, *J* = 11.8, 4.8 Hz, H-6u), 3.868 (1H, dd, *J* = 11.8, 2.5 Hz, H-6d), 3.899 (1H, dd, *J* = 9.7, 9.1 Hz, H-3), 4.246 (1H, dddd, *J* = 10.1, 4.8, 2.5, 0.4 Hz, H-5), 4.269 (2H, t, *J* = 6.6 Hz, H-1”), 5.152 (1H, d, *J* = 3.7 Hz, H-1), 7.070 (2H, s, H-*meta*)

^{13}C NMR (150.95 MHz, MeOD): 14.73 (C-12”), 24.03 (C-11”), 27.44 (C-3”), 30.08 (C-2”), 30.66 (C-4”), 30.76 (C-9”), 30.95, 30.98, 31.04, 31.04 (C-5”, C-6”, C-7”, C-8”), 33.36 (C-10”), 62.43 (C-6),

66.45 (C-1"), 71.21 (C-4), 73.70 (H-2), 75.24 (C-3), 75.49 (C-5), 105.50 (C-1), 110.30 (C-*meta*), 128.44 (C-*para*), 139.74 (C-*ipso*), 152.35 (C-*ortho*), 168.18 (CO)

3′-*O*-α-D-Glucopyranosyl quercetin

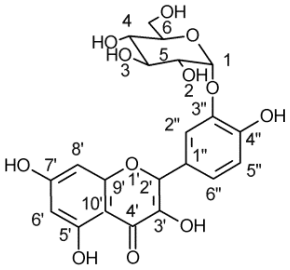

^{1}H NMR (600.23 MHz, MeOD): 3.533 (1H, dd, *J* = 9.7, 9.0 Hz, H-4), 3.652 (1H, dd, *J* = 9.7, 3.7 Hz, H-2), 3.821 (1H, m, H-6u), 3.85[a] (1H, m, H-5), 3.878 (1H, m, H-6d), 3.932 (1H, dd, *J* = 9.7, 9.0 Hz, H-3), 5.423 (1H, d, *J* = 3.7 Hz, H-1), 6.202 (1H, d, *J* = 2.1 Hz, H-6'), 6.434 (1H, d, *J* = 2.1 Hz, H-8'), 6.998 (1H, d, *J* = 8.6 Hz, H-5"), 7.865(1H, dd, *J* = 8.6, 2.2 Hz, H-6"), 8.182 (1H, d, *J* = 2.2 Hz, H-2"); [a] HSQC readout

^{13}C NMR (150.95 MHz, MeOD): 62.49 (C-6), 71.48 (C-4), 73.78 (C-2), 74.89 (C-5), 75.19 (C-3), 94.95 (C-8'), 99.70 (C-6'), 102.14 (C-1), 104.80 (C-10'), 117.57 (C-5"), 119.46 (C-2"), 124.57 (C-1"), 125.58 (C-6"), 137.67 (C-3'), 146.60 (C-3"), 147.82 (C-2'), 151.36 (C-4"), 158.58 (C-9'), 162.79 (C-5'), 166.21 (C-7'), 177.68 (C-4')

4′-*O*-α-D-Glucopyranosyl quercetin

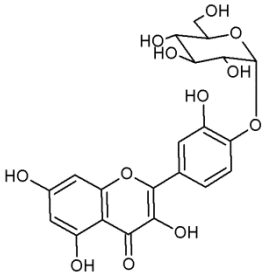

^{1}H NMR (600.23 MHz, MeOD): 3.472 (1H, dd, *J* = 9.7, 9.0 Hz, H-4), 3.648 (1H, dd, *J* = 9.7, 3.7 Hz, H-2), 3.75[a] (2H, m, H-5, H-6u), 3.829 (1H, m, H-6d), 3.929 (1H, dd, *J* = 9.7, 9.0 Hz, H-3), 5.515 (1H, d, *J* = 3.7 Hz, H-1), 6.214 (1H, d, *J* = 2.0 Hz, H-6'), 6.425 (1H, d, *J* = 2.0 Hz, H-8'), 7.424 (1H, d, *J* = 8.7 Hz, H-5"), 7.729 (1H, dd, *J* = 8.7, 2.2 Hz, H-6"), 7.790 (1H, d, *J* = 2.2 Hz, H-2"); [a] HSQC readout

^{13}C NMR (150.95 MHz, MeOD): 62.65 (C-6), 71.66 (C-4), 73.74 (C-2), 75.03 (C-5), 75.14 (C-3), 94.77 (C-8'), 99.65 (C-6'), 101.07 (C-1), 104.89 (C-10'), 117.01 (C-2"), 118.35 (C-5"), 121.52 (C-6"), 127.95 (C-1"), 138.28 (C-3'), 147.31 (C-2'), 148.10 (C-4"), 148.64 (C-3"), 158.64 (C-9'), 162.89 (C-5'), 166.15 (C-7'), 177.83 (C-4')

3′-*O*-α-D-Glucopyranosyl catechin

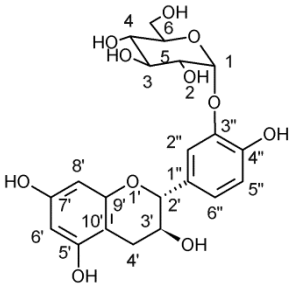

^{1}H NMR (600.23 MHz, MeOD): 2.523 (1H, dd, *J* = 16.1, 8.5 Hz, H-4'u), 2.913 (1H, dd, *J* = 16.1, 5.6 Hz, H-4'd), 3.468 (1H, dd, *J* = 9.6, 9.0 Hz, H-4), 3.600 (1H, dd, *J* = 9.7, 3.7 Hz, H-2), 3.752 (1H, dd, *J* = 11.6, 4.4 Hz, H-6u), 3.797 (1H, ddd, *J* = 9.6, 4.4, 2.3 Hz, H-5), 3.826 (1H, dd, *J* = 11.6, 2.3 Hz, H-6d), 3.894 (1H, dd, *J* = 9.7, 9.0 Hz, H-3), 4.009 (1H, ddd, *J* = 8.5, 8.0, 5.6 Hz, H-3'), 4.59[a] (1H, m, H-2'), 5.351 (1H, d, *J* = 3.7 Hz, H-1), 5.869 (1H, d, *J* = 2.3 Hz, H-8'), 5.953 (1H, d, *J* = 2.3 Hz, H-6'), 6.876 (1H, d, *J* = 8.2 Hz, H-5"), 7.007 (1H, ddd, *J* = 8.2, 2.0, 0.5 Hz, H-6"), 7.330 (1H, d, *J* = 2.0 Hz, H-2"); [a] HSQC readout

^{13}C NMR (150.95 MHz, MeOD): 29.30 (C-4'), 62.57 (C-6), 69.08 (C-3'), 71.57 (C-4), 73.77 (H-2), 74.81 (C-5), 75.20 (C-3), 83.10 (C-2'), 95.83 (C-8'), 96.68 (C-6'), 101.23 (C-10'), 101.93 (C-1), 117.22 (C-5"), 118.93 (C-2"), 124.30 (C-6"), 132.60 (C-1"), 146.59 (C-3"), 149.05 (C-4"), 157.22 (C-9'), 157.87 (C-5'), 158.16 (C-7')

3´-*O*-α-D-Glucopyranosyl epicatechin

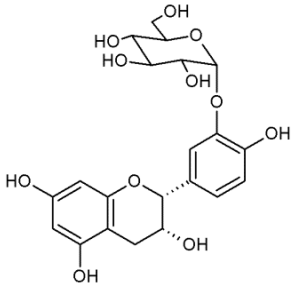

^{1}H NMR (600.23 MHz, MeOD): 2.766 (1H, ddd, *J* = 16.6, 2.8, 0.5 Hz, H-4'u), 2.892 (1H, dd, *J* = 16.6, 4.5 Hz, H-4'd), 3.443 (1H, dd, *J* = 9.8, 9.0 Hz, H-4), 3.600 (1H, dd, *J* = 9.7, 3.7 Hz, H-2), 3.746 (1H, dd, *J* = 11.8, 5.3 Hz, H-6u), 3.805 (1H, ddd, *J* = 9.8, 5.3, 2.3 Hz, H-5), 3.855 (1H, dd, *J* = 11.8, 2.3 Hz, H-6d), 3.899 (1H, dd, *J* = 9.7, 9.0 Hz, H-3), 4.217 (1H, ddd, *J* = 4.5, 2.8, 1.4 Hz, H-3'), 4.88[a] (1H, m, H-2'), 5.375 (1H, d, *J* = 3.7 Hz, H-1), 5.946 (1H, d, *J* = 2.3 Hz, H-6'), 5.966 (1H, d, *J* = 2.3 Hz, H-8'), 6.867 (1H, d, *J* = 8.3 Hz, H-5"), 7.086 (1H, ddd, *J* = 8.3, 2.1, 0.6 Hz, H-6"), 7.448 (1H, d, *J* = 2.1 Hz, H-2"); [a] HSQC readout

^{13}C NMR (150.95 MHz, MeOD): 29.65 (C-4'), 62.80 (C-6), 67.73 (C-3'), 71.77 (C-4), 73.82 (H-2), 74.80 (C-5), 75.22 (C-3), 80.03 (C-2'), 96.27 (C-6'), 96.77 (C-8'), 100.34 (C-10'), 101.77 (C-1), 116.93 (C-5"), 118.46 (C-2"), 123.53 (C-6"), 132.76 (C-1"), 146.39 (C-3"), 148.45 (C-4"), 157.60 (C-9'), 157.98 (C-7'), 158.31 (C-5')

1-*O*-α-D-Cellobiopyranosyl hydroquinone

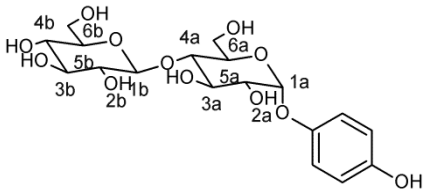

^{1}H NMR (600.23 MHz, D_2O): 3.065 (1H, dd, *J* = 9.4, 7.9 Hz, H-2b), 3.160 (1H, dd, *J* = 9.8, 9.0 Hz, H-4b), 3.233 (1H, ddd, *J* = 9.8, 5.7, 2.1 Hz, H-5b), 3.247 (1H, dd, *J* = 9.4, 9.0 Hz, H-3b), 3.48[a] (2H, m, H-4a, H-6bu), 3.49[a] (1H, m, H-2a), 3.580 (2H, m, H-6a), 3.664 (1H, dd, *J* = 12.3, 2.1 Hz, H-6bd), 3.695 (1H, ddd, H-5a), 3.751 (1H, dd, Σ*J* = 18.7 Hz, H-3a), 4.270 (1H, d, *J* = 7.9 Hz, H-1b), 5.222 (1H, d, *J* = 3.7 Hz, H-1a), 6.608 (2H, m, Σ*J* = 9.0 Hz, H-*meta*), 6.811 (2H, m, Σ*J* = 9.0 Hz, H-*ortho*); [a] HSQC readout

^{13}C NMR (150.95 MHz, D_2O): 59.87 (C-6a), 60.85 (C-6b), 69.72 (C-4b), 71.17 (C-2a), 71.34 (C-5a), 71.80 (C-3a), 73.43 (C-2b), 75.77 (C-3b), 76.25 (C-5b), 78.64 (C-4a), 98.20 (C-1a), 102.76 (C-1b), 116.50 (C-*meta*), 119.34 (C-*ortho*), 150.02 (C-*ipso*), 151.43 (C-*para*)

1-*O*-α-D-Cellotriopyranosyl hydroquinone

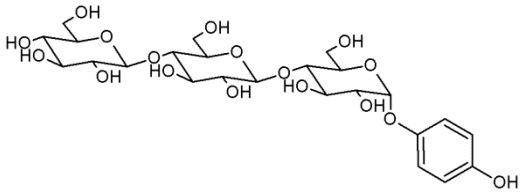

^{1}H NMR (600.23 MHz, D_2O): 3.053 (1H, dd, *J* = 9.6, 8.0 Hz, H-2c), 3.112 (1H, dd, *J* = 9.0, 8.0 Hz, H-2b), 3.153 (1H, dd, H-4c), 3.224 (1H, m, H-5c), 3.246 (1H, dd, H-3c), 3.37[a] (1H, m, H-5b), 3.39[a] (1H, m, H-3b), 3.41[a] (1H, m, H-4b), 3.471 (1H, dd, H-6cu), 3.48[a] (1H, m, H-4a), 3.49[a] (1H, m, H-2a), 3.568 (1H, m, H-6a), 3.571 (1H, dd, H-6bu), 3.597 (1H, m, H-6bd), 3.652 (1H, m, H-6cd), 3.699 (1H, m, H-5a), 3.731 (1H, m, H-6bd), 3.756 (1H, dd, Σ*J* = 18.8 Hz, H-3a), 4.247 (1H, d, *J* = 8.0 Hz, H-1c), 4.296 (1H, d, *J* = 8.0 Hz, H-1b), 5.224 (1H, d, *J* = 3.8 Hz, H-1a), 6.611 (2H, m, Σ*J* = 9.0 Hz, H-*meta*), 6.814 (2H, m, Σ*J* = 9.0 Hz, H-*ortho*); [a] HSQC readout

^{13}C NMR (150.95 MHz, D_2O): 59.85 (C-6a), 60.19 (C-6b), 60.82(C-6c), 69.70 (C-4c), 71.19 (C-2a), 71.36 (C-5a), 71.76 (C-3a), 73.21 (C-2b), 73.40 (C-2c), 74.33 (C-3b), 75.09 (C-5b), 75.74 (C-3c), 76.23 (C-5c), 78.54 (C-4a), 78.68 (C-4b), 98.23 (C-1a), 102.54 (C-1b), 102.82 (C-1c), 116.51 (C-*meta*), 119.37 (C-*ortho*), 150.03 (C-*ipso*), 151.44 (C-*para*)

1-*O*-β-D-Cellobiopyranosyl hydroquinone

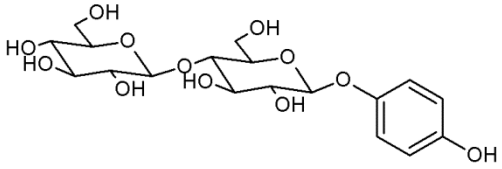

^{1}H NMR (600.23 MHz, MeOD): 3.262 (1H, dd, *J* = 9.2, 7.9 Hz, H-2b), 3.336 (1H, dd, *J* = 9.6, 8.8 Hz, H-4b), 3.381 (1H, ddd, *J* = 9.6, 5.8, 2.3 Hz, H-5b), 3.403 (1H, dd, *J* = 9.2, 8.8 Hz, H-3b), 3.496 (1H, dd, *J* = 9.1, 7.8 Hz, H-2a), 3.535 (1H, ddd, H-5a), 3.621 (1H, dd, *J* = 9.1, 8.8 Hz, H-3a), 3.677 (1H, dd, *J* = 9.6, 8.8 Hz, H-4a), 3.694 (1H, dd, *J* = 11.9, 5.8 Hz, H-6bu), 3.911 (1H, dd, *J* = 11.9, 2.3 Hz, H-6bd), 3.916 (2H, m, H-6a), 4.462 (1H, d, *J* = 7.9 Hz, H-1b), 4.791 (1H, d, *J* = 7.8 Hz, H-1a), 6.718 (2H, m, Σ*J* = 9.0 Hz, H-*meta*), 6.977 (2H, m, Σ*J* = 9.0 Hz, H-*ortho*)

^{13}C NMR (150.95 MHz, MeOD): 61.99 (C-6a), 62.73 (C-6b), 71.67 (C-4b), 75.01 (C-2a), 75.22 (C-2b), 76.62 (C-3a), 76.84 (C-5a), 78.15 (C-3b), 78.41 (C-5b), 80.64 (C-4a), 103.72 (C-1a), 104.87 (C-1b), 116.92 (C-*meta*), 119.77 (C-*ortho*), 152.61 (C-*ipso*), 154.17 (C-*para*)

1-*O*-β-D-Cellotriopyranosyl hydroquinone

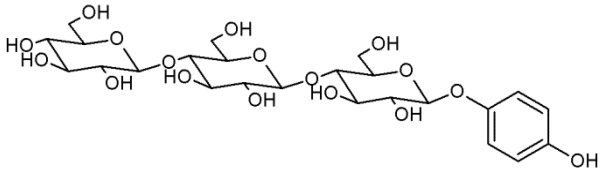

^{1}H NMR (600.23 MHz, D_2O): 3.052 (1H, dd, *J* = 9.4, 7.9 Hz, H-2c), 3.108 (1H, dd, *J* = 9.1, 8.0 Hz, H-2b), 3.152 (1H, dd, *J* = 9.9, 9.0 Hz, H-4c), 3.223 (1H, ddd, *J* = 9.9, 5.9, 2.2 Hz, H-5c), 3.244 (1H, dd, *J* = 9.4, 9.0 Hz, H-3c), 3.306 (1H, m, H-2a), 3.365 (1H, m, H-5b), 3.391 (1H, m, H-3b), 3.419 (1H, m, H-4b), 3.45[a] (1H, m, H-5a), 3.46[a] (1H, m, H-3a), 3.469 (1H, dd, H-6cu), 3.47[a] (1H, m, H-4a), 3.571 (1H, dd, *J* = 12.3, 4.7 Hz, H-6bu), 3.578 (1H, dd, *J* = 12.4, 4.4 Hz, H-6au), 3.652 (1H, dd, *J* = 12.4, 2.2 Hz, H-6cd), 3.713 (1H, dd, *J* = 12.4, 2.0 Hz, H-6ad), 3.727 (1H, dd, *J* = 12.3, 2.1 Hz, H-6bd), 4.246 (1H, d, *J* = 7.9 Hz, H-1c), 4.293 (1H, d, *J* = 8.0 Hz, H-1b), 4.740 (1H, d, *J* = 7.9 Hz, H-1a), 6.605 (2H, m, Σ*J* = 9.0 Hz, H-*meta*), 6.789 (2H, m, Σ*J* = 9.0 Hz, H-*ortho*); [a] HSQC readout

^{13}C NMR (150.95 MHz, D_2O): 60.05 (C-6a), 60.14 (C-6b), 60.82(C-6c), 69.70 (C-4c), 73.01 (C-2a), 73.19 (C-2b), 73.39 (C-2c), 74.30 (C-3b), 74.35 (C-3a), 75.07 (C-5b), 75.14 (C-5a), 75.73 (C-3c), 76.23 (C-5c), 78.49 (C-4a), 78.64 (C-4b), 101.41 (C-1a), 102.60 (C-1b), 102.81 (C-1c), 116.47 (C-*meta*), 118.70 (C-*ortho*), 150.62 (C-*ipso*), 151.54 (C-*para*)

Methyl gallyl 4-*O*-α-D-cellobiopyranoside

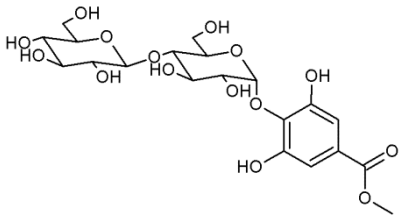

^{1}H NMR (600.23 MHz, MeOD): 3.288 (1H, dd, *J* = 9.2, 7.9 Hz, H-2b), 3.342 (1H, dd, *J* = 9.6, 8.6 Hz, H-4b), 3.384 (1H, ddd, *J* = 9.6, 5.7, 2.2 Hz, H-5b), 3.410 (1H, dd, *J* = 9.2, 8.6 Hz, H-3b), 3.673 (1H, dd, *J* = 9.6, 3.8 Hz, H-2a), 3.703 (1H, dd, *J* = 11.9, 5.7 Hz, H-6bu), 3.719 (1H, dd, *J* = 10.2, 8.8 Hz, H-4a), 3.849 (1H, dd, *J* = 12.1, 2.4 Hz, H-6au), 3.862 (3H, s, H-1'), 3.920 (1H, dd, *J* = 11.9, 2.2 Hz, H-6bd), 4.016 (1H, dd, *J* = 12.1, 3.4 Hz, H-6ad), 4.022 (1H, dd, *J* = 9.6, 8.8 Hz, H-3a), 4.386 (1H, ddd, *J* = 10.2, 3.4, 2.4 Hz, H-5a), 4.484 (1H, d, *J* = 7.9 Hz, H-1b), 5.169 (1H, d, *J* = 3.8 Hz, H-1a), 7.062 (2H, s, H-*meta*)

^{13}C NMR (150.95 MHz, MeOD): 52.86 (C-1'), 61.62 (C-6a), 62.79 (C-6b), 71.71 (C-4b), 73.60 (C-2a), 73.74 (C-3a), 73.80 (C-5a), 75.23 (C-2b), 78.17 (C-3b), 78.44 (C-5b), 80.09 (C-4a), 104.83 (C-1a), 104.86 (C-1b), 110.30 (C-*meta*), 128.09 (C-*para*), 139.60 (C-*ipso*), 152.45 (C-*ortho*), 168.61 (CO)

Methyl gallyl 4-*O*-α-D-cellotriopyranoside

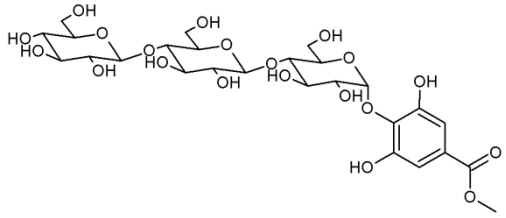

^{1}H NMR (600.23 MHz, MeOD): 3.252 (1H, dd, *J* = 9.2, 7.9 Hz, H-2c), 3.34[a] (1H, m, H-4c), 3.358 (1H, dd, *J* = 9.2, 7.9 Hz, H-2b), 3.369 (1H, ddd, *J* = 9.6, 5.6, 2.2 Hz, H-5c), 3.393 (1H, dd, *J* = 9.2, 8.6 Hz, H-3c), 3.517 (1H, ddd, *J* = 9.6, 4.3, 2.4 Hz, H-5b), 3.570 (1H, dd, *J* = 9.2, 8.8 Hz, H-3b), 3.629 (1H, dd, *J* = 9.6, 8.8 Hz, H-4b), 3.672 (1H, dd, *J* = 9.6, 3.8 Hz, H-2a), 3.687 (1H, dd, *J* = 11.9, 5.6 Hz, H-6cu), 3.724 (1H, dd, *J* = 10.1, 8.9 Hz, H-4a), 3.845 (1H, dd, *J* = 12.2, 2.4 Hz, H-6au), 3.863 (3H, s, H-1'), 3.899 (1H, dd, *J* = 12.2, 4.3 Hz, H-6bu), 3.904 (1H, dd, *J* = 11.9, 2.2 Hz, H-6cd), 3.952 (1H, dd, *J* = 12.2, 2.4 Hz, H-6bd), 4.024 (1H, dd, *J* = 12.2, 3.3 Hz, H-6ad), 4.030 (1H, dd, *J* = 9.6, 8.9 Hz, H-3a), 4.388 (1H, ddd, *J* = 10.1, 3.3, 2.4 Hz, H-5a), 4.431 (1H, d, *J* = 7.9 Hz, H-1c), 4.523 (1H, d, *J* = 7.9 Hz, H-1b), 5.175 (1H, d, *J* = 3.8 Hz, H-1a), 7.063 (2H, s, H-*meta*); [a] HSQC readout

^{13}C NMR (150.95 MHz, MeOD): 52.86 (C-1'), 61.55 (C-6a), 61.84 (C-6b), 62.73 (C-6c), 71.66 (C-4c), 73.61 (C-2a), 73.70 (C-3a), 73.79 (C-5a), 74.93 (C-2b), 75.20 (C-2c), 76.49 (C-3b), 76.97 (C-5b), 78.15 (C-3c), 78.43 (C-5c), 79.94 (C-4a), 80.51 (C-4b), 104.60 (C-1b), 104.80 (C-1a), 104.92 (C-1c), 110.30 (C-*meta*), 128.09 (C-*para*), 139.60 (C-*ipso*), 152.48 (C-*ortho*), 168.61 (CO)

Ethyl gallyl 4-*O*-α-D-cellobiopyranoside

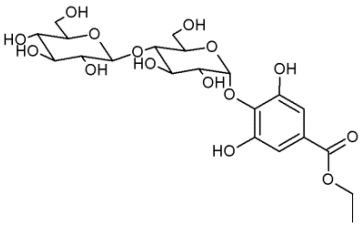

^{1}H NMR (600.23 MHz, MeOD): 1.375 (3H, t, *J* = 7.1 Hz, H-2'), 3.288 (1H, dd, *J* = 9.2, 7.9 Hz, H-2b), 3.342 (1H, dd, *J* = 9.6, 8.6 Hz, H-4b), 3.384 (1H, ddd, *J* = 9.6, 5.8, 2.2 Hz, H-5b), 3.409 (1H, dd, *J* = 9.2, 8.6 Hz, H-3b), 3.674 (1H, dd, *J* = 9.6, 3.8 Hz, H-2a), 3.703 (1H, dd, *J* = 11.9, 5.8 Hz, H-6bu), 3.719 (1H, dd, *J* = 10.1, 8.9 Hz, H-4a), 3.852 (1H, dd, *J* = 12.2, 2.4 Hz, H-6au), 3.920 (1H, dd, *J* = 11.9, 2.2 Hz, H-6bd), 4.015 (1H, dd, *J* = 12.2, 3.3 Hz, H-6ad), 4.022 (1H, dd, *J* = 9.6, 8.9 Hz, H-3a), 4.320 (2H, q, *J* = 7.1 Hz, H-1'), 4.386 (1H, ddd, *J* = 10.1, 3.3, 2.4 Hz, H-5a), 4.484 (1H, d, *J* = 7.9 Hz, H-1b), 5.168 (1H, d, *J* = 3.8 Hz, H-1a), 7.066 (2H, s, H-*meta*)

^{13}C NMR (150.95 MHz, MeOD): 14.86 (C-2'), 61.63 (C-6a), 62.35 (C-1'), 62.80 (C-6b), 71.72 (C-4b), 73.60 (C-2a), 73.75 (C-3a), 73.81 (C-5a), 75.24 (C-2b), 78.18 (C-3b), 78.44 (C-5b), 80.11 (C-4a), 104.86 (C-1a, C-1b), 110.26 (C-*meta*), 128.42 (C-*para*), 139.56 (C-*ipso*), 152.41 (C-*ortho*), 168.13 (CO)

Propyl gallyl 4-*O*-α-D-cellobiopyranoside

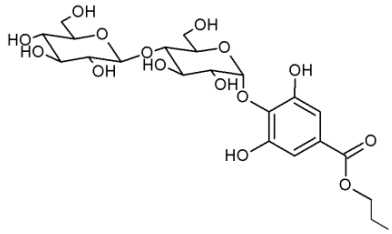

^{1}H NMR (600.23 MHz, MeOD): 1.048 (3H, t, *J* = 7.4 Hz, H-3'), 1.787 (2H, m, H-2'), 3.288 (1H, dd, *J* = 9.2, 7.9 Hz, H-2b), 3.342 (1H, dd, *J* = 9.6, 8.7 Hz, H-4b), 3.384 (1H, ddd, *J* = 9.6, 5.7, 2.2 Hz, H-5b), 3.409 (1H, dd, *J* = 9.2, 8.7 Hz, H-3b), 3.673 (1H, dd, *J* = 9.6, 3.8 Hz, H-2a), 3.703 (1H, dd, *J* = 11.9, 5.7 Hz, H-6bu), 3.720 (1H, dd, *J* = 10.1, 8.9 Hz, H-4a), 3.851 (1H, dd, *J* = 12.2, 2.5 Hz, H-6au), 3.920 (1H, dd, *J* = 11.9, 2.2 Hz, H-6bd), 4.015 (1H, dd, *J* = 12.2, 3.2 Hz, H-6ad), 4.023 (1H, dd, *J* = 9.6, 8.9 Hz, H-3a), 4.232 (2H, t, *J* = 6.6 Hz, H-1'), 4.386 (1H, ddd, *J* = 10.1, 3.3, 2.4 Hz, H-5a), 4.485 (1H, d, *J* = 7.9 Hz, H-1b), 5.172 (1H, d, *J* = 3.8 Hz, H-1a), 7.071 (2H, s, H-*meta*)

^{13}C NMR (150.95 MHz, MeOD): 11.09 (C-3'), 23.45 (C-2'), 61.64 (C-6a), 62.80 (C-6b), 67.91 (C-1'), 71.72 (C-4b), 73.61 (C-2a), 73.76 (C-3a), 73.80 (C-5a), 75.24 (C-2b), 78.19 (C-3b), 78.45 (C-5b),

80.11 (C-4a), 104.85 (C-1a), 104.87 (C-1b), 110.25 (C-*meta*), 128.40 (C-*para*), 139.57 (C-*ipso*), 152.44 (C-*ortho*), 168.19 (CO)

Propyl gallyl 4-*O*-α-D-cellotriopyranoside

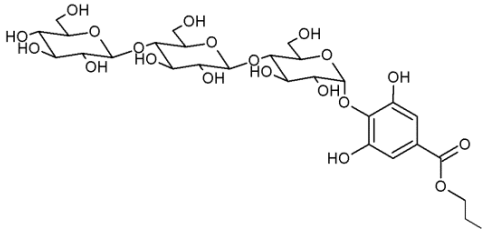

^{1}H NMR (600.23 MHz, MeOD): 1.047 (3H, t, *J* = 7.4 Hz, H-3'), 1.787 (2H, m, H-2'), 3.254 (1H, dd, *J* = 9.2, 7.9 Hz, H-2c), 3.34[a] (1H, m, H-4c), 3.359 (1H, dd, *J* = 9.2, 7.9 Hz, H-2b), 3.371 (1H, ddd, *J* = 9.6, 5.7, 2.2 Hz, H-5c), 3.394 (1H, dd, *J* = 9.2, 8.6 Hz, H-3c), 3.518 (1H, ddd, *J* = 9.6, 4.2, 2.4 Hz, H-5b), 3.572 (1H, dd, *J* = 9.2, 8.8 Hz, H-3b), 3.630 (1H, dd, *J* = 9.6, 8.8 Hz, H-4b), 3.674 (1H, dd, *J* = 9.6, 3.8 Hz, H-2a), 3.688 (1H, dd, *J* = 11.9, 5.7 Hz, H-6cu), 3.724 (1H, dd, *J* = 10.1, 9.0 Hz, H-4a), 3.848 (1H, dd, *J* = 12.1, 2.4 Hz, H-6au), 3.900 (1H, dd, *J* = 12.0, 4.2 Hz, H-6bu), 3.906 (1H, dd, *J* = 11.9, 2.2 Hz, H-6cd), 3.953 (1H, dd, *J* = 12.0, 2.4 Hz, H-6bd), 4.024 (1H, dd, *J* = 12.1, 3.3 Hz, H-6ad), 4.032 (1H, dd, *J* = 9.6, 9.0 Hz, H-3a), 4.232 (2H, t, *J* = 6.6 Hz, H-1'), 4.389 (1H, ddd, *J* = 10.1, 3.3, 2.4 Hz, H-5a), 4.432 (1H, d, *J* = 7.9 Hz, H-1c), 4.524 (1H, d, *J* = 7.9 Hz, H-1b), 5.180 (1H, d, *J* = 3.8 Hz, H-1a), 7.071 (2H, s, H-*meta*); [a] HSQC readout

^{13}C NMR (150.95 MHz, MeOD): 11.09 (C-3'), 23.44 (C-2'), 61.56 (C-6a), 61.85 (C-6b), 62.73 (C-6c), 67.91 (C-1'), 71.67 (C-4c), 73.61 (C-2a), 73.70 (C-3a), 73.78 (C-5a), 74.93 (C-2b), 75.20 (C-2c), 76.49 (C-3b), 76.97 (C-5b), 78.15 (C-3c), 78.43 (C-5c), 79.95 (C-4a), 80.52 (C-4b), 104.60 (C-1b), 104.80 (C-1a), 104.92 (C-1c), 110.25 (C-*meta*), 128.38 (C-*para*), 139.55 (C-*ipso*), 152.45 (C-*ortho*), 168.19 (CO)

3-*O*-α-D-Cellobiopyranosyl resveratrol

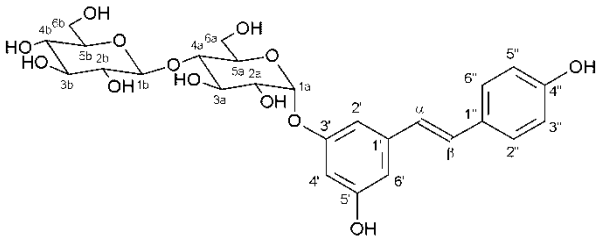

^{1}H NMR (600.23 MHz, MeOD): 3.270 (1H, dd, *J* = 9.1, 7.9 Hz, H-2b), 3.345 (1H, dd, *J* = 9.3, 8.6 Hz, H-4b), 3.384 (1H, ddd, *J* = 9.3, 5.6, 2.2 Hz, H-5b), 3.401 (1H, dd, *J* = 9.1, 8.6 Hz, H-3b), 3.655 (1H, dd, *J* = 9.8, 3.7 Hz, H-2a), 3.708 (1H, dd, *J* = 11.9, 5.6 Hz, H-6bu), 3.710 (1H, dd, *J* = 9.7, 8.7 Hz, H-4a), 3.788 (1H, dd, *J* = 12.1, 2.6 Hz, H-6au), 3.819 (1H, ddd, *J* = 9.7, 3.3, 2.6 Hz, H-5a), 3.921 (1H, dd, *J* = 11.9, 2.2 Hz, H-6bd), 3.941 (1H, dd, *J* = 12.1, 3.3 Hz, H-6ad), 4.001 (1H, dd, *J* = 9.8, 8.7 Hz, H-3a), 4.462 (1H, d, *J* = 7.9 Hz, H-1b), 5.506 (1H, d, *J* = 3.7 Hz, H-1a), 6.516 (1H, dd, Σ*J* = 4.3 Hz, H-4'), 6.644 (1H, dd, Σ*J* = 3.6 Hz, H-6'), 6.798 (2H, m, Σ*J* = 8.7 Hz, H-3", H-5"), 6.834 (1H, dd, Σ*J* = 3.6 Hz, H-2'), 6.869 (1H, d, *J* = 16.3 Hz, H-α), 7.028 (1H, d, *J* = 16.3 Hz, H-β), 7.387 (1H, m, Σ*J* = 8.7 Hz, H-2", H-6")

^{13}C NMR (150.95 MHz, MeOD): 61.77 (C-6a), 62.75 (C-6b), 71.68 (C-4b), 73.10 (C-5a), 73.39 (C-2a), 73.70 (C-3a), 75.25 (C-2b), 78.15 (C-3b), 78.44 (C-5b), 80.85 (C-4a), 99.16 (C-1a), 104.61 (C-4'), 104.96 (C-1b), 107.58 (C-2'), 108.67 (C-6'), 116.80 (C-3", C-5"), 126.95 (C-α), 129.20 (C-2", C-6"), 130.26 (C-β), 130.58 (C-1"), 141.77 (C-1'), 158.82 (C-4"), 159.97 (C-5'), 160.12 (C-3')

3-*O*-α-D-Cellotriopyranosyl resveratrol

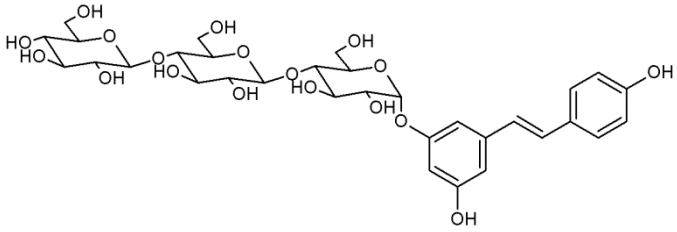

^{1}H NMR (600.23 MHz, MeOD): 3.255 (1H, dd, *J* = 9.2, 7.9 Hz, H-2c), 3.329 (1H, m, H-4b), 3.344 (2H, m, H-4c, H-2b), 3.374 (1H, m, H-5c), 3.399 (1H, m, H-3c), 3.525 (1H, m, H-5b), 3.567 (1H, m, H-3b), 3.638 (1H, m, H-4b), 3.661 (1H, dd, *J* = 9.8, 3.7 Hz, H-2a), 3.688 (1H, m, H-6cu), 3.723 (1H, dd, *J* = 9.9, 8.8 Hz, H-4a), 3.787 (1H, m, H-6au), 3.822 (1H, m, H-5a), 3.906 (1H, m, H-6cd), 3.911 (1H, m, H-6bu), 3.950 (1H, m, H-6ad), 3.954 (1H, m, H-6bd), 4.009 (1H, dd, *J* = 9.8, 8.8 Hz, H-3a), 4.437 (1H, d, *J* = 7.9 Hz, H-1c), 4.507 (1H, d, *J* = 7.9 Hz, H-1b), 5.512 (1H, d, *J* = 3.7 Hz, H-1a), 6.517 (1H, dd, Σ*J* = 4.3 Hz, H-4'), 6.648 (1H, dd, Σ*J* = 3.3 Hz, H-6'), 6.791 (2H, m, Σ*J* = 8.6 Hz, H-3", H-5"), 6.831 (1H, dd, Σ*J* = 3.4 Hz, H-2'), 6.868 (1H, d, *J* = 16.3 Hz, H-α), 7.028 (1H, d, *J* = 16.3 Hz, H-β), 7.386 (1H, m, Σ*J* = 8.6 Hz, H-2", H-6")
^{13}C NMR (150.95 MHz, MeOD): 61.67 (C-6a), 61.76 (C-6b), 62.70 (C-6c), 71.66 (C-4c), 73.09 (C-5a), 73.39 (C-2a), 73.62 (C-3a), 74.94 (C-2b), 75.19 (C-2c), 76.41 (C-3b), 76.95 (C-5b), 78.12 (C-3c), 78.42 (C-5c), 80.43 (C-4b), 80.64 (C-4a), 99.15 (C-1a), 104.67 (C-1b), 104.90 (C-1c), 107.58 (C-2'), 108.69 (C-6'), 116.81 (C-3", C-5"), 126.93 (C-α), 129.19 (C-2", C-6"), 130.27 (C-β), 130.56 (C-1"), 141.78 (C-1'), 158.83 (C-4"), 159.98 (C-5'), 160.10 (C-3')

3-*O*-β-D-Cellobiopyranosyl resveratrol

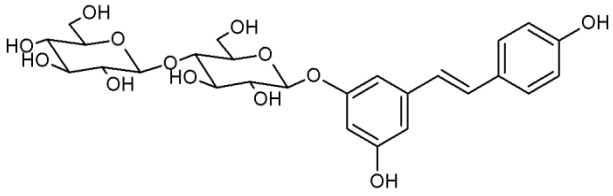

^{1}H NMR (600.23 MHz, MeOD): 3.275 (1H, dd, *J* = 9.2, 7.9 Hz, H-2b), 3.34[a] (1H, m, H-4b), 3.386 (1H, ddd, *J* = 9.6, 5.8, 2.3 Hz, H-5b), 3.407 (1H, dd, *J* = 9.2, 8.8 Hz, H-3b), 3.537 (1H, dd, *J* = 9.0, 7.8 Hz, H-2a), 3.627 (1H, ddd, *J* = 9.4, 4.2, 2.5 Hz, H-5a), 3.659 (1H, dd, *J* = 9.0, 8.7 Hz, H-3a), 3.693 (1H, dd, *J* = 9.4, 8.7 Hz, H-4a), 3.700 (1H, dd, *J* = 11.9, 5.8 Hz, H-6bu), 3.918 (1H, dd, *J* = 11.9, 2.3 Hz, H-6bd), 3.928 (1H, dd, *J* = 12.3, 4.2 Hz, H-6au), 3.982 (1H, dd, *J* = 12.3, 2.5 Hz, H-6ad), 4.472 (1H, d, *J* = 7.9 Hz, H-1b), 4.956 (1H, d, *J* = 7.8 Hz, H-1a), 6.464 (1H, dd, Σ*J* = 2.2 Hz, H-4'), 6.643 (1H, dd, Σ*J* = 3.6 Hz, H-6'), 6.787 (2H, m, Σ*J* = 8.6 Hz, H-3", H-5"), 6.79[a] (1H, m, H-2'), 6.869 (1H, d, *J* = 16.2 Hz, H-α), 7.030 (1H, d, *J* = 16.2 Hz, H-β), 7.386 (1H, m, Σ*J* = 9.0 Hz, H-2", H-6"); [a] HSQC readout
^{13}C NMR (150.95 MHz, MeOD): 62.05 (C-6a), 62.78 (C-6b), 71.71 (C-4b), 75.02 (C-2a), 75.27 (C-2b), 76.69 (C-3a), 77.03 (C-5a), 78.21 (C-3b), 78.47 (C-5b), 80.67 (C-4a), 102.46 (C-1a), 104.42(C-4'), 104.92 (C-1b), 107.44 (C-2'), 108.65 (C-6'), 116.83 (C-3", C-5"), 126.97 (C-α), 129.24 (C-2", C-6"), 130.32 (C-β), 130.62 (C-1"), 141.75 (C-1'), 158.83 (C-4"), 159.94 (C-3'), 160.70 (C-5')

3-*O*-β-D-Cellotriopyranosyl resveratrol

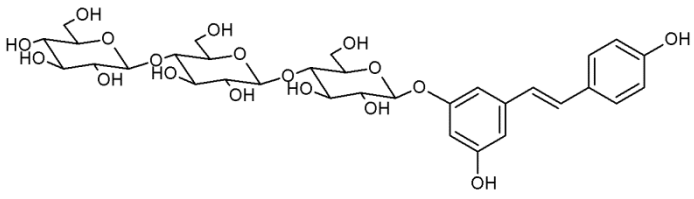

^{1}H NMR (600.23 MHz, MeOD): 3.252 (1H, dd, *J* = 9.2, 7.9 Hz, H-2c), 3.328 (1H, dd, J = 9.6, 8.8 Hz, H-4c), 3.370 (1H, ddd, *J* = 9.6, 5.8, 2.3 Hz, H-5c), 3.393 (1H, dd, *J* = 9.2, 8.8 Hz, H-3b), 3.536 (1H, dd, *J* = 9.0, 7.8 Hz, H-2a), 3.628 (1H, ddd, *J* = 9.5, 4.0, 2.5 Hz, H-5a), 3.665 (1H, dd, *J* = 9.0, 8.7 Hz, H-3a), 3.687 (1H, dd, *J* = 11.9, 5.8 Hz, H-6cu), 3.703 (1H, dd, *J* = 9.5, 8.7 Hz, H-4a), 3.905 (1H, dd, *J* = 11.9, 2.3 Hz, H-6cd), 3.938 (1H, dd, *J* = 12.4, 4.0 Hz, H-6au), 3.981 (1H, dd, *J* =

12.4, 2.5 Hz, H-6ad), 4.431 (1H, d, *J* = 7.9 Hz, H-1c), 4.956 (1H, d, *J* = 7.8 Hz, H-1a), 6.464 (1H, dd, Σ*J* = 2.2 Hz, H-4'), 6.644 (1H, dd, Σ*J* = 3.8 Hz, H-6'), 6.788 (2H, m, Σ*J* = 8.7 Hz, H-3", H-5"), 6.79[a] (1H, m, H-2'), 6.870 (1H, d, *J* = 16.2 Hz, H-α), 7.030 (1H, d, *J* = 16.2 Hz, H-β), 7.387 (1H, m, Σ*J* = 9.0 Hz, H-2", H-6"); [a] HSQC readout

^{13}C NMR (150.95 MHz, MeOD): 61.93 (C-6a), 62.74 (C-6c), 71.67 (C-4c), 74.99 (C-2a), 75.20 (C-2c), 76.60 (C-3a), 76.97 (C-5a), 78.15 (C-3c), 78.43 (C-5c), 80.48 (C-4a), 102.44 (C-1a), 104.38(C-4'), 104.92 (C-1c), 107.41 (C-2'), 108.62 (C-6'), 116.80 (C-3", C-5"), 126.94 (C-α), 129.22 (C-2", C-6"), 130.30 (C-β), 130.59 (C-1"), 141.73 (C-1'), 158.81 (C-4"), 159.92 (C-3'), 160.67 (C-5')

3´-*O*-α-D-Cellobiopyranosyl epicatechin

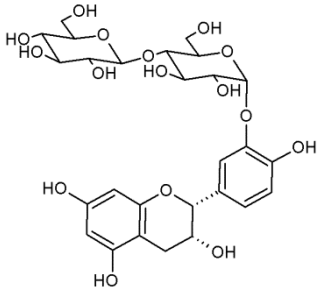

^{1}H NMR (600.23 MHz, MeOD): 2.765 (1H, ddd, *J* = 16.6, 2.8, 0.5 Hz, H-4'u), 2.888 (1H, dd, *J* = 16.6, 4.5 Hz, H-4'd), 3.272 (1H, dd, *J* = 9.2, 7.9 Hz, H-2b), 3.342 (1H, m, H-4b), 3.38[a] (1H, m, H-5b), 3.402 (1H, dd, *J* = 9.2, 8.6 Hz, H-3b), 3.669 (1H, dd, *J* = 9.7, 3.7 Hz, H-2a), 3.70[a] (1H, m, H-6bu), 3.703 (1H, dd, *J* = 9.8, 8.7 Hz, H-4a), 3.86[a] (1H, m, H-6au), 3.92[a] (1H, m, H-6bd), 3.93[a] (1H, m, H-5a), 3.95[a] (1H, m, H-6ad), 4.026 (1H, dd, *J* = 9.7, 8.7 Hz, H-3a), 4.211 (1H, ddd, *J* = 4.5, 2.8, 1.4 Hz, H-3'), 4.462 (1H, d, *J* = 7.9 Hz, H-1b), 4.88[a] (1H, m, H-2'), 5.397 (1H, d, *J* = 3.7 Hz, H-1a), 5.939 (1H, d, *J* = 2.3 Hz, H-6'), 5.965 (1H, d, *J* = 2.3 Hz, H-8'), 6.867 (1H, d, *J* = 8.2 Hz, H-5"), 7.073 (1H, ddd, *J* = 8.2, 2.0, 0.7 Hz, H-6"), 7.427 (1H, d, *J* = 2.0 Hz, H-2"); [a] HSQC readout

^{13}C NMR (150.95 MHz, MeOD): 29.62 (C-4'), 61.87 (C-6a), 62.76 (C-6b), 67.74 (C-3'), 71.69 (C-4b), 73.24 (C-5a), 73.57 (H-2a), 73.66 (C-3a), 75.23 (C-2b), 78.14 (C-3b), 78.44 (C-5b), 80.01 (C-2'), 80.65 (C-4a), 96.24 (C-6'), 96.76 (C-8'), 100.32 (C-10'), 101.27 (C-1a), 104.93 (C-1b), 116.99 (C-5"), 118.23 (C-2"), 123.54 (C-6"), 132.77 (C-1"), 146.27 (C-3"), 148.44 (C-4"), 157.59 (C-9'), 158.00 (C-7'), 158.33 (C-5')

CHAPTER 9

Turning bulk sugars into prebiotics: Chemoenzymatic synthesis of kojibiose from sucrose and glucose

Parts of this chapter have been published:

T. Verhaeghe, K. De Winter, M. Berland, R. De Vreese, M. D'hooghe, B. Offmann, and T. Desmet, **2016**, Converting bulk sugars into prebiotics: Semi-rational design of a transglucosidase with controlled selectivity, *Chemical Communications*, DOI: 10.1039/C5CC09940D.

Parts of this chapter will be submitted for publication:

K. De Winter, T. Verhaeghe, A. Van Canneyt, and T. Desmet, **2016**, Highly efficient synthesis of kojibiose: Process intensification, crystallization, and characterization, *Journal of Agricultural and Food Chemistry*, ***In preparation***.

1 ABSTRACT

Over the past decade, prebiotics have gained increasing attention in the field of nutrition and gastroenterology. Although these compounds are known to stimulate the growth of beneficial bacterial populations, the variety of prebiotics is limited to date. Indeed, application testing of promising carbohydrates is often hampered by their limited availability, as is the case for the naturally occurring disaccharide kojibiose (2-*O*-α-D-glucopyranosyl-D-glucopyranoside). In this work, the synthesis of kojibiose was evaluated using different SP variants. The L341I_Q345S variant of *Bifidobacterium adolescentis* sucrose phosphorylase was found to efficiently synthesize kojibiose, while remaining fully active after 1 week incubation at 55 °C. The use of an integrated approach during the design of the process, allowed the synthesis and isolation of kojibiose up to concentrations of 1.5 M. The produced kojibiose could be conveniently purified by treatment with baker's yeast and was subsequently crystallized to obtain 3 kg crystalline kojibiose with a purity of 99.8 %.

2 INTRODUCTION

Over the past decade, the intimate relation between the gut microbiome and our physiology has been vastly described. Indeed, these micro-organisms play pivotal roles in our metabolism and immune response, as well as in several diseases like obesity, inflammatory bowel disease and type 2 diabetes[5, 235]. As a result, prebiotics, carbohydrates that stimulate the growth of beneficial bacterial populations in the human gut, have gained increasing attention[236, 237]. Commonly applied prebiotics include inulin[1], trans- galactooligosaccharides[2], resistant starches[3] and mannan oligosaccharides[4]. Despite these examples, the current menu of prebiotics is rather limited and expanding their scope is highly desired[238-240].

In that respect, kojibiose (2-*O*-α-D-glucopyranosyl-D-glucopyranoside) is a very promising compound. Preliminary studies indicated that kojibiose and its derived oligosaccharides can selectively stimulate beneficial gut populations. Indeed, the α-1,2 bond is largely resistant to the action of enzymes in the digestive tract, but can be cleaved by specific micro-organisms such as lactobacilli[241-243]. Besides its prebiotic properties, kojibiose is not metabolized by common oral bacteria and has therefore attracted attention as a low-calorie sweetener for the prevention of tooth decay[243]. Moreover, kojibiose has been described to inhibit α-glucosidase I[244]. These inhibitors are known to be candidate drugs for the treatment of HIV-1 infections[245], while their inhibitory properties could limit the digestion of dietary carbohydrates. Kojibiose might therefore also find application in the treatment of diabetes, obesity and cardiovascular diseases[246].

However, in depth studies on the health-promoting properties of kojibiose are hampered by its high price and limited availability[241]. Although kojibiose is present in honey, beer, sake and koji, the amounts are far too low for practical isolation[247-249]. In parallel to the production of glycosides, also the chemical synthesis of kojibiose suffers from low yields and the generation of toxic waste[250-252]. Alternatively, isolation after partial acetolysis of dextran produced by *Leuconostoc mesenteroides* has been described. However, the latter procedure involves multiple steps requiring chemical reagents among which acetic anhydride, sulfuric acid, chloroform and methanol, while the

kojibiose yield is limited to 17 %[253]. Therefore, the enzymatic synthesis of kojibiose has been vastly explored. Examples include the use of α-glucosidases[254] and α-glucoamylases[255], glucansucrase[256, 257] and kojibiose phosphorylase[258]. Unfortunately, these processes suffer from low yields and the generation of side products. More recently a procedure using dextransucrase and galactosidase as biocatalysts was developed[259]. Although the latter strategy is certainly the most efficient and sustainable way to obtain kojibiose to date, it requires multiple enzymatic and yeast treatment steps, while the overall yield of 38 % can be considered average at best. Moreover, the purity of the obtained kojibiose was limited to 65 %. Higher purities could only be achieved by preparative liquid chromatography while freeze-drying was applied to obtain a powdered product[259].

In an attempt to overcome these drawbacks, the sucrose phosphorylase (SP) from *Bifidobacterium adolescentis* has very recently been engineered towards the synthesis of kojibiose[43]. Indeed, although the latter enzyme is able to convert sucrose and glucose to glucobioses, kojibiose accounted for only 33 % of the formed disaccharides (Figure 9.1). Moreover, substantial amounts of sucrose are hydrolyzed to fructose and glucose by the wild type enzyme. Interestingly, a number of variants with improved selectivity towards the synthesis of kojibiose were obtained[43]. In this chapter, these variants were thoroughly evaluated for the production of kojibiose. The reaction conditions were optimized, and a sustainable downstream processing methodology was established. Finally, the reaction was scaled to 10 L, illustrating the robustness and industrial applicability of the latter procedure.

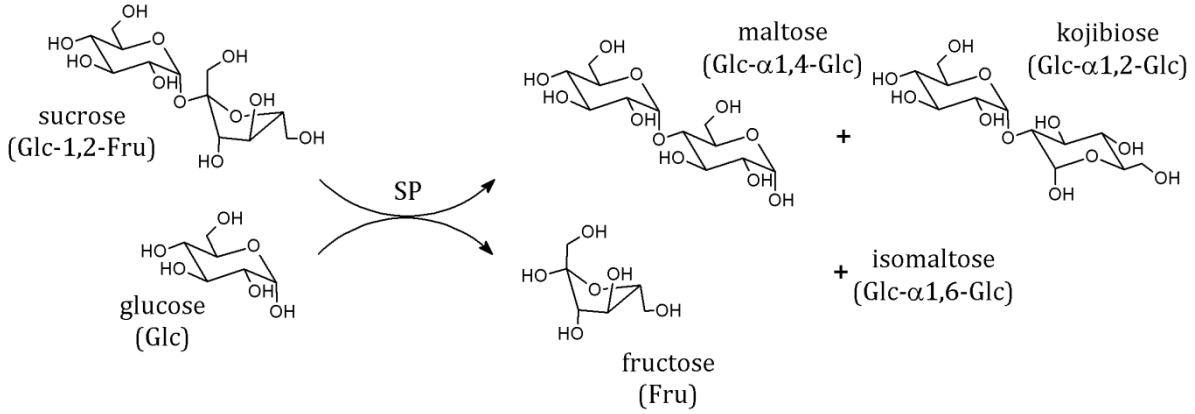

Figure 9.1 Reactions catalyzed by the SP from *Bifidobacterium adolescentis* in the presence of sucrose and glucose. Maltose and kojibiose are the main products, while only traces of isomaltose are formed.

3 RESULTS & DISCUSSION

3.1 Selection of SP variant for the production of kojibiose

Although recent research resulted in several SP mutants with enhanced properties towards the synthesis of kojibiose[43], these variants haven't been evaluated under production conditions to date. To that end, the most promising variants (L341I, L341I_Q345S, L341I_Q345N, and L341I_Y344A_Q345N) were studied in detail. The substrate concentration was varied between 0.1 and 1 M, while heat purified enzyme was added to concentrations between 1 and 4 mg/mL. From these experiments, a variety of parameters were obtained (Table S9.1). The average values for all parameters were then calculated to allow a straightforward comparison of the different variants (Table 9.1).

Table 9.1 Performance of various SP variants for the synthesis of kojibiose. The averages of all values calculated in Table S9.1 are reported.

Enzyme	Sel.[a] (%)	Conv.[b] (%)	Yield (%)	Hydr.[c] (%)	Efficiency (%)	Productivity (g/g/h)
L341I	79.7	95.7	43.5	34.8	51.5	5.7
L341I_Q345S	97.1	67.8	51.1	30.7	67.1	5.4
L341I_Q345N	98.3	38.7	23.4	36.0	62.6	1.6
L341I_Y344A_Q345N	100.0	28.9	7.4	19.5	77.8	0.3

[a] Selectivity, [b] Conversion, [c] Hydrolysis

Triple mutant L341I_Y344A_Q345N displays both the highest selectivity and efficiency, while hydrolysis is limited to only 19.5 %. Indeed, the enzyme produces no other glucobioses (selectivity of 100 %), which, combined with the reduced hydrolysis, results in an efficiency of nearly 78 %. Unfortunately, this increased selectivity comes at the expense of a severely reduced productivity. As a result, the average conversion remained below 30 %, while a kojibiose yield of only 7.4 % was observed. In contrast, single mutant L341I reached nearly 96 % conversion, while exhibiting the highest productivity. However, kojibiose accounted for only 80 % of the formed glucobioses, while hydrolysis amounted to roughly 35 %. Consequentially, the efficiency of the L341I variant was found to be rather limited. Interestingly, both double mutants exhibit intermediate properties. In particular, the L341I_Q345S mutant combines a high

selectivity with an enhanced productivity, resulting in the best kojibiose yield of all variants. In addition, the hydrolysis of the latter variant was found to be substantially lower compared to the L341I_Q345N mutant. Therefore, mutant L341I_Q345S was identified to be the most promising variant for the production of kojibiose.

3.2 Stability of the L341I_Q345S mutant

Although variants with improved properties were revealed, altering the structure of enzymes is known to influence their stability[260, 261]. Therefore, the thermostability of mutant L341I_Q345S, the wild type, and both single mutants was evaluated (Figure 9.2).

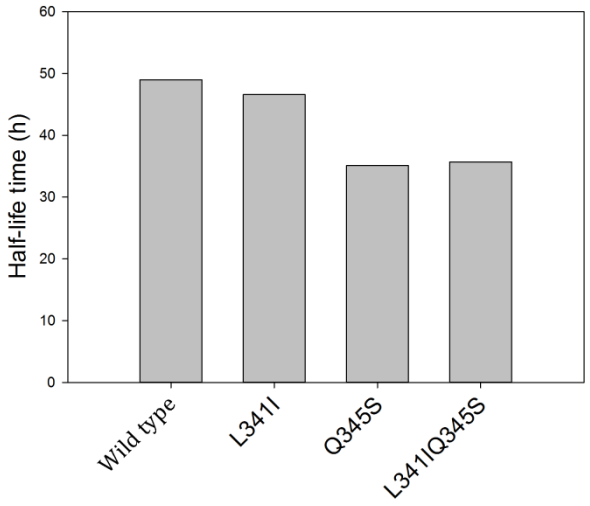

Figure 9.2 Stability of selected SP mutants at 60 °C. The time required to reduce the initial activity to 50 % (t_{50}) was calculated calculated from the equations obtained by fitting the linear part of the stability curves.

When incubating the enzymes at 60 °C, a significant difference in thermostability was observed. The half-life time of the L341I_Q345S mutant was found to be decreased by roughly 30 %. A similar result was obtained for the Q345S variant, while the thermostability of the L341I mutant was comparable with the wild type enzyme. The reduced stability of the L341I_Q345S variant can thus be solely contributed to mutation Q345S. Despite this decreased stability, all variants remained fully active after one week incubation at 55 °C, thus enabling their application at the industrial scale.

3.3 Optimization of substrate concentrations and downstream processing: an integrated approach

Industrial carbohydrate conversions are preferably run at elevated temperatures with high substrate concentrations[96]. Although the L341I_Q345S variant proved to be stable at 55 °C, the use of high sucrose and glucose concentrations might hamper the efficient isolation of kojibiose. Indeed, *Saccharomyces cerevisiae* is known to metabolize all contaminating carbohydrates (sucrose, glucose, fructose, maltose)[262], while kojibiose isn't consumed by the yeast[259]. However, these conversions are typically performed at moderate carbohydrate concentrations, not exceeding 200 g/L total carbohydrates[259, 263]. Therefore, the reaction mixtures obtained by converting 0.25, 0.5, 1 and 1.5 M sucrose and glucose to kojibiose, were subjected to treatment with 30 g/L baker's yeast at pH 7.0 and 30 °C (Figure 9.3).

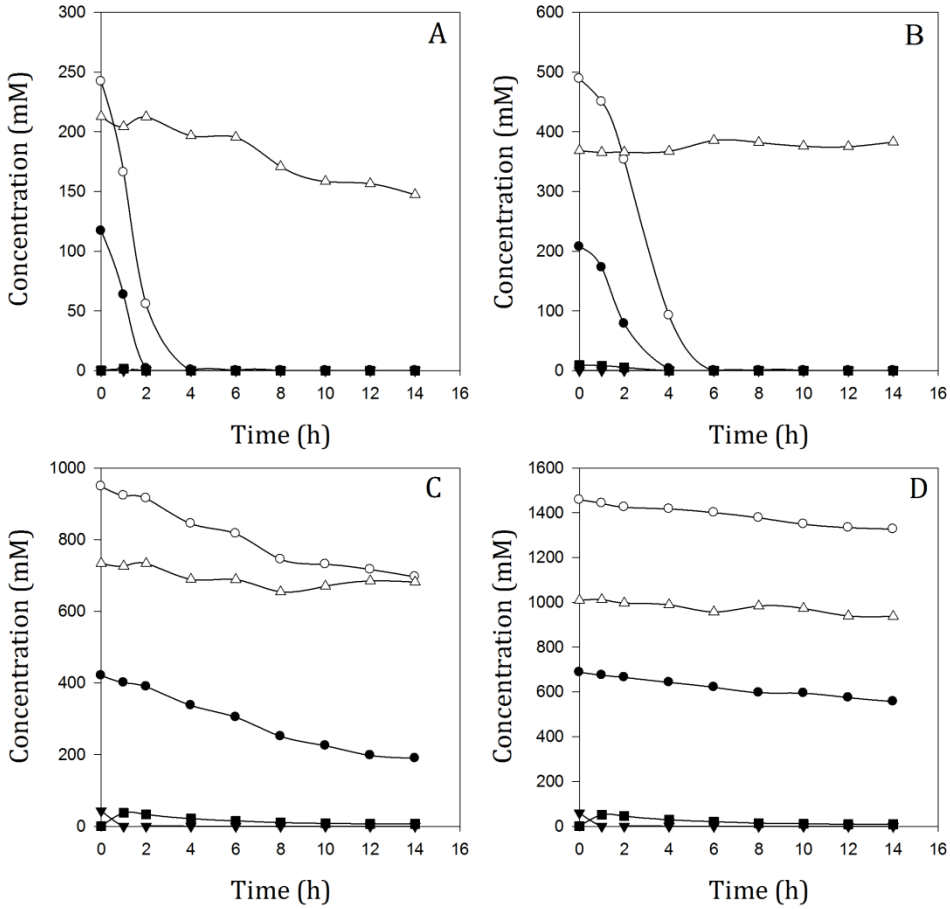

Figure 9.3 Yeast treatment of reaction mixtures obtained by converting 0.25 (A), 0.5 (B), 1 (C) and 1.5 (D) M sucrose and glucose to equilibrium. Baker's yeast was added to 30 g/L, and the reactions were incubated at 30 °C and pH 7.0. The concentration of glucose (●), fructose (○), sucrose (▼), kojibiose (△) and maltose (■) was followed in time.

Interestingly, the addition of 30 g/L *S. cerevisiae* allowed the elimination of all contaminating carbohydrates after 4 and 6 h, when starting from 250 and 500 mM sucrose and glucose, respectively. In contrast to the reaction starting from 500 mM substrate, baker's yeast was found to slowly metabolize kojibiose after 6 h when starting from 250 mM sucrose and glucose. Unfortunately, higher substrate concentrations severely hampered the yeast's action. As a result, roughly 70 and 90 % of the undesired contaminants remained present after 14 h when using substrate concentrations of 1 and 1.5 M respectively. Extended incubation of these reaction mixtures (up to 7 days) failed to remove all undesired carbohydrates. Similar results were obtained when incubating the baker's yeast at pH 5.0, indicating the limited effect of the acidity on the performance of *S. cerevisiae* for the latter conversions (Figure S9.1).

Although reacting 500 mM sucrose and glucose with the L341I_Q345S variant easily outperforms the most efficient method for the synthesis of kojibiose to date[259], higher kojibiose concentrations would be desirable. At the end of the enzymatic conversion, all sucrose is converted, resulting in roughly 350 mM kojibiose, while also approximately 500 mM fructose and 200 mM glucose are present (Figure 9.3). Reducing the amount of the latter side products, would allow higher kojibiose titers during the yeast treatment. Therefore, the use of glucose isomerase (GI) was evaluated to convert the stoichiometrically formed fructose to glucose, which can then be used as acceptor (Figure 9.4).

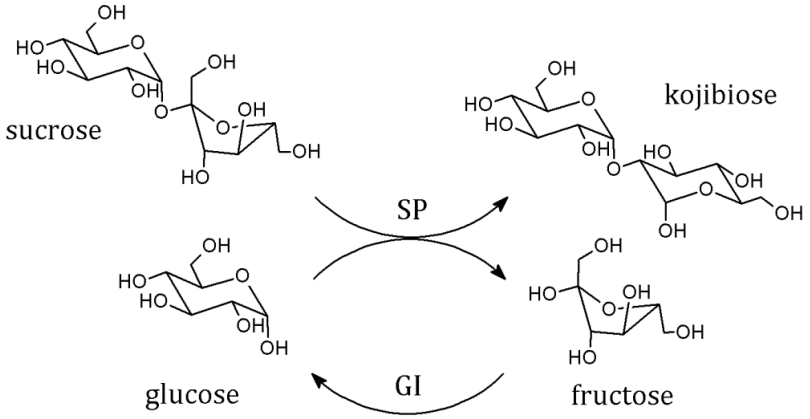

Figure 9.4 Synthesis of kojibiose from sucrose and glucose by the *Bifidobacterium adolescentis* L341I_Q345S SP. Glucose isomerase (GI) was used to convert the formed fructose to the acceptor substrate glucose.

The latter adaptation was found to allow the use of higher sucrose and lower glucose concentrations, while producing more kojibiose (Table 9.2).

Table 9.2 Performance of *Bifidobacterium adolescentis* L341I_Q345S SP under various reaction conditions. All reactions were performed at 55 °C in the presence of 2 mg/mL heat purified L341I_Q345S.

Sucrose (mM)	Glucose (mM)	GI	Reaction time (h)	Kojibiose (mM)	Atom efficiency (%)	Yeast reaction (h)[a]
250	250	-[d]	24	201	52.7	4
500	500	-[d]	24	374	49.0	6
1000	1000	-[d]	48	754	49.4	-[b]
1500	1500	-[d]	69	1008	44.0	-[b]
1500	300	+[e]	69	1135	68.5	-[b]
800	200	+[e]	48	596	65.8	9
1600	200	+[e]	69	1332	78.1	11
1800	200	+[e]	69	1507	79.1	12
2000	200	+[e]	69	1664	79.0	P[c]

[a] Time required to remove >99 % of the contaminating carbohydrates. [b] The contaminating carbohydrates could not be removed by yeast treatment. [c] Kojibiose precipitated during yeast treatment. [d] No glucose isomerase was added. [e] 20 g/L glucose isomerase was added after 2h.

Combining the use of glucose isomerase with high sucrose and low glucose concentrations, was found to significantly increase the atom efficiency (Table 9.2). The latter parameter, which is a measure for the efficient use of substrates, could be increased to 79 %; a tremendous improvement compared to the recently reported 19 % for the synthesis from lactose and glucose[259]. Moreover, kojibiose concentrations exceeding 1.5 M were readily achieved. Much to our surprise, we were able to remove all contaminating carbohydrates, when reacting 1.8 M sucrose with 0.2 M glucose. In contrast, when using 1.5 M sucrose and 0.3 M glucose, we failed to purify kojibiose. The latter phenomenon was studied in detail by adding kojibiose to 1 M final concentration after the enzymatic conversion of 500 mM sucrose and glucose (Figure 9.5).

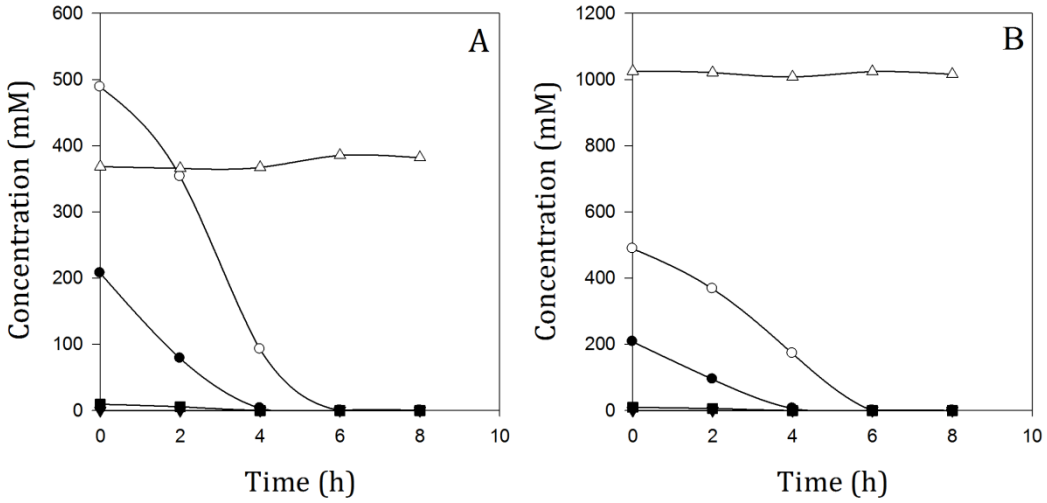

Figure 9.5 Effect of kojibiose on the performance of *Saccharomyces cerevisiae.* Yeast treatments were performed on reaction mixtures obtained by converting 500 mM sucrose and glucose to equilibrium (A) and an identical reaction mixture supplemented with kojibiose to 1 M (B). Baker's yeast was added to 30 g/L, and the reactions were incubated at 30 °C. The concentration of glucose (●), fructose (○), sucrose (▼), kojibiose (△) and maltose (■) was followed in time.

Remarkably, the presence of 1 M kojibiose did not significantly influence the performance of *S. cerevisiae* (Figure 9.5). Nevertheless, previous experiments demonstrated the inhibitory effect of such elevated carbohydrate concentrations (Figure 9.3). Therefore, this inhibition is solely related to high fructose and glucose concentrations, while the presence of kojibiose doesn't significantly influence the yeast's performance. Indeed, reacting 1.8 M sucrose with 0.2 M glucose, resulted in a combined total of 786 mM fructose and glucose, while the reaction starting from 1.5 M sucrose and 0.3 M glucose yielded more than 1 M of the latter carbohydrates. In conclusion, the combined glucose and fructose concentration should be kept well below 1 M. Although further increasing the sucrose concentration to 2 M resulted in an impressive kojibiose concentration approaching 1.7 M, such high concentrations were found to result in precipitation during the yeast treatment.

3.4 Crystallization of kojibiose

As described above, reacting 1.8 M sucrose with 0.2 M glucose resulted in 1.5 M kojibiose. Although all contaminating carbohydrates could be successfully removed by yeast treatment, obtaining the desired product in crystalline form often remains a challenge[53]. Indeed, *S. cerevisiae* is known to produce metabolites (mainly glycerol

and/or organic acids), which might hamper the crystallization of kojibiose[259]. Although the concentration of these contaminants increased with increasing substrate concentrations, we were able to obtain kojibiose crystals by performing an evaporative step at 50 °C to a Brix of 60, followed by cooling crystallization at 4 °C. Remarkably, the addition of glycerol up to 300 mM did not affect the crystallization of kojibiose under these conditions.

Encouraged by these results, the crystallization of kojibiose was studied in detail. To that end, the concentration of kojibiose prior to the cooling crystallization step was altered between 75 and 42 ° Bx, corresponding to 2.07 and 1.16 M respectively (Figure S9.2). These mixtures were then overnight cooled from 50 °C to room temperature, and subsequently cooled to 4 °C, after which crystal growth was continued during 24 h. Next, the (microscopic) appearance of the crystals (Figure S9.3 and S9.4), crystallization yield, whiteness and purity of the obtained kojibiose crystals were evaluated (Table 9.3).

Table 9.3 Cooling crystallization of kojibiose. The performance at different Brixes was evaluated by determining the crystallization yield and measuring the whiteness and purity of all crystals.

Brix (° Bx)	ICUMSA score	Purity HPAEC-PAD (%)	Purity HPLC-RI (%)	Crystallization Yield (%)
75	400.0	96.40	98.41	85.5
60	379.0	96.66	94.16	72.5
55	217.5	98.08	99.87	74.9
50	196.5	98.47	99.90	74.2
48	129.8	99.81	99.98	72.3
46	168.4	98.08	99.95	58.2
44	164.9	98.17	99.86	51.7
42	789.5	96.12	89.45	46.2

Although the highest crystallization yield was achieved at Brix 75, the obtained purity of the crystals was limited to 96 %. Decreasing the Brix resulted in lower crystallization yields, but also significantly improved the purity of the obtained crystals. Interestingly, Brix 48 was found to combine a high crystallization yield, with a purity exceeding 99.8 %. Also, the crystals obtained at Brix 48 presented the lowest ICUMSA score, reflecting their whiteness. Moreover, the latter crystals were visible with the naked eye

(Figure S9.4). Indeed, in contrast to cooling crystallization at higher Brixes, the presence of large kojibiose needle shaped crystals was confirmed by microscopic analysis up to Brix 50 (Figure S9.4)[264].

In conclusion, crystallization at Brix 48 resulted in white crystals with a purity exceeding 99.8 % (Figure 9.6). The corresponding crystallization yield of 72 % could be conveniently increased to 96 % by performing a second crystallization on the supernatant, yielding 99 % pure kojibiose. Alternatively, the sucrose concentration was increased from 1.8 to 2 M, resulting in the spontaneous crystallization of kojibiose upon cooling (Table 9.2). Although the latter procedure avoids the use of *S. cerevisiae*, the purity of the obtained crystals was limited to 97.5 %. Despite the presence of minor amounts of glucose and fructose, this procedure allows the straightforward isolation of kojibiose, and was identified a valuable alternative for obtaining bulk kojibiose.

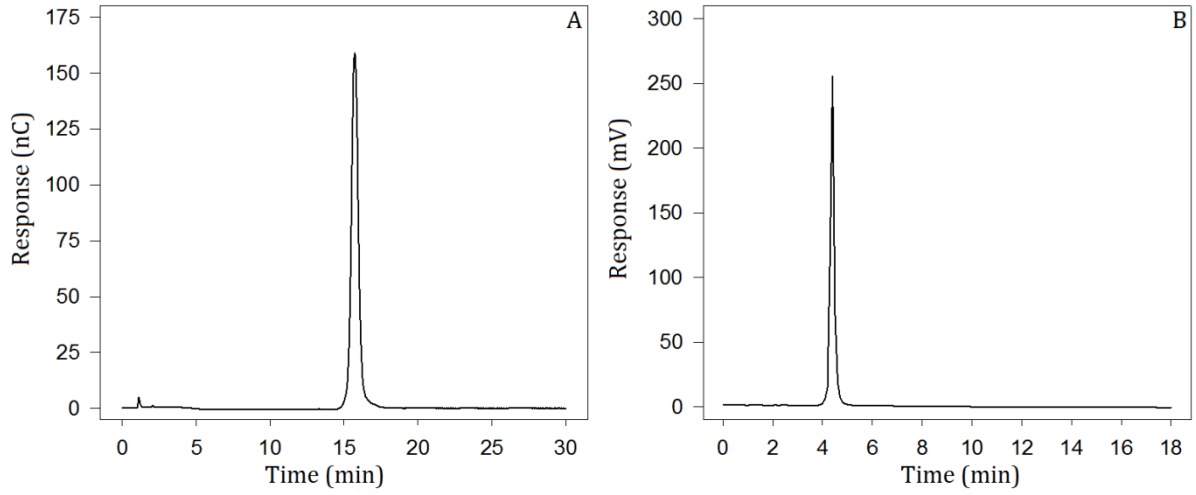

Figure 9.6 Purity of kojibiose crystals obtained by reacting 1.8 M sucrose with 0.2 M glucose, followed by cooling crystallization at Brix 48. The crystals were analyzed by HPAEC-PAD (A) and HPLC-RI (B). The small peak at 1 min in the HPAEC-PAD profile corresponds to the injection peak.

3.5 Proof of concept: production at 10 L scale

Finally, the scalability and industrial applicability of the developed process was illustrated by performing the synthesis of kojibiose at 10 L scale (Figure 9.7). As a result, roughly 3 kg of kojibiose with a purity exceeding 99.8 % was obtained, while crystallization of the supernatant resulted in approximately 1 kg of 99 % pure kojibiose. In contrast to the current production strategies for kojibiose, we thus developed a

sustainable, cost-effective and scalable biocatalytic process for the production of highly pure kojibiose. Moreover, the substrates sucrose and glucose are cheap and readily available bulk sugars.

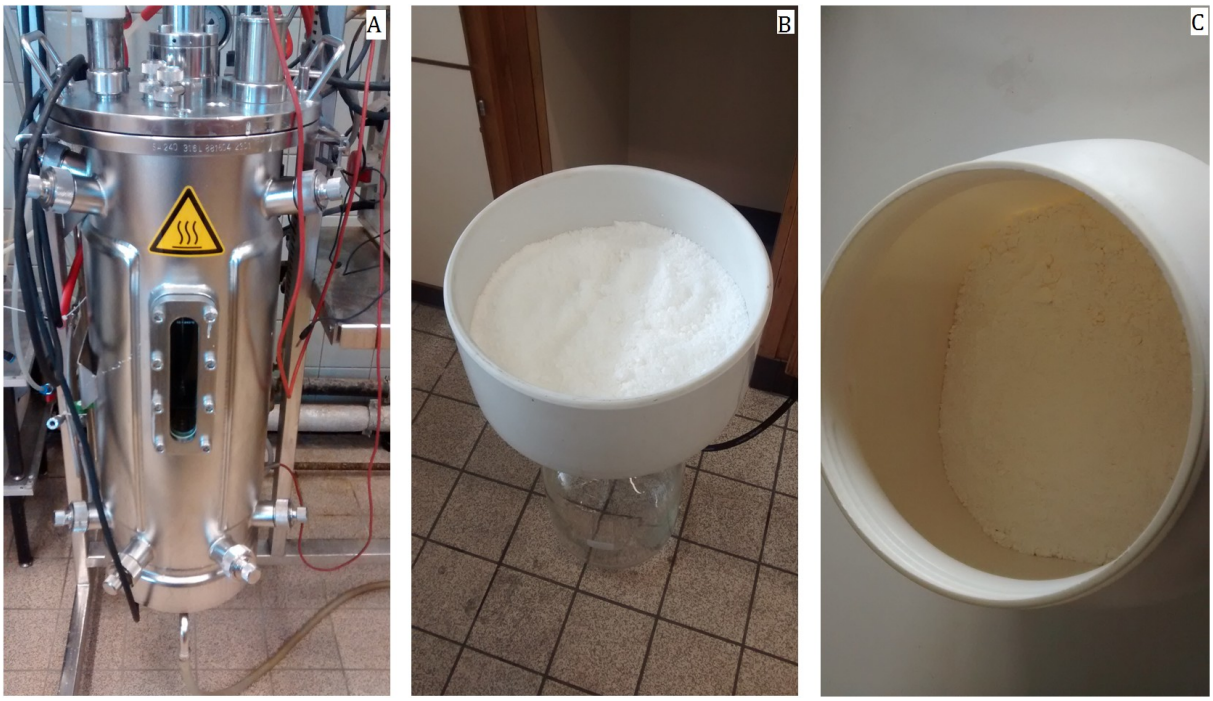

Figure 9.7 Large scale production of kojibiose. Synthesis of kojibiose in a 30 L reactor (A), washing and drying of the crystals (B), storage of 3 kg highly pure kojibiose (C).

4 CONCLUSION

Following the work on the synthesis of various α- (CHAPTER 2, 3 and 4) and β-glucosides (CHAPTER 5), this chapter illustrates the applicability of disaccharide phosphorylases for the synthesis of specialty carbohydrates. A variety of SP variants were evaluated under a broad range of process conditions, indentifying variant L341I_Q345S as the most promising biocatalyst. Indeed, an integrated approach, optimizing both reaction conditions and downstream processing at the same time quickly led to the synthesis and purification of kojibiose at concentrations exceeding 1.5 M. Moreover, the atom efficiency of the latter process was increased to an impressive 79 % through the use of glucose isomerase. The optimized process finally allowed the isolation of 3 kg crystalline kojibiose with a purity of 99.8 %. In conclusion, we developed a sustainable, cost-effective and scalable biocatalytic process for the production of highly pure kojibiose, starting from renewable, cheap and readily available bulk sugars.

5 MATERIALS & METHODS

5.1 Enzyme production, purification and quantification

The recombinant SP from *B. adolescentis*, the L341I, Q345S, L341IQ345S, L341I_Q345N, and L341I_Y344A_Q345N variant were routinely grown as described in CHAPTER 2. The obtained pellets were lysed in 2 mM MOPS buffer at pH 7.0 (CHAPTER 2), and partially purified by 15 min incubation at 58 °C, followed by centrifugation (18 000 g, 4 °C, 30 min). Alternatively, the *N*-terminal His_6-tagged proteins were purified by nickel-nitrilotriacetic acid metal affinity chromatography. The protocol as described by the supplier (Qiagen) was used, and the obtained enzyme solutions were washed with MOPS buffer (50 mM, pH 7.0) and concentrated using Centricons (Amicon Ultra 30K, Millipore). Protein concentrations were measured with the BCA Protein Assay kit (Pierce), using bovine serum albumin as standard. All assays were performed in triplicate and had a CV of less than 10 %.

5.2 Quantification of reaction products

The concentration of carbohydrates was followed by high performance anion exchange chromatography (HPAEC) (Dionex ICS-3000, Thermo Scientific), using a CarboPac PA20 pH-stable column and pulsed amperometric detection (PAD). Separation of sucrose, glucose, fructose, trehalose, kojibiose, nigerose, maltose, isomaltose, was achieved using a 30 min protocol. After 13 min of isocratic elution with 30 mM NaOH, the concentration was gradually increased to 100 mM in 5 min, kept constant for 3 min and decreased again to 30 mM within 1 min, followed by an equilibration period of 8 min. The temperature and flow rate were set at 30 °C and 0.5 mL/min respectively. Alternatively, the purity of the crystallised kojibiose was analyzed by HPLC using an Aminex HPX-87H column (Bio-Rad), equilibrated at 30°C. The eluent consisted of 5 mM H_2SO_4 in milliQ at a flow rate of 0.6 mL/min. Adequate detection was achieved with a refractive index detector. These measurements were used to calculate the following parameters, whereby $sucrose_0$ represents the initial sucrose concentration.

$$Selectivity\ (\%) = \frac{[kojibiose]}{[kojibiose] + [maltose] + [isomaltose]} * 100$$

$$Conversion\ (\%) = \left(1 - \frac{[sucrose]}{[sucrose]_0}\right) * 100$$

$$Yield\ (\%) = \frac{[kojibiose]}{[sucrose]_0} * 100$$

$$Hydrolysis\ (\%) = \frac{[fructose] - [kojibiose] - [maltose] - [isomaltose]}{[fructose]} * 100$$

$$Efficiency\ (\%) = \frac{[kojibiose]}{[fructose]} * 100$$

$$Productivity\ (\frac{g\ kojibiose}{g\ protein * h}) = \frac{[kojibiose\ (M)] * 342.3 \frac{g}{mol}}{\left[protein\ (\frac{g}{L})\right] * time\ (h)}$$

$$Atom\ Efficiency\ (\%) = \frac{mass\ of\ atoms_{desired\ product}}{mass\ of\ atoms_{reactants}} * 100$$

5.3 Stability assays

The kinetic thermostability of the wild type SP, the L341I, Q345S and L341I_Q345S variant was determined by diluting 0.5 mg/mL His-tag purified enzyme in a 50 mM MOPS buffer at pH 7.0. The mixtures were incubated in a water bath at 55 or 60 °C, and samples were placed on ice at regular intervals. Next, the samples were added to a substrate solution containing 500 mM sucrose and glucose dissolved in a 50 mM MOPS buffer at pH 7.0. The residual activity was determined by incubating the reaction mixtures at 55 °C, and following the kojibiose concentration using the HPAEC-PAD method described above. The t_{50}-values, which is the time required to reduce the initial enzymatic activity by 50 %, were calculated from the equations obtained by fitting the linear part of the stability curves.

5.4 Biocatalytic synthesis of kojibiose

The synthesis of kojibiose was performed by dissolving varying amounts of glucose and sucrose in milliQ water. Unless stated otherwise, 2 mg/mL of the heat purified SP variants was used, and the reaction mixtures were incubated at 55 °C. The pH of this buffer free system was set at 7.0, and remained constant throughout all conversions. If required, glucose isomerase (Sweetzyme® IT Extra, Novozymes) was added to 20 g/L after 2 h.

5.5 Purification of kojibiose

Prior to the yeast treatment, immobilized glucose isomerase was removed by filtration over a Whatman paper, and SP was inactivated by heating the solutions to 90 °C during 10 min. The purification of various reaction mixtures was then performed by adding 30 g/L spray dried baker's yeast (Algist Bruggeman) in 50 mL falcons with perforated lids. The reactions were incubated at 30 °C and 50 rpm on a thermoshaker (Eppendorf). Unless stated otherwise, no buffers were added, resulting in a gradual pH drop from 7.0 to roughly 5.0 at the end of the yeast treatment. Alternatively, the pH was kept constant at 7.0 or 5.0 throughout the fermentation by performing the yeast treatments in a 50 mM MOPS or sodium acetate buffer. Upon depletion of all contaminating carbohydrates, the yeast was removed by centrifugation (5 000 g, 4 °C, 15 min) using a Sorvall RC-6+ centrifuge (Thermo Scientific). Finally, the solution was filtered over a vacuum filtration system with a pore size of 0.22 µm (Corning) to remove any suspended solids.

5.6 Crystallization of kojibiose

Prior to the cooling crystallization, the kojibiose solutions were evaporated *in vacuo* to varying concentrations by means of a rotavapor (Büchi R-200). The temperature and pressure were set at 50 °C and 50 mbar respectively, while the kojibiose concentration, expressed as Brix (°Bx), was determined by a series of ATAGO hand refractometers. Next the samples were cooled overnight from 50 °C to room temperature, while shaking on a rotary shaker at 20 rpm. The samples were subsequently cooled to 4 °C over a period of 4 h, and crystal growth was allowed for another 24 h at 4 °C and 20 rpm. Next, the kojibiose crystals were isolated by filtration over a Whatman paper, washed with ethanol and dried to the air.

5.7 Properties of kojibiose crystals

The purity of the obtained kojibiose crystals was determined using HPAEC-PAD and HPLC-RI as described in section 5.2, while the microscopic appearance was evaluated using an Olympus CH30 microscope at 100x and 400x total magnification. The crystallization yield and whiteness of the crystals, expressed by the ICUMSA score were calculated as follows:

$$Crystallization\ Yield\ (\%) = \frac{mass\ of\ kojibiose\ crystals}{mass\ of\ kojibiose_{in\ solution\ before\ crystallization}} * 100$$

$$ICUMSA\ 420\ Carbohydrate\ Score = \frac{(Absorbance_{420nm}\ of\ carbohydrate\ solution * 1000)}{c * b}$$

with *c* the carbohydrate concentration (g/mL) and *b* the path length (cm).

5.8 Large scale production of kojibiose

Large scale production of kojibiose was performed by dissolving 6 kg sucrose and 350 g glucose to a total volume of 10 L in milliQ water. The mixture was supplemented with 1 mg/mL heat purified *B. adolescentis* L341I_Q345S SP, and incubated at 55 °C and 35 rpm in a 30 L Biostat C reactor (B. Braun Biotech). After 4 h, 200 g of prewashed Sweetzyme® IT Extra (Novozymes) was added, and the formation of kojibiose was continued during 4 days. Next, the immobilized glucose isomerase was conveniently removed by filtration over a fritted column with a hot water jacket at 55 °C. The obtained solution was then heated to 90 °C during 10 min, cooled to 30 °C, and supplemented with 300 g baker's yeast. Once all contaminating carbohydrates were removed, the yeast was separated by vacuum filtration over a Seitz® K series depth filter. The residue was then evaporated *in vacuo* at 50 °C to a Brix of 48, cooled overnight to room temperature, and subsequently incubated during 24 h at 4 °C and 20 rpm. The obtained crystals were washed with 2 L ethanol over a Seitz® K Series Depth Filter, and dried to the air.

6 SUPPLEMENTARY INFORMATION

Table S9.1 Performance of various SP variants for the synthesis of kojibiose. The reported parameters were calculated after 8 h incubation at 55 °C.

Enzyme	Sucrose (mM)	Glucose (mM)	Enzyme (mg/mL)	Selectivity (%)	Conversion (%)	Yield (%)	Hydrolysis (%)	Efficiency (%)	Productivity (g kojibiose/(g protein*h))
L341I	100	100	1	86.1	100.0	34.7	66.8	28.6	1.5
L341I	250	250	1	81.4	100.0	47.3	39.3	49.5	5.1
L341I	500	500	1	78.8	95.9	49.8	33.8	52.2	10.7
L341I	500	250	1	79.1	93.8	36.3	49.1	40.3	7.8
L341I	1000	1000	1	77.5	67.9	38.1	17.2	64.2	16.3
L341I	100	100	3	85.2	100.0	33.8	67.6	27.6	0.5
L341I	250	250	3	80.7	100.0	47.6	43.3	45.7	1.7
L341I	500	500	3	77.3	100.0	58.0	10.2	69.4	4.1
L341I	500	250	3	76.2	100.0	41.2	22.2	59.2	2.9
L341I	1000	1000	3	74.4	100.0	47.7	8.4	78.1	6.8
L341I_Q354S	100	100	1	98.7	99.7	63.1	64.0	35.6	2.7
L341I_Q354S	250	250	1	97.6	43.4	45.0	37.0	61.5	4.8
L341I_Q354S	500	500	1	96.8	31.4	36.5	24.7	72.9	7.8
L341I_Q354S	500	250	1	97.3	35.5	25.8	36.4	61.9	5.5
L341I_Q354S	1000	1000	1	96.2	47.1	29.0	13.5	83.2	12.4
L341I_Q354S	100	100	3	99.0	100.0	52.3	47.7	51.8	0.7
L341I_Q354S	250	250	3	97.6	99.9	68.0	31.7	66.7	2.4
L341I_Q354S	500	500	3	96.0	78.6	71.5	17.7	79.0	5.1

L341I_Q354S	500	250	3	96.1	69.3	63.0	29.1	68.1	4.5
L341I_Q354S	1000	1000	3	95.4	73.7	56.7	5.1	90.6	8.1
L341I_Q354N	100	100	2	100.0	61.5	25.4	43.4	56.6	0.5
L341I_Q354N	250	250	2	100.0	14.9	19.1	86.5	13.5	1.0
L341I_Q354N	500	500	2	97.5	19.2	17.2	4.1	90.0	1.8
L341I_Q354N	500	250	2	98.7	24.9	13.0	43.0	56.3	1.4
L341I_Q354N	1000	1000	2	96.6	42.7	16.5	22.4	75.0	3.5
L341I_Q354N	100	100	4	100.0	85.3	34.7	48.2	51.8	0.4
L341I_Q354N	250	250	4	99.4	37.0	28.5	40.3	59.3	0.8
L341I_Q354N	500	500	4	98.0	34.2	24.0	28.9	69.7	1.3
L341I_Q354N	500	250	4	97.7	29.8	21.7	39.2	59.4	1.2
L341I_Q354N	1000	1000	4	95.5	37.4	34.2	12.0	84.0	3.7
L341I_Y344A_Q354N	100	100	4	100.0	39.3	11.4	40.9	59.1	0.1
L341I_Y344A_Q354N	250	250	4	100.0	13.9	7.4	24.7	75.3	0.2
L341I_Y344A_Q354N	500	500	4	100.0	14.7	8.7	12.3	91.2	0.5
L341I_Y344A_Q354N	500	250	4	100.0	17.1	6.4	23.2	76.8	0.3
L341I_Y344A_Q354N	1000	1000	4	100.0	59.4	3.1	22.1	77.9	0.3

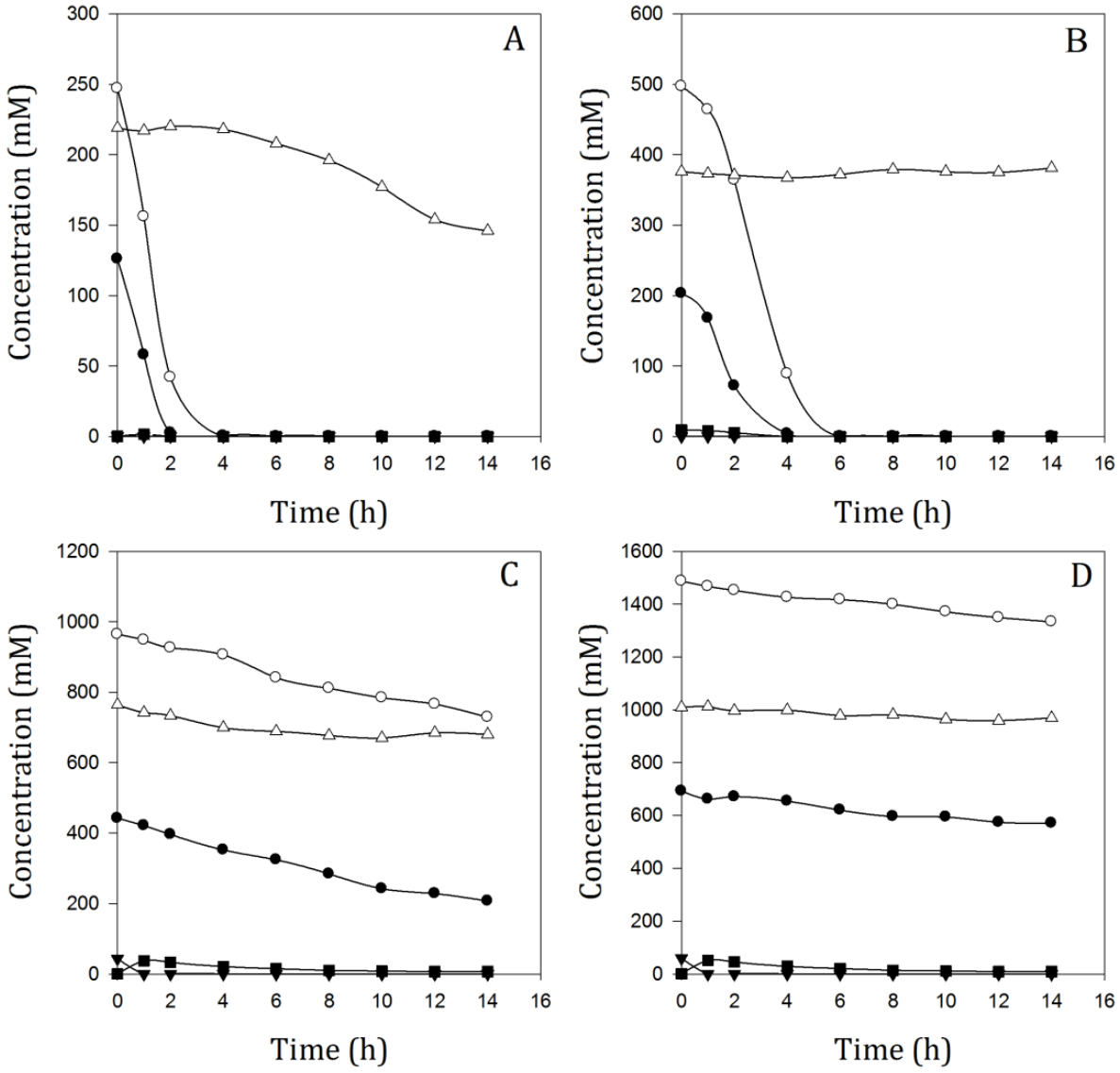

Figure S9.1 Yeast treatment of reaction mixtures obtained by converting 0.25 (A), 0.5 (B), 1 (C) and 1.5 (D) M sucrose and glucose to equilibrium. Baker's yeast was added to 30 g/L, and the reactions were incubated at 30 °C and pH 5. The concentration of glucose (●), fructose (○), sucrose (▼), kojibiose (△) and maltose (■) were followed in time.

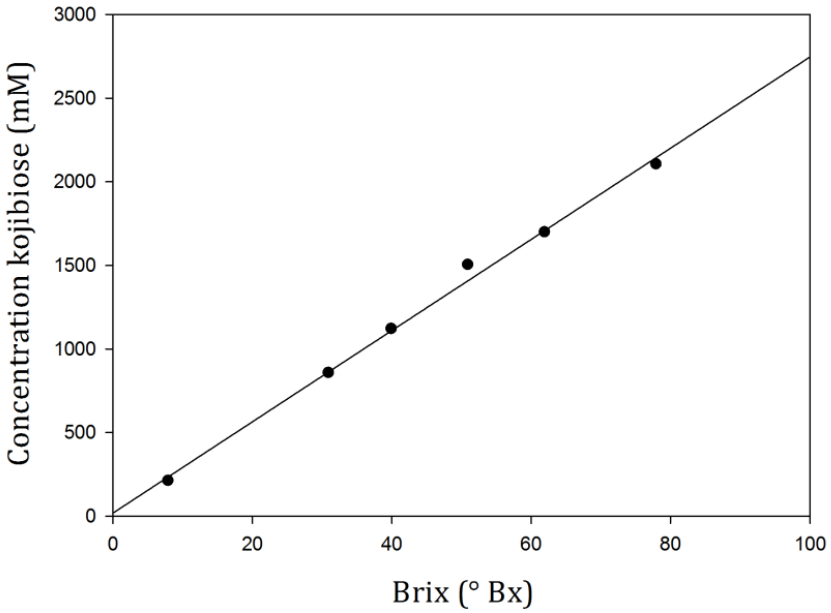

Figure S9.2 Relation between the Brix (° Bx) and kojibiose concentration (mM).

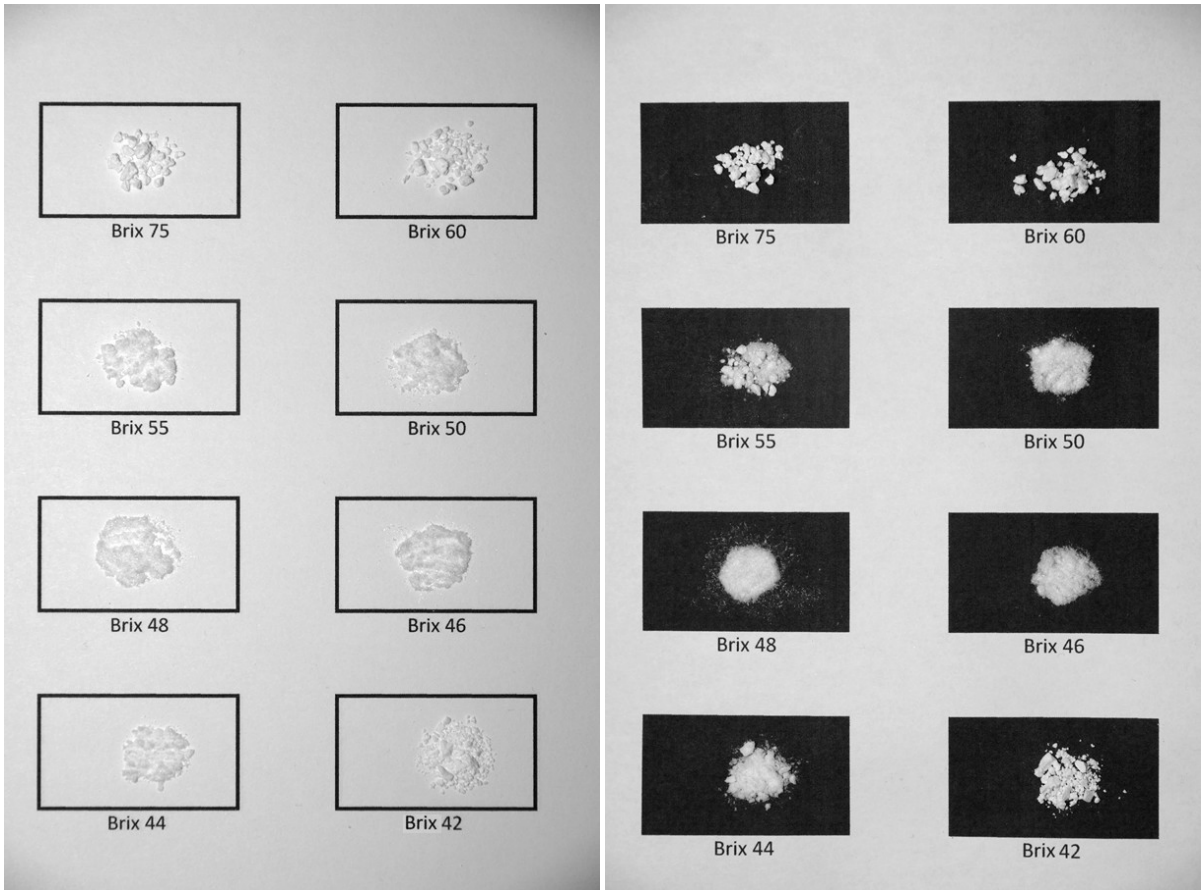

Figure S9.3 Appearance of kojibiose crystals obtained by cooling crystallization at various kojibiose concentrations.

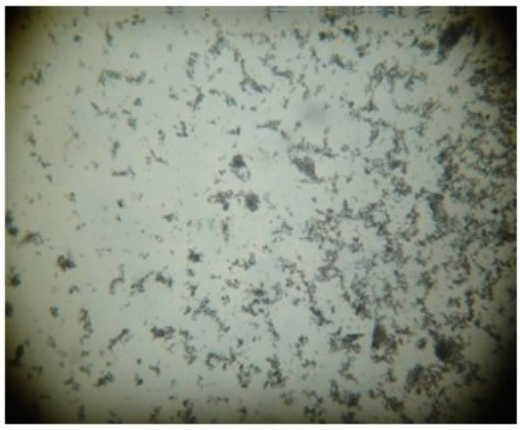

Brix 75 (100x)

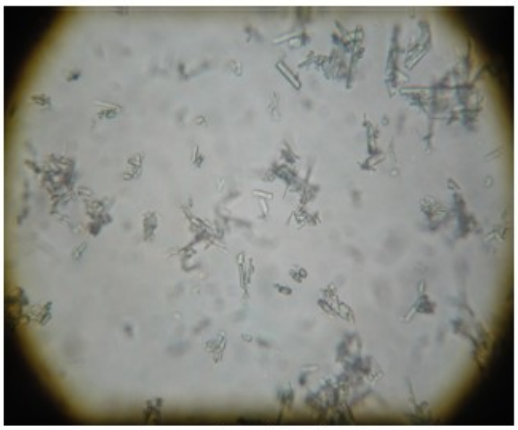

Brix 75 (400x)

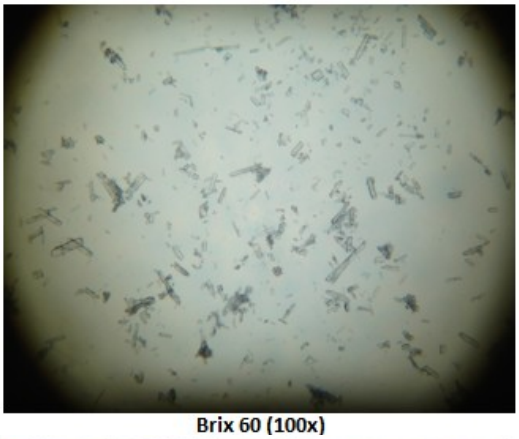

Brix 60 (100x)

Brix 60 (400x)

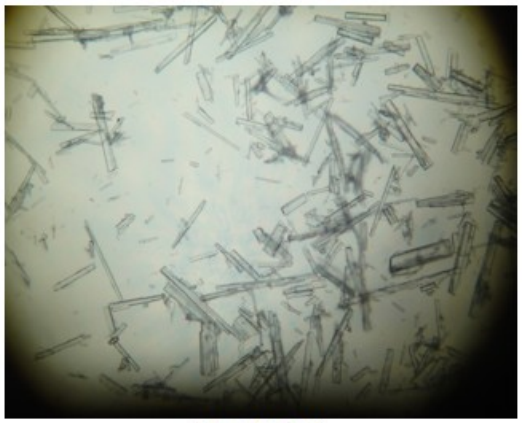

Brix 55 (100x)

Brix 55 (400x)

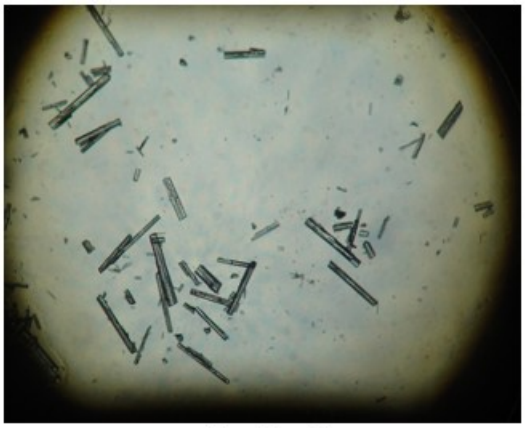

Brix 50 (100x)

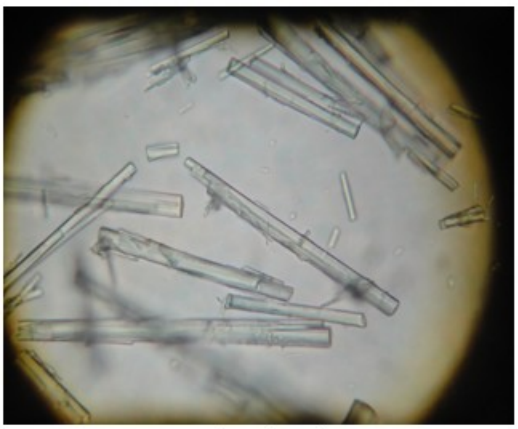

Brix 50 (400x)

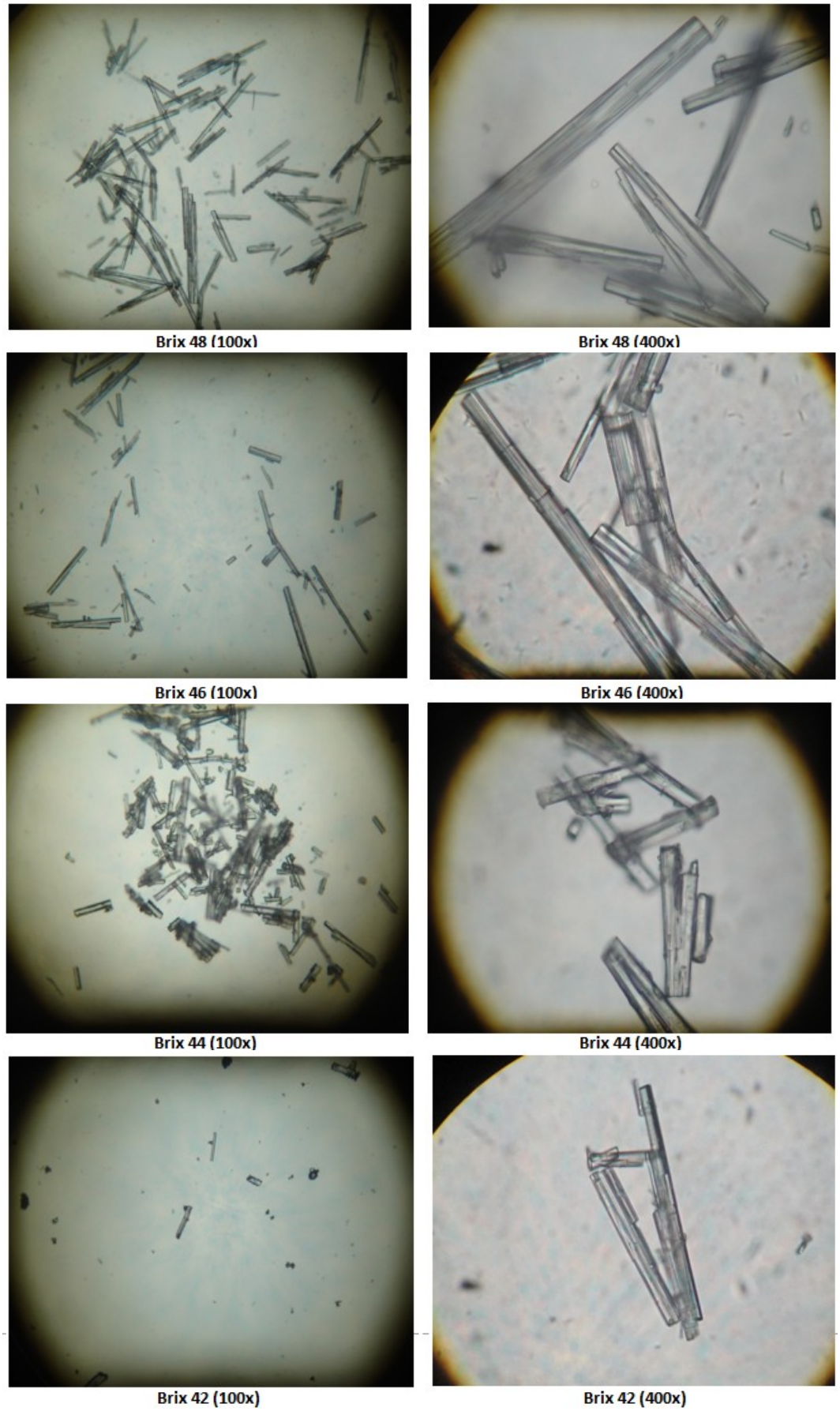

Figure S9.4 Microscopic appearance of kojibiose crystals obtained by cooling crystallization at various kojibiose concentrations.

General discussion and future perspectives

During this PhD thesis, numerous technologies, resulting in the synthesis and isolation of various glycosides, were developed. An overview of the most frequently used enzymes, substrates and techniques is shown in Figure D.1, which might be helpful to follow the discussion below. Remarkably, the technologies developed during this research allow the production of α-glucosides, β-glucosides, α-cellobiosides, β-cellobiosides and kojibiose, requiring only the cheap and readily available sucrose as carbohydrate source.

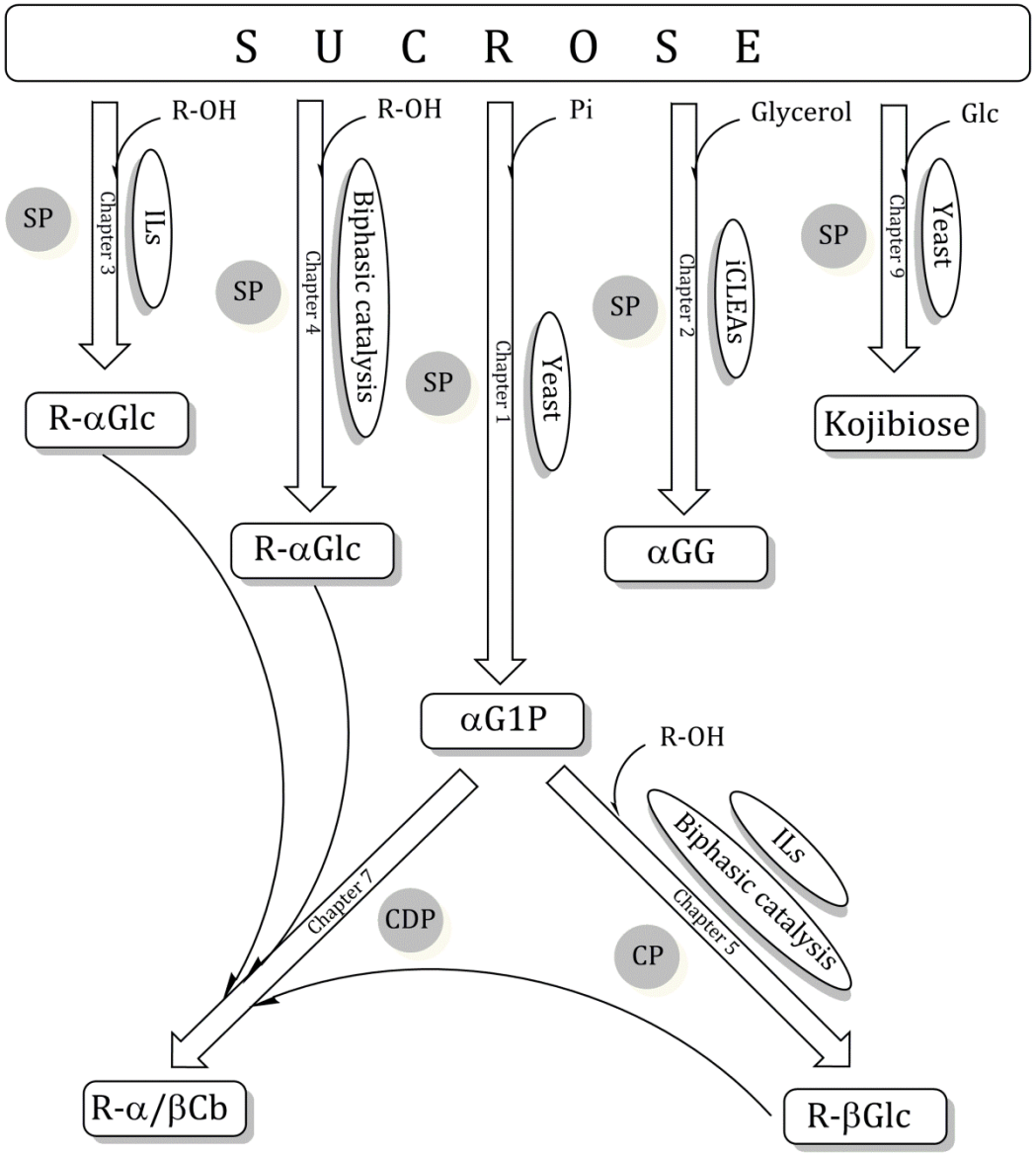

Figure D.1 Schematic overview of the glycosylation reactions performed with glycoside phosphorylases during this research. Abbreviations: R-OH, acceptor; Pi, inorganic phosphate; SP, sucrose phosphorylase; CP, cellobiose phosphorylase; CDP, cellodextrin phosphorylase; ILs, ionic liquids; iCLEAs, imprinted cross-linked enzyme aggregates; Yeast, yeast treatment with *Saccharomyces cerevisiae*; αG1P, α-D-glucose 1-phosphate ; Glc, glucose; Cb, cellobioiside and αGG, α-glucosyl glycerol.

1 SUGARY PHOSPHATES

Glycosyl phosphates are efficient glycosyl donors for both chemical and enzymatic glycosylation reactions[47]. Indeed, α-D-glucose 1-phosphate (αG1P) is the preferred donor for many glycoside phosphorylases, including cellobiose phosphorylase (CP) and cellodextrin phosphorylase (CDP). Although these 'sugary phosphates' can be chemically synthesized, the required procedures suffer from low yields, a lack of anomeric selectivity, and the generation or large quantities of toxic waste[50]. Biocatalytic synthesis through the action of kinases on the other hand, requires ATP as phosphate donor. Interestingly, glycoside phosphorylases require only cheap inorganic phosphate and a di- or oligosaccharide for the synthesis of various glycosyl phosphates.

The latter concept has been repeatedly applied for the synthesis of αG1P from sucrose and inorganic phosphate with sucrose phosphorylase (SP) immobilized on corn stover[64], diethylaminoethyl cellulose[65], and Eupergit C[52]. Despite these endeavors, the industrial applicability is hampered by the limited operational temperature of 30 or 37 °C. Indeed, the combination of such temperatures and the presence of carbohydrates will inevitably give rise to microbial contamination. In contrast, the production process for αG1P described in CHAPTER 1 was continuously performed at 60 °C during 2 weeks. The use of this elevated temperature was facilitated by choosing a thermostable SP, and further improving its stability by multipoint covalent immobilization[44].

Moreover, combining heat purification with immobilization on Sepabeads EC-HFA, allowed the synthesis of αG1P up to 179 g/L/h. Consequently, one would be capable of producing 4 tons of αG1P on a daily basis, by immobilizing the SP obtained from a 320 L fermentation on 1 m^3 of Sepabeads EC-HFA. As a result, the limited availability of αG1P has been clearly overcome, allowing its use as glucosyl donor at the industrial scale. Although the synthesis of β-D-glucose 1-phosphate and α-D-galactose 1-phosphate have been described using the trehalose phosphorylase from *Thermoanaerobacter brockii*[53] and a tailor made lactose phosphorylase[54] respectively, both production processes could most likely be enhanced by immobilizing the enzymes on Sepabeads. Indeed, the latter modification would allow continuous operation in a packed bed reactor, while boosting the thermostability.

2 SWEET STABILIZATION

Stabilization of proteins by polyols and carbohydrates is a well known phenomenon. Sucrose, for example, can stabilize the native state of proteins against both chemical denaturants and temperature[265]. Studies on the protein-buffer interaction revealed that sucrose is preferentially excluded from the protein domain, thereby increasing the free energy of the system. Thermodynamically this results in protein stabilization, as the unfolded state of the protein becomes thermodynamically even less favorable in the presence of sucrose[266].

The results obtained during this research indicate that the latter stabilization also applies to SP. Indeed, the addition of sucrose to concentrations exceeding 0.2 M was found to inhibit *tert*-butyl alcohol mediated precipitation of SP (CHAPTER 2). Moreover, the addition of sucrose resulted in a 25-fold increased half-life when SP was dissolved in 20 % DMSO or AMMOENG 101. Comparable results, obtained with the well-known protectant trehalose[117], indicate that the observed stabilization originates from non-specific interactions at the protein surface (CHAPTER 3). CHAPTER 4, on its turn, revealed the necessity of high sucrose concentrations to obtain proper glucosylation in biphasic reaction systems. Interestingly, this stabilization also applies to immobilized SP variants. While previous research already showed that sucrose increases the yield of multipoint covalent immobilization[44], the results obtained in CHAPTER 1 with SP Sepabeads clearly show its stabilizing effect on SP Sepabeads. Immobilized SP is known to lose roughly 25 % of its activity after 16 h incubation at 60 °C. Nevertheless, we found that the activity of SP Sepabeads in the presence of sucrose, remained constant up to extended reaction times of 2 weeks.

In addition, the presence of sucrose was found to also boost the solubility of hydrophobic compounds such as quercetin and resveratrol (CHAPTER 3). Interestingly, sucrose is the preferred donor substrate of SP. Therefore, all these effects can be considered additional benefits, as sucrose has to be added as substrate, regardless of its stabilizing and solubilizing properties. The addition of sucrose or trehalose might also be applied to stabilize other glycoside phosphorylases. However, depending on the intended reaction, the use of these additional disaccharides might complicate product isolation.

3 BAKERS' YEAST: A POWERFUL CLEAN-UP TOOL?

Saccharomyces cerevisiae, or bakers' yeast, is known to metabolize a variety of carbohydrates, including the monosaccharides D-glucose, D-fructose, D-mannose and D-galactose, as well as disaccharides such as maltose and sucrose. Other carbohydrates like D-xylose, lactose and cellobiose, are largely resistant; allowing the use of baker's yeast to purify these compounds[262]. Indeed, the non-resistant monosaccharides enter the anaerobic glycolysis, resulting in the formation of pyruvic acid. The latter is then decarboxylated, thereby liberating CO_2 and acetaldehyde, which is on its turn reduced to ethanol. The formed CO_2 and ethanol can be conveniently removed by simple evaporation. Consequently, the use of a microorganism can be considered an environmentally friendly alternative compared to chromatography.

During this research, baker's yeast was applied to purify a variety of compounds. In CHAPTER 1, *S. cerevisiae* was successfully used to purify αG1P from a reaction mixture that also contained sucrose, phosphate, fructose and traces of glucose. The extracellular invertase was found to quickly hydrolyze sucrose, after which glucose and fructose were sequentially metabolized. The latter strategy allowed the isolation of large quantities of crystalline αG1P, thereby avoiding the use of labor intensive chromatography steps. Also kojibiose was found to be largely resistant to baker's yeast, while all other carbohydrates present in the reaction mixture were metabolized by *S. cerevisiae* (CHAPTER 9). Although these conversions are typically performed at moderate carbohydrate concentrations[259, 263], the presence of 1 M kojibiose (on top of a combined total of roughly 150 g/L fructose and glucose) did not significantly influence the performance of *S. cerevisiae*.

The latter surprising observation illustrates that one should, however, always carefully evaluate the suitability of treatment with baker's yeast. Indeed, the complexity of the yeast metabolism is hidden behind this seemingly straightforward operation. Methyl gallyl 4-*O*-α-D-glucopyranoside, as produced in CHAPTER 4, was readily metabolized by *S. cerevisiae*, while the glucosides of quercetin were largely resistant[267]. Moreover, *S. cerevisiae* is known to produce metabolites (mainly glycerol and/or organic acids), which might hamper crystallization of the desired products[259]. All in all, treatment with baker's yeast can be considered a valuable alternative to remove common mono- and

disaccharides during the enzymatic preparation of carbohydrates or glycosides. Nevertheless, the latter purification strategy should be carefully evaluated for each application, thereby monitoring the concentration of all compounds, and assessing the formation of stress metabolites.

4 IMPRINTING AND CROSS-LINKING: A HAPPY MARRIAGE

Molecular imprinting is an attractive alternative to mutagenesis for changing the specificity of biocatalysts[82]. Indeed, modification of the three-dimensional structure of proteins by noncovalent interactions with an imprinting molecule, has been vastly reported[83]. In order to achieve these effects, the enzymes are typically contacted with an imprinting molecule under mild denaturing conditions. Unfortunately, imprinted enzymes are only able to maintain their new conformation when transferred to a non-aqueous environment or when immobilized by cross-linking. Although the latter strategy was successfully applied for the creation of a galactose oxidase from a glucose oxidase, a complex radical polymerization procedure, requiring transfer to organic solvents and derivatization of the enzyme was required[88].

In CHAPTER 2, a molecular imprinting technique using glutaraldehyde mediated cross-linking, instead of radical polymerization in pure organic solvents, was developed. This procedure can be performed in an aqueous environment and gives rise to a new enzyme formulation called imprinted cross-linked enzyme aggregate (iCLEA). Proof of concept was delivered by imprinting SP with α-glucosyl glycerol. As a consequence, the enzyme's specific activity towards glycerol was increased two-fold while simultaneously providing an exceptional stability at 60 °C. The applicability of the latter technique for the synthesis of octyl β-D-glucopyranoside with CP, was evaluated in CHAPTER 5. Interestingly, imprinting with octyl β-D-glucopyranoside did not significantly increase the transglycosylation activity of the enzyme. However, the addition of octanol roughly doubled the rate of octyl β-D-glucopyranoside synthesis, while the activity of the iCLEA towards glucose was decreased by 45 %. In contrast to imprinting SP (CHAPTER 2), the acceptor molecule rather than the glucoside was found to enhance the desired glycosylation activity of CP. The latter difference may be explained by the reaction mechanism of both enzymes. Indeed, while SP is a retaining phosphorylase using a

double displacement mechanism, CP is an inverting phosphorylase following a single displacement mechanism.

The results obtained in CHAPTER 2 and 5 indentified the newly developed iCLEA technology as a valuable tool for enzyme engineering. The latter strategy allows to simultaneously boost the specificity and stability of biocatalysts; two common targets of enzyme engineering experiments. The availability of the desired product as imprinting molecule can be considered the main disadvantage. Moreover, certain compounds, such as sucrose, were found to inhibit precipitation of enzymes, while some affinity between the enzyme and imprinting molecule is generally required. Although iCLEAs can be conveniently recycled, they are unfortunately not suited for operation in packed-bed columns. Nevertheless, the potential of iCLEAs reaches far beyond phosphorylases, and could find widespread application in the field of enzyme engineering.

5 IONIC LIQUIDS: THE GREEN ALTERNATIVE?

Although disaccharide phosphorylases have received increasing attention as promising biocatalysts for glycoside synthesis, these enzymes typically have a very low affinity for non-carbohydrate acceptors. For hydrophobic acceptors, concentrations compensating for the high K_m values are not readily achieved in aqueous solutions. Enzymatic glycosylation of these compounds is, therefore, commonly performed in the presence of organic cosolvents, such as DMSO or methanol. However, these solvents are not compatible with numerous applications of carbohydrate-derived products, while their presence often leads to the partial inactivation biocatalysts. Ionic liquids (ILs), in contrast, have emerged recently as a new class of solvents for biocatalytic applications. These 'green' solvents consist of salts with a low melting point (<100 °C), possess no vapor pressure and are consequentially inflammable. Their ability to dissolve both polar and hydrophobic substrates has already been exploited in glycosylation reactions. Nevertheless, the use of ILs as cosolvents for glycoside phosphorylases hasn't been considered to date.

In CHAPTER 3, the ability of a range of ILs to dissolve medium- and long-chain alcohols, flavonoids, alkaloids, phenolics and terpenes, was scrutinized. The addition of 20 % ILs resulted in a remarkable increase in solubility, without affecting the ability to dissolve

1 M sucrose. Interestingly, both [EMIM][dca] and AMMOENG 101 proved to have better dissolving properties than DMSO. In contrast to [EMIM][dca], the IL AMMOENG 101 was found to be also much less deleterious to the stability of SP than for example DMSO or methanol. Consequently, the use of the IL AMMOENG 101 enabled the synthesis of complex glucosides, including 3-*O*-α-D-glucopyranosyl (*E*)-resveratrol. Similar results were obtained in CHAPTER 5 for CP. Indeed, whereas common organic cosolvents and the ILs BMIM][dca], [BMIM][I] and [BMIM][BF_4] were found to destabilize CP, the IL AMMOENG 101 was found to efficiently balance acceptor solubility and enzyme stability. The α-L-rhamnosidase originating from *Aspergillus terreus*, on the other hand, was found to be incompatible with most ILs. Although glycosylation was observed in the presence of the IL AMMOENG 101, the enzyme performed much better in the presence of DMSO, polyethylene glycol or acetone (CHAPTER 6).

The results obtained during this research confirmed the compatibility of ILs with enzymatic glycosylation reactions. In particular, the IL AMMOENG 101 was identified as a powerful tool for glycosylation reactions with disaccharide phosphorylases. Moreover, the latter IL could find widespread application to dissolve various chemicals, from rather hydrophilic to very hydrophobic, regardless of their type. Nevertheless, the stability and activity of the applied biocatalysts should be carefully monitored upon the addition of ILs. Unfortunately, product isolation can also be hampered by the presence of these salts, as they often cannot be removed by simple evaporation. Although the recuperation of ILs through extraction with organic solvents, adsorption and membrane-based processes has been described, the recovery of these compounds remains a challenge to date[268]. Indeed, some successful examples of the adsorption of ILs onto solid supports such as activated carbon[269], silica[270], aluminum oxide[271] and cation exchange resins[272] exist. However, the availability of adsorption/desorption data and the requirement of complex chromatography equipment, limits the applicability of the latter methods to date. Nanofiltration, on the other hand, has been used to separate the IL [BMIM][BF_4] from a mixture containing bromophenol blue and lactose. After three filtration steps, 93 % of the IL passed through a Desal DVA 00 membrane, while 7 % remained in the lactose containing solution[273]. Nevertheless, the recovery efficiency depends on the target IL and the type and concentration of contaminants present[268]. Also here, insufficient knowledge and research limits the application of membrane based

process for the recuperation of ILs. In conclusion, the use of ILs should be considered 'a' green alternative, rather than 'the' green alternative.

6 BIPHASIC CATALYSIS: BACK TO THE FUTURE

Besides the addition of cosolvents, the application of liquid-liquid biphasic systems containing water and a water-immiscible organic solvent, was also considered to counter the low affinity of glycoside phosphorylases towards alternative substrates. The aqueous phase typically contains the biocatalysts and carbohydrates, while hydrophobic substrates are dissolved in the organic phase. Stirring or shaking will transfer these substrates from the organic to the aqueous phase, where they can be converted by the enzymes. Improved enzyme stability and ease of product recovery, while simultaneously avoiding substrate and product inhibition, are among the major advantages of biphasic catalysis. Consequently, the latter technique has been used for decades[130], enabling the synthesis of various oligosaccharides[131] and glycosides[132, 133]. Nevertheless, no reports on the use of biphasic catalysis for the synthesis of glycosides with disaccharide phosphorylases are available to date.

Therefore, the synthesis of glycosides with the SP from *B. adolescentis* was evaluated in the presence of a variety of water-immiscible solvents (CHAPTER 4). Although glycosylation was observed using butyl acetate, methyl-*tert*-butylether, octane, diethyl ether, cyclohexene and pentane, ethyl acetate (EtOAc) displayed superior characteristics. Indeed, the ethyl ester of acetic acid was found to dissolve a broad range of acceptor compounds, while being less deleterious to the stability and activity of SP compared to the other solvents. Careful optimization resulted in the following optimal reaction conditions: 62.5 % aqueous MOPS buffer at pH 7.5 containing 2 M sucrose and 50 U/mL SP, and 37.5 % EtOAc supplemented with 100 mg/mL acceptor. The latter system allowed the glucosylation of aliphatic alcohols, monoterpenoids, aromatic alcohols and phenolics, as well as a range of antioxidants (CHAPTER 8). Moreover, biphasic catalysis was found to outperform the previously described synthesis of 2-*O*-α-D-glucopyranosyl pyrogallol with the IL AMMOENG 101. Indeed, the yield of the cosolvent system reached only 17.4 %, while roughly 60 % of the initial pyrogallol could be converted when using a biphasic system. Surprisingly, this difference was caused by the higher transfer/hydrolysis ratio when using biphasic catalysis. Consequently, less

hydrolysis, which ultimately leads to the formation of glucobioses, and thus a lower yield, occurs.

Biphasic catalysis was also found to be compatible with the CP mediated synthesis of β-glucosides (CHAPTER 5). However, in contrast to SP, the transfer/hydrolysis ratio of CP was not influenced by the choice for cosolvent or biphasic catalysis. Increasing the amount of EtOAc from 20 to 37.5 % did not significantly influence the stability of CP, while CLEAs and iCLEAs were found to be suitable catalysts for biphasic glycosylation reactions. Apart from glucosides, also the synthesis and isolation of a broad range of α-L-rhamnosides was facilitated through biphasic catalysis (CHAPTER 6). Despite being developed decades ago, the use of biphasic catalysis should still be considered a valuable tool when designing challenging enzymatic glycosylation reactions.

7 FLAVORS AND FRAGRANCES

Various food-processing operations, ranging from premature harvesting to extended storage and physical treatments, may cause a loss of aroma, calling for subsequent supplementation with flavors and fragrances[274]. Moreover, the demand for these olfactory compounds in the cosmetics and toiletries market increases rapidly. Consequently, the ever expanding flavor and fragrance market is forecast to annually increase by 4.4 %, reaching an astonishing US$26.5 billion in 2016[275]. The beginning of the modern flavor industry was marked by the isolation, identification, and synthesis of vanillin in 1874[276]. Ever since, many flavors and fragrances haves been produced by chemical synthesis or extraction from plants[277]. However, the steadily increasing market forced suppliers to search for alternative sources, including biotechnological processes[278, 279]. According to US and European food legislations, natural flavor substances can only be prepared either by physical processes (extraction from natural sources) or by enzymatic or microbial processes. The latter classification further increased the interest for biotechnological solutions, as compounds labeled 'natural' are more profitable compared to the less appreciated 'nature-identical' ones[280].

Glycosylation is known to result in a modified perception of flavors and fragrances. The coupling of a glucose moiety to L-menthol for example, results in its delayed release, eventually giving rise to a prolonged sensation of freshness[12]. However, the evaluation

of such glycosides is typically hampered by their limited availability. Therefore, the ability of glycoside phosphorylases to glucosylate compounds with olfactory properties was thoroughly evaluated. The use of SP allowed the α-glucosylation of the monoterpenoids geraniol and β-citronellol, aromatic alcohols such as benzyl alcohol, anisyl alcohol, cinnamyl alcohol and vanillyl alcohol, as well as the phenylpropanoid eugenol and vanillin (CHAPTER 4). Similar results were obtained with CP, resulting in the β-glucosides of geraniol, β-citronellol, anisyl alcohol, cinnamyl alcohol, 2-phenylethanol and vanillin (CHAPTER 5). In addition, a variety of rhamnosides with olfactory properties including anisyl α-L-rhamnopyranoside, 2-phenylethyl α-L-rhamnopyranoside and cinnamyl α-L-rhamnopyranoside were obtained in CHAPTER 6.

In conclusion, the application of glycoside phosphorylases and the α-L-rhamnosidase from *A. terreus*, allowed the modification of various flavors and fragrances. The created library forms an ideal basis to study the effect of glycosylation on such compounds in detail. Indeed, the use of different enzymes resulted in both α and β-glucosides, as well as α-L-rhamnosides. The latter achievements should allow the mandatory research to evaluate their applicability at the industrial scale.

8 ANTIOXIDANTS: GLYCOSYLATION AND CHARACTERIZATION

Antioxidants find widespread application in the rubber, plastics, cosmetics, health care and food packaging industries. These compounds are also commonly added to foods, mainly to avoid oxidation of fats and proteins, which quickly leads to the undesirable formation of aldehydes, ketones and organic acids. According to Transparency Market Research, the global antioxidants market will annually grow by 5.6 %, thereby expanding from US$2,1 billion in 2013 to roughly US$3,1 billion in 2020[281]. As a result, the quest for antioxidants with altered properties continues to date. Many chemical modifications of both natural and synthetic antioxidants have been described, including coupling to a carbohydrate moiety[220]. Indeed, the latter modification is of particular interest to improve the solubility of flavonoids, enhance the stability of labile compounds, and modulate the uptake of for example quercetin in the small intestine[223].

The results obtained in CHAPTER 4, 5 and 7 illustrated the potential of respectively SP, CP and CDP for the enzymatic glycosylation of antioxidants. Therefore, these enzymes, and

a recently reported mutant of the *Thermoanaerobacterium thermosaccharolyticum* SP (TtSPP), were used to synthesize an antioxidant library with an extended structural diversity (CHAPTER 8). The aglycons were varied from simple phenols, over a series of gallate esters, to complex polyphenols such as resveratrol, quercetin and catechin. Moreover, the use of different enzymes allowed the isolation of multiple regio-isomers, anomers, as well as a range of α and β-cellobiosides and cellotriosides.

The application potential of the obtained glycosides was subsequently assessed by determining their solubility, stability and radical scavenging abilities. Glucosylation was found to significantly improve the solubility of numerous antioxidants, while α-glucosides could generally be dissolved to higher concentrations compared to their β-linked counterparts. Although the coupling of additional β-(1,4)-linked glucose moieties was found to decrease solubility, all cellobiosides and cellotriosides could be dissolved to higher concentrations than their respective aglycons. In contrast to the solubility, the stability of all glycosides increased significantly, regardless their anomeric configuration. The glycosylation position, on the other hand, significantly affected the stability of the glucosylated antioxidants, while cellobiosides are generally more stable compared to glucosides.

Moreover, the point of attachment, the anomeric configuration, and the glycosidic chain length were all found to influence the scavenging abilities of these glycosides. Despite decreased activities, most glycosylated compounds were identified as potent antioxidants, exhibiting lower EC_{50} values than the commonly used BHT. All together, the use of glycoside phosphorylases allowed the creation of a vast library of new antioxidants. Depending on the desired properties, α-glucosylation should be applied to maximize solubility, while the synthesis of cellobiosides and cellotriosides increased the stability to the largest extent. However, different methods to determine the antioxidant capacity are based on different strategies, often yielding other conclusions. Alkyl gallyl 3-glucosides, for example, were found to be better DPPH scavengers than the corresponding 4-glucosides, while the opposite was observed for ABTS radicals (CHAPTER 8). The antioxidant capacity indexes obtained by these chemical assays should, therefore, not be extrapolated to *in vivo* performance. Indeed, antioxidant action is not limited to scavenging of free radicals (which are certainly not DPPH or ABTS radicals),

but also includes upregulation of antioxidant and detoxifying enzymes, modulation of redox cell signaling and gene expression[282]. Consequently, subjecting the antioxidant library to cellular assays, such as the cellular antioxidant activity assay[283], might help to further grasp the true potential of these novel compounds.

9 KOJIBIOSE: A SWEET STORY

Over the past decade, the increasing consumer awareness regarding the intimate relation between the gut microbiome and our physiology, has driven the market for prebiotics. Global sales of these carbohydrates, which selectively stimulate the growth of beneficial bacterial populations in the human intestinal tract, are predicted to grow from US$11.16 billion in 2012 to a staggering US$15.90 billion in 2019[284]. Although the use of inulin, trans-galacto-oligosaccharides, resistant starches and mannan oligosaccharides was established in recent years, the current menu of prebiotics is rather limited. Expanding the range of prebiotics is therefore highly desirable. Unfortunately, in depth studies on the health-promoting properties of novel compounds is often hampered by their high price and limited availability. In that respect, kojibiose is a prime example. Preliminary studies indicated that kojibiose and its derived oligosaccharides can selectively stimulate beneficial gut populations. Besides its prebiotic properties, kojibiose is not metabolized by common oral bacteria and has therefore also attracted attention as a low-calorie sweetener for the prevention of tooth decay[243]. Nevertheless, its high price and limited availability (164 euro for 1 mg[285]) aren't in line with the requirements for prebiotics.

Recently, a number of SP variants with improved selectivity towards the synthesis of kojibiose were reported[43]. Evaluation of these mutants under a broad range of process conditions, indentified variant L341I_Q345S as the most promising biocatalyst (CHAPTER 9). Careful optimization quickly allowed the synthesis and isolation of kojibiose up to 350 mM. The use of glucose isomerase, while simultaneously evaluating the synthesis and purification of kojibiose, eventually paved the way to an intensified process. Indeed, kojibiose could be synthesized to concentrations in excess of 1.5 M, while the atom efficiency was boosted to an impressive 79 %. The reaction mixture was subsequently purified by treatment with bakers' yeast, after which kojibiose crystals with a purity exceeding 99.8 % were obtained. Scaling the reaction to 10 L yielded

roughly 3 kg of pure kojibiose, indicating the industrial applicability of the latter process. Moreover, the substrates sucrose and glucose are cheap and readily available bulk sugars.

In conclusion, the combination of both enzyme and process engineering enabled the efficient conversion of sucrose and glucose to the valuable kojibiose. Large quantities of kojibiose are now available, which can be used to further evaluate its true application potential. Apart from determining the sweetness of kojibiose, additional tests to evaluate its prebiotic properties should be conducted. Such experiments should certainly include monitoring the microbial community and its metabolic activity in different colon compartments using a human intestinal microbial ecosystem (SHIME)[286], and digestive tests to evaluate the stability of kojibiose prior to its arrival in the colon[287]. In addition, kojibiose has been described to inhibit α-glucosidase I[244], which could limit the digestion of dietary carbohydrates. The latter could be studied in detail by performing digestive experiments on a mixture of dietary carbohydrates in the presence and absence of various amounts of kojibiose.

10 FUTURE PERSPECTIVES

Over the past decade, many efforts in the field of enzyme engineering, aimed to expand the application potential of glycoside phosphorylases, have been described. During this research, also process engineering was identified a valuable tool to improve the performance of these enzymes. However, as illustrated in CHAPTER 7 and 9, combining both strategies is most likely the shortest road to success. Rather than exploring the use of cosolvents, biphasic catalysis, and the isolation of the desired product after extended enzyme engineering efforts, both approaches should be developed simultaneously. The latter strategy allows to identify the true required characteristics of the biocatalyst in an early stage, enabling a more focused engineering plan.

Efforts to decrease the K_m through enzyme engineering, for example, would not be useful if one would be able to perform the conversions at elevated substrate concentrations (well above the current K_m of the enzyme). However, if the biocatalyst would appear to suffer from substrate or product inhibition, working at lower substrate concentrations would be a strong incentive to improve the enzyme's affinity.

Alternatively, in the case of substrate inhibition, a steady feed of substrate could be applied, avoiding inhibition and consequently also the need for enzyme engineering. If product inhibition were to occur, the continuous removal of product, if technically possible, might be a useful alternative. In case multiple products are formed, for example, increasing the selectivity of a biocatalyst might significantly reduce the required efforts to isolate a certain compound. Hence, although the technology to isolate the product might be available, enzyme engineering (if successful) would allow to skip this operation. All in all, both enzyme and process engineering should always be considered at any stage in the development of a novel biocatalytic production process.

Such strategy could, for example, be applied to synthesize sophorose (2-*O*-β-D-glucopyranosyl-D-glucopyranoside), a strong inducer of enzymes involved in the degradation of lignocellulose[288]. To that end, cellobiose phosphorylase could be engineered to change its strict (1,4)-regioselectivity to a (1,2)-selectivity. If successful, the pricy sophorose (117 euro for 10 mg[289]) could be synthesized from the readily available αG1P (which can easily be obtained from sucrose as shown in CHAPTER 1) and glucose in a single step. Purification and isolation of sophorose could be achieved as described for kojibiose in CHAPTER 9. Alternatively, both SP and CP could be engineered to accept other monosaccharides besides glucose. Activity towards alternative acceptors such as mannose and xylose would give rise to a variety of kojibiose and sophorose analogues, which might harbor interesting properties. The structural diversity of these compounds could even be further expanded by coupling additional β-(1,4)-linked glucose residues with CDP (as shown in CHAPTER 7), although enzyme engineering might be required to do so.

In addition to expanding the acceptor specificity of glycoside phosphorylases, also the donor specificity of these enzymes can be changed. The latter has been nicely illustrated for the production of α-D-galactose 1-phosphate (αGal1P) from lactose with an engineered CP[54], which was subsequently used to synthesize a range of lactolipids with CDP[193]. Unfortunately, such processes are often limited by the availability of the required sugar phosphates. The recent breakthrough in the production of sucrose analogues[290], however, could enable the synthesis of for example α-D-mannose 1-phosphate and α-D-xylose 1-phosphate with (an engineered) SP. Efforts in this direction

might expand the scope of glycoside phosphorylases from glucosylation to galactosylation, mannosylation and xylosylation.

From a process engineering point of view, integrating membrane separation technology more closely with the production of glycosides would be of great value. Indeed, membrane separation generally uses less energy and solvents, thereby boosting the potential for industrial application, and reducing the overall footprint of the process[291]. In CHAPTER 5, a hydrophobic membrane was found to be very efficient for the isolation of octyl β-D-glucopyranoside. However, the use of hydrophobic membranes is mainly limited to the isolation of hydrophobic compounds, and would be less suited to isolate glycosides of phenolic compounds such as pyrogallol, hydroquinone or catechol. Supported liquid membranes, on the other hand, provide an interesting alternative. These membranes are constructed by impregnating a microporous membrane with a water immiscible organic solvent containing a selective transport carrier. The latter technique has already been successfully used to isolate fructose from a fermentation broth, by impregnating a polypropylene support with a solution of a phenylboronic acid derivatives in 2-nitrophenyl octyl ether[292]. Moreover, the use of a selective membrane would enable the continuous addition of substrates and selective extraction of the product, thereby avoiding stability or activity problems caused by elevated substrate or product concentrations. Despite the work on resorcinarene based supported liquid membranes for the isolation of methyl glycosides[293], insufficient knowledge and research are limiting the application of this technique to date. The availability of a large number of glycosides, however, provides the opportunity to develop selective membranes for such compounds.

Recently, a full-length ancestor of sucrose phosphorylase and sucrose 6'-phosphate phosphorylase was constructed[43]. Despite being believed to be more promiscuous, a present-day thermostable SP was found to be a better template for enzyme engineering. Nevertheless, this less specialized ancestor might be an ideal starting point for molecular imprinting experiments. The technology developed in CHAPTER 2 can easily be transferred to ancestor enzymes, which might result in a novel application for these ancient biocatalysts.

Finally, this research revealed the potential of sucrose to generate a large variety of glycosides and carbohydrates. Both the anomeric configuration and chain length could be conveniently altered by using different phosphorylase enzymes. Further expanding the acceptor promiscuity of these enzymes, would therefore be highly desirable. In that respect, glycoside hydrolases and transferases provide an interesting opportunity. Converting these types of enzymes to phosphorylases by means of enzyme engineering would vastly expand their application potential. Indeed, although many specificities have been reported, glycoside phosphorylases suffer from low yields when used in the synthesis direction, whereas glycoside transferases require expensive nucleotide activated sugars.

References

1. N. Kaur and A.K. Gupta, **2002**, Applications of inulin and oligofructose in health and nutrition, *Journal of Biosciences*, 27, 703-714.

2. D.B.A. Silk, A. Davis, J. Vulevic, G. Tzortzis and G.R. Gibson, **2009**, Clinical trial: the effects of a trans-galactooligosaccharide prebiotic on faecal microbiota and symptoms in irritable bowel syndrome, *Alimentary Pharmacology & Therapeutics*, 29, 508-518.

3. M.G. Sajilata, R.S. Singhal and P.R. Kulkarni, **2006**, Resistant starch - A review, *Comprehensive Reviews in Food Science and Food Safety*, 5, 1-17.

4. F. Fernandez, M. Hinton and B. Van Gils, **2002**, Dietary mannan-oligosaccharides and their effect on chicken caecal microflora in relation to *Salmonella Enteritidis* colonization, *Avian Pathology*, 31, 49-58.

5. M. Roberfroid, **2007**, Prebiotics: the concept revisited, *Journal of Nutrition*, 137, 830-837.

6. A. Varki, **1993**, Biological role of oligosaccharides: all of the theories are correct, *Glycobiology*, 3, 97-130.

7. T. Kwon, C.T. Kim and J.H. Lee, **2007**, Transglucosylation of ascorbic acid to ascorbic acid 2-glucoside by a recombinant sucrose phosphorylase from *Bifidobacterium longum*, *Biotechnology Letters*, 29, 611-615.

8. V. Kren and T. Rezanka, **2008**, Sweet antibiotics - the role of glycosidic residues in antibiotic and antitumor activity and their randomization, *Fems Microbiology Reviews*, 32, 858-889.

9. P. Torres, A. Poveda, J. Jimenez-Barbero, J. Luis Parra, F. Comelles, A.O. Ballesteros and F.J. Plou, **2011**, Enzymatic synthesis of α-glucosides of resveratrol with surfactant activity, *Advanced Synthesis & Catalysis*, 353, 1077-1086.

10. V. Kren and L. Martinkova, **2001**, Glycosides in medicine: the role of glycosidic residue in biological activity, *Current Medicinal Chemistry*, 8, 1313-1338.

11. G.R. Fenwick, J. Lutomski and C. Nieman, **1990**, Liquorice, *Glycyrrhiza glabra* L. Composition, uses and analysis, *Food Chemistry*, 38, 119-143.

12. H. Nakagawa, M. Yoshiyama, S. Shimura, K. Kirimura and S. Usami, **1998**, Anomer-selective glucosylation of L-menthol by Yeast α-glucosidase, *Bioscience Biotechnology and Biochemistry*, 62, 1332-1336.

13. S. Muthana, H.Z. Cao and X. Chen, **2009**, Recent progress in chemical and chemoenzymatic synthesis of carbohydrates, *Current Opinion in Chemical Biology*, 13, 573-581.

14. W. von Rybinski and K. Hill, **1998**, Alkyl polyglycosides - Properties and applications of a new class of surfactants, *Angewandte Chemie-International Edition*, 37, 1328-1345.

15. X. Zhu and R.R. Schmidt, **2009**, New principles for glycoside-bond formation, *Angewandte Chemie-International Edition*, 48, 1900-1934.

16. R.R. Schmidt and M. Hoffmann, **1983**, Synthesis of C-α- and C-β-D-glucopyranosyl derivatives from *O*-(α-D-glucopyranosyl) trichloroacetimidate, *Angewandte Chemie-International Edition in English*, 22, 406-406.

17. T.K. Lindhorst, ed., *Essentials of Carbohydrate Chemistry and Biochemistry*, Wiley-VCH, Weinheim **2007**.

18. T. Desmet, W. Soetaert, P. Bojarova, V. Kren, L. Dijkhuizen, V. Eastwick-Field and A. Schiller, **2012**, Enzymatic Glycosylation of Small Molecules: Challenging Substrates Require Tailored Catalysts, *Chemistry-a European Journal*, 18, 10786-10801.

19. B.M. de Roode, M.C.R. Franssen, A. Van der Padt and R.M. Boom, **2003**, Perspectives for the industrial enzymatic production of glycosides, *Biotechnology Progress*, 19, 1391-1402.

20. B. Henrissat and G.J. Davies, **2000**, Glycoside hydrolases and glycosyltransferases. Families, modules, and implications for genomics, *Plant Physiology*, 124, 1515-1519.

21. F. van Rantwijk, M.W.V. Oosterom and R.A. Sheldon, **1999**, Glycosidase-catalysed synthesis of alkyl glycosides, *Journal of Molecular Catalysis B-Enzymatic*, 6, 511-532.

22. J. Seibel, H.J. Jordening and K. Buchholz, **2006**, Glycosylation with activated sugars using glycosyltransferases and transglycosidases, *Biocatalysis and Biotransformation*, 24, 311-342.

23. D. Bowles, J. Isayenkova, E.K. Lim and B. Poppenberger, **2005**, Glycosyltransferases: managers of small molecules, *Current Opinion in Plant Biology*, 8, 254-263.

24. K.F. Johnson, **1999**, Synthesis of oligosaccharides by bacterial enzymes, *Glycoconjugate Journal*, 16, 141-146.

25. S. Masada, Y. Kawase, M. Nagatoshi, Y. Oguchi, K. Terasaka and H. Mizukami, **2007**, An efficient chemoenzymatic production of small molecule glucosides with in situ UDP-glucose recycling, *Febs Letters*, 581, 2562-2566.

26. C.A.G.M. Weijers, M.C.R. Franssen and G.M. Visser, **2008**, Glycosyltransferase-catalyzed synthesis of bioactive oligosaccharides, *Biotechnology Advances*, 26, 436-456.

27. T. Desmet and W. Soetaert, **2011**, Enzymatic glycosyl transfer: mechanisms and applications, *Biocatalysis and Biotransformation*, 29, 1-18.

28. J. Seibel, R. Beine, R. Moraru, C. Behringer and K. Buchholz, **2006**, A new pathway for the synthesis of oligosaccharides by the use of non-Leloir glycosyltransferases, *Biocatalysis and Biotransformation*, 24, 157-165.

29. T. Desmet and W. Soetaert, **2012**, Broadening the synthetic potential of disaccharide phosphorylases through enzyme engineering, *Process Biochemistry*, 47, 11-17.

30. C. Moulis, G. Vaca-Medina, S. Suwannarangsee, P. Monsan, G. Potocki-Veronese and M. Remaud-Simeon, **2008**, One-step synthesis of isomaltooligosaccharide syrups and dextrans of controlled size using engineered dextransucrase, *Biocatalysis and Biotransformation*, 26, 141-151.

31. P. Monsan, M. Remaud-Simeon and I. Andre, **2010**, Transglucosidases as efficient tools for oligosaccharide and glucoconjugate synthesis, *Current Opinion in Microbiology*, 13, 1-8.

32. E. Champion, I. Andre, C. Moulis, J. Boutet, K. Descroix, S. Morel, P. Monsan, L.A. Mulard and M. Remaud-Simeon, **2009**, Design of α-transglucosidases of controlled specificity for programmed chemoenzymatic synthesis of antigenic oligosaccharides, *Journal of the American Chemical Society*, 131, 7379-7389.

33. A. Bertrand, S. Morel, F. Lefoulon, Y. Rolland, P. Monsan and M. Remaud-Simeon, **2006**, Leuconostoc mesenteroides glucansucrase synthesis of flavonoid glucosides by acceptor reactions in aqueous-organic solvents, *Carbohydrate Research*, 341, 855-863.

34. J.R. Knowles, **1980**, Enzyme-catalyzed phosphoryl transfer reactions, *Annual Review of Biochemistry*, 49, 877-919.

35. A. Percy, H. Ono, D. Watt and K. Hayashi, **1997**, Synthesis of β-n-glucopyranosyl (1 -> 4)-D-arabinose, β-D-glucopyranosyl-(1 -> 4)-L-fucose and β-D-glucopyranosyl-(1 -> 4)-D-altrose catalysed by cellobiose phosphorylase from *Cellvibrio gilvus*, *Carbohydrate Research*, 305, 543-548.

36. A. Percy, H. Ono and K. Hayashi, **1998**, Acceptor specificity of cellobiose phosphorylase from *Cellvibrio gilvus*: synthesis of three branched trisaccharides, *Carbohydrate Research*, 308, 423-429.

37. K. Sheth and Alexande.Jk, **1967**, Cellodextrin phosphorylase from *Clostridium thermocellum*, *Biochimica Et Biophysica Acta*, 148, 808-&.

38. M. Reichenbecher, F. Lottspeich and K. Bronnenmeier, **1997**, Purification and properties of a cellobiose phosphorylase (CepA) and a cellodextrin phosphorylase (CepB) from the cellulolytic thermophile *Clostridium stercorarium*, *European Journal of Biochemistry*, 247, 262-267.

39. T. Giang Hai, T. Desmet, M.R.M. De Groeve and W. Soetaert, **2011**, Probing the active site of cellodextrin phosphorylase from *Clostridium stercorarium*: Kinetic characterization, ligand docking, and site-directed mutagenesis, *Biotechnology Progress*, 27, 326-332.

40. C. Goedl, T. Sawangwan, M. Mueller, A. Schwarz and B. Nidetzky, **2008**, A high-yielding biocatalytic process for the production of 2-O-(α-D-glucopyranosyl)-sn-glycerol, a natural osmolyte and useful moisturizing ingredient, *Angewandte Chemie International Edition*, 47, 10086-10089.

41. M.R. De Groeve, M. De Baere, L. Hoflack, T. Desmet, E.J. Vandamme and W. Soetaert, **2009**, Creating lactose phosphorylase enzymes by directed evolution of cellobiose phosphorylase, *Protein Engineering Design and Selection*, 22, 393-399.

42. M.R. De Groeve, L. Remmery, A. Van Hoorebeke, J. Stout, T. Desmet, S.N. Savvides and W. Soetaert, **2010**, Construction of cellobiose phosphorylase variants with broadened acceptor specificity towards anomerically substituted glucosides, *Biotechnology and Bioengineering*, 107, 413-420.

43. T. Verhaeghe, **2014**, Improving the glycosylation potential of sucrose phosphorylase through enzyme engineering, *Department of Biochemical and microbial technology*, 233p.

44. A. Cerdobbel, T. Desmet, K. De Winter, J. Maertens and W. Soetaert, **2010**, Increasing the thermostability of sucrose phosphorylase by multipoint covalent immobilization, *Journal of Biotechnology*, 150, 125-130.

45. A. Cerdobbel, K. De Winter, T. Desmet and W. Soetaert, **2010**, Sucrose phosphorylase as cross-linked enzyme aggregate: Improved thermal stability for industrial applications, *Biotechnology Journal*, 5, 1192–1197.

46. T. Bulter and L. Elling, **1999**, Enzymatic synthesis of nucleotide sugars, *Glycoconjugate Journal*, 16, 147-159.

47. O.J. Plante, R.B. Andrade and P.H. Seeberger, **1999**, Synthesis and use of glycosyl phosphates as glycosyl donors, *Org. Lett.*, 1, 211-214.

48. H. Fujinaka, J. Nakamura, H. Kobayashi, M. Takizawa, D. Murase, V. Tokimitsu and T. Suda, **2006**, Glucose 1-phosphate increases active transport of calcium in intestine, *Archives of Biochemistry and Biophysics*, 460, 152-160.

49. C.L. Ronchera-Oms, N.V. Jimenez and J. Peidro, **1995**, Stability of parenteral nutrition admixtures containing organic phosphates, *Clinical Nutrition*, 14, 373-380.

50. S. Timmons and D. Jakeman, **2008**, Stereospecific synthesis of sugar-1-phosphates and their conversion to sugar nucleotides, *Carbohydrate Research*, 343, 865-874.

51. H.M. Zhao and W.A. van der Donk, **2003**, Regeneration of cofactors for use in biocatalysis, *Current Opinion in Biotechnology*, 14, 583-589.

52. C. Goedl, A. Schwarz, A. Minani and B. Nidetzky, **2007**, Recombinant sucrose phosphorylase from *Leuconostoc mesenteroides*: characterization, kinetic studies of transglucosylation, and application of immobilised enzyme for production of α-D-glucose 1-phosphate, *Journal of Biotechnology*, 129, 77-86.

53. J. Van der Borght, T. Desmet and W. Soetaert, **2010**, Enzymatic production of β-D-glucose 1-phosphate from trehalose, *Biotechnology Journal*, 5, 986-993.

54. M.R. De Groeve, V. Depreitere, T. Desmet and W. Soetaert, **2009**, Enzymatic production of α-D-galactose 1-phosphate by lactose phosphorolysis, *Biotechnol Letters*, 31, 1873-1877.

55. C. Goedl, T. Sawangwan, P. Wildberger and B. Nidetzky, **2010**, Sucrose phosphorylase: a powerful transglucosylation catalyst for the synthesis of α-D-glucosides as industrial fine chemicals, *Biocatalysis and Biotransformation*, 28, 10-21.

56. T. Sawangwan, C. Goedl and B. Nidetzky, **2009**, Single-step enzymatic synthesis of (R)-2-*O*-α-D-glucopyranosyl glycerate, a compatible solute from micro-organisms that functions as a protein stabiliser, *Organic and Biomolecular Chemistry*, 7, 4267-4270.

57. C. Vieille and J.G. Zeikus, **1996**, Thermozymes: Identifying molecular determinants of protein structural and functional stability, *Trends in Biotechnology*, 14, 183-190.

58. M.E. Bruins, A.E.M. Janssen and R.M. Boom, **2001**, Thermozymes and their applications - A review of recent literature and patents, *Applied Biochemistry and Biotechnology*, 90, 155-186.

59. V.G.H. Eijsink, S. Gaseidnes, T.V. Borchert and B. van den Burg, **2005**, Directed evolution of enzyme stability, *Biomolecular Engineering*, 22, 21-30.

60. M. Sorgedrager, D. Verdoes, H. Van der Meer and R. Sheldon, **2008**, Cross-linked enzyme aggregates in a membrane slurry reactor. Continuous production of 6-APA by enzymatic hydrolysis of penicillin., *Chimica oggi-chemistry today*, 26, 23-25.

61. A. Lejeune, M. Vanhove, J. Lamotte-Brasseur, R.H. Pain, J.M. Frere and A. Matagne, **2001**, Quantitative analysis of the stabilization by substrate of *Staphylococcus aureus* PC1 beta-lactamase, *Chemistry & Biology*, 8, 831-842.

62. A. Hedoux, J.F. Willart, R. Ionov, F. Affouard, Y. Guinet, L. Paccou, A. Lerbret and M. Descamps, **2006**, Analysis of sugar bioprotective mechanisms on the thermal denaturation of lysozyme from Raman scattering and differential scanning calorimetry investigations, *Journal of Physical Chemistry B*, 110, 22886-22893.

63. J.H. Ashby, H.B. Clarke, E.M. Crook and S.P. Datta, **1955**, Thermodynamic quantities for the dissociation equilibria of biologically important compounds, *Biochemical Journal*, 59, 203-208.

64. A. Guibert and P. Monsan, **1988**, Production and purification of sucrose phosphorylase from *Leuconostoc mesenteroides*: applications to the production of glucose 1-phosphate., *Annals of the New York Academy of Sciences*, 542, 307-311.

65. M.C.B. Pimentel and M.S.S. Ferreira, **1991**, Immobilized sucrose phosphorylase from *Leuconostoc mesenteroides*, *Applied Biochemistry and Biotechnology*, 27, 37-43.

66. W. Soetaert, D. Schwengers, K. Buchholz and E.J. Vandamme, in *Carbohydrate Bioengineering*, eds. S. B. Petersen, B. Svensson and S. Pedersen, **1995**, pp. 351-358.

67. S.H. Bhosale, M.B. Rao and V.V. Deshpande, **1996**, Molecular and industrial aspects of glucose isomerase, *Microbiology Reviews*, 60, 280-300.

68. D. Aerts, T. Verhaeghe, M. De Mey, T. Desmet and W. Soetaert, **2011**, A constitutive expression system for high-throughput screening, *Engineering in Life Sciences*, 11, 10-19.

69. S. Waffenschmidt and L. Jaenicke, **1987**, Assay of reducing sugars in the nanomole range with 2,2'-bicinchoninate, *Analytical Biochemistry*, 165, 337-340.

70. W. Werner, H.G. Rey and H. Wielinge, **1970**, Properties of a new chromogen for determination of glucose in blood according to god/pod-method, *Zeitschrift für analytische Chemie*, 252, 224-228.

71. T. Koga, K. Nakamura, Y. Shirokane, K. Mizusawa, S. Kitao and M. Kikuchi, **1991**, Purification and some properties of sucrose phosphorylase from *Leuconostoc mesenteroides*, *Agricultural and Biological Chemistry*, 55, 1805-1810.

72. R. Silverstein, J. Voet, D. Reed and R.H. Abeles, **1967**, Purification and mechanism of action of sucrose phosphorylase, *The Journal of Biological Chemistry*, 242, 1338-1346.

73. B. Henrissat, **1991**, A classification of glycosyl hydrolases based on amino-acid sequence similarities, *Biochemical Journal* 280, 309-316.

74. C. Goedl, A. Schwarz, M. Mueller, L. Brecker and B. Nidetzky, **2008**, Mechanistic differences among retaining disaccharide phosphorylases: insights from kinetic analysis of active site mutants of sucrose phosphorylase and α,α-trehalose phosphorylase, *Carbohydrate Research*, 343, 2032-2040.

75. D. Sprogoe, L.A.M. van den Broek, O. Mirza, J.S. Kastrup, A.G.J. Voragen, M. Gajhede and L.K. Skov, **2004**, Crystal structure of sucrose phosphorylase from *Bifidobacterium adolescentis*, *Biochemistry*, 43, 1156-1162.

76. U.T. Bornscheuer, **2003**, Immobilizing enzymes: How to create more suitable biocatalysts, *Angewandte Chemie-International Edition*, 42, 3336-3337.

77. D. Aerts, T.F. Verhaeghe, B.I. Roman, C.V. Stevens, T. Desmet and W. Soetaert, **2011**, Transglucosylation potential of six sucrose phosphorylases toward different classes of acceptors, *Carbohydrate Research*, 346, 1860-1867.

78. R.A. Sheldon, **2011**, Cross-Linked Enzyme Aggregates as Industrial Biocatalysts, *Organic Process Research & Development*, 15, 213-223.

79. A. Cerdobbel, K. De Winter, D. Aerts, R. Kuipers, H.-J. Joosten, W. Soetaert and T. Desmet, **2011**, Increasing the thermostability of sucrose phosphorylase by a combination of sequence- and structure-based mutagenesis, *Protein Engineering Design & Selection*, 24, 829-834.

80. P. Wildberger, C. Luley-Goedl and B. Nidetzky, **2011**, Aromatic interactions at the catalytic subsite of sucrose phosphorylase: Their roles in enzymatic glucosyl transfer probed with Phe(52) -> Ala and Phe(52) -> Asn mutants, *Febs Letters*, 585, 499-504.

81. J. Wiesbauer, C. Goedl, A. Schwarz, L. Brecker and B. Nidetzky, **2009**, Substitution of the catalytic acid–base Glu237 by Gln suppresses hydrolysis during glucosylation of phenolic acceptors catalyzed by *Leuconostoc mesenteroides* sucrose phosphorylase *Journal of Molecular Catalysis B: Enzymatic*, 65, 24-29.

82. M. Stahl, U. Jeppssonwistrand, M.O. Mansson and K. Mosbach, **1991**, Induced stereo- and substrate selectivity of bioimprinted alpha-chymotrypsin in anhydrous organic media, *Journal of the American Chemical Society*, 113, 9366-9368.

83. E. Verheyen, J.P. Schillemans, M. van Wijk, M.A. Demeniex, W.E. Hennink and C.F. van Nostrum, **2011**, Challenges for the effective molecular imprinting of proteins, *Biomaterials*, 32, 3008-3020.

84. A.A. Vaidya, B.S. Lele, M.G. Kulkarni and R.A. Mashelkar, **2001**, Creating a macromolecular receptor by affinity imprinting, *Journal of Applied Polymer Science*, 81, 1075-1083.

85. J.U. Klein, M.J. Whitcombe, F. Mulholland and E.N. Vulfson, **1999**, Template-mediated synthesis of a polymeric receptor specific to amino acid sequences, *Angewandte Chemie-International Edition*, 38, 2057-2060.

86. F. Peissker and L. Fischer, **1999**, Crosslinking of imprinted proteases to maintain a tailor-made substrate selectivity in aqueous solutions, *Bioorganic & Medicinal Chemistry*, 7, 2231-2237.

87. J. Kaulpiboon, P. Pongsawasdi and W. Zimmermann, **2007**, Molecular imprinting of cyclodextrin glycosyltransferases from *Paenibacillus sp* A11 and *Bacillus macerans* with gamma-cyclodextrin, *Febs Journal*, 274, 1001-1010.

88. A. Vaidya, A. Borck, A. Manns and L. Fischer, **2004**, Altering glucose oxidase to oxidize D-galactose through crosslinking of imprinted protein, *Chembiochem*, 5, 132-135.

89. M. Wang, W. Qi, C. Jia, Y. Ren, R. Su and Z. He, **2011**, Enhancement of activity of cross-linked enzyme aggregates by a sugar-assisted precipitation strategy: Technical development and molecular mechanism, *Journal of Biotechnology*, 156, 30-38.

90. S. Kitao, S. Yoshida, T. Horiuchi, H. Sekine and I. Kusakabe, **1994**, Formation of kojibiose and nigerose by sucrose phosphorylase, *Bioscience Biotechnology and Biochemistry*, 58, 790-791.

91. F.L. Cabirol, P.L. Tan, B. Tay, S. Cheng, U. Hanefeld and R.A. Sheldon, **2008**, *Linum usitatissimum* hydroxynitrile lyase cross-linked enzyme aggregates: A recyclable enantioselective catalyst, *Advanced Synthesis and Catalysis*, 350, 2329-2338.

92. O.H. Lowry, N.J. Rosebrough, A.L. Farr and R.J. Randall, **1951**, Protein measurement with the Foling phenol reagent, *Journal of Biological Chemistry*, 193, 265-275.

93. S. Blanchard and J.S. Thorson, **2006**, Enzymatic tools for engineering natural product glycosylation, *Current Opinion in Chemical Biology*, 10, 263-271.

94. V. Kren, in *Glycoscience*, eds. B. Fraser-Reid, K. Tatsuta and J. Thiem, Springer, Berlin, **2008**, pp. 2589-2644.

95. I. Yamamoto, N. Muto, E. Nagata, T. Nakamura and Y. Suzuki, **1990**, Formation of a stable L-ascorbic acid α-glucoside by mammalian α-glucosidase-catalyzed transglucosylation, *Biochimica Et Biophysica Acta*, 1035, 44-50.

96. K. Buchholz and J. Seibel, **2008**, Industrial carbohydrate biotransformations, *Carbohydrate Research*, 343, 1966-1979.

97. M.M. Palcic, **2011**, Glycosyltransferases as biocatalysts, *Current Opinion in Chemical Biology*, 15, 226-233.

98. M. Kitaoka and K. Hayashi, **2002**, Carbohydrate-processing phosphorolytic enzymes, *Trends in Glycoscience and Glycotechnology*, 14, 35-50.

99. C. Luley-Goedl and B. Nidetzky, **2010**, Carbohydrate synthesis by disaccharide phosphorylases: Reactions, catalytic mechanisms and application in the glycosciences, *Biotechnology Journal*, 5, 1324-1338.

100. M.H. Shin, N.Y. Cheong, J.H. Lee and K.H. Kim, **2009**, Transglucosylation of caffeic acid by a recombinant sucrose phosphorylase in aqueous buffer and aqueous-supercritical CO_2 media, *Food Chemistry*, 115, 1028-1033.

101. K. De Winter, W. Soetaert and T. Desmet, **2012**, An Imprinted Cross-Linked Enzyme Aggregate (iCLEA) of Sucrose Phosphorylase: Combining Improved Stability with Altered Specificity, *International Journal of Molecular Sciences*, 13, 11333-11342.

102. Q.B. Liu, M.H.A. Janssen, F. van Rantwijk and R.A. Sheldon, **2005**, Room-temperature ionic liquids that dissolve carbohydrates in high concentrations, *Green Chemistry*, 7, 39-42.

103. F. van Rantwijk and R.A. Sheldon, **2007**, Biocatalysis in ionic liquids, *Chemical Reviews*, 107, 2757-2785.

104. N. Galonde, K. Nott, A. Debuigne, M. Deleu, C. Jerome, M. Paquot and J.-P. Wathelet, **2012**, Use of ionic liquids for biocatalytic synthesis of sugar derivatives, *Journal of Chemical Technology and Biotechnology*, 87, 451-471.

105. U. Kragl, M. Eckstein and N. Kaftzik, **2002**, Enzyme catalysis in ionic liquids, *Current Opinion in Biotechnology*, 13, 565-571.

106. S. Ferdjani, M. Ionita, B. Roy, M. Dion, Z. Djeghaba, C. Rabiller and C. Tellier, **2011**, Correlation between thermostability and stability of glycosidases in ionic liquid, *Biotechnology Letters*, 33, 1215-1219.

107. M. Lang, T. Kamrat and B. Nidetzky, **2006**, Influence of ionic liquid cosolvent on transgalactosylation reactions catalyzed by thermostable β-glycosylhydrolase celB from *Pyrococcus furiosus*, *Biotechnology and Bioengineering*, 95, 1093-1100.

108. U. Kragl, N. Kaftzik, S.H. Schofer, M. Eckstein, P. Wasserscheid and C. Hilgers, **2001**, Enzyme catalysis in the presence of ionic liquids, *Chimica oggi-chemistry today*, 19, 22-24.

109. Y. Bi, Z. Wang, Y. Mao, S. Zheng, H. Zhang and H. Shi, **2012**, Ionic liquid effects on the activity of β-glycosidase for the synthesis of salidroside in cosolvent systems, *Chinese Journal of Catalysis*, 33, 1161-1165.

110. Z. Kerem, D. Chetrit, O. Shoseyov and G. Regev-Shoshani, **2006**, Protection of lipids from oxidation by epicatechin, trans-resveratrol, and gallic and caffeic acids in intestinal model systems, *Journal of Agricultural and Food Chemistry*, 54, 10288-10293.

111. T. Cvetkovic, P. Vlahovic, V. Savic, D. Pavlovic, G. Kokic and V.B. Djordjevic, **2000**, Quercetine protects liver from oxidative stress induced by glycerole, *Journal of Hepatology*, 32, 214-214.

112. M. Murias, N. Handler, T. Erker, K. Pleban, G. Ecker, P. Saiko, T. Szekeres and W. Jager, **2004**, Resveratrol analogues as selective cyclooxygenase-2 inhibitors: synthesis and structure-activity relationship, *Bioorganic and Medicinal Chemistry*, 12, 5571-5578.

113. J.L. Anderson, J. Ding, T. Welton and D.W. Armstrong, **2002**, Characterizing ionic liquids on the basis of multiple solvation interactions, *Journal of the American Chemical Society*, 124, 14247-14254.

114. X. Zhang, X. Zhang, H. Dong, Z. Zhao, S. Zhang and Y. Huang, **2012**, Carbon capture with ionic liquids: overview and progress, *Energy & Environmental Science*, 5, 6668-6681.

115. C. Kohlmann, N. Robertz, S. Leuchs, Z. Dogan, S. Luetz, K. Bitzer, S. Na'amnieh and L. Greiner, **2011**, Ionic liquid facilitates biocatalytic conversion of hardly water soluble ketones, *Journal of Molecular Catalysis B-Enzymatic*, 68, 147-153.

116. D.Y. Xu, Y. Yang and Z. Yang, **2011**, Activity and stability of cross-linked tyrosinase aggregates in aqueous and nonaqueous media, *Journal of Biotechnology*, 152, 30-36.

117. J.K. Kaushik and R. Bhat, **2003**, Why is trehalose an exceptional protein stabilizer? An analysis of the thermal stability of proteins in the presence of the compatible osmolyte trehalose, *Journal of Biological Chemistry*, 278, 26458-26465.

118. A. Szabo, M. Kotorman, I. Laczko and L.M. Simon, **2009**, Influence of carbohydrates on stability of papain in aqueous tetrahydrofuran mixture, *Journal of Chemical Technology and Biotechnology*, 84, 133-138.

119. M. Pazhang, K. Khajeh, B. Ranjbar and S. Hosseinkhani, **2006**, Effects of water-miscible solvents and polyhydroxy compounds on the structure and enzymatic activity of thermolysin, *Journal of Biotechnology*, 127, 45-53.

120. M.T. Reetz, P. Soni, L. Fernandez, Y. Gumulya and J.D. Carballeira, **2010**, Increasing the stability of an enzyme toward hostile organic solvents by directed evolution based on iterative saturation mutagenesis using the B-FIT method, *Chemical Communications*, 46, 8657-8658.

121. K.M. Polizzi, A.S. Bommarius, J.M. Broering and J.F. Chaparro-Riggers, **2007**, Stability of biocatalysts, *Current Opinion in Chemical Biology*, 11, 220-225.

122. R.H. Cichewicz and S.A. Kouzi, **1998**, Biotransformation of resveratrol to piceid by *Bacillus cereus*, *Journal of Natural Products*, 61, 1313-1314.

123. H. Shim, W.P. Hong and Y. Ahn, **2003**, Enzymatic preparation of phenolic glucosides by *Streptococcus mutans*, *Bulletin of the Korean Chemical Society*, 24, 1680-1682.

124. A. Wong and I. Toth, **2001**, Lipid, sugar and liposaccharide based delivery systems, *Current Medicinal Chemistry*, 8, 1123-1136.

125. S. Kitao and H. Sekine, **1994**, α-D-glucosyl transfer to phenolic compounds by sucrose phosphorylase from *Leuconostoc mesenteroides* and production of α-arbutin, *Bioscience Biotechnology and Biochemistry*, 58, 38-42.

126. S. Kitao, T. Ariga, T. Matsuda and H. Sekine, **1993**, The syntheses of catechin glucosides by transglycosylation with *Leuconostoc mesenteroides* sucrose phosphorylase, *Bioscience Biotechnology and Biochemistry*, 57, 2010-2015.

127. S. Kitao, T. Matsudo, T. Sasaki, T. Koga and M. Kawamura, **2000**, Enzymatic synthesis of stable, odorless, and powdered furanone glucosides by sucrose phosphorylase, *Bioscience, Biotechnology, and Biochemistry*, 64, 134-141.

128. K. De Winter, K. Verlinden, V. Kren, L. Weignerova, W. Soetaert and T. Desmet, **2013**, Ionic liquids as cosolvents for glycosylation by sucrose phosphorylase: balancing acceptor solubility and enzyme stability, *Green Chemistry*, 15, 1949–1955.

129. G. Carrea and P. Cremonesi, **1987**, Enzyme-catalyzed steroid transformations in water-organic solvent two-phase systems, *Methods in Enzymology*, 136, 150-157.

130. D.K. Eggers, H.W. Blanch and J.M. Prausnitz, **1989**, Extractive catalysis: Solvent effects on equilibria of enzymatic reactions in two-phase systems, *Enzyme and Microbial Technology*, 11, 84-89.

131. K. Wang, Y. Lu, W.Q. Liang, S. Di Wang, Y. Jiang, R. Huang and Y.H. Liu, **2012**, Enzymatic synthesis of galacto-oligosaccharides in an organic-aqueous biphasic system by a novel β-galactosidase from a metagenomic library, *Journal of Agricultural and Food Chemistry*, 60, 3940-3946.

132. T. Hansson, M. Andersson, E. Wehtje and P. Adlercreutz, **2001**, Influence of water activity on the competition between β-glycosidase catalysed transglycosylation and hydrolysis in aqueous hexanol, *Enzyme and Microbial Technology*, 29, 527-534.

133. S.J. Kwon, H.-C. Jung and J.-G. Pan, **2007**, Transgalactosylation in a water-solvent biphasic reaction system with β-galactosidase displayed on the surfaces of *Bacillus subtilis* spores, *Applied and Environmental Microbiology*, 73, 2251-2256.

134. A.B. Tayade, P. Dhar, M. Sharma, R.S. Chauhan, O.P. Chaurasia and R.B. Srivastava, **2013**, Antioxidant capacities, phenolic contents, and GC/MS analysis of *Rhodiola imbricata Edgew.* root extracts from Trans-Himalaya, *Journal of Food Science*, 78, 402-410.

135. K.P. Mishra, L. Ganju and S.B. Singh, **2012**, Anti-cellular and immunomodulatory potential of aqueous extract of *Rhodiola imbricata rhizome*, *Immunopharmacology and Immunotoxicology*, 34, 513-518.

136. I. Mook-Jung, H. Kim, W.Z. Fan, Y. Tezuka, S. Kadota, H. Nishijo and M.W. Jung, **2002**, Neuroprotective effects of constituents of the oriental crude drugs, *Rhodiola sacra*, *R-sachalinensis* and *Tokaku-joki-to*, against β-amyloid toxicity, oxidative stress and apoptosis, *Biological & Pharmaceutical Bulletin*, 25, 1101-1104.

137. L. Becker, **2007**, Final report on the amended safety assessment of propyl gallate, *International Journal of Toxicology*, 26, 89-118.

138. T. Kalaivani, C. Rajasekaran and L. Mathew, **2011**, Free radical scavenging, cytotoxic, and memolytic activities of an active antioxidant compound ethyl gallate from leaves of *Acacia Nilotica* (L.) *Journal of Food Science*, 76, 144-149.

139. D. Auriol, R. ter Halle and F. Lefèvre, in *Practical Methods for Biocatalysis and Biotransformations 2*, eds. J. Whittall and W. P. Sutton, Wiley, Chichester, **2012**, pp. 232-235

140. K. Kino, Y. Shimizu, S. Kuratsu and K. Kirimura, **2007**, Enzymatic synthesis of α-anomer-selective D-glucosides using maltose phosphorylase, *Bioscience, Biotechnology, and Biochemistry*, 71, 1598-1600.

141. K. De Winter, T. Desmet, T. Devlamynck, L. Van Renterghem, T. Verhaeghe, H. Pelantova, V. Kren and W. Soetaert, **2014**, Biphasic catalysis with disaccharide phosphorylases: Chemoenzymatic synthesis of α-D-glucosides using sucrose phosphorylase, *Organic Process Research & Development*, 18, 781-787.

142. K. Kino, R. Satake, T. Morimatsu, S. Kuratsu, Y. Shimizu, M. Sato and K. Kirimura, **2008**, A new method of synthesis of alkyl β-glycosides using sucrose as sugar donor, *Bioscience, Biotechnology, and Biochemistry*, 72, 2415-2417.

143. C. Pop, L. Vlase and M. Tamas, **2009**, Natural resources containing arbutin. Determination of arbutin in the leaves of *Bergenia crassifolia* (L.) fritsch acclimated in Romania, *Notulae Botanicae Horti Agrobotanici Cluj-Napoca*, 37, 129-132.

144. J. Kurosu, T. Sato, K. Yoshida, T. Tsugane, S. Shimura, K. Kirimura, K. Kino and S. Usami, **2002**, Enzymatic synthesis of α-arbutin by α-anomer-selective-glucosylation of hydroquinone using lyophilized cells of *Xanthomonas campestris* WU-9701, *Journal of Bioscience and Bioengineering*, 93, 328-330.

145. G. Schindler, U. Patzak, B. Brinkhaus, A. von Nieciecki, J. Wittig, N. Krahmer, I. Glockl and M. Veit, **2002**, Urinary excretion and metabolism of arbutin after oral administration of Arctostaphylos uvae ursi extract as film-coated tablets and aqueous solution in healthy humans, *Journal of Clinical Pharmacology*, 42, 920-927.

146. A. Ducret, M. Trani and R. Lortie, **2002**, Screening of various glycosidases for the synthesis of octyl glucoside, *Biotechnology and Bioengineering*, 77, 752-757.

147. Y. Bhatia, S. Mishra and V.S. Bisaria, **2002**, Microbial β-glucosidases: Cloning, properties, and applications, *Critical Reviews in Biotechnology*, 22, 375-407.

148. J.K. Alexander, **1961**, Characteristics of cellobiose phosphorylase, *Journal of Bacteriology*, 81, 903-910.

149. M. Hidaka, M. Kitaoka, K. Hayashi, T. Wakagi, H. Shoun and S. Fushinobu, **2006**, Structural dissection of the reaction mechanism of cellobiose phosphorylase, *Biochemistry Journal*, 398, 37-43.

150. J.K. Alexander, **1968**, Synthesis of 4-*O*-β-D-glucopyranosyl-D-xylose, 4-*O*-β-D-glucopyranosyl-D-arabinose, 4-*O*-β-D-glucopyranosyl-2-deoxy-D-glucose, 4-*O*-β-D-glucopyranosyl-D-mannose, and 4-*O*-β-D-glucopyranosyl-D-glucosamine by cellobiose phosphorylase from *Clostridium thermocellum*, *Archives of Biochemistry and Biophysics*, 123, 240-246.

151. M.R. De Groeve, G.H. Tran, A. Van Hoorebeke, J. Stout, T. Desmet, S.N. Savvides and W. Soetaert, **2010**, Development and application of a screening assay for glycoside phosphorylases, *Analytical Biochemistry*, 401, 162-167.

152. H. Nakai, M.A. Hachem, B.O. Petersen, Y. Westphal, K. Mannerstedt, M.J. Baumann, A. Dilokpimol, H.A. Schols, J.O. Duus and B. Svensson, **2010**, Efficient chemoenzymatic oligosaccharide synthesis by reverse phosphorolysis using cellobiose phosphorylase and cellodextrin phosphorylase from *Clostridium thermocellum*, *Biochimie*, 92, 1818-1826.

153. E.N. Vulfson, R. Patel and B.A. Law, **1990**, Alkyl-β-glucoside synthesis in a water-organic two-phase system, *Biotechnology Letters*, 12, 397-402.

154. R.A. Sheldon, **2007**, Enzyme immobilization: The quest for optimum performance, *Advanced Synthesis & Catalysis*, 349, 1289-1307.

155. L.Q. Cao, L. van Langen and R.A. Sheldon, **2003**, Immobilised enzymes: carrier-bound or carrier-free?, *Current Opinion in Biotechnology*, 14, 387-394.

156. J.D. Gawronski and D.R. Benson, **2004**, Microtiter assay for glutamine synthetase biosynthetic activity using inorganic phosphate detection, *Analytical Biochemistry*, 327, 114-118.

157. S. Perez, M.A. Rodriguez-Carvajal and T. Doco, **2003**, A complex plant cell wall polysaccharide: rhamnogalacturonan II. A structure in quest of a function, *Biochimie*, 85, 109-121.

158. L. Weignerova, P. Marhol, D. Gerstorferova and V. Kren, **2012**, Preparatory production of quercetin-3-β-D-glucopyranoside using alkali-tolerant thermostable α-L-rhamnosidase from *Aspergillus terreus*, *Bioresource Technology*, 115, 222-227.

159. H.S. Yu, J.M. Gong, C.Z. Zhang and F.X. Jin, **2002**, Purification and characterization of ginsenoside-α-L-rhamnosidase, *Chemical & Pharmaceutical Bulletin*, 50, 175-178.

160. Y. Oda, K. Saito, A. Ohara-Takada and M. Mori, **2002**, Hydrolysis of the potato glycoalkaloid α-chaconine by filamentous fungi, *Journal of Bioscience and Bioengineering*, 94, 321-325.

161. L.Y. Deng, D.L. Kasper, T.P. Krick and M.R. Wessels, **2000**, Characterization of the linkage between the type III capsular polysaccharide and the bacterial cell wall of group B *Streptococcus*, *Journal of Biological Chemistry*, 275, 7497-7504.

162. G. Spagna, R.N. Barbagallo, A. Martino and P.G. Pifferi, **2000**, A simple method for purifying glycosidases: α-L-rhamnopyranosidase from *Aspergillus niger* to increase the aroma of Moscato wine, *Enzyme and Microbial Technology*, 27, 522-530.

163. O. Benavente-Garcia, J. Castillo, F.R. Marin, A. Ortuno and J.A. Del Rio, **1997**, Uses and properties of Citrus flavonoids, *Journal of Agricultural and Food Chemistry*, 45, 4505-4515.

164. G. Faury, J. Molinari, E. Rusova, B. Mariko, S. Raveaud, P. Huber, V. Velebny, A.M. Robert and L. Robert, **2011**, Receptors and aging: Structural selectivity of the rhamnose-receptor on fibroblasts as shown by Ca^{2+}-mobilization and gene-expression profiles, *Archives of Gerontology and Geriatrics*, 53, 106-112.

165. J. Laboureau, J.-T. Simonnet, P. Portes and K. Lucet-Levannier, **2010**, Association de monosaccharides avec des agents antioxydants et son utilization en cosmetique, *European Patent*, EP2204164.

166. H. Duplan, V. Raufast, A. Mavon, I. Ceruti, N. Castex-Rizzi and M. Charveron, **2009**, Bioavailability and pharmacological effect of a new pentyl rhamnoside on the inflamed skin, *Journal of Investigative Dermatology*, 129, 800-800.

167. D. Gerstorferova, B. Fliedrova, P. Halada, P. Marhol, V. Kren and L. Weignerova, **2012**, Recombinant α-L-rhamnosidase from *Aspergillus terreus* in selective trimming of rutin, *Process Biochemistry*, 47, 828-835.

168. M. Trani, A. Ducret and R. Lortie, **2004**, Influence of water-miscible solvents on hydrolytic activity of crude almond β-glucosidase, *Journal of Molecular Catalysis B-Enzymatic*, 28, 15-18.

169. M.R. Martearena, S. Blanco and G. Ellenrieder, **2003**, Synthesis of alkyl α-L-rhamnosides by water soluble alcohols enzymatic glycosylation, *Bioresource Technology*, 90, 297-303.

170. S. Papanikolaou, **2001**, Enzyme-catalyzed synthesis of alkyl β-glucosides in a water-alcohol two-phase system, *Bioresource Technology*, 77, 157-161.

171. I. Mladenoska, E. Winkelhausen and S. Kuzmanova, **2008**, Transgalactosylation/hydrolysis ratios of various β-galactosidases catalyzing alkyl β-galactoside synthesis in single-phased alcohol media, *Food Technology and Biotechnology*, 46, 311-316.

172. E. Rajnochova, J. Dvorakova, Z. Hunkova and V. Kren, **1997**, Reverse hydrolysis catalysed by β-*N*-acetylhexosaminidase from *Aspergillus oryzae*, *Biotechnology Letters*, 19, 869-872.

173. B. Baderschneider, G. Skouroumounis and P. Winterhalter, **1997**, Isolation of two glucosidic precursors of β-damascenone from riesling wine, *Natural Product Letters*, 10, 111-114.

174. J. Vetter, **2000**, Plant cyanogenic glycosides, *Toxicon*, 38, 11-36.

175. I. London-Shafir, S. Shafir and D. Eisikowitch, **2003**, Amygdalin in almond nectar and pollen - facts and possible roles, *Plant Systematics and Evolution*, 238, 87-95.

176. S.M. Jeon, S.H. Bok, M.K. Jang, Y.H. Kim, K.T. Nam, T.S. Jeong, Y.B. Park and M.S. Choi, **2002**, Comparison of antioxidant effects of naringin and probucol in cholesterol-fed rabbits, *Clinica Chimica Acta*, 317, 181-190.

177. M. Puri and U.C. Banerjee, **2000**, Production, purification, and characterization of the debittering enzyme naringinase, *Biotechnology Advances*, 18, 207-217.

178. M.H. Ribeiro, **2011**, Naringinases: occurrence, characteristics, and applications, *Applied Microbiology and Biotechnology*, 90, 1883-1895.

179. D. Balzer, **1996**, Properties of alkyl polyglucosides, *Tenside Surfactants Detergents*, 33, 102-110.

180. M.K. Matsson, B. Kronberg and P.M. Claesson, **2004**, Adsorption of alkyl polyglucosides on the solid/water interface: Equilibrium effects of alkyl chain length and head group polymerization, *Langmuir*, 20, 4051-4058.

181. F.A. Hughes and B.W. Lew, **1970**, Physical and functional properties of some higher alkyl polyglucosides, *Journal of the American Oil Chemists Society*, 47, 162-167.

182. R. Spilker, B. Menzebach, U. Schneider and I. Venn, **1996**, Analysis of alkyl polyglucosides, *Tenside Surfactants Detergents*, 33, 21-25.

183. X. Jin, S.F. Zhang, J.Z. Yang and Y.K. Li, **2004**, The potential of alkyl polyglucosides and polyethylene glycol glucosides coatings for improving the storage and shelf-life of pineapples, *Tenside Surfactants Detergents*, 41, 109-112.

184. M.W. Sulek, M. Ogorzalek, T. Wasilewski and E. Klimaszewska, **2013**, Alkyl polyglucosides as components of water based lubricants, *Journal of Surfactants and Detergents*, 16, 369-375.

185. K. Hill, **2000**, Fats and oils as oleochemical raw materials, *Pure and Applied Chemistry*, 72, 1255-1264.

186. G.T. Richard, S. Morel, R.M. Willemot, P. Monsan and M. Remaud-Simeon, **2003**, Glucosylation of α-butyl and α-octyl D-glucopyranosides by dextransucrase and alternansucrase from *Leuconostoc mesenteroides*, *Carbohydrate Research*, 338, 855-864.

187. Y.K. Kim, M. Kitaoka, M. Krishnareddy, Y. Mori and K. Hayashi, **2002**, Kinetic studies of a recombinant cellobiose phosphorylase (CBP) of the *Clostridium thermocellum* YM4 strain expressed in *Escherichia coli*, *Journal of Biochemistry*, 132, 197-203.

188. J. Lou, K.A. Dawson and H.J. Strobel, **1997**, Cellobiose and cellodextrin metabolism by the ruminal bacterium *Ruminococcus albus*, *Current Microbiology*, 35, 221-227.

189. L.R. Lynd, P.J. Weimer, W.H. van Zyl and I.S. Pretorius, **2002**, Microbial cellulose utilization: Fundamentals and biotechnology, *Microbiology and Molecular Biology Reviews*, 66, 506-577.

190. B.L. Cantarel, P.M. Coutinho, C. Rancurel, T. Bernard, V. Lombard and B. Henrissat, **2009**, The carbohydrate-active enyymes database (CAZy): an expert resource for glycogenomics, *Nucleic Acids Research* 37, 233-238.

191. M. Hidaka, Y. Honda, M. Kitaoka, S. Nirasawa, K. Hayashi, T. Wakagi, H. Shoun and S. Fushinobu, **2004**, Chitobiose phosphorylase from *Vibrio proteolyticus*, a member of glycosyl transferase family 36, has a clan GH-L-like $(\alpha/\alpha)_6$ barrel fold, *Structure*, 12, 937-947.

192. E. Samain, C. Lancelonpin, F. Ferigo, V. Moreau, H. Chanzy, A. Heyraud and H. Driguez, **1995**, Phosphorolytic synthesis of cellodextrins, *Carbohydrate Research*, 271, 217-226.

193. H.G. Tran, T. Desmet, K. Saerens, H. Waegeman, S. Vandekerckhove, M. D'Hooghe, I. Van Bogaert and W. Soetaert, **2012**, Biocatalytic production of novel glycolipids with cellodextrin phosphorylase, *Bioresource Technology*, 115, 84-87.

194. W. Nerinckx, T. Desmet, K. Piens and M. Claeyssens, **2005**, An elaboration on the syn-anti proton donor concept of glycoside hydrolases: electrostatic stabilisation of the transition state as a general strategy, *Febs Letters*, 579, 302-312.

195. W. Nerinckx, T. Desmet and M. Claeyssens, **2003**, A hydrophobic platform as a mechanistically relevant transition state stabilising factor appears to be present in the active centre of all glycoside hydrolases, *Febs Letters*, 538, 1-7.

196. R.D. Whitaker, Y. Cho, J. Cha, H.L. Carrell, J.P. Glusker, P.A. Karplus and C.A. Batt, **1995**, Probing the roles of active site residues in D-xylose isomerase, *Journal of Biological Chemistry*, 270, 22895-22906.

197. A.M. Lambeir, M. Lauwereys, P. Stanssens, N.T. Mrabet, J. Snauwaert, H. van Tilbeurgh, G. Matthyssens, I. Lasters, M. De Maeyer, S.J. Wodak, J. Jenkins, M. Chiadmi and J. Janin, **1992**, Protein engineering of xylose (glucose) isomerase from *Actinoplanes missouriensis*. 2. Site-directed mutagenesis of the xylose binding site, *Biochemistry*, 31, 5459-5466.

198. B.A. van der Veen, G. Potocki-Veronese, C. Albenne, G. Joucla, P. Monsan and M. Remaud-Simeon, **2004**, Combinatorial engineering to enhance amylosucrase performance: construction, selection, and screening of variant libraries for increased activity, *Febs Letters*, 560, 91-97.

199. S. Emond, I. Andre, K. Jaziri, G. Potocki-Veronese, P. Mondon, K. Bouayadi, H. Kharrat, P. Monsan and M. Remaud-Simeon, **2008**, Combinatorial engineering to enhance thermostability of amylosucrase, *Protein Science*, 17, 967-976.

200. E. Krieger, K. Joo, J. Lee, J. Lee, S. Raman, J. Thompson, M. Tyka, D. Baker and K. Karplus, **2009**, Improving physical realism, stereochemistry, and side-chain accuracy in homology modeling: Four approaches that performed well in CASP8, *Proteins-Structure Function and Bioinformatics*, 77, 114-122.

201. E. Krieger, G. Koraimann and G. Vriend, **2002**, Increasing the precision of comparative models with YASARA NOVA - a self-parameterizing force field, *Proteins-Structure Function and Genetics*, 47, 393-402.

202. Y. Honda, M. Kitaoka and K. Hayashi, **2004**, Reaction mechanism of chitobiose phosphorylase from *Vibrio proteolyticus*: identification of family 36 glycosyltransferase in *Vibrio*, *Biochemical Journal*, 377, 225-232.

203. O. Trott and A.J. Olson, **2010**, Software news and update Autodock Vina: Improving the speed and accuracy of docking with a new scoring function, efficient optimization, and multithreading, *Journal of Computational Chemistry*, 31, 455-461.

204. D. Seeliger and B.L. de Groot, **2010**, Ligand docking and binding site analysis with PyMOL and Autodock/Vina, *Journal of Computer-Aided Molecular Design*, 24, 417-422.

205. Y. Duan, C. Wu, S. Chowdhury, M.C. Lee, G.M. Xiong, W. Zhang, R. Yang, P. Cieplak, R. Luo, T. Lee, J. Caldwell, J.M. Wang and P. Kollman, **2003**, A point-charge force field for molecular mechanics simulations of proteins based on condensed-phase quantum mechanical calculations, *Journal of Computational Chemistry*, 24, 1999-2012.

206. J. Sanchis, L. Fernandez, J.D. Carballeira, J. Drone, Y. Gumulya, H. Hoebenreich, D. Kahakeaw, S. Kille, R. Lohmer, J.J.P. Peyralans, J. Podtetenieff, S. Prasad, P. Soni, A. Taglieber, S. Wu, F.E. Zilly and M.T. Reetz, **2008**, Improved PCR method for the creation of saturation mutagenesis libraries in directed evolution: application to difficult-to-amplify templates, *Applied Microbiology and Biotechnology*, 81, 387-397.

207. E. Choe and D.B. Min, **2009**, Mechanisms of antioxidants in the oxidation of foods, *Comprehensive Reviews in Food Science and Food Safety*, 8, 345-358.

208. M. Namiki, **1990**, Antioxidants antimutagens in food, *Critical Reviews in Food Science and Nutrition*, 29, 273-300.

209. B. Saad, Y.Y. Sing, M.A. Nawi, N. Hashim, A.S.M. Ali, M.I. Saleh, S.F. Sulaiman, K.M. Talib and K. Ahmad, **2007**, Determination of synthetic phenolic antioxidants in food items using reversed-phase HPLC, *Food Chemistry*, 105, 389-394.

210. C.A. RiceEvans and N.J. Miller, **1996**, Antioxidant activities of flavonoids as bioactive components of food, *Biochemical Society Transactions*, 24, 790-795.

211. J.W. Finley, A.-N. Kong, K.J. Hintze, E.H. Jeffery, L.L. Ji and X.G. Lei, **2011**, Antioxidants in foods: state of the science important to the food industry, *Journal of Agricultural and Food Chemistry*, 59, 6837-6846.

212. S.T. Mayne, **2003**, Antioxidant nutrients and chronic disease: Use of biomarkers of exposure and oxidative stress status in epidemiologic research, *Journal of Nutrition*, 133, 933-940.

213. R.G. Berger, S. Lunkenbein, A. Strohle and A. Hahn, **2012**, Antioxidants in food: Mere myth or magic medicine?, *Critical Reviews in Food Science and Nutrition*, 52, 162-171.

214. D.G. Soares, A.C. Andreazza and M. Salvador, **2003**, Sequestering ability of butylated hydroxytoluene, propyl gallate, resveratrol, and vitamins C and E against ABTS, DPPH, and hydroxyl free radicals in chemical and biological systems, *Journal of Agricultural and Food Chemistry*, 51, 1077-1080.

215. A.S. Meyer, M. Heinonen and E.N. Frankel, **1998**, Antioxidant interactions of catechin, cyanidin, caffeic acid, quercetin, and ellagic acid on human LDL oxidation, *Food Chemistry*, 61, 71-75.

216. F. Shahidi and Y. Zhong, **2010**, Novel antioxidants in food quality preservation and health promotion, *European Journal of Lipid Science and Technology*, 112, 930-940.

217. B.G. Kim, B.R. Jung, Y. Lee, H.G. Hur, Y. Lim and J.H. Ahn, **2006**, Regiospecific flavonoid 7-*O*-methylation with *Streptomyces avermitilis O*-methyltransferase expressed in *Escherichia coli*, *Journal of Agricultural and Food Chemistry*, 54, 823-828.

218. R. Mateos, M. Trujillo, G. Pereira-Caro, A. Madrona, A. Cert and J.L. Espartero, **2008**, New lipophilic tyrosyl esters. Comparative antioxidant evaluation with hydroxytyrosyl esters, *Journal of Agricultural and Food Chemistry*, 56, 10960-10966.

219. A. Trincone, E. Pagnotta and A. Tramice, **2012**, Enzymatic routes for the production of mono- and di-glucosylated derivatives of hydroxytyrosol, *Bioresource Technology*, 115, 79-83.

220. X. Wu, J. Chu, B. Wu, S. Zhang and B. He, **2013**, An efficient novel glycosylation of flavonoid by β-fructosidase resistant to hydrophilic organic solvents, *Bioresource Technology*, 129, 659-662.

221. L. Bungaruang, A. Gutmann and B. Nidetzky, **2013**, Leloir glycosyltransferases and natural product glycosylation: biocatalytic synthesis of the C-glucoside nothofagin, a major antioxidant of redbush herbal tea, *Advanced Synthesis & Catalysis*, 355, 2757-2763.

222. M. Plaza, T. Pozzo, J. Liu, K.Z.G. Ara, C. Turner and E.N. Karlsson, **2014**, Substituent effects on *in vitro* antioxidizing properties, stability, and solubility in flavonoids, *Journal of Agricultural and Food Chemistry*, 62, 3321-3333.

223. P.C.H. Hollman, M. Bijsman, Y. van Gameren, E.P.J. Cnossen, J.H.M. de Vries and M.B. Katan, **1999**, The sugar moiety is a major determinant of the absorption of dietary flavonoid glycosides in man, *Free Radical Research*, 31, 569-573.

224. M.E. Dirks-Hofmeister, T. Verhaeghe, K. De Winter and T. Desmet, **2015**, Creating space for large acceptors: Rational biocatalyst design for resveratrol glycosylation in an aqueous system, *Angewandte Chemie International Edition*, 54, 9289–9292.

225. J.A. Rothwell, A.J. Day and M.R.A. Morgan, **2005**, Experimental determination of octanol-water partition coefficients of quercetin and related flavonoids, *Journal of Agricultural and Food Chemistry*, 53, 4355-4360.

226. Y.H. Moon, J.H. Lee, J.S. Ahn, S.H. Nam, D.K. Oh, D.H. Park, H.J. Chung, S. Kang, D.F. Day and D. Kim, **2006**, Synthesis, structure analyses, and characterization of novel epigallocatechin gallate (EGCG) glycosides using the glucansucrase from *Leuconostoc mesenteroides* B-1299CB, *Journal of Agricultural and Food Chemistry*, 54, 1230-1237.

227. Y. Kaminaga, A. Nagatsu, T. Akiyama, N. Sugimoto, T. Yamazaki, T. Maitani and H. Mizukami, **2003**, Production of unnatural glucosides of curcumin with drastically enhanced water solubility by cell suspension cultures of *Catharanthus roseus*, *Febs Letters*, 555, 311-316.

228. A. Noguchi, M. Inohara-Ochiai, N. Ishibashi, H. Fukami, T. Nakayama and M. Nakao, **2008**, A novel glucosylation enzyme: Molecular cloning, expression, and characterization of *Trichoderma viride* JCM22452 α-amylase and enzymatic synthesis of some flavonoid monoglucosides and oligoglucosides, *Journal of Agricultural and Food Chemistry*, 56, 12016-12024.

229. D. Zielinska, W. Wiczkowski and M.K. Piskula, **2008**, Determination of the relative contribution of quercetin and its glucosides to the antioxidant capacity of onion by cyclic voltammetry and spectrophotometric methods, *Journal of Agricultural and Food Chemistry*, 56, 3524-3531.

230. J. Takebayashi, R. Ishii, J. Chen, T. Matsumoto, Y. Ishimi and A. Tai, **2010**, Reassessment of antioxidant activity of arbutin: Multifaceted evaluation using five antioxidant assay systems, *Free Radical Research*, 44, 473-478.

231. J. Xie and K.M. Schaich, **2014**, Re-evaluation of the 2,2-diphenyl-1-picrylhydrazyl free radical (DPPH) assay for antioxidant activity, *Journal of Agricultural and Food Chemistry*, 62, 4251-4260.

232. D.P. Makris and J.T. Rossiter, **2001**, Domestic processing of onion bulbs (*Allium cepa*) and asparagus spears (*Asparagus officinalis*): Effect on flavonol content and antioxidant status, *Journal of Agricultural and Food Chemistry*, 49, 3216-3222.

233. K. Valentova, J. Vrba, M. Bancirova, J. Ulrichova and V. Kren, **2014**, Isoquercitrin: pharmacology, toxicology, and metabolism, *Food and Chemical Toxicology*, 68, 267-282.

234. J. Xiao and P. Hoegger, **2015**, Stability of dietary polyphenols under the cell culture conditions: avoiding erroneous conclusions, *Journal of Agricultural and Food Chemistry*, 63, 1547-1557.

235. M. Blaser, P. Bork, C. Fraser, R. Knight and J. Wang, **2013**, The microbiome explored: recent insights and future challenges, *Nature Reviews Microbiology*, 11, 213-217.

236. K. Kukkonen, E. Savilahti, T. Haahtela, K. Juntunen-Backman, R. Korpela, T. Poussa, T. Tuure and M. Kuitunen, **2007**, Probiotics and prebiotic galacto-oligosaccharides in the prevention of allergic diseases: A randomized, double-blind, placebo-controlled trial, *Journal of Allergy and Clinical Immunology*, 119, 192-198.

237. M. Roberfroid, G.R. Gibson, L. Hoyles, A.L. McCartney, R. Rastall, I. Rowland, D. Wolvers, B. Watzl, H. Szajewska, B. Stahl, F. Guarner, F. Respondek, K. Whelan, V. Coxam, M.-J. Davicco, L. Leotoing, Y. Wittrant, N.M. Delzenne, P.D. Cani, A.M. Neyrinck and A. Meheust,

2010, Prebiotic effects: metabolic and health benefits, *British Journal of Nutrition*, 104, 1-63.

238. G.A. Preidis and J. Versalovic, **2009**, Targeting the human microbiome with antibiotics, probiotics, and prebiotics: Gastroenterology enters the metagenomics era, *Gastroenterology*, 136, 2015-2031.

239. P. Hemarajata and J. Versalovic, **2013**, Effects of probiotics on gut microbiota: mechanisms of intestinal immunomodulation and neuromodulation, *Therapeutic Advances in Gastroenterology*, 6, 39-51.

240. P.D. Cani and N.M. Delzenne, **2011**, The gut microbiome as therapeutic target, *Pharmacology & Therapeutics*, 130, 202-212.

241. M.L. Sanz, G.R. Gibson and R.A. Rastall, **2005**, Influence of disaccharide structure on prebiotic selectivity *in vitro*, *Journal of Agricultural and Food Chemistry*, 53, 5192-5199.

242. H. Chaen, T. Nishimoto, T. Nakada, S. Fukuda, M. Kurimoto and Y. Tsujisaka, **2001**, Enzymatic synthesis of kojioligosaccharides using kojibiose phosphorylase, *Journal of Bioscience and Bioengineering*, 92, 177-182.

243. J. Hodoniczky, C.A. Morris and A.L. Rae, **2012**, Oral and intestinal digestion of oligosaccharides as potential sweeteners: A systematic evaluation, *Food Chemistry*, 132, 1951-1958.

244. S. Ogawa, M. Ashiura and C. Uchida, **1998**, Synthesis of α-glucosidase inhibitors: kojibiose-type pseudodisaccharides and a related pseudotrisaccharide, *Carbohydrate Research*, 307, 83-95.

245. E.B. de Melo, A.d.S. Gomes and I. Carvalho, **2006**, α- And β-glucosidase inhibitors: Chemical structure and biological activity, *Tetrahedron*, 62, 10277-10302.

246. O.J. Phung, J.M. Scholle, M. Talwar and C.I. Coleman, **2010**, Effect of noninsulin antidiabetic drugs added to metformin therapy on glycemic control, weight gain, and hypoglycemia in type 2 diabetes, *Jama-Journal of the American Medical Association*, 303, 1410-1418.

247. T. Watanabe and K. Aso, **1959**, Isolation of kojibiose from honey, *Nature*, 183, 1740-1740.

248. K. Matsuda, **1959**, Studies on the disaccharides in koji extract and sake. V. Isolation and identification of kojibiose, *Nippon Nogeikagaku Kaishi*, 719-723.

249. A. Sato and K. Aso, **1957**, Kojibiose (2-O-α-D-glucopyranosyl-D-glucose): isolation and structure: isolation from hydrol, *Nature*, 180, 984-985.

250. K. Matsuda, H. Watanabe, K. Fujimoto and K. Aso, **1961**, Isolation of nigerose and kojibiose from dextrans, *Nature*, 191, 278.

251. M.L. Wolfrom, D.R. Lineback and A. Thompson, **1963**, Isopropyl tetra-*O*-acetyl-α-D-glucopyranoside - a synthesis of kojibiose, *Journal of Organic Chemistry*, 28, 860-861.

252. K. Igarashi, J. Irisawa and T. Honma, **1975**, Syntheses of α-D-linked disaccharides, *Carbohydrate Research*, 39, 341-343.

253. J. Duke, N. Little and Goldstei.Ij, **1973**, Preparation of cyrstalline α-kojibiose octaacetate from dextran B-1299-S: Its conversion into *p*-nitrophenyl and *p*-isothiocyanatophenyl β-kojibioside, *Carbohydrate Research*, 27, 193-198.

254. H. Fujimoto, H. Nishida and K. Ajisaka, **1988**, Enzymatic syntheses of glucobioses by a condensation reaction with α-glucosidase, β-glucosidase and glucoamylase, *Agricultural and Biological Chemistry*, 52, 1345-1351.

255. L. Cantarella, Z.L. Nikolov and P.J. Reilly, **1994**, Dissaccharide production by glucoamylase in aqueous ether mixtures, *Enzyme and Microbial Technology*, 16, 383-387.

256. P. Monsan and F. Ouarne, in *Prebiotics and probiotics science and technology*, eds. D. Chalarampopoulos and R. A. Ratstall, Springer, Berlin, **2010**, pp. 293-336.

257. Y. Brison, T. Pijning, Y. Malbert, É. Fabre, L. Mourey, S. Morel, G. Potocki-Véronèse, P. Monsan, S. Tranier, M. Remaud-Siméon and B.W. Dijkstra, **2012**, Functional and Structural Characterization of α-(1→2) Branching Sucrase Derived from DSR-E Glucansucrase, *Journal of Biological Chemistry*, 287, 7915-7924.

258. H. Chaen, T. Nishimoto, T. Nakada, S. Fukuda, M. Kurimoto and Y. Tsujisaka, **2001**, Enzymatic synthesis of novel oligosaccharides from L-sorbose, maltose, and sucrose using kojibiose phosphorylase, *Journal of Bioscience and Bioengineering*, 92, 173-176.

259. M. Diez-Municio, A. Montilla, F. Javier Moreno and M. Herrero, **2014**, A sustainable biotechnological process for the efficient synthesis of kojibiose, *Green Chemistry*, 16, 2219-2226.

260. R.J.M. Russell and G.L. Taylor, **1995**, Engineering thermostability: lessons from thermophilic proteins, *Current Opinion in Biotechnology*, 6, 370-374.

261. S. Khan and M. Vihinen, **2010**, Performance of protein stability predictors, *Human Mutation*, 31, 675-684.

262. S.H. Yoon, R. Mukerjea and J.F. Robyt, **2003**, Specificity of yeast (*Saccharomyces cerevisiae*) in removing carbohydrates by fermentation, *Carbohydrate Research*, 338, 1127-1132.

263. Z. Li, M. Xiao, L. Lu and Y. Li, **2008**, Production of non-monosaccharide and high-purity galactooligosaccharides by immobilized enzyme catalysis and fermentation with immobilized yeast cells, *Process Biochemistry*, 43, 896-899.

264. F. Yamauchi and K. Aso, **1961**, Crystalline α-kojibiose, *Nature*, 189, 753-&.

265. G. Graziano, **2012**, How does sucrose stabilize the native state of globular proteins?, *International Journal of Biological Macromolecules*, 50, 230-235.

266. J.C. Lee and S.N. Timasheff, **1981**, The stabilization of proteins by sucrose, *Journal of Biological Chemistry*, 256, 7193-7201.

267. S. De Laet, **2015**, Glycosylated phenolic antioxidants: chemoenzymatic synthesis and properties, *Master of Science in Bioscience Engineering: Chemistry and Bioprocess Technology*.

268. M. Ngoc Lan, K. Ahn and Y.-M. Koo, **2014**, Methods for recovery of ionic liquids. A review, *Process Biochemistry*, 49, 872-881.

269. P. Virtanen, J.-P. Mikkola, E. Toukoniitty, H. Karhu, K. Kordas, K. Eranen, J. Warna and T. Salmi, **2009**, Supported ionic liquid catalysts-From batch to continuous operation in preparation of fine chemicals, *Catalysis Today*, 147, 144-148.

270. Z. Zhang, L. Wu, J. Dong, B.-G. Li and S. Zhu, **2009**, Preparation and sorption/desorption behavior of an ionic liquid supported on porous silica particles, *Industrial & Engineering Chemistry Research*, 48, 2142-2148.

271. J. Lemus, J. Palomar, M.A. Gilarranz and J.J. Rodriguez, **2009**, Characterization of supported ionic liquid phase (SILP) materials prepared from different supports, *Adsorption-Journal of the International Adsorption Society*, 17, 561-571.

272. J.B. Binder and R.T. Raines, **2010**, Fermentable sugars by chemical hydrolysis of biomass, *Proceedings of the National Academy of Sciences of the United States of America*, 107, 4516-4521.

273. J. Krockel and U. Kragl, **2003**, Nanofiltration for the separation of nonvolatile products from solutions containing ionic liquids, *Chemical Engineering & Technology*, 26, 1166-1168.

274. U. Krings and R.G. Berger, **1998**, Biotechnological production of flavours and fragrances, *Applied Microbiology and Biotechnology*, 49, 1-8.

275. World flavors & fragrances, *Freedionia*, **2012**.

276. F. Tiemann and W. Haarmann, **1874**, Ueber das Coniferin und seine Umwandlung in das aromatische Princip der Vanille, *Berichte der Deutschen Chemischen Gesellschaft*, 7, 608-623.

277. C. Chapuis and D. Jacoby, **2001**, Catalysis in the preparation of fragrances and flavours, *Applied Catalysis a-General*, 221, 93-117.

278. S. Hagedorn and B. Kaphammer, **1994**, Microbial biocatalysis in the generation of flavor and fragrance chemicals, *Annual Review of Microbiology*, 48, 773-800.

279. F.W. Welsh, W.D. Murray and R.E. Williams, **1989**, Microbiological and enzymatic production of flavor and fragrance chemicals, *Critical Reviews in Biotechnology*, 9, 105-169.

280. S. Serra, C. Fuganti and E. Brenna, **2005**, Biocatalytic preparation of natural flavours and fragrances, *Trends in Biotechnology*, 23, 193-198.

281. N. Ghumare, Antioxidants market - Global industry analysis, size, share, growth, trends and forecast, 2014-2020, *Transparency Market Research*, **2014**.

282. C. Lopez-Alarcon and A. Denicola, **2013**, Evaluating the antioxidant capacity of natural products: A review on chemical and cellular-based assays, *Analytica Chimica Acta*, 763, 1-10.

283. K.L. Wolfe and R.H. Liu, **2007**, Cellular antioxidant activity (CAA) assay for assessing antioxidants, foods, and dietary supplements, *Journal of Agricultural and Food Chemistry*, 55, 8896-8907.

284. Prebiotics market - Global industry analysis, size, share, growth, trends and forecast, 2013 - 2019, *Transparency Market Research*, **2015**.

285. Sigma-Aldrich, K4769 SIGMA Kojibiose, http://www.sigmaaldrich.com/catalog/product/sigma/k4769?lang=en&region=BE, Accessed 2015-09-30, **2015**.

286. T. Van de Wiele, N. Boon, S. Possemiers, H. Jacobs and W. Verstraete, **2004**, Prebiotic effects of chicory inulin in the simulator of the human intestinal microbial ecosystem, *Fems Microbiology Ecology*, 51, 143-153.

287. J.H. Cummings, G.T. Macfarlane and H.N. Englyst, **2001**, Prebiotic digestion and fermentation, *American Journal of Clinical Nutrition*, 73, 415-420.

288. M. Mandels, E.T. Reese and F.W. Parrish, **1962**, Sophorose as an inducer of cellulase in *Trichoderma viride*, *Journal of Bacteriology*, 83, 400-408.

289. Carbosynth, MFCD00150664 Sophorose, http://www.carbosynth.com/carbosynth/website.nsf/(w-productdisplay)/DAA24139989A6CC6802571C0002BA2A3, Accessed 2015-09-30, **2015**.

290. J. Seibel, R. Moraru, S. Gotze, K. Buchholz, S. Na'amnieh, A. Pawlowski and H.J. Hecht, **2006**, Synthesis of sucrose analogues and the mechanism of action of *Bacillus subtilis* fructosyltransferase (levansucrase), *Carbohydrate Research*, 341, 2335-2349.

291. H. Strathmann, **2001**, Membrane separation processes: Current relevance and future opportunities, *Aiche Journal*, 47, 1077-1087.

292. M. Di Luccio, B.D. Smith, T. Kida, C.P. Borges and T.L.M. Alves, **2000**, Separation of fructose from a mixture of sugars using supported liquid membranes, *Journal of Membrane Science*, 174, 217-224.

293. K. Touaj, N. Tbeur, M. Hor, J.-F. Verchere and M. Hlaibi, **2009**, A supported liquid membrane (SLM) with resorcinarene for facilitated transport of methyl glycopyranosides: Parameters and mechanism relating to the transport, *Journal of Membrane Science*, 337, 28-38.

Summary

Glycosylation of small molecules can substantially alter their physicochemical and biological properties, thereby extending their application potential in various industries. Prominent examples include the prolonged stability of ascorbic acid in cosmetic formulations, the modified perception of flavors and fragrances, and the enhanced solubility of therapeutic flavonoids. Despite the continuous development of new procedures, chemical synthesis of glycosides still suffers from low yields and the generation of toxic waste. Biocatalytic approaches have, therefore, gained increasing attention as attractive alternatives, enabling one-step reactions with high regio- and stereoselectivity. Nevertheless, few enzymes are available to perform glycosylation reactions cost-efficiently at the industrial scale. Indeed, glycosyl transferases require relatively expensive nucleotide-activated sugars, while glycoside hydrolases suffer from low yields when used in the synthetic direction. Consequently, disaccharide phosphorylases have received increasing attention in recent years as promising biocatalysts for glycoside synthesis. These enzymes catalyze the reversible phosphorolysis of glycosidic bonds, and thus only require a glycosyl phosphate as donor substrate for synthetic reactions.

First, a continuous production process for α-D-glucose 1-phosphate (αG1P), the preferred donor for many glycoside phosphorylases, was developed. The use of sucrose phosphorylase (SP) from *Bifidobacterium adolescentis* immobilized on Sepabeads EC-HFA allowed the synthesis of αG1P up to 179 g/L/h. Interestingly, the substrate sucrose was found to stabilize the biocatalyst, which remained fully active after 2 weeks of continuous operation at 60 °C. The produced αG1P could be conveniently purified by yeast treatment and was recovered in crystalline form with a yield of 86 %. The limited availability of specificities however, still hampers the use of glycoside phosphorylases for synthetic purposes. In that respect, molecular imprinting was explored to modify the three-dimensional structure of SP by noncovalent interactions with an imprinting molecule. The developed procedure can be performed in an aqueous environment and gives rise to a new enzyme formulation called imprinted cross-linked enzyme aggregates (iCLEAs). Proof of concept was delivered by imprinting SP with α-glucosyl glycerol, thereby doubling the enzyme's specific activity towards glycerol, while simultaneously providing an exceptional stability at 60 °C.

Unfortunately, disaccharide phosphorylases typically have a very low affinity for non-carbohydrate acceptors. Although concentrations compensating for the high K_m values can be achieved by the addition of organic cosolvents, the commonly used DMSO and methanol are not compatible with numerous applications of carbohydrate-derived products. Moreover, their presence often leads to the partial inactivation of the biocatalyst. Ionic liquids (ILs), in contrast, have emerged as a new class of solvents for biocatalytic applications. These 'green' solvents consist of salts with a low melting point (<100 °C), possess no vapor pressure and are inflammable. The addition of various ILs was found to significantly increase the solubility of for example resveratrol and quercetin, without affecting the ability to dissolve 1 M sucrose. Interestingly, both [EMIM][dca] and AMMOENG 101 proved to have better dissolving properties than DMSO. In contrast to [EMIM][dca], the IL AMMOENG 101 was found to be also much less deleterious to the stability of SP than for example DMSO or methanol. Consequently, the use of the IL AMMOENG 101 enabled the synthesis and isolation of the desirable 3-*O*-α-D-glucopyranosyl (*E*)-resveratrol. Alternatively, the application of liquid-liquid biphasic systems containing water and a water-immiscible organic solvent, was also considered to counter this low affinity towards alternative substrates. Careful optimization allowed the glucosylation of aliphatic alcohols, monoterpenoids, aromatic alcohols and phenolics with the SP from *B. adolescentis*. In addition a series of alkyl gallyl 4-*O*-α-D-glucopyranosides was successfully synthesized. These glucosylations were achieved by reacting 62.5 % aqueous MOPS buffer at pH 7.5 containing 2 M sucrose and 50 U/mL SP, and 37.5 % EtOAc supplemented with 100 mg/mL acceptor. Consequently, the use of ILs and biphasic catalysis was identified a valuable alternative for glycosylation reactions with SP.

Next, the previously developed techniques were applied for the synthesis of β-D-glucosides and α-L-rhamnosides with the cellobiose phosphorylase (CP) originating from *Clostridium thermocellum* and the α-L-rhamnosidase from *Aspergillus terreus*, respectively. Interestingly, CP was found to be compatible with the IL AMMOENG 101 and EtOAc, allowing the glycosylation of aliphatic alcohols, monoterpenoids, aromatic alcohols and phenolics. The stability of the biocatalyst was significantly improved by cross-linking the enzyme, resulting in an impressive half-life of 11 days at 50 °C. Moreover, the efficiency of the CLEAs for the synthesis of octyl β-D-glucopyranoside

could be roughly doubled by molecular imprinting with octanol. In parallel, the recombinant α-L-rhamnosidase originating from *A. terreus* was used for the reverse rhamnosylation of various small organic compounds. A full factorial experimental design setup was applied to identify the importance of temperature, substrate concentrations, solvent type and concentration as well as the acidity of the reaction mixture. Careful optimization of these parameters allowed the synthesis and isolation of a range of α-L-rhamnosides among which cyclohexyl α-L-rhamnopyranoside, anisyl α-L-rhamnopyranoside and 2-phenylethyl α-L-rhamnopyranoside. In addition, α-L-rhamnosylation of phenolic hydroxyls in phenols such as hydroquinone, resorcinol, catechol and phenol was observed, which is a rather unique reaction catalyzed by glycosidases.

Next, the previously obtained α- and β-glucosides were glycosylated with the cellodextrin phosphorylase (CDP) from *Clostridium stercorarium*. The specific activity of the enzyme towards various glucosides was assessed, revealing β-(1,4)-glucosylation of aliphatic and phenolic α/β-glucosides. In addition, three proposed positions in the +2 subsite were mutated to alanine, and proved to be determinants for the specificity of CDP. Remarkably, the specific activity of variant W168A towards octyl β-D-glucopyranoside was found to be higher than the activity of the WT towards its natural substrate cellobiose, revealing the potential of this newly created biocatalyst for the synthesis of alkyl polyglucosides. Moreover, SP, CP and CDP were successfully combined for the glycosylation of a wide variety of antioxidants. The resulting antioxidant library, containing α/β-glucosides, different regio-isomers, cellobiosides and cellotriosides was then characterized. The glucosylation position was found to significantly influence the solubility of these compounds, while α-glucosides could be dissolved to higher concentrations compared to their β-linked counterparts. Moreover, glycosylation improved the stability of all evaluated antioxidants. Also, the point of attachment, the anomeric configuration, and the glycosidic chain length were found to influence the scavenging abilities of these glycosides. Despite decreased activities, most glycosylated compounds were identified as potent antioxidants, outperforming the commonly used 2,6-bis(1,1-dimethylethyl)-4-methylphenol (BHT).

Finally, a production process for the promising prebiotic kojibiose was developed. To that end, a number of recently reported SP variants with improved selectivity towards kojibiose, were evaluated under process conditions. Initial experiments allowed the synthesis and isolation of kojibiose up to 350 mM using the L341I_Q345S variant of *B. adolescentis* SP. Moreover, an integrated approach, optimizing both reaction conditions and downstream processing at the same time quickly led to the synthesis and purification of kojibiose to concentrations in excess of 1.5 M. In addition, the atom efficiency of the latter process was increased to an impressive 79 % through the use of glucose isomerase, allowing the isolation of 3 kg crystalline kojibiose with a purity of 99.8 %. Thus, we developed a sustainable, cost-effective and scalable biocatalytic process for the production of highly pure kojibiose, starting from renewable, cheap and readily available bulk sugars. In conclusion, the synthetic potential of glycoside phosphorylases for the production of glycosides and specialty carbohydrates was demonstrated during this PhD research.

Samenvatting

Glycosylatie kan de fysicochemische en biologische eigenschappen van organische verbindingen sterk beïnvloeden. Hierdoor zullen typisch ook hun toepassingsmogelijkheden in verschillende industriële takken veranderen. De verhoogde stabiliteit van ascorbinezuur in cosmetische formulaties, wijzigingen in het waarnemen van smaak- of geurstoffen, en de verhoogde oplosbaarheid van therapeutische flavonoiden zijn hiervan slechts enkele voorbeelden. Ondanks de onafgebroken ontwikkeling van nieuwe technieken, wordt de chemische synthese van glycosides nog steeds gekenmerkt door lage opbrengsten en het aanmaken van grote hoeveelheden toxisch afval. Bijgevolg is de interesse in biokatalytische alternatieven, die één-staps reacties met hoge regio- en steriosleCtiviteit toelaten, sterk toegenomen. Ondanks deze voordelen, zijn echter weinig enzymen in staat deze glycosylatiereacties op een economisch verantwoorde manier te katalyseren. De vaak gebruikte glycosyl transferasen hebben immers dure nucleotide-geactiveerde suikers nodig, terwijl het gebruik van glycoside hydrolasen in de synthese richting leidt tot lage opbrengsten. Bijgevolg krijgen disaccharide fosforylasen steeds meer aandacht als veelbelovend alternatief voor de synthese van glycosides. Deze enzymen katalyseren de omkeerbare fosforylatie van glycosidische bindingen, en hebben dus enkel een glycosyl fosfaat nodig als donor substraat voor synthetische reacties.

In eerste instantie werd een continu productieproces voor α-D-glucose 1-fosfaat (αG1P), het donor substraat voor verschillende glycoside fosforylasen, ontwikkeld. Immobilisatie van het *Bifidobacterium adolescentis* sucrose fosforylase (SP) op Sepabeads EC-HFA, liet de synthese van 179 g/L/u αG1P toe. Bovendien bleek de aanwezigheid van sucrose de biokatalysator sterk te stabiliseren, dewelke nog steeds over zijn volledige activiteit beschikte na 2 weken katalyse bij 60 °C. Het geproduceerde αG1P kon nadien eenvoudig opgezuiverd worden met behulp van een gistbehandeling, waarna kristallisatie leidde tot zuiver αG1P. De beperkte beschikbaarheid van specificiteiten, bemoeilijkt echter het gebruik van deze glycoside fosforylasen. In die optiek, werd moleculaire imprinting onderzocht als alternatief om de driedimensionele structuur van SP aan te passen. De ontwikkelde procedure kan uitgevoerd worden in een waterig milieu, en geeft aanleiding tot een nieuw preparaat dat 'imprinted cross-linked enzyme aggregate' (iCLEA) genoemd wordt. De specifieke activiteit van SP voor

glycerol kon verdubbeld worden door imprinten met α-glucosyl glycerol, terwijl de bekomen iCLEAs uitzonderlijk stabiel bleken bij 60 °C.

Dissacharide fosforylasen hebben jammer genoeg een lage affiniteit voor niet-suiker acceptoren. Hoewel concentraties die compenseren voor deze hoge K_m waardes bereikt kunnen worden door het toevoegen van organische cosolventen, is het typisch gebruikte DMSO niet compatibel met de meeste toepassingen van de beoogde producten. Bovendien leidt hun aanwezigheid ook vaak tot een gedeeltelijke inactivatie van de biokatalysator. Ionische vloeistoffen (ILs), daarentegen, krijgen steeds meer aandacht als nieuwe klasse solventen voor biokatalytische processen. Deze 'groene' solventen bestaan uit zouten met een laag smeltpunt (<100 °C), bezitten geen dampdruk en zijn niet ontvlambaar. Het toevoegen van deze ILs bleek de oplosbaarheid van resveratrol en quercetine sterk te verhogen, en dit terwijl nog steeds 1 M sucrose kon opgelost worden. Verder onderzoek toonde aan dat zowel [EMIM][dca] als AMMOENG 101 beter presteerden dan DMSO voor het oplossen van diverse componenten. In tegenstelling tot [EMIM][dca], bleek SP veel stabieler te zijn in de IL AMMOENG 101 dan in het typisch gebruikte DMSO. Het gebruik van AMMOENG 101 liet de synthese en isolatie van ondermeer 3-*O*-α-D-glucopyranosyl (*E*)-resveratrol toe. Daarnaast werd ook vloeistof-vloeistof bifase katalyse onderzocht om de lage affiniteit voor alternatieve substraten te compenseren. Het zorgvuldig optimaliseren van de reactiecondities leidde uiteindelijk tot de glucosylatie van diverse verbindingen, waaronder alifatische alcoholen, monoterpenen, aromatische alcoholen en fenolen met het SP van *B. adolescentis*. Bovendien kon tevens een reeks alkyl gallyl 4-*O*-α-D-glucopyranosides gesynthetiseerd worden. Deze reacties werden uitgevoerd door 62.5 % MOPS buffer op pH 7.5, die 2 M sucrose en 50 U/mL SP bevatte, toe te voegen bij 37.5 % EtOAc met 100 mg/mL acceptor. Bijgevolg kunnen zowel het gebruik van ILs als bifase katalyse bestempeld worden als waardevolle technieken voor glycosylatiereacties met SP.

Vervolgens werden de reeds ontwikkelde technieken toegepast voor de synthese van β-D-glucosides en α-L-rhamnosides met het cellobiose fosforylase (CP) van *Clostridium thermocellum* en het α-L-rhamnosidase van *Aspergillus terreus*, respectievelijk. Onderzoek toonde aan dat CP net als SP compatibel is met de IL AMMOENG 101 en EtOAc, wat de glycosylatie van alifatische alcoholen, monoterpenen, aromatische

alcoholen en fenolen toeliet. De stabiliteit van CP kon eveneens sterk verhoogd worden door cross-linking, wat leide tot een verbluffende half-waarde tijd van 11 dagen bij 50 °C. Bovendien kon de efficientie van de CP CLEAs voor de synthese van octyl β-D-glucopyranoside verdubbeld worden door imprinting met octanol. Daarnaast werd het α-L-rhamnosidase van *A. terreus* gebruikt voor de rhamnosylering van verschillende kleine organische moleculen. Experimenten werden opgesteld om het belang van de temperatuur, substraat concentraties, solvent type en concentratie, alsook de pH van het reactiemedium te bepalen. Vervolgens werden deze parameters geoptimaliseerd, wat de synthese en isolatie van een reeks α-L-rhamnosides waaronder cyclohexyl α-L-rhamnopyranoside, anisyl α-L-rhamnopyranoside en 2-phenylethyl α-L-rhamnopyranoside toeliet. Tot onze verbazing, bleek ook de α-L-rhamnosylatie van kleine fenolen zoals hydroquinone, resorcinol, catechol en fenol mogelijk.

Aansluitend op de synthese van α- en β-glucosides met SP en CP respectievelijk, werd de verlenging van deze glucosides met het cellodextrine fosforylase (CDP) van *Clostridium stercorarium* ontwikkeld. De specifieke activiteit van CDP voor verschillende glucosides werd onderzocht, waaruit β-(1,4)-glucosylatie van alifatische en fenolische α/β-glucosides mogelijk bleek. Ook werden enkele posities in de +2 subsite gemuteerd naar alanine, dewelke cruciaal bleken voor de specificiteit van CDP. Geheel onverwacht, bleek de specifieke activiteit van de W168A variant voor octyl β-D-glucopyranoside hoger te zijn dan de activiteit van het wild type op cellobiose, wat het nut van deze mutant voor de synthese van alkyl polyglucosides (APGs) duidelijk aantoont. Naast de synthese van APGs, werden SP, CP en CDP eveneens succesvol gecombineerd voor de glycosylatie van een waaier antioxidanten. De resulterende antioxidant bibliotheek, die zowel α/β-glucosides, verschillende regio-isomeren, als cellobiosides en cellotriosides bevat, werd vervolgens gekarakteriseerd. De glycosylatiepositie beïnvloedde de oplosbaarheid van deze componenten sterk, terwijl α-glucosides typisch beter oplosbaar bleken in vergelijking met de corresponderende β-glucosides. Daarnaast verhoogt glycosylatie de stabiliteit van alle geteste antioxidanten, terwijl de plaats van aanhechting, de anomerische configuratie, alsook de ketenlengte van het suikerdeel de radicaalvangende eigenschappen van deze glycosides bepaalt. Ondanks verlaagde activiteiten, bleken de meeste glycosides nog steeds beter te presteren dan 2,6-bis(1,1-dimethylethyl)-4-methylfenol (BHT).

Tenslotte werd een productieproces voor het veelbelovende prebioticum kojibiose ontwikkeld. Daartoe werden een reeks recent gerapporteerde SP varianten onderworpen aan verschillende reactiecondities. Initiële experimenten leidden snel tot de synthese en isolatie van 350 mM kojibiose, gebruik makende van de *B. adolescentis* SP L341I_Q345S variant. Het toepassen van een geïntegreerde benadering, waarbij zowel de reactiecondities als de productopzuivering tegelijkertijd werden ontwikkeld, leidde uiteindelijk tot kojibiose concentraties hoger dan 1.5 M. Bovendien kon de atoom efficiëntie van dit proces verhoogd worden tot een indrukwekkende 79 % door gebruik te maken van glucose isomerase. Uiteindelijk werd 3 kg kristallijn kojibiose met een zuiverheid van 99.8 % geïsoleerd uit één enkele reactie. Het ontwikkelde procec is dus schaalbaar, en maakt enkel gebruik van hernieuwbare, goedkope en in bulk beschikbare suikers. Het synthetische potentieel van glycoside fosforylasen voor de productie van glycosides en speciale suikers werd bijgevolg duidelijk aangetoond tijdens dit doctoraatsonderzoek.

Curriculum vitae

Personalia

Name	**KAREL DE WINTER**
Professional address	Center for Industrial Biotechnology and Biocatalysis Faculty of Bioscience Engineering Ghent University Coupure Links 653 9000 Ghent
E-mail	Karel.DeWinter@ugent.be
Nationality	Belgian
Place of birth	Zottegem
Date of birth	September 23rd, 1987

Education

2010-2016 **PhD in Applied Biological Sciences**, Faculty of Bioscience Engineering, Ghent University, Ghent

PhD thesis: Expanding the application potential of glycoside phosphorylases through process engineering

Promotors: prof. dr. Tom Desmet and prof. dr. ir. Wim Soetaert

2008-2010 **MSc in Bioscience Engineering – Chemistry and Bioprocess Technology**, Faculty of Bioscience Engineering, Ghent University, Ghent
With greatest honor

MSc thesis: Increasing the thermostability of sucrose phosphorylase by covalent immobilization

Promotors: prof. dr. Tom Desmet and prof. dr. ir. Wim Soetaert

2005-2008 **BSc in Bioscience Engineering – Chemistry and Bioprocess Technology**, Faculty of Bioscience Engineering, Ghent University, Ghent
With great honor

Conferences and courses

International Scientific Conference on Probiotics and Prebiotics - IPC2015, June 23rd – June 25th, 2015, Budapest (Hungary)

Oral presentation: K. De Winter, T. Verhaeghe and T. Desmet, **2015**, Turning bulk sugars into prebiotics: highly efficient production of kojibiose from sucrose and glucose

Biorefinery for Biomolecules (Graduate School VLAG), April 15th – April 16th, 2015, Wageningen (The Netherlands)

Poster presentation: K. De Winter and T. Desmet, **2015**, Ionic liquids and sucrose phosphorylase

4th international conference on Novel Enzymes (Ghent University), October 14th – October 17th, 2014, Ghent (Belgium)

Poster presentation: K. De Winter, W. Soetaert and T. Desmet, **2014**, Disaccharide phosphorylases for the efficient synthesis of glycosides

25th Joint Glycobiology meeting (Ghent University), September 14th – September 16th, 2014, Ghent (Belgium)

Oral presentation: K. De Winter and T. Desmet, **2014**, Disaccharide phosphorylases as efficient biocatalysts for glycoside synthesis

Knowledge for Growth 2014 (FlandersBio), May 8th, 2014, Ghent (Belgium)

Poster presentation: K. De Winter and T. Desmet, **2014**, Ionic liquids and sucrose phosphorylase: Balancing acceptor solubility and enzyme stability

CINBIOS-workshop: een Roadmap voor Industriële Biotechnologie in Vlaanderen (CINBIOS), March 28th, 2014, Mechelen (Belgium)

10th Carbohydrate Bioengineering Meeting – CBM2013, April 21st – April 24th, 2013, Prague (Czech Republic)

Oral presentation: K. De Winter and T. Desmet, **2013**, Disaccharide phosphorylases as efficient biocatalysts for glycoside synthesis

CINBIOS Forum for Industrial Biotechnology & the Biobased Economy (CINBIOS), October 23rd, 2012, Mechelen (Belgium)

Poster presentation: K. De Winter, W. Soetaert and T. Desmet, **2012**, Imprinted cross-linked enzyme aggregates (iCLEAs): Combining improved stability with altered specificity

Biocat 2012 (Hamburg University of Technology), September 2nd – September 6th, 2012, Hamburg (Germany)
Poster presentation: K. De Winter, W. Soetaert and T. Desmet, **2012**, Imprinted cross-linked enzyme aggregates (iCLEAs): Combining improved stability with altered specificity

Ghent Bio-economy Summer School (Ghent University), August 7th – August 10th, 2012, Ghent (Belgium)
Poster presentation: K. De Winter, W. Soetaert and T. Desmet, **2012**, Sucrose phosphorylase iCLEAs: enhancing stability and specificity

Catalyzing Bio-Economy – Biocatalysts for Industrial Biotechnology (Dechema e.V.), April 24th – April 25th, 2012, Frankfurt am Main (Germany)
Oral presentation: K. De Winter, A. Cerdobbel and T. Desmet, **2012**, Engineering the thermostability of sucrose phosphorylase

Biotransformations 2011 (Dechema e.V.), August 22nd – August 25th, 2011, Bad Herrenalb (Germany)
Poster presentation: K. De Winter, A. Cerdobbel and T. Desmet, **2011**, Sucrose phosphorylase CLEAs: Improved thermal stability for industrial applications

16th European Carbohydrate Symposium (Eurocarb-16), July 3rd – July 7th, 2011, Sorrento (Italy)

Knowledge for Growth 2011 (FlandersBio), May 5th, 2011, Ghent (Belgium)
Poster presentation: K. De Winter, A. Cerdobbel and T. Desmet, **2011**, Sucrose phosphorylase CLEAs: Improved thermal stability for industrial applications

International mobility

Institute of Microbiology - Laboratory of Biotransformation (Academy of Sciences of the Czech Republic), 2011-2012, November 24th – January 31st , Prague (Czech Republic)
Supervisor: prof. dr. Vladimir Kren

Peer-reviewed publications

T. Verhaeghe, **K. De Winter**, M. Berland, R. De Vreese, M. D'hooghe, B. Offmann, and T. Desmet, **2016**, Converting bulk sugars into prebiotics: Semi-rational design of a transglucosidase with controlled selectivity, *Chemical communications*, DOI: 10.1039/C5CC09940D.

K. De Winter, G. Dewitte, M.E. Dirks-Hofmeister, S. De Laet, H. Pelantova, V. Kren, and T. Desmet, **2015**, Chemoenzymatic glycosylation of phenolic antioxidants: phosphorylase mediated synthesis and characterization, *Journal of Agricultural and Food Chemistry*, 63, 10131-10139.

K. De Winter, L. Van Renterghem, K. Wuyts, H. Pelantova, V. Kren, W. Soetaert and T. Desmet, **2015**, Chemoenzymatic synthesis of β-D-glucosides using cellobiose phosphorylase from *Clostridium thermocellum*, *Advanced Synthesis & Catalysis*, 357, 1961-1969

K. Mollet, L. Decuyper, S. Vander Meeren, N. Piens, **K. De Winter**, T. Desmet and M. D'hooghe, **2015**, Synthesis of 2-aryl-3-(2-cyanoethyl) aziridines and their chemical and enzymatic hydrolysis towards γ-lactams and γ-lactones, *Organic & Biomolecular Chemistry*, 13, 2716-2725

M.E. Dirks-Hofmeister, T. Verhaeghe, **K. De Winter** and T. Desmet, **2015**, Creating space for large acceptors: Rational biocatalyst design for resveratrol glycosylation in an aqueous system, *Angewandte Chemie International Edition*, 54, 9289-9292

K. De Winter, G. Dewitte, H.G. Tran and T. Desmet, **2015**, Biocatalytic production of novel glycolipids, *Practical methods for biocatalysis and biotransformations 3*, 119-125 (BookChapter)

K. De Winter, T. Desmet, T. Devlamynck, L. Van Renterghem, T. Verhaeghe, H. Pelantova, V. Kren and W. Soetaert, **2014**, Biphasic catalysis with disaccharide phosphorylases: Chemoenzymatic synthesis of α-D-glucosides using sucrose phosphorylase, *Organic Process Research & Development*, 18, 781-787

K. De Winter, K. Verlinden, V. Kren, L. Weignerova, W. Soetaert and T. Desmet, **2013**, Ionic liquids as cosolvents for glycosylation by sucrose phosphorylase: balancing acceptor solubility and enzyme stability, *Green Chemistry*, 15, 1949-1955

K. De Winter, D. Simcikova, B. Schalck, L. Weignerova, H. Pelantova, W. Soetaert, V. Kren, and T. Desmet, **2013**, Chemoenzymatic synthesis of α-L-rhamnosides using recombinant α-L-rhamnosidase from *Aspergillus terreus*, *Bioresource Technology*, 147, 640-644

K. De Winter, W. Soetaert and T. Desmet, **2012**, An imprinted cross-linked enzyme aggregate (iCLEA) of sucrose phosphorylase: Combining improved stability with altered specificity, *International Journal of Molecular Sciences*, 13, 11333-11344

K. De Winter, T. Desmet, A. Cerdobbel and W. Soetaert, **2012**, Preparation and use of sucrose phosphorylase as cross-linked enzyme aggregate (CLEA), *Practical methods for biocatalysis and biotransformations 2*, 240-244 (BookChapter)

A. Cerdobbel, **K. De Winter**, D. Aerts, R. Kuipers, H.-J. Joosten, W. Soetaert and T. Desmet, **2011**, Increasing the thermostability of sucrose phosphorylase by a combination of sequence- and structure-based mutagenesis, *Protein Engineering Design & Selection*, 24, 829-834

K. De Winter, A. Cerdobbel, W. Soetaert and T. Desmet, **2011**, Operational stability of immobilized sucrose phosphorylase: Continuous production of α-glucose 1-phosphate at elevated temperatures, *Process Biochemistry*, 46, 2074-2078

A. Cerdobbel, T. Desmet, **K. De Winter**, J. Maertens and W. Soetaert, **2010**, Increasing the thermostability of sucrose phosphorylase by multipoint covalent immobilization, *Journal of Biotechnology*, 150, 125-130

A. Cerdobbel, **K. De Winter**, T. Desmet and W. Soetaert, **2010**, Sucrose phosphorylase as cross-linked enzyme aggregate: Improved thermal stability for industrial applications, *Biotechnology Journal*, 5, 1192-1197

Manuscripts in preparation

K. De Winter, T. Verhaeghe, A. Van Canneyt, and T. Desmet, **2016**, Highly efficient synthesis of kojibiose: Process intensification, crystallization, and characterization, *Journal of Agricultural and Food Chemistry*, ***In preparation***.

Patents

K. De Winter and T. Desmet, Production of specific glucosides with cellobiose phosphorylase, *EP 15152108.5*

M.E. Dirks-Hofmeister, T. Verhaeghe, **K. De Winter** and T. Desmet, Mutant sucrose phosphorylases with improved glycosylation activity towards polyphenols, *EP 15167263.1*

T. Verhaeghe, **K. De Winter** and T. Desmet, A sucrose phosphorylase for the production of kojibiose, *EP 14193238.4*

K. De Winter, W. Soetaert, D. Aerts, T. Verhaeghe and T. Desmet, A thermostable sucrose and sucrose-6'-phosphate phosphorylase, *WO 2014/060452*

Student guidance

Practical courses

Microbiology (2011)
Biocatalysis – enzyme kinetics (2012, 2014)
Biocatalysis – computer excercises (2013)

BSc thesis

L. Bernaerts, M. Carron, N. De Wit and E. De Wolf, **2014-2015,** Antioxidanten: Veel geblaat, weinig wol?

MSc thesis

S. De Laet, **2014-2015**, Glycosylated phenolic antioxidants: chemoenzymatic synthesis and properties

A. Van Canneyt, **2014-2015**, Demonstrating the necessity of enzyme engineering: towards a highly efficient process for the synthesis of kojibiose

B. De Schrijver, **2014-2015**, Synthese en biokatalytische hydrolyse van 4-(cyaanalkyl)azetidin-2-onen

G. Dewitte, **2013-2014**, Exploring the glycosylation potential of cellodextrin phosphorylase through a combination of enzyme and process engineering

L. Van Renterghem, **2013-2014**, Biocatalytic synthesis of glucosides through the combinatorial action of sucrose and cellobiose phosphorylase

L. Decuyper, **2013-2014**, Synthese van 2-aryl-3-(2-cyaanethyl)aziridinen en hun biokatalytische omzetting tot γ-lactonen en γ-lactamen

J. Bomon, **2013-2014**, Chemische synthese en enzymatische hydrolyse van 4-(cyaanmethyl) azetidin-2-onen

K. Wuyts, **2012-2013**, Cellobiose phosphorylase revisited: A promising tool for the synthesis of glucosides

T. Devlamynck, **2012-2013**, Biocatalytic glycosylation of organic compounds in biphasic systems

B. Schalck, **2012-2013**, Production and application of α-L-rhamnosidase for the glycosylation of small organic molecules

S. Vander Meeren, **2012-2013**, Synthese en enzymatische hydrolyse van trans-2-aryl-3-(2-cyaanethyl)aziridinen

K. Verlinden, **2011-2012**, Biokatalytische productie van geglycosyleerde verbindingen in groene solventen